

International Journal of Modern Physics B
© World Scientific Publishing Company

INFLUENCE FUNCTIONAL FOR DECOHERENCE OF INTERACTING ELECTRONS IN DISORDERED CONDUCTORS

JAN VON DELFT

*Fakultät für Physik, Arnold Sommerfeld Center for Theoretical Physics,
and Center for NanoScience
Ludwig-Maximilians-Universität München
Theresienstr. 37, 80333, München, Germany
vondelft@lmu.de*

Received November 16, 2007

In this review, we rederive the controversial influence functional approach of Golubev and Zaikin (GZ) for interacting electrons in disordered metals in a way that allows us to show its equivalence, before disorder averaging, to diagrammatic Keldysh perturbation theory. By representing a certain Pauli factor ($\delta - 2\bar{\rho}^0$) occurring in GZ's effective action in the frequency domain (instead of the time domain, as GZ do), we also achieve a more accurate treatment of recoil effects. With this change, GZ's approach reproduces, in a remarkably simple way, the standard, generally accepted result for the decoherence rate. – The main text and appendices A.1 to A.3 of the present review are comparatively brief, and have been published previously; for convenience, they are included here again (with minor revisions). The bulk of the review is contained in several additional, lengthy appendices containing the relevant technical details.

Keywords: interactions, disorder, decoherence, weak localization

1. Introduction

A few years ago, Golubev and Zaikin (GZ) developed an influence functional approach for describing interacting fermions in a disordered conductor^{2,3,4,5,6,7}. Their key idea was as follows: to understand how the diffusive behavior of a given electron is affected by its interactions with other electrons in the system, which constitute its effective environment, the latter should be integrated out, leading to an influence functional, denoted by $e^{-\frac{1}{\hbar}(i\tilde{S}_R + \tilde{S}_I)}$, in the path integral $\int \tilde{\mathcal{D}}' \mathbf{R}$ describing its dynamics. To derive the effective action $(i\tilde{S}_R + \tilde{S}_I)$, GZ devised a strategy which, when implemented with sufficient care, *properly incorporates the Pauli principle* – this is essential, since both the particle and its environment originate from the same system of indistinguishable fermions, a feature which makes the present problem conceptually interesting and sets it apart from all other applications of influence functionals that we are aware of.

GZ used their new approach to calculate the electron decoherence rate $\gamma_\varphi(T)$ in disordered conductors, as extracted from the magnetoconductance in the weak lo-

calization regime, and found it to be finite at zero temperature^{2,3,4,5,6,7}, $\gamma_\varphi^{\text{GZ}}(T \rightarrow 0) = \gamma_\varphi^{0,\text{GZ}}$, in apparent agreement with some experiments⁸. However, this result contradicts the standard view, based on the work of Altshuler, Aronov and Khmelnitskii (AAK)¹⁰, that $\gamma_\varphi^{\text{AAK}}(T \rightarrow 0) = 0$, and hence elicited a considerable controversy⁹. GZ's work was widely questioned,^{11,12,13,14,15,16} with the most detailed and vigorous critique coming from Aleiner, Altshuler and Gershenson (AAG)¹⁷ and Aleiner, Altshuler and Vavilov (AAV)^{18,19}, but GZ rejected each critique^{4,5,6,9} with equal vigor. It is important to emphasize that the debate here was about a well-defined theoretical model, and not about experiments which do or do not support GZ's claim.

The fact that GZ's final results for $\gamma_\varphi^{\text{GZ}}(T)$ have been questioned, however, does not imply that their influence functional approach, as such, is fundamentally flawed. To the contrary, we show in this review that it is sound in principle, and that *the standard result $\gamma_\varphi^{\text{AAK}}(T)$ can be reproduced using GZ's method*, provided that it is applied with slightly more care to correctly account for recoil effects (i.e. the fact that the energy of an electron changes when it absorbs or emits a photon). We believe that this finding conclusively resolves the controversy in favor of AAK and company; hopefully, it will also serve to revive appreciation for the merits of GZ's influence functional approach.

The premise for understanding how $\gamma_\varphi^{\text{AAK}}$ can be reproduced with GZ's methods was that we had carried out a painfully detailed analysis and rederivation of GZ's approach, as set forth by them in two lengthy papers from 1999 and 2000, henceforth referred to as GZ99³ and GZ00⁴. Our aim was to establish to what extent their method is related to the standard Keldysh diagrammatic approach. As it turned out, the two methods are essentially equivalent, and GZ obtained unconventional results only because a certain "Pauli factor" ($\tilde{\delta} - 2\tilde{\rho}^0$) occurring in \tilde{S}_R was not treated sufficiently carefully, where $\tilde{\rho}^0$ is the single-particle density matrix. That their treatment of this Pauli factor was dubious had of course been understood and emphasized before: first and foremost it was correctly pointed out by AAG¹⁷ that GZ's treatment of the Pauli factor caused their expression for $\gamma_\varphi^{\text{GZ}}$ to acquire an artificial ultraviolet divergence, which then produces the term $\gamma_\varphi^{0,\text{GZ}}$, whereas no such divergence is present in diagrammatic calculations. GZ's treatment of ($\tilde{\delta} - 2\tilde{\rho}^0$) was also criticized, in various related contexts, by several other authors^{11,12,15,16,18}. However, none of these works (including our own¹⁵, which, in retrospect, missed the main point, namely recoil) had attempted to diagnose the nature of the Pauli factor problem *with sufficient precision to allow a successful remedy to be devised within the influence functional framework*.

This will be done in the present review. Working in the time domain, GZ represent ($\tilde{\delta} - 2\tilde{\rho}^0(t)$) as $1 - 2n_0[\tilde{h}_0(t)/2T]$, where n_0 is the Fermi function and $\tilde{h}_0(t)$ the free part of the electron energy. GZ assumed that $\tilde{h}_0(t)$ does not change during the diffusive motion, because scattering off impurities is elastic. Our diagnosis is that this assumption *unintentionally neglects recoil effects* (as first pointed out by

Eriksen and Hedegard¹¹), because the energy of an electron actually does change at each interaction vertex, i.e. each time it emits or absorbs a photon. The remedy (not found by Eriksen and Hedegard) is to transform from the time to the frequency domain, in which $(\tilde{\delta} - 2\tilde{\rho}^0)$ is represented by $1 - 2n_0[\hbar(\tilde{\varepsilon} - \tilde{\omega})] = \tanh[\hbar(\tilde{\varepsilon} - \tilde{\omega})/2T]$, where $\hbar\tilde{\omega}$ is the energy change experienced by an electron with energy $\hbar\tilde{\varepsilon}$ at an interaction vertex. Remarkably, this simple change of representation from the time to the frequency domain is sufficient to recover $\gamma_\varphi^{\text{AAK}}$. Moreover, the ensuing calculation is free of ultraviolet or infrared divergencies, and no cut-offs of any kind have to be introduced by hand.

The main text of the present review has two central aims: firstly, to concisely explain the nature of the Pauli factor problem and its remedy; and secondly, to present a transparent calculation of γ_φ , using only a few lines of simple algebra. (Actually, we shall only present a “rough” version of the calculation here, which reproduces the qualitative behavior of $\gamma_\varphi^{\text{AAK}}(T)$; an improved version, which achieves quantitative agreement with AAK’s result for the magnetoconductance [with an error of at most 4% for quasi-1-D wires], has been published in a separate analysis by Marquardt, von Delft, Smith and Ambegaokar²⁰. The latter consists of two parts, referred to as MDSA-I and DMSA-II below, which use alternative routes to arrive at conclusions that fully confirm the analysis of this review.)

We have made an effort to keep the main text reasonably short and to the point; once one accepts its starting point [Eqs. (1) to Eq. (4)], the rest of the discussion can easily be followed step by step. Thus, as far as possible, the main text avoids technical details of interest only to the experts. These have been included in a set of five lengthy and very detailed appendices, B to F, in the belief that when dealing with a controversy, *all* relevant details should be publicly accessible to those interested in “the fine print”. For the benefit of those readers (presumably the majority) with no time or inclination to read lengthy appendices, a concise appendix A summarizes (without derivations) the main steps and approximations involved in obtaining the influence functional.

The main text and appendices A.1 to A.3 have already been published previously¹, but for convenience are included here again (with minor revisions, and an extra sketch in Fig. 1), filling the first 23 pages. The content of the remaining appendices is as follows: In App. A.4 we address GZ’s claim that a strictly nonperturbative approach is needed for obtaining γ_φ , and explain why we disagree (as do many others^{17,18,19}). In App. B, we rederive the influence functional and effective action of GZ, following their general strategy in spirit, but introducing some improvements. The most important differences are: (i) instead of using the coordinate-momentum path integral $\int \mathcal{D}\mathbf{R} \int \mathcal{D}\mathbf{P}$ of GZ, we use a “coordinates-only” version $\int \tilde{\mathcal{D}}\mathbf{R}$, since this enables the Pauli factor to be treated more accurately; and (ii), we are careful to perform thermal weighting at an initial time $t_0 \rightarrow -\infty$ (which GZ do not do), which is essential for obtaining properly energy-averaged expressions and for reproducing perturbative results: the standard diagrammatic Keldysh

perturbation expansion for the Cooperon in powers of the interaction propagator is generated if, *before disorder averaging*, the influence functional is expanded in powers of $(i\tilde{S}_R + \tilde{S}_I)/\hbar$. In App. C we review how a general path integral expression derived for the conductivity in App. B can be rewritten in terms of the familiar Cooperon propagator, and thereby related to the standard relations familiar from diagrammatic perturbation theory. In particular, we review the Fourier transforms required to obtain a path integral $\tilde{P}_{\text{eff}}^\varepsilon(\tau)$ properly depending on both the energy variable $\hbar\varepsilon$ relevant for thermal weighting and the propagation time τ needed to traverse the closed paths governing weak localization. Appendix D gives an explicit time-slicing definition of the “coordinates-only” path integral $\int \tilde{\mathcal{D}}' \mathbf{R}$ used in App. B. Finally, for reference purposes, we collect in Apps. E and F some standard material on the diagrammatic technique (although this is bread-and-butter knowledge for experts in diagrammatic methods and available elsewhere, it is useful to have it summarized here in a notation consistent with the rest of our analysis). App. E summarizes the standard Keldysh approach in a way that emphasizes the analogy to our influence functional approach, and App. F collects some standard and well-known results used for diagrammatic disorder averaging. Disorder averaging is discussed last for a good reason: one of the appealing features of the influence functional approach is that most of the analysis can be performed *before* disorder averaging, which, if at all, only has to be performed at the very end.

2. Main Results of Influence Functional Approach

We begin by summarizing the main result of GZ’s influence functional approach. Our notations and also the content of some of our formulas are not identical to those of GZ, and in fact differ from their’s in important respects. Nevertheless, we shall refer to them as “GZ’s results”, since we have (re)derived them (see App. B for details) in the spirit of GZ’s approach.

The Kubo formula represents the DC conductivity σ_{DC} in terms of a retarded current-current correlator $\langle [\hat{j}(1), \hat{j}(2)] \rangle$. This correlator can (within various approximations discussed in App. B.5.6, B.5.7, B.6.3 and A.3) be expressed as follows in terms of a path integral $\tilde{P}_{\text{eff}}^\varepsilon$ representing the propagation of a pair of electrons with average energy $\hbar\varepsilon$, thermally averaged over energies:

$$\sigma_{\text{DC}} = \frac{2}{d} \int dx_2 \mathbf{j}_{11'} \cdot \mathbf{j}_{22'} \int (d\varepsilon) [-n'(\hbar\varepsilon)] \int_0^\infty d\tau \tilde{P}_{21',\text{eff}}^{12',\varepsilon}(\tau), \quad (1a)$$

$$\tilde{P}_{21',\text{eff}}^{12',\varepsilon}(\tau) = \int_{\mathbf{R}^F(-\frac{\tau}{2})=\mathbf{r}_{2'}}^{\mathbf{R}^F(\frac{\tau}{2})=\mathbf{r}_1} \int_{\mathbf{R}^B(-\frac{\tau}{2})=\mathbf{r}_2}^{\mathbf{R}^B(\frac{\tau}{2})=\mathbf{r}_{1'}} \tilde{\mathcal{D}}' \mathbf{R} e^{\frac{1}{\hbar} [i(\tilde{S}_0^F - \tilde{S}_0^B) - (i\tilde{S}_R + \tilde{S}_I)](\tau)}. \quad (1b)$$

The propagator $\tilde{P}_{21',\text{eff}}^{12',\varepsilon}(\tau)$, defined for a given impurity configuration, is written in terms of a forward and backward path integral $\int_{\mathbf{R}^F} \int_{\mathbf{R}^B} \tilde{\mathcal{D}}' \mathbf{R}$ between the specified initial and final coordinates and times. It gives the amplitude for a pair of electron trajectories, with average energy $\hbar\varepsilon$, to propagate from $\mathbf{r}_{2'}$ at time $-\frac{1}{2}\tau$ to \mathbf{r}_1 at

$\frac{1}{2}\tau$ or from $\mathbf{r}_{1'}$ at time $\frac{1}{2}\tau$ to \mathbf{r}_2 at $-\frac{1}{2}\tau$, respectively. [The sense in which both τ and ε can be specified at the same time is discussed in App. A.3, and in more detail in App. C.4, Eqs. (C.21) to (C.24)]. We shall call these the forward and backward paths, respectively, using an index $a = F, B$ to distinguish them. $\tilde{S}_0^a = \tilde{S}_0^{F/B}$ are the corresponding free actions, which determine which paths will dominate the path integral. The weak localization correction to the conductivity, $\sigma_{\text{DC}}^{\text{WL}}$, arises from the ‘‘Cooperon’’ contributions to σ_{DC} , illustrated in Fig. 1(b), for which the coordinates $\mathbf{r}_1, \mathbf{r}'_1, \mathbf{r}_2$ and \mathbf{r}'_2 all lie close together, and which feature self-returning random walks through the disordered potential landscape for pairs of paths $\mathbf{R}^{F/B}$, with path B being the time-reversed version of path F , i.e. $\mathbf{R}^F(t_3) = \mathbf{R}^B(-t_3)$ for $t_3 \in (-\frac{1}{2}\tau, \frac{1}{2}\tau)$. The effect of the other electrons on this propagation is encoded in the influence functional $e^{-(i\tilde{S}_R + \tilde{S}_I)/\hbar}$ occurring in Eq. (1b). The effective action $i\tilde{S}_R + \tilde{S}_I$ turns out to have the form [for a more explicit version, see Eq. (A.7) in App. A; or, for an equivalent but more compact representation, see Eqs. (B.94) and (B.97) of Sec. B.6.3]:

$$\left\{ \begin{array}{l} i\tilde{S}_R(\tau) \\ \tilde{S}_I(\tau) \end{array} \right\} = -\frac{1}{2}i \sum_{a,a'=F,B} s_a \int_{-\frac{\tau}{2}}^{\frac{\tau}{2}} dt_{3a} \int_{-\frac{\tau}{2}}^{t_{3a}} dt_{4a'} \left\{ \begin{array}{l} \tilde{\mathcal{L}}_{3_a 4_{a'}}^{a'} \\ s_{a'} \tilde{\mathcal{L}}_{3_a 4_{a'}}^K \end{array} \right\}. \quad (2)$$

Here s_a stands for $s_{F/B} = \pm 1$, and the shorthand $\tilde{\mathcal{L}}_{3_a 4_{a'}} = \tilde{\mathcal{L}}[t_{3a} - t_{4_{a'}}, \mathbf{R}^a(t_{3a}) - \mathbf{R}^{a'}(t_{4_{a'}})]$ describes, in the coordinate-time representation, an interaction propagator linking two vertices on contours a and a' . It will be convenient below to Fourier transform to the momentum-frequency representation, where the propagators $\tilde{\mathcal{L}}^K$ and $\tilde{\mathcal{L}}^{a'}$ can be represented as follows $[(d\bar{\omega})(d\bar{\mathbf{q}}) \equiv (d\bar{\omega} d\bar{\mathbf{q}})/(2\pi)^4]$:

$$\tilde{\mathcal{L}}_{3_a 4_{a'}}^K \equiv \int (d\bar{\omega})(d\bar{\mathbf{q}}) e^{i(\bar{\mathbf{q}}[\mathbf{R}^a(t_{3a}) - \mathbf{R}^{a'}(t_{4_{a'}})] - \bar{\omega}(t_{3a} - t_{4_{a'}}))} \tilde{\mathcal{L}}_{\bar{\mathbf{q}}}^K(\bar{\omega}), \quad (3a)$$

$$\tilde{\mathcal{L}}_{3_a 4_{a'}}^{a'} \equiv \begin{cases} [(\tilde{\delta} - 2\tilde{\rho}^0)\tilde{\mathcal{L}}^R]_{3_a 4_F} & \text{if } a' = F, \\ [\tilde{\mathcal{L}}^A(\tilde{\delta} - 2\tilde{\rho}^0)]_{4_B 3_a} & \text{if } a' = B, \end{cases} \quad (3b)$$

$$\equiv \int (d\bar{\omega})(d\bar{\mathbf{q}}) e^{is_{a'}(\bar{\mathbf{q}}[\mathbf{R}^a(t_{3a}) - \mathbf{R}^{a'}(t_{4_{a'}})] - \bar{\omega}(t_{3a} - t_{4_{a'}}))} \tilde{\mathcal{L}}_{\bar{\mathbf{q}}}^{a'}(\bar{\omega}). \quad (3c)$$

[Note the sign $s_{a'}$ in the Fourier exponential in Eq. (3c); it reflects the opposite order of indices in Eq. (3b), namely 34 for F vs. 43 for B .] Here $\tilde{\mathcal{L}}^K$ is the Keldysh interaction propagator, while $\tilde{\mathcal{L}}^{F/B}$, to be used when time $t_{4_{a'}}$ lies on the forward or backward contours, respectively, represent ‘‘effective’’ retarded or advanced propagators, modified by a ‘‘Pauli factor’’ $(\tilde{\delta} - 2\tilde{\rho}^0)$ (involving a Dirac-delta $\tilde{\delta}_{ij}$ and single-particle density matrix $\tilde{\rho}_{ij}^0$ in coordinate space), the precise meaning of which will be discussed below. $\tilde{\mathcal{L}}_{\bar{\mathbf{q}}}^{K,R,A}(\bar{\omega})$ denote the Fourier transforms of the standard Keldysh, retarded, or advanced interaction propagators. For the screened Coulomb interaction in the unitary limit, they are given by

$$\tilde{\mathcal{L}}_{\bar{\mathbf{q}}}^R(\bar{\omega}) = [\tilde{\mathcal{L}}_{\bar{\mathbf{q}}}^A(\bar{\omega})]^* = -\frac{E_{\bar{\mathbf{q}}}^0 - i\bar{\omega}}{2\nu E_{\bar{\mathbf{q}}}^0} = -\frac{[\bar{\mathcal{D}}_{\bar{\mathbf{q}}}^0(\bar{\omega})]^{-1}}{2\nu E_{\bar{\mathbf{q}}}^0}, \quad (4a)$$

6 Jan von Delft

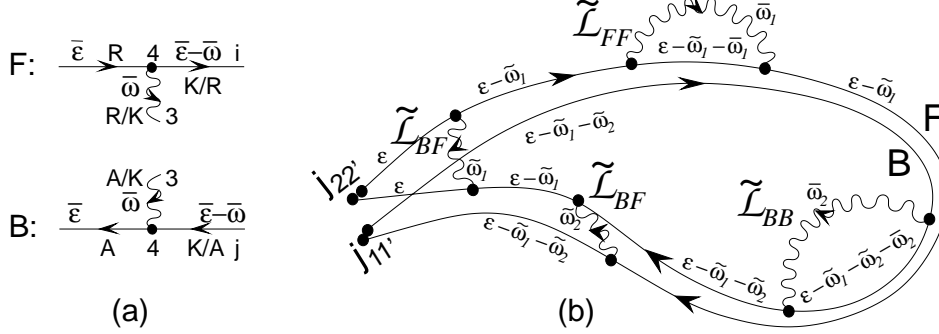


Fig. 1. (a) Structure of vertices on the forward or backward contours of Keldysh perturbation theory. F: the combinations $\tilde{G}_{i_F 4_F}^K \tilde{\mathcal{L}}_{34_F}^R$ and $\tilde{G}_{i_F 4_F}^R \tilde{\mathcal{L}}_{34_F}^K$ occur if vertex 4 lies on the upper forward contour. B: the combinations $\tilde{\mathcal{L}}_{4_B 3}^A \tilde{G}_{4_B j_B}^K$ and $\tilde{\mathcal{L}}_{4_B 3}^K \tilde{G}_{4_B j_B}^A$ occur if vertex 4 lies on the lower contour. Arrows point from the second to first indices of propagators. (b) Sketch of a pair of time-reversed paths connecting the points at which the current operators $\mathbf{j}_{11'}$, $\mathbf{j}_{22'}$ act [cf. Eq. (1a)], decorated by several (wavy) interaction propagators $\tilde{\mathcal{L}}_{aa'}^{R/A/K}(\omega)$. In the Keldysh formalism, the electron lines represent the electron propagators $\tilde{G}^{R/A}(\omega)$ or $\tilde{G}^K(\omega) = \tanh(\hbar\omega/2T)[\tilde{G}^R - \tilde{G}^A](\omega)$. The effective action defined in Eqs. (2) to (4a) in effect neglects the frequency transfers ω_i in the arguments of all retarded and advanced electron Green's functions [$\tilde{G}^{R/A}(\varepsilon - \omega_i - \dots) \rightarrow \tilde{G}^{R/A}(\varepsilon)$], but, for every occurrence of the combination $\tilde{\mathcal{L}}^{R/A}(\omega_i)\tilde{G}^K(\varepsilon - \omega_i)$, retains it in the factor $\tanh[\hbar(\varepsilon - \omega_i)/\hbar]$ of the accompanying \tilde{G}^K function. The latter prescription ensures that a crucial feature of the Keldysh approach is retained in the influence functional formalism, too, namely that all integrals $\int d\omega_i$ over frequency transfer variables are limited to the range $|\hbar\omega_i| \lesssim T$ [which is why the neglect of ω_i in $\tilde{G}^{R/A}(\varepsilon - \omega_i - \dots)$ is justified]. In contrast, GZ also neglect the $-\omega_i$ in $\tanh[\hbar(\varepsilon - \omega_i)/\hbar]$ [see Sec. 4], which amounts to neglecting recoil. As a result, their $\int d\omega_i$ integrals are no longer limited to $|\hbar\omega_i| \lesssim T$, i.e. artificial ultraviolet divergencies occur, which produce GZ's temperature-independent contribution $\gamma_\varphi^{0,\text{GZ}}$ to the decoherence rate [see Eq. (11)]. Thus, $\gamma_\varphi^{0,\text{GZ}}$ is an artefact of GZ's neglect of recoil, as is their claimed ‘‘decoherence at zero temperature’’.

$$\overline{\mathcal{L}}_{\bar{q}}^K(\bar{\omega}) = 2i \coth(\hbar\bar{\omega}/2T) \text{Im}[\overline{\mathcal{L}}_{\bar{q}}^R(\bar{\omega})], \quad (4b)$$

$$\overline{\mathcal{C}}_{\bar{q}}^0(\bar{\omega}) = \frac{1}{E_{\bar{q}} - i\bar{\omega}}, \quad \overline{\mathcal{D}}_{\bar{q}}^0(\bar{\omega}) = \frac{1}{E_{\bar{q}}^0 - i\bar{\omega}}, \quad (4c)$$

$$E_{\bar{q}}^0 = D\bar{q}^2, \quad E_{\bar{q}} = D\bar{q}^2 + \gamma_H, \quad (4d)$$

where, for later reference, we have also listed the Fourier transforms of the bare diffuson $\overline{\mathcal{D}}^0$ and Cooperon $\overline{\mathcal{C}}^0$ (where γ_H is the dephasing rate of the latter in the presence of a magnetic field, D the diffusion constant and ν the density of states per spin). Finally, $\overline{\mathcal{L}}_{\bar{q}}^{\alpha'}$ in Eq. (3c) is defined as

$$\overline{\mathcal{L}}_{\bar{q}}^{F/B}(\bar{\omega}) = \tanh[\hbar(\varepsilon - \bar{\omega})/2T] \overline{\mathcal{L}}_{\bar{q}}^{R/A}(\bar{\omega}), \quad (4e)$$

where $\hbar\varepsilon$ is the same energy as that occurring in the thermal weighting factor $[-n'(\hbar\varepsilon)]$ in Eq. (1a).

Via the influence functional, the effective action (2) concisely incorporates the effects of interactions into the path integral approach. \tilde{S}_I describes the *classical*

part of the effective environment, and if one would replace the factor $\coth(\hbar\bar{\omega}/2T)$ in $\tilde{\mathcal{L}}_q^K(\bar{\omega})$ by $2T/\hbar\bar{\omega}$ (as is possible for high temperatures) it corresponds to the contribution calculated by AAK¹⁰. With \tilde{S}_R , GZ succeeded to additionally also include the quantum part of the environment, and in particular, via the Pauli factor $(\tilde{\delta} - 2\tilde{\rho}^0)$, to properly account for the Pauli principle.

Casual readers are asked to simply accept the above equations as starting point for the remainder of this review, and perhaps glance through App. A to get an idea of the main steps and approximations involved in deriving them. Those interested in a detailed derivation are referred to App. B (where $\tilde{S}_{R/I}$ are obtained in Sec. B.5.8). It is also shown there [Sec. B.6] that the standard results of diagrammatic Keldysh perturbation theory can readily be reproduced from the above formalism by expanding the influence functional $e^{-(i\tilde{S}_R + \tilde{S}_I)/\hbar}$ in powers of $(i\tilde{S}_R + \tilde{S}_I)/\hbar$. For present purposes, simply note that such an equivalence is entirely plausible in light of the fact that our effective action (2) is linear in the effective interaction propagators $\tilde{\mathcal{L}}$, a structure typical for generating functionals for Feynman diagrams.

3. Origin of the Pauli Factor

The occurrence of the Pauli factor $(\tilde{\delta} - 2\tilde{\rho}^0)$ in \tilde{S}_R was first found by GZ in precisely the form displayed in the position-time representation of the effective action used in Eq. (2). However, their subsequent treatment of this factor differs from ours, in a way that will be described below. In particular, they did not represent this factor in the frequency representation, as in our Eq. (4e), and this is the most important difference between our analysis and theirs.

The origin of the Pauli factor in the form given by our Eq. (4e) can easily be understood if one is familiar with the structure of Keldysh perturbation theory. [For a detailed discussion, see Sec. B.6.2.] First recall two exact relations for the noninteraction Keldysh electron propagator: in the coordinate-time representation, it contains a Pauli factor,

$$\tilde{G}_{ij}^K = \int dx_k (\tilde{G}^R - \tilde{G}^A)_{ik} (\tilde{\delta} - 2\tilde{\rho}^0)_{kj} = \int dx_k (\tilde{\delta} - 2\tilde{\rho}^0)_{ik} (\tilde{G}^R - \tilde{G}^A)_{kj} \quad (5a)$$

which turns into a tanh in the coordinate frequency representation:

$$\tilde{G}_{ij}^K(\bar{\omega}) = \tanh(\hbar\bar{\omega}/2T) [\tilde{G}_{ij}^R(\bar{\omega}) - \tilde{G}_{ij}^A(\bar{\omega})]. \quad (5b)$$

Now, in the Keldysh approach, retarded or advanced interaction propagators always occur [see Fig. 1(a)] together with Keldysh electron propagators, in the combinations $\tilde{G}_{i_F 4_F}^K \tilde{\mathcal{L}}_{34_F}^R$ or $\tilde{\mathcal{L}}_{4_B 3}^A \tilde{G}_{4_B j_B}^K$, where the indices denote coordinates and times. [Likewise, the Keldysh interaction propagators always come in the combinations $\tilde{G}_{i_F 4_F}^R \tilde{\mathcal{L}}_{34_F}^K$ or $\tilde{\mathcal{L}}_{4_B 3}^K \tilde{G}_{4_B j_B}^A$.] In the momentum-frequency representation, the combinations involving \tilde{G}^K therefore turn into $\bar{\mathcal{L}}_q^{R/A}(\bar{\omega}) [\bar{G}^R - \bar{G}^A]_{q-\bar{q}}(\bar{\varepsilon} - \bar{\omega}) \tanh[\hbar(\bar{\varepsilon} - \bar{\omega})/2T]$. Thus, *in the frequency representation the Pauli factor is represented as*

$\tanh[\hbar(\bar{\varepsilon} - \bar{\omega})/2T]$. Here the variable $\hbar\bar{\varepsilon}$ represents the energy of the electron line on the upper (or lower) Keldysh contour before it enters (or after it leaves) an interaction vertex at which its energy decreases (or increases) by $\hbar\bar{\omega}$ [see Fig. 1(a)]. The subtraction of $\bar{\omega}$ in the argument of \tanh thus reflects the physics of recoil: emitting or absorbing a photon causes the electron energy to change by $\hbar\bar{\omega}$, and it is this changed energy $\hbar(\bar{\varepsilon} - \bar{\omega})$ that enters the Fermi functions for the relevant final or initial states.

Of course, in Keldysh perturbation theory, $\hbar\bar{\varepsilon}$ will have different values from one vertex to the next, reflecting the history of energy changes of an electron line as it proceeds through a Feynman diagram [as illustrated in Fig. 1(b)]. It is possible to neglect this complication in the influence functional approach, if one so chooses, by always using one and the same energy in Eq. (4e), which then should be chosen to be the same as that occurring in the thermal weighting factor $[-n'(\hbar\varepsilon)]$, i.e. $\hbar\bar{\varepsilon} = \hbar\varepsilon$. This approximation, which we shall henceforth adopt, is expected to work well if the relevant physics is dominated by low frequencies, at which energy transfers between the two contours are sufficiently small [$\hbar(\bar{\varepsilon} - \varepsilon) \ll T$, so that the electron “sees” essentially the same Fermi function throughout its motion. [For a detailed discussion of this point, see App. B.6.2.]

Though the origin and necessity of the Pauli factor is eminently clear when seen in conjunction with Keldysh perturbation theory, it is a rather nontrivial matter to derive it cleanly in the functional integral approach [indeed, this is the main reason for the length of our appendices!]. The fact that GZ got it completely right in the position-time representation of Eq. (2) is, in our opinion, a significant and important achievement. It is regrettable that they did not proceed to consider the frequency representation (4e), too, which in our opinion is more useful.

4. Calculating τ_φ à la GZ

To calculate the decoherence rate $\gamma_\varphi = 1/\tau_\varphi$, one has to find the long-time decay of the Cooperon contribution to the propagator $\tilde{P}_{\text{eff}}^\varepsilon(\tau)$ of Eq. (1). To do this, GZ proceeded as follows: using a saddle-point approximation for the path integral for the Cooperon, they replaced the sum over all pairs of self-returning paths $\mathbf{R}^{F/B}(t_{3_F/B})$ by just the contribution $\langle e^{-\frac{1}{\hbar}(i\tilde{S}_R + \tilde{S}_I)(\tau)} \rangle_{\text{rw}}$ of the classical “random walk” paths $\mathbf{R}_{\text{rw}}(t)$ picked out by the classical actions \tilde{S}_0^g , namely $\mathbf{R}^F(t_{3_F}) = \mathbf{R}_{\text{rw}}(t_{3_F})$ and $\mathbf{R}^B(t_{3_B}) = \mathbf{R}_{\text{rw}}(-t_{3_B})$, for which the paths on the forward and backward Keldysh contours are *time-reversed* partners. The subscript “rw” indicates that each such classical path is a self-returning random walk through the given disorder potential landscape, and $\langle \rangle_{\text{rw}}$ means averaging over all such paths. Next, in the spirit of Chakravarty and Schmid²¹, they replace the average of the exponent over all time-reversed pairs of self-returning random walks, by the exponent of the average, $e^{-F(\tau)}$, where $F(\tau) = \frac{1}{\hbar} \langle i\tilde{S}_R + \tilde{S}_I \rangle_{\text{rw}}$ (cf. Eq. (67) of GZ99³). This amounts to expanding the exponent to first order, then averaging, and then reexponentiating. The function $F(\tau)$ thus defined increases with time, starting from $F(0) = 0$, and

the decoherence time τ_φ can be defined as the time at which it becomes of order one, i.e. $F(\tau_\varphi) \approx 1$.

To evaluate $\langle i\tilde{S}_R + \tilde{S}_I \rangle_{\text{rw}}$, GZ Fourier transform the functions $\tilde{\mathcal{L}}_{3_a 4'_a} = \tilde{\mathcal{L}}[t_{34}, \mathbf{R}^a(t_3) - \mathbf{R}^{a'}(t_4)]$ occurring in $\tilde{S}_{R/I}$, and average the Fourier exponents using²¹ the distribution function for diffusive motion, which gives probability that a random walk that passes point $\mathbf{R}_{\text{rw}}(t_4)$ at time t_4 will pass point $\mathbf{R}_{\text{rw}}(t_3)$ at time t_3 , i.e. that it covers a distance $\mathbf{R} = \mathbf{R}_{\text{rw}}(t_3) - \mathbf{R}_{\text{rw}}(t_4)$ in time $|t_{34}|$:

$$\begin{aligned} \left\langle e^{i\bar{\mathbf{q}} \cdot [\mathbf{R}_{\text{rw}}(t_3) - \mathbf{R}_{\text{rw}}(t_4)]} \right\rangle_{\text{rw}} &\simeq \int d^{\bar{d}} \mathbf{R} \left(\frac{\pi}{D|t_{34}|} \right)^{\bar{d}/2} e^{-\mathbf{R}^2 / (4D|t_{34}|)} e^{i\bar{\mathbf{q}} \cdot \mathbf{R}} \\ &= e^{-\bar{\mathbf{q}}^2 D|t_{34}|} \rightarrow \tilde{C}_{\bar{\mathbf{q}}}^0(|t_{34}|) = e^{-E_{\bar{\mathbf{q}}}|t_{34}|}. \end{aligned} \quad (6)$$

(Here $t_{34} = t_3 - t_4$.) The arrow in the second line makes explicit that if we also account for the fact that such time-reversed pairs of paths are dephased by a magnetic field, by adding a factor $e^{-\gamma_H|t_{34}|}$, the result is simply equal to the bare Cooperon in the momentum-time representation.

Actually, the above way of averaging is somewhat inaccurate, as was pointed out to us by Florian Marquardt: it neglects the fact that the diffusive trajectories between t_3 and t_4 are part of a larger, *self-returning* trajectory, starting and ending at $\mathbf{r}_1 \simeq \mathbf{r}_2$ at times $\mp \frac{1}{2}\tau$. It is actually not difficult to include this fact, see MDSA-I²⁰, and this turns out to quantitatively improve the numerical prefactor for τ_φ (e.g. in Eq. (18) below). However, for the sake of simplicity, we shall here be content with using Eq. (6), as GZ did.

Finally, GZ also assumed that the Pauli factor $(\tilde{\delta} - 2\tilde{\rho}^0)$ in \tilde{S}_R remains unchanged throughout the diffusive motion: they use a coordinate-momentum path integral $\int \mathcal{D}\mathbf{R} \int \mathcal{D}\mathbf{P}$ [instead of our coordinates-only version $\int \tilde{\mathcal{D}}'\mathbf{R}$], in which $(\tilde{\delta} - 2\tilde{\rho}^0)$ is replaced by $[1 - 2n_0(\tilde{h}_0)] = \tanh(\tilde{h}_0/2T)$, and the free-electron energy $\tilde{h}_0[\mathbf{R}(t_a), \mathbf{P}(t_a)]$ is argued to be unchanged throughout the diffusive motion, since impurity scattering is elastic [cf. p. 9205 of GZ99³: “ n depends only on the energy and not on time because the energy is conserved along the classical path”]. Indeed, this is true *between* the two interaction events at times t_3 and t_4 , so that the averaging of Eq. (6) *is* permissible. However, as emphasized above, the full trajectory stretches from $-\frac{1}{2}\tau$ to t_4 to t_3 to $\frac{1}{2}\tau$, and the electron energy *does* change, by $\pm\hbar\bar{\omega}$, at the interaction vertices at t_4 and t_3 . Thus, *GZ’s assumption of a time-independent Pauli factor neglects recoil effects*. As argued in the previous section, these can straightforwardly taken into account using Eq. (4e), which we shall use below. In contrast, GZ’s assumption of time-independent n amounts dropping the $-\hbar\bar{\omega}$ in our $\tanh[\hbar(\varepsilon - \bar{\omega})/2T]$ function.

If one uses GZ’s assumptions to average Eq. (2), but uses the proper $\tanh[\hbar(\varepsilon - \bar{\omega})/2T]$ function, one readily arrives at

$$\left\{ \begin{array}{l} \langle i\tilde{S}_R \rangle_{\text{rw}} \\ \langle \tilde{S}_I \rangle_{\text{rw}} \end{array} \right\} = 2\text{Re} \left[-\frac{1}{2}i \int (d\bar{\omega})(d\bar{\mathbf{q}}) \left\{ \begin{array}{l} \tilde{\mathcal{L}}_{\bar{\mathbf{q}}}^F(\bar{\omega}) \\ \tilde{\mathcal{L}}_{\bar{\mathbf{q}}}^K(\bar{\omega}) \end{array} \right\} [f^{\text{self}} - f^{\text{vert}}](\tau) \right], \quad (7)$$

10 *Jan von Delft*

where $f^{\text{self}} - f^{\text{vert}}$ are the first and second terms of the double time integral

$$\int_{-\frac{\tau}{2}}^{\frac{\tau}{2}} dt_3 \int_{-\frac{\tau}{2}}^{t_3} dt_4 e^{-i\bar{\omega}t_{34}} \left\langle e^{i\mathbf{q}\cdot[\mathbf{R}_{\text{rw}}(t_3) - \mathbf{R}_{\text{rw}}(t_4)]} - e^{i\mathbf{q}\cdot[\mathbf{R}_{\text{rw}}(-t_3) - \mathbf{R}_{\text{rw}}(t_4)]} \right\rangle_{\text{rw}}, \quad (8)$$

corresponding to self-energy ($a = a' = F$) and vertex ($a \neq a' = F$) contributions, and the $2\text{Re}[\]$ in Eq. (7) comes from adding the contributions of $a' = F$ and B . Performing the integrals in Eq. (8), we find

$$f^{\text{self}}(\tau) = \bar{\mathcal{C}}_{\bar{q}}^0(-\bar{\omega})\tau + [\bar{\mathcal{C}}_{\bar{q}}^0(-\bar{\omega})]^2 \left[e^{-\tau(E_{\bar{q}} + i\bar{\omega})} - 1 \right], \quad (9a)$$

$$f^{\text{vert}}(\tau) = \bar{\mathcal{C}}_{\bar{q}}^0(\bar{\omega}) \left[\frac{e^{-i\bar{\omega}\tau} - 1}{-i\bar{\omega}} + \frac{e^{-E_{\bar{q}}\tau} - 1}{E_{\bar{q}}} \right]. \quad (9b)$$

Of all terms in Eqs. (9), the first term of f^{self} , which is linear in τ , clearly grows most rapidly, and hence dominates the leading long-time behavior. Denoting the associated contribution to Eq. (7) by $\frac{1}{\hbar} \langle i\tilde{S}_R/\tilde{S}_I \rangle_{\text{rw}}^{\text{leading,self}} \equiv \tau\gamma_{\varphi}^{R/I,\text{self}}$, the corresponding rates $\gamma_{\varphi}^{R/I,\text{self}}$ obtained from Eqs. (7) and (9) are:

$$\gamma_{\varphi}^{R,\text{self}} = \frac{1}{\hbar} \int (d\bar{\omega})(d\bar{q}) \tanh \left[\frac{\hbar(\varepsilon - \bar{\omega})}{2T} \right] 2\text{Re} \left[\frac{\frac{1}{2}i(E_{\bar{q}}^0 - i\bar{\omega})}{2\nu E_{\bar{q}}^0(E_{\bar{q}} + i\bar{\omega})} \right], \quad (10a)$$

$$\gamma_{\varphi}^{I,\text{self}} = \frac{1}{\hbar} \int (d\bar{\omega})(d\bar{q}) \coth \left[\frac{\hbar\bar{\omega}}{2T} \right] 2\text{Re} \left[\frac{\bar{\omega}}{2\nu E_{\bar{q}}^0(E_{\bar{q}} + i\bar{\omega})} \right]. \quad (10b)$$

Let us compare these results to those of GZ, henceforth using $\gamma_H = 0$. Firstly, both our $\gamma_{\varphi}^{I,\text{self}}$ and $\gamma_{\varphi}^{R,\text{self}}$ are nonzero. In contrast, in their analysis GZ concluded that $\langle \tilde{S}_R \rangle_{\text{rw}} = 0$. The reason for the latter result is, evidently, their neglect of recoil effects: indeed, if we drop the $-\hbar\bar{\omega}$ from the tanh-factor of Eq. (10a), we would find $\gamma_{\varphi}^R = 0$ and thereby recover GZ's $i\bar{\omega}$ result, since the real part of the factor in square brackets is odd in $\bar{\omega}$.

Secondly and as expected, we note that Eq. (10b) for $\gamma_{\varphi}^{I,\text{self}}$ agrees with that of GZ, as given by their equation (71) of GZ99³ for $1/\tau_{\varphi}$, i.e. $\gamma_{\varphi}^{I,\text{self}} = \gamma_{\varphi}^{\text{GZ}}$. [To see the equivalence explicitly, use Eq. (A.9).] Noting that the $\int d\bar{\omega}$ -integral in Eq. (10b) evidently diverges for large $\bar{\omega}$, GZ cut off this divergence at $1/\tau_{\text{el}}$ (arguing that the diffusive approximation only holds for time-scales longer than τ_{el} , the elastic scattering time). For example, for quasi-1-dimensional wires, for which $\int (d\bar{q}) = a^{-2} \int dq/(2\pi)$ can be used (a^2 being the cross section, so that $\sigma_1 = a^2 \sigma_{\text{DC}}^{\text{Drude}}$ is the conductivity per unit length, with $\sigma_{\text{DC}}^{\text{Drude}} = 2e^2\nu D$), they obtain (cf. (76) of GZ99³):

$$\frac{1}{\tau_{\varphi}^{\text{GZ}}} \simeq \frac{e^2\sqrt{2D}}{\hbar\sigma_1} \int_{\frac{1}{\tau_{\text{GZ}}}}^{\frac{1}{\tau_{\text{el}}}} \frac{(d\bar{\omega})}{\omega^{1/2}} \coth \left[\frac{\hbar\bar{\omega}}{2T} \right] \simeq \frac{e^2}{\pi\hbar\sigma_1} \sqrt{\frac{2D}{\tau_{\text{el}}}} \left[\frac{2T\sqrt{\tau_{\text{el}}\tau_{\varphi}^{\text{GZ}}}}{\hbar} + 1 \right]. \quad (11)$$

[The use of a self-consistently-determined lower frequency cut-off is explained in Sec. 6]. Thus, they obtained a temperature-independent contribution $\gamma_{\varphi}^{0,\text{GZ}}$ from the +1 term, which is the result that ignited the controversy.

However, we thirdly observe that, due to the special form of the retarded interaction propagator in the unitary limit, the real parts of the last factors in square brackets of Eqs. (10a) and (10b) are actually *equal* (for $\gamma_H = 0$). Thus, the ultraviolet divergence of $\gamma_\varphi^{I,\text{self}}$ is *cancelled* by a similar divergence of $\gamma_\varphi^{R,\text{self}}$. Consequently, the total decoherence rate coming from self-energy terms, $\gamma_\varphi^{\text{self}} = \gamma_\varphi^{I,\text{self}} + \gamma_\varphi^{R,\text{self}}$, is free of ultraviolet divergencies. Thus we conclude that the contribution $\gamma_\varphi^{0,\text{GZ}}$ found by GZ is an artefact of their neglect of recoil, as is their claimed “decoherence at zero temperature”.

5. Dyson Equation and Cooperon Self Energy

The above results for $\gamma_\varphi^{R,\text{self}} + \gamma_\varphi^{I,\text{self}}$ turn out to agree completely with those of a standard calculation of the Cooperon self energy $\tilde{\Sigma}$ using diagrammatic impurity averaging [details of which are summarized in Appendix F]. We shall now summarize how this comes about.

Calculating $\tilde{\Sigma}$ is an elementary exercise within diagrammatic perturbation theory, first performed by Fukuyama and Abrahams²². However, to facilitate comparison with the influence functional results derived above, we proceed differently: We have derived [Sec. B.6.1] a general expression²³, before impurity averaging, for the Cooperon self-energy of the form $\tilde{\Sigma} = \sum_{aa'} \left[\tilde{\Sigma}_{aa'}^I + \tilde{\Sigma}_{aa'}^R \right]$, which keeps track of which terms originate from $i\tilde{S}_R$ or \tilde{S}_I , and which contours $a, a' = F/B$ the vertices sit on. This expression agrees, as expected, with that of Keldysh perturbation theory, before disorder averaging; it is given by Eq. (A.10) and illustrated by Fig. A1 in App. A. We then disorder average using standard diagrammatic techniques. For reference purposes, some details of this straightforward exercise are collected in Appendix F.2.

For present purposes, we shall consider only the “self-energy contributions” ($a = a'$) to the Cooperon self energy, and neglect the “vertex contributions” ($a \neq a'$), since above we likewise extracted $\gamma_\varphi^{R/I}$ from the self-energy contributions to the effective action, $\langle \tilde{S}_{R/I} \rangle_{\text{rw}}^{\text{leading,self}}$. After impurity averaging, the Cooperon then satisfies a Dyson equation of standard form, $\bar{\mathcal{C}}_{\mathbf{q}}^{\text{self}}(\omega) = \bar{\mathcal{C}}_{\mathbf{q}}^0(\omega) + \bar{\mathcal{C}}_{\mathbf{q}}^0(\omega) \bar{\Sigma}_{\mathbf{q}}^{\text{self}}(\omega) \bar{\mathcal{C}}_{\mathbf{q}}^{\text{self}}(\omega)$, with standard solution:

$$\bar{\mathcal{C}}_{\mathbf{q}}^{\text{self}}(\omega) = \frac{1}{E_{\mathbf{q}} - i\omega - \bar{\Sigma}_{\mathbf{q}}^{\text{self}}(\omega)}, \quad (12)$$

where $\bar{\Sigma}^{R/I,\text{self}} = \sum_a \bar{\Sigma}_{aa}^{R/I,\text{self}}$, with $\bar{\Sigma}_{\mathbf{q},FF}^{R/I,\text{self}}(\omega) = \left[\bar{\Sigma}_{\mathbf{q},BB}^{R/I,\text{self}}(-\omega) \right]^*$, and

$$\bar{\Sigma}_{\mathbf{q},FF}^{I,\text{self}}(\omega) \equiv -\frac{1}{\hbar} \int (d\bar{\omega})(d\bar{\mathbf{q}}) \coth \left[\frac{\hbar\bar{\omega}}{2T} \right] \text{Im} \left[\bar{\mathcal{L}}_{\bar{\mathbf{q}}}^R(\bar{\omega}) \right] \bar{\mathcal{C}}_{\mathbf{q}-\bar{\mathbf{q}}}^0(\omega - \bar{\omega}), \quad (13a)$$

$$\bar{\Sigma}_{\mathbf{q},FF}^{R,\text{self}}(\omega) \equiv \frac{1}{\hbar} \int (d\bar{\omega})(d\bar{\mathbf{q}}) \left\{ \tanh \left[\frac{\hbar(\varepsilon + \frac{1}{2}\omega - \bar{\omega})}{2T} \right] \frac{1}{2} i \bar{\mathcal{L}}_{\bar{\mathbf{q}}}^R(\bar{\omega}) \right\} \quad (13b)$$

$$\times \left[\overline{\mathcal{C}}_{\mathbf{q}-\bar{\mathbf{q}}}^0(\omega - \bar{\omega}) + [\overline{\mathcal{D}}_{\bar{\mathbf{q}}}^0(\bar{\omega})]^2 \left([\overline{\mathcal{C}}_{\mathbf{q}}^0(\omega)]^{-1} + [\overline{\mathcal{D}}_{\bar{\mathbf{q}}}^0(\bar{\omega})]^{-1} \right) \right].$$

In Eq. (13b), the terms proportional to $(\overline{\mathcal{D}}^0)^2 [(\overline{\mathcal{C}}^0)^{-1} + (\overline{\mathcal{D}}^0)^{-1}]$ stem from the so-called Hikami contributions, for which an electron line changes from $\tilde{G}^{R/A}$ to $\tilde{G}^{A/R}$ to $\tilde{G}^{R/A}$ at the two interaction vertices. As correctly emphasized by AAG¹⁷ and AAV¹⁸, such terms are missed by GZ's approach of averaging only over time-reversed pairs of paths, since they stem from paths that are not time-reversed pairs.

Now, the standard way to define a decoherence rate for a Cooperon of the form (12) is as the “mass” term that survives in the denominator when $\omega = E_{\mathbf{q}} = 0$, i.e. $\gamma_{\varphi}^{\text{self}} = -\overline{\Sigma}_{\mathbf{0}}^{\text{self}}(0) = -2\text{Re} \left[\overline{\Sigma}_{\mathbf{0},FF}^{I+R,\text{self}}(0) \right]$. In this limit the contribution of the Hikami terms vanishes identically, as is easily seen by using the last of Eqs. (4a), and noting that $\text{Re}[i(\overline{\mathcal{D}}^0)^{-1}(\overline{\mathcal{D}}^0)^2(\overline{\mathcal{D}}^0)^{-1}] = \text{Re}[i] = 0$. (The realization of this fact came to us as a surprise, since AAG and AAV had argued that GZ's main mistake was their neglect of Hikami terms^{17,18}, thereby implying that the contribution of these terms is not zero, but essential.) The remaining (non-Hikami) terms of Eq. (13b) agree with the result for $\tilde{\Sigma}$ of AAV¹⁸ and reproduce Eqs. (10) given above, in other words:

$$\gamma_{\varphi}^{\text{self}} = [-\overline{\Sigma}_{\mathbf{0}}^{\text{self}}(0)] = \frac{1}{\tau \hbar} \langle i\tilde{S}_R + \tilde{S}_I \rangle_{\text{rw}}^{\text{leading,self}}. \quad (14)$$

Thus, the Cooperon mass term $-\overline{\Sigma}_{\mathbf{0}}^{\text{self}}(0)$ agrees identically with the coefficient of τ in the leading terms of the averaged effective action of the influence functional. This is no coincidence: it simply reflects the fact that averaging in the exponent amounts to reexponentiating the *average of the first order term* of an expansion of the exponential, while in calculating the self energy one of course *also* averages the first order term of the Dyson equation. It is noteworthy, though, that for the problem at hand, where the unitary limit of the interaction propagator is considered, it suffices to perform this average exclusively over pairs of time-reversed paths — more complicated paths are evidently not needed, in contrast to the expectations voiced by AAG¹⁷ and AAV¹⁸.

The latter expectations do apply, however, if one considers forms of the interaction propagator $\overline{\mathcal{L}}_{\bar{\mathbf{q}}}^R(\bar{\omega})$ more general than the unitary limit of (4a) (i.e. not proportional to $[\overline{\mathcal{D}}_{\bar{\mathbf{q}}}^0(\bar{\omega})]^{-1}$). Then, the Hikami contribution to $\gamma_{\varphi}^{\text{self}} = -\overline{\Sigma}_{\mathbf{0}}^{\text{self}}(0)$ indeed does not vanish; instead, by noting that for $\omega = \mathbf{q} = \gamma_H = 0$ the second line of Eq. (13b) can always be written as $2\text{Re}[\overline{\mathcal{D}}_{\bar{\mathbf{q}}}^0(\bar{\omega})]$, we obtain

$$\begin{aligned} \gamma_{\varphi}^{\text{self}} = & \frac{1}{\hbar} \int (d\bar{\omega})(d\bar{\mathbf{q}}) \left\{ \coth \left[\frac{\hbar\bar{\omega}}{2T} \right] + \tanh \left[\frac{\hbar(\varepsilon - \bar{\omega})}{2T} \right] \right\} \\ & \times \text{Im} \left[\overline{\mathcal{L}}_{\bar{\mathbf{q}}}^R(\bar{\omega}) \right] \frac{2E_{\bar{\mathbf{q}}}^0}{(E_{\bar{\mathbf{q}}}^0)^2 + \bar{\omega}^2}, \end{aligned} \quad (15)$$

which is the form given by AAV¹⁸.

6. Vertex Contributions

Eq. (10b) for $\gamma_\varphi^{I,\text{self}}$ has the deficiency that its frequency integral is *infrared* divergent (for $\bar{\omega} \rightarrow 0$) for the quasi-1 and 2-dimensional cases, as becomes explicit once its $\bar{\mathbf{q}}$ -integral has been performed [as in Eq. (11)]. This problem is often dealt with by arguing that small-frequency environmental fluctuations that are slower than the typical time scale of the diffusive trajectories are, from the point of view of the diffusing electron, indistinguishable from a static field and hence cannot contribute to decoherence. Thus, a low-frequency cutoff γ_φ is inserted by hand into Eqs. (10) [i.e. $\int_0^\infty d\bar{\omega} \rightarrow \int_{\gamma_\varphi}^\infty d\bar{\omega}$], and γ_φ determined selfconsistently. This procedure was motivated in quite some detail by AAG¹⁷, and also adopted by GZ in GZ99³ [see Eq. (11) above]. However, as emphasized by GZ in a subsequent paper, GZ00⁴, it has the serious drawback that it does not necessarily reproduce the correct functional form for the Cooperon in the time domain; e.g., in $\bar{d} = 1$ dimensions, the Cooperon is known¹⁰ to decay as $e^{-a(\tau/\tau_\varphi)^{3/2}}$, i.e. with a nontrivial power in the exponent, whereas a ‘‘Cooperon mass’’ would simply give $e^{-\tau/\tau_\varphi}$.

A cheap fix for this problem would be to take the above idea of a self-consistent infrared cutoff one step further, arguing that the Cooperon will decay as $e^{-\tau\gamma_\varphi^{\text{self}}(\tau)}$, where $\gamma_\varphi^{\text{self}}(\tau)$ is a *time-dependent* decoherence rate, whose time-dependence enters via a time-dependent infrared cutoff. Concretely, using Eqs. (13) and (10), one would write

$$\gamma_\varphi^{\text{self}}(\tau) = 2 \int_{1/\tau}^\infty (d\bar{\omega}) \bar{\omega} \left\{ \coth \left[\frac{\hbar\bar{\omega}}{2T} \right] + \frac{1}{2} \sum_{s=\pm} s \tanh \left[\frac{\hbar(\varepsilon - s\bar{\omega})}{2T} \right] \right\} \times \int \frac{(d\bar{\mathbf{q}})}{\hbar\nu} \frac{1}{(D\bar{\mathbf{q}}^2)^2 + \bar{\omega}^2}. \quad (16)$$

It is straightforward to check [using steps analogous to those used below to obtain Eq. (18)] that in $\bar{d} = 1$ dimensions, the leading long-time dependence is $\gamma_\varphi^{\text{self}}(\tau) \propto \tau^{1/2}$, so that this cheap fix does indeed produce the desired $e^{-a(\tau/\tau_\varphi)^{3/2}}$ behavior.

The merits of this admittedly rather ad hoc cheap fix can be checked by doing a better calculation: It is well-known that the proper way to cure the infrared problems is to include ‘‘vertex contributions’’, having interactions vertices on opposite contours. In fact, the original calculation of AAK¹⁰ in effect did just that. Likewise, although GZ neglected vertex contributions in GZ99³, they subsequently included them in GZ00⁴, exploiting the fact that in the influence functional approach this is as straightforward as calculating the self-energy terms: one simply has to include the contributions to $\langle i\tilde{S}_R/\tilde{S}_I \rangle_{\text{rw}}$ of the vertex function $-f^{\text{vert}}$ in Eq. (7), too. The leading contribution comes from the first term in Eq. (9b), to be called $\langle i\tilde{S}_R/\tilde{S}_I \rangle_{\text{rw}}^{\text{leading,vert}}$, which gives a contribution identical to $\langle i\tilde{S}_R/\tilde{S}_I \rangle_{\text{rw}}^{\text{leading,self}}$, but multiplied by an extra factor of $-\frac{\sin(\bar{\omega}\tau)}{\bar{\omega}\tau}$ under the integral. Thus, if we collect all contributions to Eq. (7) that have been termed ‘‘leading’’, our final result for the

14 *Jan von Delft*

averaged effective action is $\frac{1}{\hbar}(i\tilde{S}_R + \tilde{S}_I)_{\text{rw}}^{\text{leading}} \equiv F_{\bar{d}}(\tau)$, with

$$F_{\bar{d}}(\tau) = \tau \int (d\bar{\omega}) \bar{\omega} \left\{ \coth \left[\frac{\hbar\bar{\omega}}{2T} \right] + \tanh \left[\frac{\hbar(\varepsilon - \bar{\omega})}{2T} \right] \right\} \left(1 - \frac{\sin(\bar{\omega}\tau)}{\bar{\omega}\tau} \right) \times \int \frac{(d\bar{q})}{\hbar\nu} \frac{1}{(D\bar{q}^2)^2 + \bar{\omega}^2}. \quad (17)$$

This is our main result: an expression for the decoherence function $F_{\bar{d}}(\tau)$ that is both ultraviolet and infrared convergent (as will be checked below), due to the $(\coth + \tanh)$ and $(1 - \sin)$ -combinations, respectively. Comparing this to Eqs. (16), we note that $F_{\bar{d}}(\tau)$ has precisely the same form as $\tau\gamma_{\varphi}^{\text{self}}(\tau)$, except that the infrared cutoff now occurs in the $\int(d\bar{\omega})$ integrals through the $(1 - \sin)$ combination. Thus, the result of including vertex contributions fully confirms the validity of using the cheap fix replacement $\int_0(d\bar{\omega}) \rightarrow \int_{1/\tau}(d\bar{\omega})$, the only difference being that the cutoff function is smooth instead of sharp (which will somewhat change the numerical prefactor of τ_{φ}).

It turns out to be possible to also obtain Eq. (17) [and in addition *all* the “subleading” terms of Eq. (7)] by purely diagrammatic means: to this end, one has to set up and solve a Bethe-Salpeter equation. This is a Dyson-type equation, but with interaction lines transferring energies between the upper and lower contours, so that a more general Cooperon $\bar{C}_{\mathbf{q}}^{\varepsilon}(\Omega_1, \Omega_2)$, with three frequency variables, is needed. Such an analysis will be published in DMSA-II²⁰.

To wrap up our rederivation of standard results, let us perform the integrals in Eq. (17) for $F_{\bar{d}}(\tau)$ for the quasi-1-dimensional case $\bar{d} = 1$. The $\int(d\bar{q})$ -integral yields $\bar{\omega}^{-3/2}\sqrt{D/2}/(\sigma_1\hbar/e^2)$. To do the frequency integral, we note that since the $(\coth + \tanh)$ -combination constrains the relevant frequencies to be $|\hbar\bar{\omega}| \lesssim T$, the integral is dominated by the small-frequency limit of the integrand, in which $\coth(\hbar\bar{\omega}/2T) \simeq 2T/\hbar\bar{\omega}$, whereas \tanh , making a subleading contribution, can be neglected. The frequency integral then readily yields

$$F_1(\tau) = \frac{4}{3\sqrt{\pi}} \frac{T\tau/\hbar}{g_1(\sqrt{D}\tau)} \equiv \frac{4}{3\sqrt{\pi}} \left(\frac{\tau}{\tau_{\varphi}} \right)^{3/2}, \quad (18)$$

so that we correctly obtain the known $e^{-a(\tau/\tau_{\varphi})^{3/2}}$ decay for the Cooperon. Here $g_{\bar{d}}(L) = (\hbar/e^2)\sigma_{\bar{d}}L^{\bar{d}-2}$ represents the dimensionless conductance, which is $\gg 1$ for good conductors. The second equality in Eq. (18) defines τ_{φ} , where we have exploited the fact that the dependence of F_1 on τ is a simple $\tau^{3/2}$ power law, which we made dimensionless by introducing the decoherence time τ_{φ} . [Following AAG¹⁷, we purposefully arranged numerical prefactors such that none occur in the final Eq. (19) for τ_{φ} below.] Setting $\tau = \tau_{\varphi}$ in Eq. (18) we obtain the self-consistency relation and solution (cf. Eq. (2.38a) of AAG¹⁷):

$$\frac{1}{\tau_{\varphi}} = \frac{T/\hbar}{g_{\bar{d}}(\sqrt{D}\tau_{\varphi})}, \quad \Rightarrow \quad \tau_{\varphi} = \left(\frac{\hbar^2\sigma_1}{Te^2\sqrt{D}} \right)^{2/3}. \quad (19)$$

The second relation is the celebrated result of AAK, which diverges for $T \rightarrow 0$. This completes our recalculation of $\gamma_\varphi^{\text{AAK}}$ using GZ's influence functional approach.

Eq. (18) can be used to calculate the magnetoconductance for $\bar{d} = 1$ via

$$\sigma_{\text{DC}}^{\text{WL}}(H) = -\frac{\sigma_{\text{DC}}^{\text{Drude}}}{\pi\nu\hbar} \int_0^\infty d\tau \tilde{C}_{r=0}^0(\tau) e^{-F_1(\tau)}. \quad (20)$$

(Here, of course, we have to use $\gamma_H \neq 0$ in $\tilde{C}_{r=0}^0(\tau)$). Comparing the result to AAK's result for the magnetoconductance (featuring an Ai' function for $\bar{d} = 1$), one finds qualitatively correct behavior, but deviations of up to 20% for small magnetic fields H . The reason is that our calculation was not sufficiently accurate to obtain the correct numerical prefactor in Eq. (18). [GZ did not attempt to calculate it accurately, either]. It turns out (see MDSA-I²⁰) that if the averaging over random walks of Eq. (6) is done more accurately, following Marquardt's suggestion of ensuring that the random walks are *self-returning*, the prefactor changes in such a way that the magnetoconductance agrees with that of AAK to within an error of at most 4%. Another improvement that occurs for this more accurate calculation is that the results are well-behaved also for finite γ_H , which is not the case for our present Eq. (10a): for $\gamma_H \neq 0$, the real part of the square brackets contains a term proportional to $\gamma_H/E_{\bar{q}}^0$, which contains an infrared divergence as $\bar{q} \rightarrow 0$. This problem disappears if the averaging over paths is performed more accurately, see MDSA-I²⁰.

7. Discussion and Summary

We have shown [in Apps. B to D, as summarized in App. A] that GZ's influence functional approach to interacting fermions is sound in principle, and that standard results from Keldysh diagrammatic perturbation theory can be extracted from it, such as the Feynman rules, the first order terms of a perturbation expansion in the interaction, and the Cooperon self energy.

Having established the equivalence between the two approaches in general terms, we were able to identify precisely why GZ's treatment of the Pauli factor ($\tilde{\delta} - 2\tilde{\rho}^0$) occurring \tilde{S}_R was problematic: representing it in the time domain as $\tanh[\tilde{h}_0(t)/2T]$, they assumed it not to change during diffusive motion along time-reversed paths. However, they thereby neglected the physics of recoil, i.e. energy changes of the diffusing electrons by emission or absorption of photons. As a result, GZ's calculation yielded the result $\langle i\tilde{S}_R^{\text{GZ}} \rangle_{\text{rw}} = 0$. The ultraviolet divergence in $\langle \tilde{S}_I^{\text{GZ}} \rangle_{\text{rw}}$, which in diagrammatic approaches is cancelled by terms involving a tanh function, was thus left uncanceled, and instead was cut off at $\bar{\omega} \simeq 1/\tau_{\text{el}}$, leading to the conclusion that $\gamma_\varphi^{\text{GZ}}(T \rightarrow 0)$ is finite.

In this review, we have shown that the physics of recoil can be included very simply by passing from the time to the frequency representation, in which ($\tilde{\delta} - 2\tilde{\rho}^0$) is represented by $\tanh[\tilde{h}(\varepsilon - \bar{\omega})/2T]$. Then $\langle i\tilde{S}_R \rangle_{\text{rw}}$ is found *not* to equal to zero; instead, it cancels the ultraviolet divergence of $\langle \tilde{S}_I \rangle_{\text{rw}}$, so that the total rate $\gamma_\varphi = \gamma_\varphi^I + \gamma_\varphi^R$ reproduces the classical result $\gamma_\varphi^{\text{AAK}}$, which goes to zero for $T \rightarrow 0$.

Interestingly, to obtain this result it was sufficient to average only over pairs of time-reversed paths; more complicated paths, such as represented by Hikami terms, are evidently not needed. (However, this simplification is somewhat fortuitous, since it occurs only when considering the unitary limit of the interaction propagator; for more general forms of the latter, the contribution of Hikami terms *is* essential, as emphasized by AAG and AAV^{17,18}.)

The fact that the standard result for γ_φ *can* be reproduced from the influence functional approach is satisfying, since this approach is appealingly clear and simple, not only conceptually, but also for calculating γ_φ . Indeed, once the form of the influence functional (2) has been properly derived (wherein lies the hard work), the calculation of $\langle i\tilde{S}_R + \tilde{S}_I \rangle_{\text{rw}}$ requires little more than knowledge of the distribution function for a random walk and can be presented in just a few lines [Sec.4]; indeed, the algebra needed for the key steps [evaluating Eq. (7) to get the first terms of (9), then finding (10) and (17)] involves just a couple of pages.

We expect that the approach should be similarly useful for the calculation of other physical quantities governed by the long-time, low-frequency behavior of the Cooperon, provided that one can establish unambiguously that it suffices to include the contributions of time-reversed paths only — because Hikami-like terms, though derivable from the influence functional approach too, can not easily be evaluated in it; for the latter task, diagrammatic impurity averaging still seems to be the only reliable tool.

Acknowledgements

I dedicate this review to Vinay Ambegaokar on the occasion of his 70th birthday. He raised and sustained my interest in the present subject by telling me in 1998: “I believe GZ have a problem with detailed balance”, which turned out to be right on the mark, in that recoil and detailed balance go hand in hand. I thank D. Golubev and A. Zaikin, and, in equal measure, I. Aleiner, B. Altshuler, M. Vavilov, I. Gornyi, R. Smith and F. Marquardt, for countless patient and constructive discussions, which taught me many details and subtleties of the influence functional and diagrammatic approaches, and without which I would never have been able to reach the conclusions presented above. I also acknowledge illuminating discussions with J. Imry, P. Kopietz, J. Kroha, A. Mirlin, H. Monien, A. Rosch, I. Smolyarenko, G. Schön, P. Wölfle and A. Zawadowski. Finally, I acknowledge the hospitality of the centers for theoretical physics in Trieste, Santa Barbara, Aspen, Dresden and the Newton Institute in Cambridge, where some of this work was performed. This research was supported in part by SFB631 of the DFG, and by the National Science Foundation under Grant No. PHY99-07949.

Appendix A. Outline of GZ’s Influence Functional Approach

Without dwelling on details of derivations, we outline in this appendix how the influence functional presented in Sec. 2 is derived. (A similar summary is contained

in a previous paper by this author^{15,23}; however, it is incomplete, in that we have introduced important improvements since.) Before we start, let us point out the two main differences between our formulation and that of GZ:

(i) GZ formulated the Cooperon propagator in terms of a coordinate-momentum path integral $\int \mathcal{D}\mathbf{R} \int \mathcal{D}\mathbf{P}$, in which $(\tilde{\delta} - 2\tilde{\rho}^0)$ is represented as $[1 - 2n_0(\tilde{h}_0)] = \tanh(\tilde{h}_0/2T)$, where the free-electron energy $\tilde{h}_0[\mathbf{R}(t_a), \mathbf{P}(t_a)]$ depends on position and momentum. This formulation makes it difficult to treat the Pauli factor with sufficient accuracy to include recoil. In contrast, we achieve the latter by using a coordinates-only version $\int \tilde{\mathcal{D}}' \mathbf{R}$, in which exact relations between noninteracting Green's functions make an accurate treatment of the Pauli factor possible, upon Fourier-transforming the effective action to the frequency domain.

(ii) GZ effectively performed thermal weighting at an initial time t_0 that is not sent to $-\infty$, but (in the notation of the main text) is set to $t_0 = -\tau/2$; with the latter choice, it is impossible to correctly reproduce the first (or higher) order terms of a perturbation expansion. GZ's claim in GZ00⁴ that they have reproduced these is incorrect (see end of App. C.3), since their time integrals have $-\tau/2$ as the lower limit, whereas in the Keldysh approach they run from $-\infty$ to $+\infty$. We have found that with some (but not much) extra effort it *is* possible to properly take the limit $t_0 \rightarrow -\infty$, to correctly recover the first order perturbation terms [App. C.3] and to express the conductivity in a form containing thermal weighting in the energy domain explicitly in the form of a factor $\int (d\varepsilon)[-n'_0(\hbar\varepsilon)]\tilde{P}^\varepsilon$, where \tilde{P}^ε is an energy-dependent path integral, obtained by suitable Fourier transformation [App. C.4].

A.1. Outline of Derivation of Influence Functional

Consider a disordered system of interacting fermions, with Hamiltonian $\hat{H} = \hat{H}_0 + \hat{H}_i$:

$$\hat{H}_0 = \int dx \hat{\psi}^\dagger(x) h_0(x) \hat{\psi}(x), \quad (\text{A.1a})$$

$$\hat{H}_i = \frac{e^2}{2} \int dx_1 dx_2 : \hat{\psi}^\dagger(x_1) \hat{\psi}(x_1) : \tilde{V}_{12}^{\text{int}} : \hat{\psi}^\dagger(x_2) \hat{\psi}(x_2) : \quad (\text{A.1b})$$

Here $\int dx = \sum_\sigma \int d\mathbf{r}$, and $\hat{\psi}(x) \equiv \hat{\psi}(\mathbf{r}, \sigma)$ is the electron field operator for creating a spin- σ electron at position \mathbf{r} , with the following expansion in terms of the exact eigenfunctions $\psi_\lambda(x)$ of $h_0(x) = \frac{\hbar^2}{2m} \nabla_{\mathbf{r}}^2 + V_{\text{imp}}(\mathbf{r}) - \mu$:

$$\hat{\psi}(x) = \sum_\lambda \psi_\lambda(x) \hat{c}_\lambda, \quad [h_0(x) - \xi_\lambda] \psi_\lambda(x) = 0. \quad (\text{A.2})$$

The interaction potential $\tilde{V}_{12}^{\text{int}} = \tilde{V}^{\text{int}}(|\mathbf{r}_1 - \mathbf{r}_2|)$ acts between the normal-ordered densities at \mathbf{r}_1 and \mathbf{r}_2 . The Kubo formula for the DC conductivity of a d -dimensional conductor gives

$$\sigma_{\text{DC}} = -\text{Re} \left[\lim_{\omega_0 \rightarrow 0} \frac{1}{d\omega_0} \sum_{\sigma_1} \int dx_2 \mathbf{j}_{11'} \cdot \mathbf{j}_{22'} \tilde{J}_{11',22}(\omega_0) \Big|_{x_1=x_{1'}} \right], \quad (\text{A.3a})$$

$$\tilde{J}_{11',22'}(\omega_0) = \int_{-\infty}^{\infty} dt_{12} e^{i\omega_0 t_{12}} \theta(t_{12}) \tilde{C}_{[11',22']}, \quad (\text{A.3b})$$

$$\tilde{C}_{[11',22']} \equiv \frac{1}{\hbar} \langle [\hat{\psi}^\dagger(t_1, x_{1'}) \hat{\psi}(t_1, x_1), \hat{\psi}^\dagger(t_2, x_{2'}) \hat{\psi}(t_2, x_2)] \rangle_H, \quad (\text{A.3c})$$

where $\mathbf{j}_{11'} \equiv \frac{-ie\hbar}{2m}(\nabla_1 - \nabla_{1'})$ and a uniform applied electric field $\mathbf{E}(\omega_0)$ was represented using a uniform, time-dependent vector potential, $\mathbf{E}(\omega_0) = i\omega_0 \mathbf{A}(\omega_0)$. A path integral representation for $\tilde{C}_{[11',22']}$ can be derived using the following strategy, adapted from GZ99³: (1) introduce a source term into the Hamiltonian, in which an artificial source field $\tilde{v}_{2'2}$ couples to $\hat{\psi}^\dagger(t_2, x_{2'}) \hat{\psi}(t_2, x_2)$, and write $\tilde{C}_{[11',22]}$ as the linear response to the source field $\tilde{v}_{2'2}$ of the single-particle density matrix $\tilde{\rho}_{11'} = \langle \hat{\psi}^\dagger(t_1, x_{1'}) \hat{\psi}(t_1, x_1) \rangle_H$. (2) Decouple the interaction using a Hubbard-Stratonovitch transformation, thereby introducing a functional integral $\langle \dots \rangle_V$ over real scalar fields $V_{F/B}$, the so-called “interaction fields”, defined on the forward and backward Keldysh contours, respectively; these then constitute a dynamic, dissipative environment with which the electrons interact. (3) Derive an equation of motion for $\tilde{\rho}_{11'}^V$, the single-particle density matrix for a given, fixed configuration of the fields $V_{F/B}$, and linearize it in $\tilde{v}_{2'2}$, to obtain an equation of motion for the linear response $\delta\tilde{\rho}_{11'}^V(t)$ to the source field. (4) Formally integrate this equation of motion by introducing a path integral $\int \tilde{\mathcal{D}}'(\mathbf{R})$ over the coordinates of the single degree of freedom associated with the single-particle density matrix $\delta\tilde{\rho}_{11'}^V$. (5) Use the RPA-approximation to bring the effective action S_V that governs the dynamics of the fields $V_{F/B}$ into a quadratic form. (6) Neglect the effect of the interaction on the single-particle density matrix wherever it occurs in the exponents occurring under the path integral $\int \tilde{\mathcal{D}}' \mathbf{R}$, i.e. replace $\tilde{\rho}_{ij}^V$ there by the free single-particle density matrix

$$\tilde{\rho}_{ij}^0 = \langle \hat{\psi}^\dagger(x_j) \hat{\psi}(x_i) \rangle_0 = \sum_{\lambda} \psi_{\lambda}^*(x_j) \psi_{\lambda}(x_i) n_0(\xi_{\lambda}), \quad (\text{A.4})$$

where thermal averaging is performed using $\langle \hat{O} \rangle_0 = \text{Tr}[e^{-\beta \hat{H}_0} \hat{O}] / \text{Tr}[e^{-\beta \hat{H}_0}]$. (7) Perform the functional integral $\langle \dots \rangle_V$ (which steps (5) and (6) have rendered Gaussian) over the fields $V_{F/B}$; the environment is thereby integrated out, and its effects on the dynamics of the single particle are encoded in an influence functional of the form $e^{-i(\tilde{S}_R + \tilde{S}_I)}$. The final result of this strategy is that $\mathbf{j}_{22'} \cdot \mathbf{j}_{11'} \tilde{C}_{[11',22]}$ can be written as [cf. (II.49)]

$$\int dx_2 \mathbf{j}_{22'} \cdot \mathbf{j}_{11'} \tilde{C}_{[11',22]} = \int dx_{0_F, \bar{0}_B} \tilde{\rho}_{0_F \bar{0}_B}^0 \int_{0_F}^{1_F} \int_{\bar{0}_B}^{1'_B} \tilde{\mathcal{D}}'(\mathbf{R}) \times \frac{1}{\hbar} \left\{ \left[\hat{\mathbf{j}}(t_{2_F}) - \hat{\mathbf{j}}(t_{2_B}) \right] \hat{\mathbf{j}}(t_1) e^{-[i\tilde{S}_R + \tilde{S}_I](t_1, t_0)/\hbar} \right. \quad (\text{A.5})$$

where $\int_{j_F}^{i_F} \int_{j_B}^{i_B} \tilde{\mathcal{D}}(\mathbf{R})$ is used as a shorthand for the following forward and backward path integral between the specified initial and final coordinates and times:

$$\begin{aligned} \int_{j_F}^{i_F} \int_{j_B}^{i_B} \tilde{\mathcal{D}}(\mathbf{R}) \dots \equiv & \int_{\mathbf{R}^F(t_j^F)=\mathbf{r}_j^F}^{\mathbf{R}^F(t_i^F)=\mathbf{r}_i^F} \tilde{\mathcal{D}}' \mathbf{R}^F(t_3^F) e^{i\tilde{S}_0^F(t_i^F, t_j^F)/\hbar} \\ & \times \int_{\mathbf{R}^B(t_j^B)=\mathbf{r}_j^B}^{\mathbf{R}^B(t_i^B)=\mathbf{r}_i^B} \tilde{\mathcal{D}}' \mathbf{R}^B(t_3^B) e^{-i\tilde{S}_0^B(t_i^B, t_j^B)/\hbar} \dots \end{aligned} \quad (\text{A.6})$$

The complex weighting functional $e^{i(\tilde{S}_0^F - \tilde{S}_0^B)}$ occurring therein involves the action for a single, free electron. Expression (A.5) has a simple interpretation: thermal averaging with $\tilde{\rho}_{00}^0$ at time t_0 (for which we take the limit $\rightarrow -\infty$) is followed by propagation in the presence of interactions (described by $e^{-[i\tilde{S}_R + \tilde{S}_I]}$) from time t_0 up to time t_1 , with insertions of current vertices $\hat{\mathbf{j}}(t_{2_a})$ at time t_2 on either the upper or lower Keldysh contour, and $\hat{\mathbf{j}}(t_1)$ at the final time t_1 .

For the purpose of calculating the Cooperon propagator, we now make the following approximation in Eq. (A.5) [referred to as “approximation (ii)” in App. B]: For the first or second terms, for which the current vertex occurs at time t_{2_a} on contour $\tilde{a} = F$ or B respectively, we neglect all interaction vertices that occur on the *same* contour \tilde{a} at earlier times t_{3_a} or $t_{4_a} \in [t_0, t_{2_a}]$; however, for the opposite contour containing no current vertex, we include interaction vertices for *all* times $\in [t_0, t_1]$, with $t_0 \rightarrow -\infty$. [This turns out to be essential to obtain, after Fourier transforming, the proper thermal weighting factor $[-n'_0(\hbar\varepsilon)]$ occurring in Eq. (1a), see App. C.4.] The rationale for this approximation is that, in diagrammatic language, this approximation retains only those diagrams for which *both* current vertices $\mathbf{j}_{22'}$ and $\mathbf{j}_{11'}$ are always sandwiched between a \tilde{G}^R - and a \tilde{G}^A -function; these are the ones relevant for the Cooperon. The contributions thereby neglected correspond to the so-called “interaction corrections”. [If one so chooses, they latter *can* be kept track of, though.]

This approximation (ii) is much weaker than the one used by GZ at a similar point in their calculation: to simplify the thermal weighting factor describing the initial distribution of electrons, namely to obtain the explicit factor ρ_0 in Eq. (49) of GZ99³, they set $t_0 \rightarrow t_2$ (their t' corresponds to our t_2), and thereby perform thermal weighting at time t_2 , instead of at $-\infty$. As a consequence, in their analysis all time integrals have t_2 as lower limit, which means that (contrary to their claims in GZ00⁴) they did not correctly reproduce the Keldysh first order perturbation expansion for $\tilde{C}_{[11', 22']}$, in which all time integrals run to $-\infty$. A detailed discussion of this matter is given at the end of App. C.3. [Contrary to our initial expectations, but in agreement with those of GZ, it turns out, though, that the choice of t_0 does not have any implications for the calculation of τ_φ , which does not depend on whether one chooses $t_0 = t_2$ or sends it to $-\infty$.]

Having made the above approximation (ii), the effective action $(i\tilde{S}_R + \tilde{S}_I)$ occurring in Eq. (A.5) is found to have the following form (we use the notation $i\tilde{S}_R/\tilde{S}_I$

20 *Jan von Delft*

to write two equations with similar structure in one line, and upper or lower terms in curly brackets refer to the first or second case):

$$[i\tilde{S}_R/\tilde{S}_I](t_1, t_0) \equiv \sum_{aa'} \int_{t_0}^{t_1} dt_3 \int_{t_0}^{t_1} dt_4 (i\tilde{L}^R/\tilde{L}^I)_{3_a 4_{a'}} , \quad (\text{A.7})$$

$$(i\tilde{L}^R/\tilde{L}^I)_{3_F 4_F} = -\frac{1}{2}i \theta_{34} \tilde{\delta}_{3_F \bar{3}_F} \left\{ \begin{array}{l} [\tilde{\delta} - 2\tilde{\rho}^0]_{4_F \bar{4}_F} \\ \tilde{\delta}_{4_F \bar{4}_F} \end{array} \right\} \tilde{\mathcal{L}}_{3_F \bar{4}_F}^{R/K} , \quad (\text{A.8a})$$

$$(i\tilde{L}^R/\tilde{L}^I)_{3_B 4_F} = \frac{1}{2}i \theta_{34} \left\{ \begin{array}{l} [\tilde{\delta} - 2\tilde{\rho}^0]_{4_F \bar{4}_F} \\ \tilde{\delta}_{4_F \bar{4}_F} \end{array} \right\} \tilde{\mathcal{L}}_{3_B \bar{4}_F}^{R/K} \tilde{\delta}_{\bar{3}_B 3_B} , \quad (\text{A.8b})$$

$$(i\tilde{L}^R/\tilde{L}^I)_{3_F 4_B} = \mp \frac{1}{2}i \theta_{34} \tilde{\delta}_{3_F \bar{3}_F} \tilde{\mathcal{L}}_{4_B \bar{3}_F}^{A/K} \left\{ \begin{array}{l} [\tilde{\delta} - 2\tilde{\rho}^0]_{4_B \bar{4}_B} \\ \tilde{\delta}_{4_B \bar{4}_B} \end{array} \right\} , \quad (\text{A.8c})$$

$$(i\tilde{L}^R/\tilde{L}^I)_{3_B 4_B} = \pm \frac{1}{2}i \theta_{34} \tilde{\mathcal{L}}_{4_B \bar{3}_B}^{A/K} \tilde{\delta}_{\bar{3}_B 3_B} \left\{ \begin{array}{l} [\tilde{\delta} - 2\tilde{\rho}^0]_{4_B \bar{4}_B} \\ \tilde{\delta}_{4_B \bar{4}_B} \end{array} \right\} . \quad (\text{A.8d})$$

Here $\tilde{\delta}_{\bar{i}i} = \delta_{\sigma_i \sigma_i} \delta(\mathbf{r}_{\bar{i}} - \mathbf{r}_i)$ and $(\tilde{\mathcal{L}}^{R,A,K})_{\bar{i}a \bar{j}a'} = (\tilde{\mathcal{L}}^{R,A,K})(t_{i_a} - t_{j_{a'}}, \mathbf{r}_{\bar{i}}^a(t_{i_a}) - \mathbf{r}_{\bar{j}}^{a'}(t_{j_{a'}}))$ are the standard retarded, advanced and Keldysh interaction propagators. For each occurrence in Eqs. (A.8) of a pair of indices, one without bar, one with, e.g. 4_a and $\bar{4}_a$, the corresponding coordinates x_4^a and $x_{\bar{4}}^a$ are both associated with the *same* time t_4 , and integrated over, $\int dx_4^a dx_{\bar{4}}^a$, in the path integral $\int \mathcal{D}'(\mathbf{R})$. (This somewhat unusual aspect of the “coordinates-only” path integral used in our approach is discussed in explicit detail in App. D.4; it is needed to account for the fact that the density-matrix $\tilde{\rho}^0$ is non-local in space, and arises upon explicitly performing the $\int \mathcal{D}\mathbf{P}$ momentum path integral in GZ’s formulation.) The $\tilde{\delta}_{\bar{i}i}$ functions on the right hand side of Eqs. (A.8) will kill one of these double coordinate integrations at time t_i .

Eqs. (A.7) and (A.8) are the main result of our rederivation of the influence functional approach. They are identical in structure (including signs and prefactors) to the corresponding expressions derived by GZ (Eqs. (68) and (69) of GZ99³), as can be verified by using the relations

$$-e^2 \tilde{R}_{ij} = \tilde{\mathcal{L}}_{ij}^R = \tilde{\mathcal{L}}_{ji}^A, \quad e^2 \tilde{I}_{ij} = e^2 \tilde{I}_{ji} = -\frac{1}{2}i \tilde{\mathcal{L}}_{ij}^K, \quad (\text{A.9})$$

to relate our interaction propagators $\tilde{\mathcal{L}}_{ij}$ to the functions R_{ij} and I_{ij} used by GZ. However, whereas Eqs. (68) and (69) of GZ99³ are written in a mixed coordinate-momentum representation in which it is difficult to treat the Pauli factors $(\tilde{\delta} - 2\tilde{\rho}^0)$ sufficiently accurately, our expressions (A.8) are formulated in a coordinates-only version. Formally, the two representations are fully equivalent. The key advantage of the latter, though, is that passing to a coordinate-frequency representation (which can be done *before* disorder averaging, allows us to sort out the fate of $(\tilde{\delta} - 2\tilde{\rho}^0)$, as discussed in Sec. A.3 [and extensively in App. B.6.2].

A.2. Cooperon Self Energy before Disorder Averaging

(a)

(b)

(c)

Fig. A1. First order contributions to the irreducible self energy of the Cooperon, illustrating Eqs. (A.10). The arrows associated with each factor \tilde{G}_{ij} or $\tilde{\mathcal{L}}_{ij}$ in Eqs. (A.10) are drawn to point from the second index to the first (j to i). Filled double dots denote the occurrence of a factor $(\tilde{\delta} - 2\tilde{\rho})_{4_F \bar{4}_F}$ on the upper contour or $(\tilde{\delta} - 2\tilde{\rho})_{\bar{4}_B 4_B}$ on the lower contour. Bars on filled dots are used to indicate the barred indices to which the interaction lines depicting $\tilde{\mathcal{L}}_{\bar{i}j}$ are connected. Both filled and open single dots indicate a delta function $\tilde{\delta}$; the open dots stand for delta functions that have been inserted to exhaust dummy integrations, as discussed after Eqs. (A.8) [and, in more detail, in Sec. 6.1]. The diagrams in (b) and (c) coincide precisely with those obtained by standard Keldysh diagrammatic perturbation theory for the Cooperon self energy, as depicted, e.g., in Fig. 2 of Ref. ¹⁸. (There, impurity lines needed for impurity averaging are also depicted; in the present figure, impurity averaging has not yet been performed.)

From the formalism outlined above, it is possible to recover the standard results of diagrammatic Keldysh perturbation theory, *before disorder averaging*, by expanding the path integral (A.5) in powers of the effective action $\frac{1}{\hbar}(i\tilde{S}_R + \tilde{S}_I)$. For example, using Eqs. (A.8) [and being sufficiently careful with signs, see App. B.6.1] one readily obtains the following expressions for Cooperon self energy $\tilde{\Sigma}^{R/I} = \sum_{aa'} \tilde{\Sigma}_{aa'}^{R/I}$,

22 *Jan von Delft*

summarized diagrammatically in Fig. A1:

$$\left(\tilde{\Sigma}_{FF}^{R/I}\right)_{\bar{4}_B 3_B}^{3_F \bar{4}_F} = -\frac{i\hbar}{2} (\tilde{G}^{K/R})_{3_F \bar{4}_F} \tilde{G}_{\bar{4}_B 3_B}^A (\tilde{\mathcal{L}}^R / \tilde{\mathcal{L}}^K)_{3_F \bar{4}_F}, \quad (\text{A.10a})$$

$$\left(\tilde{\Sigma}_{BF}^{R/I}\right)_{\bar{4}_B 3_B}^{3_F \bar{4}_F} = -\frac{i\hbar}{2} (\tilde{G}^{K/R})_{3_F \bar{4}_F} \tilde{G}_{\bar{4}_B 3_B}^A (\tilde{\mathcal{L}}^R / \frac{1}{2} \tilde{\mathcal{L}}^K)_{3_B \bar{4}_F}, \quad (\text{A.10b})$$

$$\left(\tilde{\Sigma}_{FB}^{R/I}\right)_{\bar{4}_B 3_B}^{3_F \bar{4}_F} = -\frac{i\hbar}{2} \tilde{G}^{R, 3_F \bar{4}_F} (\tilde{G}^{K/A})_{\bar{4}_B 3_B} (\tilde{\mathcal{L}}^A / \frac{1}{2} \tilde{\mathcal{L}}^K)_{\bar{4}_B 3_B}^{3_F}, \quad (\text{A.10c})$$

$$\left(\tilde{\Sigma}_{BB}^{R/I}\right)_{\bar{4}_B 3_B}^{3_F \bar{4}_F} = -\frac{i\hbar}{2} \tilde{G}^{R, 3_F \bar{4}_F} (\tilde{G}^{K/A})_{\bar{4}_B 3_B} (\tilde{\mathcal{L}}^A / \tilde{\mathcal{L}}^K)_{\bar{4}_B 3_B}. \quad (\text{A.10d})$$

To obtain this, we exploited the fact that every vertex occurring in the effective action is sandwiched between retarded propagators if it sits on the upper contour, and advanced ones on the lower contour. The Keldysh functions arise from using some exact identities, valid (before impurity averaging) in the coordinate-time representation: depending on whether a vertex at time $t_{4_a'}$ sits on the forward (time-ordered) or backward (anti-time-ordered) contour ($a' = F/B$), the factor $(\tilde{\delta} - 2\tilde{\rho}^0) \tilde{\mathcal{L}}^{R/A}$ occurring in $\tilde{L}_{aa'}^R$ is sandwiched as follows (on the left hand sides below, a coordinate integration $\int dx_{4_a'}$ over the un-barred variable at vertex 4 is implied):

$$\left[\tilde{G}_{i_F 4_F}^R (\tilde{\delta} - 2\tilde{\rho}^0)_{4_F \bar{4}_F}\right] \tilde{\mathcal{L}}_{34_F}^R \tilde{G}_{\bar{4}_F j_F}^R \rightarrow \tilde{G}_{i_F 4_F}^K (\bar{\varepsilon} - \bar{\omega}) \tilde{\mathcal{L}}_{34_F}^R (\bar{\omega}) \tilde{G}_{\bar{4}_F j_F}^R (\bar{\varepsilon}), \quad (\text{A.11a})$$

$$\tilde{G}_{\bar{j}_B \bar{4}_B}^A \tilde{\mathcal{L}}_{\bar{4}_B 3}^A \left[(\tilde{\delta} - 2\tilde{\rho}^0)_{\bar{4}_B 4_B} \tilde{G}_{\bar{4}_B \bar{i}_B}^A\right] \rightarrow -\tilde{G}_{\bar{j}_B \bar{4}_B}^A (\bar{\varepsilon}) \tilde{\mathcal{L}}_{\bar{4}_B 3}^A (\bar{\omega}) \tilde{G}_{\bar{4}_B \bar{i}_B}^K (\bar{\varepsilon} - \bar{\omega}) \quad (\text{A.11b})$$

The left- and right-hand sides are written in the time and frequency domains, respectively. To obtain Keldysh functions from the left-hand side expressions, we exploit the fact that the upper or lower contours are time- or anti-time-ordered to add an extra $-\tilde{G}^{A/R} = 0$, and then exploited Eq. (5a) to obtain a factor $\pm \tilde{G}^K$ (see Sec. B.6.2).

A.3. Thermal Averaging

It remains to figure out how the thermal weighting in Eq. (1a) can be derived from our general path integral expression Eq. (A.5). This is a standard, if nontrivial, exercise in Fourier transformation, carried out (along the lines of a similar analysis by AAK¹⁰) in App. C.4. The result is an equation for the conductivity similar to but more general than Eq. (1), with $\int_0^\infty d\tau \tilde{P}_{21', \text{eff}}^{12', \varepsilon}(\tau)$ replaced by $\int_0^\infty d\tau_{12} \tilde{P}_{21', \text{eff}}^{12', \varepsilon}(\tau_{12})$, involving a slightly more complicated path integral [Eq. (C.21)], defined as

$$\tilde{P}_{21', \text{eff}}^{12', \varepsilon}(\tau) = \int_{-\infty}^{\infty} d\bar{\tau} e^{i\bar{\tau}\varepsilon} \int_{\mathbf{R}^F(-\frac{\bar{\tau}}{2}-\frac{\bar{\tau}}{2})=\mathbf{r}_{2'}}^{\mathbf{R}^F(\frac{\bar{\tau}}{2})=\mathbf{r}_1} \int_{\mathbf{R}^B(-\frac{\bar{\tau}}{2}+\frac{\bar{\tau}}{2})=\mathbf{r}_2}^{\mathbf{R}^B(\frac{\bar{\tau}}{2})=\mathbf{r}_{1'}} \tilde{\mathcal{D}}'(\mathbf{R}) e^{-[i\bar{S}_R + \bar{S}_I]/\hbar}. \quad (\text{A.12})$$

Note that the duration of the forward and backward paths differs by a time $\bar{\tau}$, in contrast to the path integral (1b) used in the main text. The combination $\int d\varepsilon \int d\bar{\tau}$

of integrals from Eqs. (1a) and (A.12) have the effect of fixing²¹ the average energy of the forward and backward trajectories to be close to the Fermi energy, with energy spread of roughly $\pm T$ (see App. C.4 for a detailed discussion). This energy ε is the same as the one that in perturbative calculations shows up in the $\tanh[\hbar(\varepsilon - \bar{\omega})/2T]$ -factors of the Keldysh electron Green's functions $\tilde{G}^K(\varepsilon - \bar{\omega})$, which play a role in determining the phase space available for electrons to get scattered upon absorbing or emitting a noise quantum. In App. C.4 we argue that the simplest way to keep track of this in the influence functional approach is to replace Eq. (A.12) by Eq. (1b), which mimicks the effect of the former's integral $\int d\bar{\tau} e^{i\varepsilon\bar{\tau}}$ by using (i) forward and backward paths of *equal* duration τ and (ii) an effective action whose time integration boundaries are fixed at $\pm\tau/2$, but which *depends explicitly on the average propagation energy ε* [via Eqs. (2), (4e), or equivalently Eqs. (B.94), (B.97)].

Note that GZ's approach in effect employs the same simplification, since they likewise have no $\int d\bar{\tau} e^{i\varepsilon\bar{\tau}}$ integral and use forward and backward paths of equal duration τ . Their effective action depends on the average energy ε , too, via the $\tanh[\hbar\varepsilon/2T]$ -factor in their \tilde{S}_R . However, lacking the $-\bar{\omega}$ recoil shift, their \tanh -terms turn out to yield zero after averaging over random walks, so that $\langle i\tilde{S}_R^{\text{GZ}} \rangle_{\text{rw}} \simeq 0$.

A.4. Perturbative vs. Nonperturbative Methods

We conclude this overview-style appendix with some general comments on whether it is sufficient to calculate τ_φ perturbatively, as we contend (in agreement with others^{17,18,19}), or whether a truly nonperturbative approach is needed, as GZ have argued in GZ00⁴. We have made an effort to keep the discussion as nontechnical as possible and accessible to casual readers that have not studied App. B in detail, although we will on occasion refer to results from the latter.

In GZ's influence functional approach, the decoherence time is defined as the scale at which the function $F(\tau) = \frac{1}{\hbar} \langle i\tilde{S}_R + \tilde{S}_I \rangle_{\text{rw}}$, which in their theory is *linear* in the interaction propagators \tilde{R}/\tilde{I} , becomes of order one. This means that τ_φ is the crossover scale between the regimes where perturbation theory is rigorously valid or breaks down, $F(\tau) \ll 1$ or $\gg 1$, respectively. To determine this scale, we contend that it is sufficient to calculate $F(\tau)$ *perturbatively* (assuming, strictly speaking, $F(\tau) \ll 1$), and then to enquire for what time the perturbative result so obtained ceases to be small, setting $F(\tau_\varphi) \simeq 1$. (This is analogous to the fact that the crossover scales T_K or T_c , the Kondo temperature in the Kondo problem or the critical temperature in the theory of superconductivity, can be calculated perturbatively as the scales where perturbation theory breaks down.) An accurate knowledge of $F(\tau)$ for $\tau \gtrsim \tau_\varphi$ would be needed only if we desired to accurately include exponentially small ($e^{-F(\tau)} \ll 1$) contributions to weak localization, which is usually deemed not worth the effort. (In contrast, for the Kondo problem or superconductivity, nonperturbative treatments *are* worth the effort, because the phenomena of interest become strong in the nonperturbative regimes.)

GZ have argued in GZ00⁴ that a perturbative treatment of weak localization is insufficient, because according to them it fails to disentangle the effects of preexponent and exponent in an Ansatz for the Cooperon of the general form $C(\tau) = A(\tau)e^{-F(\tau)}$: when this is expanded in powers of the interaction, both A and F contribute to the first-order term $C^{(1)}$. The influence functional approach avoids this problem by very naturally generating a general expression for the function F in the exponent – which in GZ’s approach turns out to be *linear* in the interaction propagator [Eq. (2), or Eq. (B.84)]. However, the problem of disentangling the exponent from the preexponent is easily avoided in the diagrammatic approach, too, by calculating not the Cooperon itself, but its *self energy*, to linear order in the interaction; Fourier transforming the resulting Cooperon $C(\omega)$ into the time domain, this automatically yields an expression of the form $A(\tau)e^{-F(\tau)}$, again with F *linear* in the interaction propagator. [The prefactor arises from wave-function renormalization effects, see DMSA-II²⁰, Eq. (14a).] Since both the influence functional and diagrammatic strategies yield results for which the exponent F is linear in the interaction (and contains contributions with a similar $\coth + \tanh$ structure), it is reasonable to expect that if both approaches are implemented with sufficient care, their answers for F should agree completely.

They do agree, in fact, if the recoil-incorporating effective action proposed in this work and featuring $\tanh[\hbar(\varepsilon \mp \bar{\omega})/2T]$ -factors is used. (This agreement is demonstrated explicitly in DMSA-II²⁰.) But they differ if GZ’s procedure is followed without modification, leading to their no-recoil $\tanh[\hbar\varepsilon/2T]$ -factors. It is important and instructive, therefore, to identify at which point of the derivation of the influence functional approach the need for a modification of GZ’s approach first manifests itself. We shall now argue that this point is reached when the order in which two distinct averaging procedures are performed, over paths \mathbf{R}^a and fields V , is tacitly interchanged, an aspect that has not been emphasized in the preceding sections.

To be concrete, let us focus on an intermediate stage of GZ’s first principles calculation of the weak localization contribution $\sigma_{\text{DC}}^{\text{WL}}$ to the conductivity. Following the enumeration of steps used in App. A.1, p. 18, this stage is reached after steps (1) to (6) [or according to the enumeration of App. B.4, p. 36, after steps **(A)** to **(G)**], resulting in the following expressions [the first of which corresponds to Eq. (B.55a)]:

$$\sigma_{\text{DC,real}} = \sum_{\sigma_1} \frac{1}{d} \int dx_2 \mathbf{j}_{11'} \cdot \mathbf{j}_{22'} \tilde{J}'_{12',21'}(0), \quad (\text{A.13a})$$

$$\tilde{J}'_{12',21'}(0) = \tilde{J}'_{12',21'}{}^{\text{free}}(0) \left\langle \left\langle e^{i(\tilde{S}_V^F - \tilde{S}_V^B)/\hbar} \right\rangle_{\text{cqp}} \right\rangle_V, \quad (\text{A.13b})$$

$$\tilde{S}_V^{F/B} = \int_{-\frac{\pi}{2} \mp \frac{\pi}{2}}^{\frac{\pi}{2}} dt_3 \tilde{h}_V^{F/B}(t_3, \mathbf{R}^{F/B}(t_3)), \quad (\text{A.13c})$$

$$\left\langle \dots \right\rangle_{\text{cqp}} = \left[\tilde{J}'_{12',21'}{}^{\text{free}}(0) \right]^{-1} \int (d\varepsilon) [-n'(\hbar\varepsilon)] \int_{-\infty}^{\infty} d\bar{\tau} e^{i\bar{\tau}\varepsilon} \quad (\text{A.13d})$$

$$\times \int_{\mathbf{R}^F(-\frac{\tau}{2}-\frac{\tau}{2})=\mathbf{r}_{2'}}^{\mathbf{R}^F(\frac{\tau}{2})=\mathbf{r}_1} \int_{\mathbf{R}^B(-\frac{\tau}{2}+\frac{\tau}{2})=\mathbf{r}_2}^{\mathbf{R}^B(\frac{\tau}{2})=\mathbf{r}_{1'}} \tilde{\mathcal{D}}'(\mathbf{R}) e^{i[\tilde{S}_0^F(\frac{\tau}{2}, -\frac{\tau}{2}-\frac{\tau}{2})-\tilde{S}_0^B(\frac{\tau}{2}, -\frac{\tau}{2}+\frac{\tau}{2})]/\hbar} \dots$$

The correlator $\tilde{J}'_{12',21'}(0)$ originates from $\tilde{\mathcal{C}}_{[11',22']}$ of Eq. (A.3c). It has here been expressed [starting from Eqs. (B.49) to (B.52), and using the results of Eqs. (C.14), (C.19a) and (C.21)] as a double average $\langle \dots \rangle_{\text{cqp}}{}_V$ over a pair of phase factors $e^{i(\tilde{S}_V^F-\tilde{S}_V^B)}$, which describe the influence of interactions, represented by fluctuating fields $V_{F/B}(t_3, \mathbf{r}_3)$, on a pair of closed quantum-mechanical paths (cqp). [The detailed form (A.13c) of the phase factors follow from Eq. (B.56), with \tilde{h}_V^a given by (B.36b); see also Eq. (B.58), and the discussion thereafter]. Eq. (A.13b) instructs us to first pick out a specific configuration of the fields $V_{F/B}(t_3, \mathbf{r}_3)$, then to calculate the average $\langle \dots \rangle_{\text{cqp}}$ of this phase factor over all closed quantum-mechanical paths with boundary conditions specified in Eq. (A.13d) [as obtained from Eq. (C.21)], and to evaluate the average over all field configurations in the end. Thus, for a given V , the set of paths making the dominant contribution will depend on V .

Now, the next step of GZ's strategy [step (7) according to App. A.1, or step (H) according to App. B.4], is to perform the average $\langle \dots \rangle_V$ over the interaction fields. To carry out this step, GZ (tacitly) interchange the order of averages [as do we in App. B.5.5], in effect replacing Eq. (A.13b) by

$$\tilde{J}'_{12',21'}(0) = \left\langle \left\langle e^{i(\tilde{S}_V^F-\tilde{S}_V^B)/\hbar} \right\rangle_V \right\rangle_{\text{cqp}} \stackrel{\text{RPA}}{\simeq} \left\langle e^{-\tilde{S}_{\text{eff}}/\hbar} \right\rangle_{\text{cqp}}, \quad (\text{A.14a})$$

$$\tilde{S}_{\text{eff}}[\mathbf{R}^a] = \frac{1}{2\hbar} \langle (\tilde{S}_V^F - \tilde{S}_V^B)(\tilde{S}_V^F - \tilde{S}_V^B) \rangle_V = i\tilde{S}_R + \tilde{S}_I. \quad (\text{A.14b})$$

Eq. (A.14a) instructs us to first pick out a specific pair of paths $\mathbf{R}^{F/B}(t_3)$, and then to calculate the influence functional $\langle e^{i(\tilde{S}_V^F-\tilde{S}_V^B)/\hbar} \rangle_V$ which describes how the chosen pair of paths are effected on average by interactions. Within the RPA approximation, the $\langle \dots \rangle_V$ average can now be done exactly, yielding an effective action \tilde{S}_{eff} that is linear in interaction correlators \tilde{R}/\tilde{I} [Eq. (B.84)]. The sum over all closed quantum paths is to be performed at the end.

Now, this seemingly innocuous change in the order of averages is without consequence only if both averages are performed exactly, as is possible in an order-for-order perturbation expansion (or, to all orders, for exactly solvable models such as the Caldeira-Leggett model). However, this is not the case in GZ's theory (or our version thereof), which proceeds to use the semiclassical approximation of replacing the sum over all closed quantum paths by a sum over only the saddle point paths that extremize the action. In principle, this can be done in at least two different ways, which we indicate schematically as follows:

$$\left\langle e^{-\frac{1}{\hbar}\tilde{S}_{\text{eff}}[\mathbf{r}^a]} \right\rangle_{\text{cqp}} \xrightarrow{\text{GZ}} \left\langle e^{-\frac{1}{\hbar}\tilde{S}_{\text{eff}}^{\text{GZ}}[\mathbf{r}_{\text{bare}}^a]} \right\rangle_{\text{bare}} \simeq e^{-\frac{1}{\hbar}\langle \tilde{S}_{\text{eff}}^{\text{GZ}}[\mathbf{r}_{\text{bare}}^a] \rangle_{\text{bare}}}, \quad (\text{A.15a})$$

$$\left\langle e^{-\frac{1}{\hbar}\tilde{S}_{\text{eff}}[\mathbf{r}^a]} \right\rangle_{\text{cqp}} \xrightarrow{\text{ideally}} \left\langle e^{-\frac{1}{\hbar}\tilde{S}_{\text{eff}}[\mathbf{r}_{\text{dressed}}^a]} \right\rangle_{\text{dressed}}. \quad (\text{A.15b})$$

Here the subscripts bare/dressed indicate that the sums over the paths on the right

side of Eq. (A.15) are taken only over those paths, with boundary conditions as specified in Eq. (A.13d), which extremize the bare action $\tilde{S}_0 = \tilde{S}_0^F - \tilde{S}_0^B$ (“bare” paths, Eq. (A.15a), used by GZ), or the full action $\tilde{S}_{\text{tot}} = \tilde{S}_0 + i\tilde{S}_{\text{eff}}$ (“dressed” paths, Eq. (A.15b), discussed below). On the far right of Eq. (A.15a) we indicated a further (uncontroversial) approximation, used by GZ and others when an exponential is to be averaged over bare paths, namely to lift the average into the exponent. In practice, [e.g. Sec. 4], the averages $\langle \dots \rangle_{\text{bare}}$ on the r.h.s. of Eq. (A.15a) are replaced by $\langle \langle \dots \rangle_{\text{bare}} \rangle_{\text{dis}} \rightarrow \langle \dots \rangle_{\text{rw}}$, where the latter average is over diffusive random walks (rw) with appropriate boundary conditions. In other words, $\langle \dots \rangle_{\text{bare}}$ is approximated by considering only semiclassical trajectories in a disordered potential landscape (while fluctuations about these semiclassical paths are neglected), and, after after implicit disorder averaging, these semiclassical trajectories are treated as random walks.

Ideally, one would of course prefer to average over dressed paths [Eq. (A.15b)], which “know” about the effects of interactions due to the role that $i\tilde{S}_{\text{eff}}$ plays in determining the saddle point trajectories. (Even more ideally, one would also take into account fluctuations about these dressed paths). In such a calculation, the $i\tilde{S}_I$ term in $i\tilde{S}_{\text{eff}}$ would cause the dressed paths $\tilde{\mathbf{R}}_{\text{dressed}}^a$ to acquire an imaginary component (we thank Igor Gornyi for alerting us to this fact), implying that the contributions of the two terms in $(i\tilde{S}_R + \tilde{S}_I)[\mathbf{R}_{\text{dressed}}^a]$ can partially cancel, even though both \tilde{S}_R and \tilde{S}_I are purely real functionals of their arguments (GZ overlooked the possibility of such a partial cancellation, because they considered only bare paths, see below. Marquardt¹⁶ has illustrated how such a partial cancellation occurs in the Caldeira-Leggett model). Note that such a dressed-path procedure would require only that $\tilde{S}_{\text{tot}}[\mathbf{R}_{\text{dressed}}^a]/\hbar \gg 1$, and would not require $\tilde{S}_{\text{eff}}[\mathbf{R}_{\text{dressed}}^a]/\hbar$ to be small. Indeed, its results would be nonperturbative in the interaction correlator \tilde{R}/\tilde{I} , since \tilde{S}_{eff} , though linear in \tilde{R}/\tilde{I} , is a non-linear functional of $\mathbf{R}_{\text{dressed}}^a$, which itself is nonlinear in \tilde{R}/\tilde{I} (as illustrated explicitly in the Caldeira-Leggett model, where all these nonlinear functions can be evaluated explicitly).

However, in the present theory, using fully dressed paths is not technically feasible. Therefore, GZ made the standard and seemingly natural choice of averaging purely over *bare* paths. Indeed, they write (just before Eq. (61) of GZ99³): “In the zero-order approximation one can neglect the terms \tilde{S}_R and \tilde{S}_I describing the effect of Coulomb interaction” so that “the path integral is dominated by the saddle-point trajectories for the action \tilde{S}_0 ”. In other words, bare paths don’t “know” about the interactions *at all*. Consequently, GZ used an effective action $\tilde{S}_{\text{eff}}^{\text{GZ}}$ obtained by treating the Pauli factor $\tilde{\delta} - 2\tilde{\rho}$ in \tilde{S}_{eff} as time-independent (arguing that the energy argument of the corresponding Fermi function is conserved during propagation), essentially replacing it by $\tanh[\hbar\varepsilon/2T]$. [See p. 9205 of GZ99³: “ n depends only on the energy and not on time because the energy is conserved along the classical path”.]

Once the approximation of using purely bare paths has been made, the ef-

fective action $\tilde{S}_{\text{eff}}^{\text{GZ}}[\mathbf{R}_{\text{bare}}^a]$ is *linear* in the interaction propagators (since $\mathbf{R}_{\text{bare}}^a$ is now independent of the interaction). This implies in our view that GZ's results are *purely perturbative*. GZ dispute this characterization, calling their approach “nonperturbative” because in their view it does not require $\tilde{S}_{\text{eff}}^{\text{GZ}}[\mathbf{R}_{\text{bare}}^a] \lesssim \hbar$, only $\tilde{S}_{\text{eff}}^{\text{GZ}}[\mathbf{R}_{\text{bare}}^a] \ll \tilde{S}_0[\mathbf{R}_{\text{bare}}^a]$. We disagree, contending that GZ do need the former condition, because without it, their use of purely bare paths would not be justified: a semiclassical treatment requires the evaluation of the action $\tilde{S}_{\text{tot}}[\mathbf{R}^a]$ to be accurate to within \hbar , implying that the effects of \tilde{S}_{eff} on the semiclassical paths can be neglected only if $\tilde{S}_{\text{eff}}^{\text{GZ}}[\mathbf{R}_{\text{bare}}^a] \lesssim \hbar$. [Note, also, that an approach that reliably evaluates $\langle \tilde{S}_{\text{eff}} \rangle$ in the regime where the result is $\lesssim \hbar$ would yield the function $F(\tau)$ in the regime where it is $\lesssim 1$, which is entirely sufficient to reliably extract τ_φ , as argued in the second paragraph of this subsection.]

While it is a matter of somewhat empty semantics whether an approach using purely bare paths can be called nonperturbative or not, the validity of such an approach can be subjected to a hard test: does the result which this approach produces for $F(\tau)$ *after* the average $\langle \dots \rangle_{\text{bare}}$ has been performed agree, in the regime $F(\tau) \ll 1$, with that obtained from Keldysh perturbation theory? (GZ's claim in GZ00⁴ that their approach agrees with Keldysh perturbation theory, is true only if the perturbation expansion is performed *before* averaging over paths, see Secs. B.6.1 and C.3). The answer is no: The perturbation expansion obtained by expanding the first-principles expression (A.13) in powers of $(\tilde{S}_V^F - \tilde{S}_V^B)/\hbar$ shows unambiguously that the paths arising in the perturbation expansion, *do* know about the interactions (in contrast to bare paths): energy conservation induces recoil at each interaction vertex, so that the electron frequencies incident and leaving a vertex differ from each other, $\bar{\varepsilon}$ vs. $\bar{\varepsilon} \mp \bar{\omega}$, in a way relevant for the Pauli factors, which depend on $\bar{\varepsilon} \mp \bar{\omega}$. This effect is negligible for retarded and advanced electron propagators, which depend only on the combination $\hbar(\bar{\varepsilon} \mp \bar{\omega}) - \xi_{\mathbf{p}} \pm i\hbar/\tau_{\text{el}}$, with $\xi_{\mathbf{p}} = \mathbf{P}^2/2m$ [Eq. (F.2)], since there energy shifts by $\hbar|\bar{\omega}| \lesssim \hbar/\tau_{\text{el}}$ are negligible. However, it is *not* negligible for the Keldysh propagator, which contains fermion functions of the form $[e^{\hbar(\bar{\varepsilon} \mp \bar{\omega}) - \varepsilon_F}/T + 1]^{-1}$ [Eq. (B.47b)], in which the largeness of $\hbar\bar{\varepsilon}$ is *cancelled* by that of ε_F . Thus, interaction events with recoil energies of order $\hbar|\bar{\omega}| \gtrsim T$ strongly change the value of the Fermi function which specifies the phase space available for a given transition. Since these recoil effects are present in the original order $\langle \langle \dots \rangle_{\text{cqp}} \rangle_V$ of doing the average but absent in the switched order $\langle e^{-\tilde{S}_{\text{eff}}^{\text{GZ}}/\hbar} \rangle_{\text{bare}}$ if GZ's version of the effective action is used, something is clearly amiss in the latter approach.

The main assertion of our own work is that for the purpose of describing decoherence in weak localization, recoil effects *can* be taken into account in the influence functional approach provided GZ's use of bare paths is supplemented by the use of an effective action that keeps track of recoil (rec):

$$\left\langle e^{-\frac{1}{\hbar}\tilde{S}_{\text{eff}}[\mathbf{r}^a]} \right\rangle_{\text{cqp}} \xrightarrow{\text{JD}} \left\langle e^{-\frac{1}{\hbar}\tilde{S}_{\text{eff}}^{\text{rec}}[\mathbf{r}_{\text{bare}}^a]} \right\rangle_{\text{bare}} \simeq e^{-\frac{1}{\hbar}\langle \tilde{S}_{\text{eff}}^{\text{rec}}[\mathbf{r}_{\text{bare}}^a] \rangle_{\text{bare}}} . \quad (\text{A.16})$$

[In practice, we perform the averages over bare paths on the r.h.s. the same way as GZ do,^{3,4} i.e. using an average over semiclassical diffusive random walks (and neglecting fluctuations about these), $\langle \langle \dots \rangle_{\text{bare}} \rangle_{\text{dis}} \rightarrow \langle \dots \rangle_{\text{rw}}$.] Here $\tilde{S}_{\text{eff}}^{\text{rec}}$ is the effective action obtained by representing $(\tilde{\delta} - 2\tilde{\rho})$ by $\tanh[\hbar(\varepsilon \mp \tilde{\omega})/2T]$ -factors [as made explicit in Eq. (B.96)]. The result for $\tilde{S}_{\text{eff}}^{\text{rec}}[\mathbf{R}_{\text{bare}}^a]$ so obtained [Eq. (2), or Eq. (B.94) with (B.97)] is linear in the interaction propagators \tilde{R}/\tilde{I} , just as GZ's effective action is, but in contrast to the latter, an expansion of $e^{-\frac{1}{\hbar}(\tilde{S}_{\text{eff}}^{\text{rec}})_{\text{bare}}}$ to first order in the exponent yields results consistent with the Keldysh perturbation expansion also if the average over paths in $\frac{1}{\hbar}(\tilde{S}_{\text{eff}}^{\text{rec}})_{\text{bare}}$ is performed explicitly first and the exponential expanded only *thereafter*. Moreover, the results for $F(\tau)$ so obtained agree fully with those from a diagrammatic Bethe-Salpeter calculation of the Cooperon (see DMSA-II²⁰). A crucial ingredient for ensuring this agreement is that the ultraviolet divergencies arising in each of the two terms in $\langle (i\tilde{S}_R^{\text{rec}} + \tilde{S}_I^{\text{rec}})[\mathbf{R}_{\text{bare}}^a] \rangle_{\text{bare}}$ cancel each other [Sec. 4]. This cancellation is possible because the functional $\tilde{S}_R^{\text{rec}}[\mathbf{R}_{\text{bare}}^a]$, despite using only bare paths, is not purely real, thereby capturing an essential feature of $\tilde{S}_{\text{eff}}^{\text{rec}}[\mathbf{R}_{\text{dressed}}^a]$ that is not present in $\tilde{S}_{\text{eff}}^{\text{GZ}}[\mathbf{R}_{\text{bare}}^a]$.

Since GZ contend that their approach is nonperturbative, they reject arguments based on perturbation theory, defending their use of purely bare paths by evoking only the standard semiclassical approximation. But the need to keep track of recoil arises within the latter framework, too, in a way very similar to that described above: The standard condition for the validity of the semiclassical approximation is that the propagation energies and momenta of the quantum particle that is to be described semiclassically should be much larger than the typical frequencies and wave numbers characterizing the potential landscape which it is moving in, so that the latter appears “smooth”. If one were to consider a single noninteracting electron propagating with energy $\hbar\bar{\varepsilon} \simeq \varepsilon_F$ through a disordered potential landscape, this implies the conditions $\varepsilon_F \gg \hbar/\tau_{\text{el}}$ (or $k_F \gg 1/l_{\text{el}}$), which certainly are satisfied in the regime of weak localization. However, GZ's theory for an electron propagating through and interacting with a Fermi sea of other electrons shows that the propagation energy enters not only in the free part of the action, but also in the Fermi function $[e^{(\hbar\bar{\varepsilon} - \varepsilon_F)/T} + 1]^{-1}$ arising from the Pauli factor $\tilde{\delta} - 2\tilde{\rho}$ in \tilde{S}_R . To ensure that this factor is treated accurately, the standard semiclassical condition $\varepsilon_F \gg \hbar/\tau_{\text{el}}$ evoked by GZ is not sufficient, since inside the Fermi function the largeness of $\hbar\bar{\varepsilon}$ is *cancelled* by the largeness of ε_F . Thus, interaction-induced changes in $\bar{\varepsilon}$ of order $\tilde{\omega} \lesssim 1/\tau_{\text{el}}$ will produce strong changes in the Fermi function between $\simeq 0$ and $\simeq 1$. These changes need to be kept track of. As argued above, this can be accomplished by the recoil contributions $\mp\tilde{\omega}$ in our $\tanh[\hbar(\varepsilon \mp \tilde{\omega})/2T]$ -factors.

Appendix B. Derivation of Influence Functional Approach

In this appendix, we rederive the influence functional approach of GZ, with the aim of establishing clearly (i) how far it can be taken without any approximations, and (ii) what the consequences are of the approximations that they eventually do

make. We generally follow the strategy they have chosen to use, but the details of our notations and derivations deviate from GZ's whenever we believe that greater compactness, clarity or generality can thereby be achieved. The most important difference is that instead of using the coordinate-momentum path integral $\int \mathcal{D}(\mathbf{R}\mathbf{P})$ of GZ, we use a coordinate-only version $\int \mathcal{D}'\mathbf{R}$, since this enables the Pauli factor to be treated more accurately.

The outline of this appendix is as follows. After a summary of our notational conventions, Secs. B.1 to B.3 define the model and decouple the interaction using a Hubbard-Stratonovich transformation within a Keldysh framework. In Sec. B.4, we summarize GZ's procedure for deriving their influence functional approach, and in Sec. B.5 repeat their steps in explicit detail, though with some changes. Finally, Sec. B.6 establishes a link between the influence functional so derived and Keldysh perturbation theory, and discusses the fate of the Pauli factor.

Notational Conventions

We begin by summarizing, for ease of reference, some notational conventions to be used throughout: We shall use the shorthands $x \equiv (\mathbf{r}, \sigma)$ for electron position and spin, and $\int dx \equiv \sum_{\sigma} \int d\mathbf{r}$. Operators will generally carry hats (e.g. \hat{H}_0), and the subscripts S , H and I will distinguish operators in the Schrödinger, Heisenberg or interaction pictures, respectively. For c -number fields, the shorthand $V_i \equiv V_i(t_i) \equiv V(t_i, \mathbf{r}_i)$ will often be used, i.e. the time argument, when not displayed explicitly, will be understood to be t_i . c -number functions depending on two different coordinates, i.e. coordinate-space matrices, will generally carry tildes [e.g. $\tilde{\rho}_{ij} = \rho(x_i, x_j)$], and their Fourier transforms w.r.t. $\mathbf{r}_i - \mathbf{r}_j$ will carry bars, e.g.

$$\bar{\rho}(\mathbf{R}_{ij}, \mathbf{p}) \equiv \int d\mathbf{r}_{ij} e^{-i\mathbf{p}\cdot\mathbf{r}_{ij}} \tilde{\rho}(\mathbf{R}_{ij} + \frac{1}{2}\mathbf{r}_{ij}, \mathbf{R}_{ij} - \frac{1}{2}\mathbf{r}_{ij}), \quad (\text{B.1})$$

where \mathbf{R}_{ij} and \mathbf{r}_{ij} will generally denote center-of-mass and relative coordinates,

$$\mathbf{R}_{ij} = (\mathbf{r}_i + \mathbf{r}_j)/2, \quad \mathbf{r}_{ij} = \mathbf{r}_i - \mathbf{r}_j. \quad (\text{B.2})$$

We do not set $\hbar = 1$ but display it explicitly throughout. Hence, the variable \mathbf{p} in Eq. (B.1) (and likewise \mathbf{k} , \mathbf{q} below) denotes a wave-number, with units of inverse length, not a momentum; the corresponding momenta will always be denoted by capital letters:

$$\mathbf{P} = \hbar\mathbf{p} \quad \mathbf{K} = \hbar\mathbf{k}, \quad \mathbf{Q} = \hbar\mathbf{q}. \quad (\text{B.3})$$

For correlation functions, the shorthand $\tilde{G}_{ij} \equiv \tilde{G}_{ij}(t_{ij}) \equiv G(t_{ij}; x_i, x_j)$ will often be used, i.e. the time argument, when not displayed explicitly, will be understood to be $t_{ij} = t_i - t_j$. [For the step function, we use $\theta_{ij} \equiv \theta(t_{ij})$.] The corresponding frequency Fourier transform w.r.t. t_{ij} will be denoted by

$$\tilde{G}_{ij}(t_{ij}) = \int (d\omega) e^{-i\omega t_{ij}} \tilde{G}_{ij}(\omega), \quad \int (d\omega) \equiv \int \frac{d\omega}{2\pi}, \quad (\text{B.4})$$

30 *Jan von Delft*

where ω has units of inverse time. If coordinate-space subscripts are not displayed explicitly, they are understood to be summed over, e.g. $[\tilde{G}(t)\tilde{G}(t')]_{ij} \equiv \int dx_k \tilde{G}_{ik}(t)\tilde{G}_{kj}(t')$. We distinguish forward and backward parts of the Keldysh contour by an index $a = F, B$ [GZ use $a = 1, 2$ instead], and use boldface for matrices in Keldysh space, e.g. $\tilde{\mathbf{G}}_{ij}$.

A pair of indices such as ii' , appearing once without prime and once with, will denote independent coordinates x_i and $x_{i'}$ referring to the same time (i.e. $t_i = t_{i'}$ is to be understood), which are, however, to be set equal at the very end of the calculation, after being differentiated upon, i.e.

$$(\nabla_i - \nabla_{i'})\tilde{\rho}_{ii'} \equiv [(\nabla_i - \nabla_{i'})\tilde{\rho}_{ii'}]_{x_i=x_{i'}}. \quad (\text{B.5})$$

We shall often encounter double summations over coordinates referring to the same time. For such coordinates we shall use the index pair $i\bar{i}$, one without bar and one with, take it to be understood that $t_{\bar{i}} \equiv t_i$, and denote the double summation by

$$\int dx_{i,\bar{i}} \equiv \sum_{\sigma_i} \int d\mathbf{r}_i d\mathbf{r}_{\bar{i}}. \quad (\text{B.6})$$

When taking the limit of infinite volume, we shall use the shorthand notation

$$\int (d\mathbf{p}) \equiv \int \frac{d\mathbf{p}}{(2\pi)^d} = \lim_{\text{Vol} \rightarrow \infty} \frac{1}{\text{Vol}} \sum_{\mathbf{p}}, \quad (\text{B.7a})$$

$$\bar{\delta}^{(d)}(\mathbf{p} - \mathbf{p}') \equiv \lim_{\text{Vol} \rightarrow \infty} \delta_{\mathbf{p},\mathbf{p}'} \text{Vol}, \quad (\text{B.7b})$$

so that $\int (d\mathbf{p})\bar{\delta}(\mathbf{p}) = 1$, i.e., $\bar{\delta}(\mathbf{p})$ equals $(2\pi)^d$ times a d -dimensional Dirac delta function. If the integrand under $\int (d\mathbf{p})$ depends only on the energy $\xi_{\mathbf{p}} = \mathbf{P}^2/2m - \varepsilon_{\text{F}}$ and if it decays at least as fast as $1/\xi_{\mathbf{p}}^2$ for $\xi_{\mathbf{p}} \rightarrow \infty$, we shall use $\int (d\mathbf{p}) \rightarrow \nu \int d\xi_{\mathbf{p}}$. Here ν denotes the density of states per spin at the Fermi surface, which in $d = 3$ or 2 dimensions is given by

$$\nu = \frac{m}{2\pi\hbar^2} \left(\frac{k_{\text{F}}}{\pi} \right)^{d-2} = \frac{d\langle n \rangle}{2\varepsilon_{\text{F}}}, \quad (\text{B.8})$$

where $\langle n \rangle = \int_{k < k_{\text{F}}} (d\mathbf{k}) = \frac{\pi}{2d} \left(\frac{k_{\text{F}}}{\pi} \right)^d$ is the average electron density per spin. The *purely* 1-dimensional case $d = 1$ will not be considered here; nevertheless, $d = 3$ or 2 of course include the case that a sample is quasi 1-dimensional, in the sense that only one of its dimensions is larger than the phasebreaking length, $L \gtrsim \sqrt{D\tau_{\varphi}}$, where $D = v_{\text{F}}^2\tau_{\text{el}}/d$ is the diffusion constant.

For quasi- \bar{d} -dimensional diffusion, the actually measured (bare) DC conductivity $\sigma_{\bar{d}}$ is related to the Drude conductivity $\sigma_{\text{DC}}^{\text{Drude}} = 2e^2\nu D$ by an extra factor $a^{d-\bar{d}}$, which accounts for the sample's transverse directions along which motion is not diffusive ($d = 3$ or 2 is the actual dimension of the sample, $\bar{d} = 3, 2$ or 1 the effective dimension for diffusive motion). Hence, it is customary to define [cf. AAK¹⁰, after Eq. (5)] $\sigma_{\bar{d}} = \sigma_{\text{DC}}^{\text{Drude}} a^{d-\bar{d}}$ as the conductivity per unit length and unit area of a 3D sample (for $\bar{d} = 3$), or the inverse square resistance of a film (for $\bar{d} = 2$),

or the inverse resistance per unit length of a wire (for $\bar{d} = 1$). Likewise, the weak localization correction to the conductivity is often expressed in terms of these actual conductivities by defining $\sigma_{\bar{d}}^{\text{WL}} \equiv \sigma_{\text{DC}}^{\text{WL}} a^{d-\bar{d}}$.

The fact that the weak localization correction is small compared to the Drude term is often made explicit by writing the prefactor of the Cooperon term as $\sigma_{\text{DC}}^{\text{Drude}}/g_{\bar{d}}(L_H)$ [see Eq. (C.9)], where $L_H = \sqrt{D\tau_H}$ is the magnetic length and

$$g_{\bar{d}}(L) \equiv (\hbar/e^2) \sigma_{\bar{d}} L^{\bar{d}-2}, \quad (\text{B.9})$$

is the so-called dimensionless conductance, defined as the conductance, in units of e^2/\hbar , of a rectangular (d -dimensional) block with volume $a^{d-\bar{d}}L^{\bar{d}}$, measured along one of the “long” directions (of length L).

For good conductors, $g_{\bar{d}}(L) = (\pi^{1-d}/d)(ak_{\text{F}})^{d-\bar{d}}(l_{\text{el}}k_{\text{F}})^{\bar{d}-1}(L/l_{\text{el}})^{\bar{d}-2}$ is large whenever L is large: we may assume $l_{\text{el}}k_{\text{F}} \gg 1$ and $ak_{\text{F}} \gg 1$ throughout, thus for $\bar{d} = 3$ or 2 , any length $L \geq l_{\text{el}}$ implies $g_{\bar{d}}(L) \gg 1$; for $\bar{d} = 1$ the function $g_1(L)$ likewise starts out being $\gg 1$ for $L \simeq l_{\text{el}}$, but decreases with increasing L ; nevertheless, it reaches $g_1(L_*) = 1$ only when L exceeds the very large length scale $L_* = (ak_{\text{F}})^{d-1}l_{\text{el}} \gg l_{\text{el}}$.

B.1. The Model and Kubo Formula

Following GZ, we consider a disordered system of interacting fermions, described by the Hamiltonian $\hat{H} = \hat{H}_0 + \hat{H}_i$, where

$$\hat{H}_0 = \int dx \hat{\psi}_S^\dagger(x) h_0(x) \hat{\psi}_S(x), \quad h_0(x) = \frac{-\hbar^2}{2m} \nabla_{\mathbf{r}}^2 + V_{\text{imp}}(\mathbf{r}) - \mu, \quad (\text{B.10})$$

$$\hat{H}_i = \frac{e^2}{2} \int dx_1 dx_2 : \hat{n}_{11S} : \tilde{V}_{12}^{\text{int}} : \hat{n}_{22S} :, \quad (\text{B.11})$$

$$: \hat{n}_{ijS} : = \hat{n}_{ijS} - \langle \hat{n}_{ijS} \rangle_0, \quad \hat{n}_{ijS} \equiv \hat{\psi}_S^\dagger(x_j) \hat{\psi}_S(x_i), \quad (\text{B.12})$$

$$\langle \hat{O} \rangle_0 = \text{Tr}\{\hat{O} \hat{\rho}_0\}, \quad \hat{\rho}_0 = e^{-\beta \hat{H}_0} / \{\text{Tr} e^{-\beta \hat{H}_0}\}. \quad (\text{B.13})$$

$V_{\text{imp}}(\mathbf{r})$ is the disorder potential. We shall assume that the interaction potential $\tilde{V}_{12}^{\text{int}} = \tilde{V}^{\text{int}}(|\mathbf{r}_1 - \mathbf{r}_2|)$, which guarantees that its Fourier transform in \bar{d} effective dimensions, $\bar{V}_{\bar{d}}^{\text{int}}(\mathbf{q}) = \bar{V}_d^{\text{int}}(|\mathbf{q}|) = a^{3-d} \int d^d r e^{-i\bar{\mathbf{q}} \cdot \mathbf{r}} \tilde{V}^{\text{int}}(r)$, is real. For example, for the Coulomb interaction, they are given by $\bar{V}_{12}^{\text{int}} = \frac{1}{|\mathbf{r}_1 - \mathbf{r}_2|}$, and

$$V_{\bar{\mathbf{q}}}^{(3)} = \frac{4\pi}{\bar{q}^2}, \quad V_{\bar{\mathbf{q}}}^{(2)} = \frac{a 2\pi}{|\bar{\mathbf{q}}|}, \quad V_{\bar{\mathbf{q}}}^{(1)} = a^2 \ln(\bar{q}^2 a^2). \quad (\text{B.14})$$

Eq. (B.12) corresponds to a normal-ordering prescription which subtracts the expectation value w.r.t. the free density matrix $\hat{\rho}_0$. The second-quantized electron field $\hat{\psi}_S(x) \equiv \hat{\psi}_S(\mathbf{r}, \sigma)$ (in the Schrödinger picture) destroys a spin- σ electron at position \mathbf{r} , and can be expanded as follows in terms of the exact eigenfunctions $\psi_\lambda(x)$ of $h_0(x)$, with eigenvalues ξ_λ :

$$\hat{\psi}_S(x) = \sum_{\lambda} \psi_\lambda(x) \hat{c}_{\lambda S}, \quad [h_0(x) - \xi_\lambda] \psi_\lambda(x) = 0. \quad (\text{B.15})$$

The current density operator has the form

$$\hat{\mathcal{J}}_S(t_1, \mathbf{r}_1) = \sum_{\sigma_1} \left[\mathbf{j}_{11'} - \frac{e^2}{m} \mathbf{A}(t_1, \mathbf{r}_1) \right] \hat{n}_{11'S}, \quad (\text{B.16})$$

where \mathbf{A} is the vector potential, $\mathbf{j}_{11'} \equiv (-ie\hbar/2m)(\nabla_1 - \nabla_{1'})$, and the convention of Eq. (B.5) was used for the indices $11'$. An external electric field, $\mathbf{E}(t_2, \mathbf{r}) = -\nabla V_{\text{ext}}(t_2, \mathbf{r}) - \partial_{t_2} \mathbf{A}(t_2, \mathbf{r})$, switched on at time t'_0 , is described by the perturbation^a

$$\hat{H}_{\text{ext}}(t_2) = \theta(t_2 - t'_0) \int dx_2 \hat{h}_S^{\text{ext}}(t_2, x_2), \quad (\text{B.17a})$$

$$\hat{h}_S^{\text{ext}}(t_2, x_2) = h_{22'}^{\text{ext}} \hat{n}_{22'S}, \quad h_{22'}^{\text{ext}} \equiv eV_{\text{ext}}(t_2, \mathbf{r}_2) - \mathbf{A}(t_2, \mathbf{r}_2) \cdot \mathbf{j}_{22'}. \quad (\text{B.17b})$$

According to the Kubo formula, the linear response of the current density to this perturbation is

$$\langle \delta \hat{\mathcal{J}}_H(t_1, \mathbf{r}_1) \rangle = \sum_{\sigma_1} \left[-\frac{e^2}{m} \mathbf{A}(t_1, \mathbf{r}_1) \langle \hat{n}_{11S} \rangle - i \int_{t'_0}^{t_1} dt_2 \int dx_2 h_{22'}^{\text{ext}} \mathbf{j}_{11'} \tilde{\mathcal{C}}_{[11', 22']} \right] \quad (\text{B.18})$$

The first term of Eq. (B.18) is the diamagnetic contribution, $\langle n \rangle = 2\nu\varepsilon_F/d$ being the average electron density per spin [cf. Eq. (B.8)]. In the second term, the correlator

$$\tilde{\mathcal{C}}_{[11', 22']} \equiv \frac{1}{\hbar} \langle [\hat{n}_{11'H}, \hat{n}_{22'H}] \rangle \quad (\text{B.19})$$

is to be evaluated with \hat{H}_{ext} set to zero, where $\hat{B}_H(t) = e^{i\hat{H}t/\hbar} \hat{B}_S e^{-i\hat{H}t/\hbar}$ describes time evolution in the Heisenberg picture, and thermal averaging is defined by $\langle \hat{O} \rangle = \text{Tr}\{\hat{O} \hat{\rho}_H\}$, where $\hat{\rho}_H = e^{-\beta\hat{H}} / \{\text{Tr} e^{-\beta\hat{H}}\}$ is the full equilibrium density matrix.

The DC conductivity is defined via the low-frequency limit of the current response to a spatially homogeneous applied AC field $\mathbf{E}(t_2) = \int (d\tilde{\omega}_0) e^{-i\tilde{\omega}_0 t_2} \mathbf{E}(\tilde{\omega}_0)$. For a d -dimensional isotropic sample it can be written as

$$\sigma_{\text{DC}} = \lim_{\omega_0 \rightarrow 0} \frac{1}{d} \frac{\partial}{\partial \mathbf{E}(\omega_0)} \cdot \langle \delta \hat{\mathcal{J}}(\omega_0) \rangle, \quad (\text{B.20})$$

where $\mathbf{E}(\omega_0)$ can be represented by either of the choices (related by a gauge transformation)

$$\mathbf{A} = 0, \quad V_{\text{ext}}(\omega_0, \mathbf{r}_2) = -\mathbf{r}_2 \cdot \mathbf{E}(\omega_0), \quad (\text{B.21a})$$

$$\mathbf{A}(\omega_0) = \frac{\mathbf{E}(\omega_0)}{i\omega_0}, \quad V_{\text{ext}} = 0. \quad (\text{B.21b})$$

GZ use choice (B.21a) (but note our footnote a), AAG use choice (B.21b). Taking the limit $t'_0 \rightarrow -\infty$, one then readily finds from Eqs. (B.20) and (B.18) that σ_{DC}

^a We use $e < 0$ for the electron charge, as do AAG¹⁷, whereas GZ use $-e < 0$, hence our potentials are related to GZ's by a minus sign: $eV_{\text{ext}}^{\text{here}} = -eV_x^{\text{GZ}}$, and likewise $eV_F^{\text{here}} = -eV_1^{\text{GZ}}$, $eV_B^{\text{here}} = -eV_2^{\text{GZ}}$ for the potentials introduced in Eq. (B.28d) below.

can be written in either of the following forms, depending on whether the electric field is represented using a scalar or a vector potential:

$$\sigma_{\text{DC}} = -\frac{e}{d} \sum_{\sigma_1} \int dx_2 \mathbf{j}_{11'} \cdot \mathbf{r}_2 \lim_{\omega_0 \rightarrow 0} \tilde{J}_{12',21'}(\omega_0), \quad (\text{B.22a})$$

$$\sigma_{\text{DC}} = \lim_{\omega_0 \rightarrow 0} \frac{1}{\omega_0} \sum_{\sigma_1} \left[\frac{1}{d} \int dx_2 \mathbf{j}_{11'} \cdot \mathbf{j}_{22'} \tilde{J}_{12',21'}(\omega_0) + \frac{ie^2 \langle \hat{n}_{11H} \rangle}{m} \right], \quad (\text{B.22b})$$

where we have introduced the retarded correlator [with $\theta_{12} \equiv \theta(t_{12})$]

$$\tilde{J}_{12',21'}(\omega_0) = \int_{-\infty}^{\infty} dt_{12} e^{i\omega_0 t_{12}} \theta_{12} \tilde{C}_{[11',22']}. \quad (\text{B.23})$$

Sometimes it is convenient to average the coordinate \mathbf{r}_1 over the volume Vol, in which case one should replace \sum_{σ_1} in Eq. (B.22) by $\int \frac{d\mathbf{x}_1}{\text{Vol}}$.

B.2. Keldysh Approach with Source Fields

We now use the Keldysh real-time approach to rewrite $\tilde{C}_{[11',22']}$ in terms of correlators whose dynamical and statistical properties are governed entirely by \hat{H}_0 : First, thermal weighting is done in the infinite past using the *free* density matrix $\hat{\rho}_0$, and then the interaction is turned on adiabatically. For arbitrary operators \hat{A}_H and \hat{B}_H , this amounts to the replacement

$$\langle \hat{A}_H(t_1) \hat{B}_H(t_2) \rangle \rightarrow \langle \hat{A}_H(t_1 - t_0) \hat{B}_H(t_2 - t_0) \rangle_0, \quad (\text{B.24})$$

where the initial time t_0 is sent to $-\infty$ so that all disturbances associated with switching on the interactions have decayed in the infinite past (the limit $t_0 \rightarrow -\infty$, will be understood but not displayed below). Second, the time evolution of all operators is expressed in the interaction representation, using the familiar operator identity

$$e^{-iH(t_i - t_0)/\hbar} = e^{-i\hat{H}_0(t_i - t_0)/\hbar} \hat{U}_I(t_i, t_0), \quad (\text{B.25a})$$

$$\hat{U}_I(t_i, t_j) = \mathcal{T} e^{-\frac{i}{\hbar} \int_{t_j}^{t_i} dt_3 \hat{H}_I(t_3)}, \quad (\text{B.25b})$$

$$\hat{A}_I(t_i) = e^{i\hat{H}_0(t_i - t_0)/\hbar} \hat{A}_S e^{-i\hat{H}_0(t_i - t_0)/\hbar}, \quad (\text{B.25c})$$

where \mathcal{T} is the time-ordering operator (the anti-time-ordering operator, needed for \hat{U}_I^\dagger , will be denoted by $\overline{\mathcal{T}}$). The correlator $\tilde{C}_{[11',22']}$ then becomes

$$\begin{aligned} \tilde{C}_{[11',22']} &= \frac{1}{\hbar} \langle \hat{U}_I^\dagger(t_1, t_0) \hat{n}_{11'I}(t_1) \hat{U}_I(t_1, t_2) \hat{n}_{22'I}(t_2) \hat{U}_I(t_2, t_0) \rangle_0 \\ &\quad - \frac{1}{\hbar} \langle \hat{U}_I^\dagger(t_2, t_0) \hat{n}_{22'I}(t_2) \hat{U}_I^\dagger(t_1, t_2) \hat{n}_{11'I}(t_1) \hat{U}_I(t_1, t_0) \rangle_0. \end{aligned} \quad (\text{B.26})$$

This expression can be recovered via functional derivatives from the following construction:

$$\tilde{C}_{[11',22']} = i \left. \frac{\delta \tilde{\rho}_{11'}(t_1, t_0)}{\delta \tilde{v}_{2'2}} \right|_{\tilde{v}=0}, \quad (\text{B.27a})$$

$$\tilde{\rho}_{11'}(t_1, t_0) \equiv \frac{\langle \hat{U}_{IB}^\dagger(t_1, t_0) \hat{n}_{11'}(t_1) \hat{U}_{IF}(t_1, t_0) \rangle_0}{\langle \hat{U}_{IB}^\dagger(t_1, t_0) \hat{U}_{IF}(t_1, t_0) \rangle_0}, \quad (\text{B.27b})$$

$$\hat{U}_{Ia}(t_1, t_0) \equiv \mathcal{T} e^{-\frac{i}{\hbar} \int_{t_0}^{t_1} dt_3 [\hat{H}_{iI}(t_3) + \hat{v}_I(t_3)]}, \quad (\text{B.27c})$$

$$\hat{v}_I(t_3) \equiv \int dx_{3,\bar{3}} \tilde{v}_{\bar{3}\bar{3}}(t_3) \hat{n}_{\bar{3}\bar{3}I}(t_3). \quad (\text{B.27d})$$

The index $a = F, B$ will be used to distinguish propagation associated with U_I or U_I^\dagger in Eq. (B.26), i.e. with the forward or backward parts of the Keldysh contour, respectively. Since $\hat{U}_{IB}^\dagger \hat{U}_{IF} = 1$, the denominator in Eq. (B.27b), included for later convenience, in fact equals unity. $\tilde{\rho}_{11'}(t_1, t_0) = \tilde{\rho}(t_1, t_0; x_1, x_{1'})$ is the *reduced single-particle density matrix*. We call it “reduced”, since the thermal average $\langle \cdot \rangle_0$ in Eq. (B.27b) traces out all electron degrees of freedom but one, to be called the “singled-out electron”, for which the others constitute an effective environment. Note that we have defined $\tilde{\rho}_{11'}(t_1, t_0)$ in the presence of a source term^b to generalize this to $\hat{v}(t_3)$, defined by Eq. (B.27d) [which uses the conventions of Eq. (B.6)] on the interval $t_3 \in [t_0, t_1]$ in terms of a real c -number “source field” $\tilde{v}_{\bar{3}\bar{3}}(t_3) = \tilde{v}(t_3; x_{\bar{3}}, x_{\bar{3}})$ that couples to the (not normal-ordered) operator $\hat{n}_{\bar{3}\bar{3}I}(t_3)$. The source field is devoid of physical meaning, and is introduced merely as a mathematical device to generate $\tilde{\mathcal{C}}_{[11', 22']}$ via functional differentiation. For $\tilde{v} = 0$, our reduced density matrix $\tilde{\rho}_{12}(t, t_0)$ corresponds to $\rho(t; \mathbf{r}_1, \mathbf{r}_2)$ of (GZ-II.20) of GZ, who simply call it “density matrix”.

In the usual Keldysh approach, all time integrals involving the interaction extend from $-\infty$ to ∞ . This can also be achieved in the present approach, if desired, by inserting a factor of $1 = \hat{U}_{IB}^\dagger(t_\infty, t_1) \hat{U}_{IF}(t_\infty, t_1)$ just to the left or right of $\hat{n}_{11'}(t_1)$ in the first or second lines of Eq. (B.26), respectively, and taking the limit $t_\infty \rightarrow \infty$, $t_0 \rightarrow -\infty$. However, the actual value chosen for t_∞ does not matter, and in the present approach, it is actually simplest to use $t_\infty = t_1$.

B.3. Hubbard-Stratonovich Transformation

Following GZ, we now decouple the interaction term \hat{H}_i in \hat{U}_{Ia} using a Hubbard-Stratonovich transformation that introduces a path-integral over a further pair of real, spin-independent c -number fields $V_a(t_3, \mathbf{r}_3)$:

$$\hat{U}_{Ia}(t_1, t_0) = \frac{\int \mathcal{D}V_a(t_3, \mathbf{r}_3) \hat{\mathcal{U}}_a(t_1, t_0) e^{iS_V^{0a}(t_1, t_0)/\hbar}}{\int \mathcal{D}V_a(t_3, \mathbf{r}_3) e^{iS_V^{0a}(t_1, t_0)/\hbar}}, \quad (\text{B.28a})$$

$$S_V^{0a}(t_1, t_0) = \int_{t_0}^{t_1} dt_3 \int \frac{d\mathbf{q}}{(2\pi)^3} \frac{\bar{V}_a(t_3, -\mathbf{q}) \bar{V}_a(t_3, \mathbf{q})}{2V^{\text{int}}(\mathbf{q})}, \quad (\text{B.28b})$$

^bFor our purposes it turns out to be sufficient to use the *same* source term \hat{v} and source field $\tilde{v}_{\bar{3}\bar{3}}$ on the forward and backward contour; to calculate correlators more general than $\tilde{\rho}_{11'}$, one would introduce a separate source term \hat{v}^a and corresponding source fields $\tilde{v}_{\bar{3}\bar{3}}^a$ for each of the forward and backward contours, $a = F/B$. The corresponding generalizations below are straightforward.

$$\hat{\mathcal{U}}_a(t_1, t_0) = \mathcal{T} e^{-\frac{i}{\hbar} \int_{t_0}^{t_1} dt_3 [\hat{V}_a(t_3) + \hat{v}_I(t_3)]}, \quad (\text{B.28c})$$

$$\hat{V}_a(t_3) = \int dx_3 eV_a(t_3, \mathbf{r}_3) : \hat{n}_{33I} : (t_3). \quad (\text{B.28d})$$

The fields $V_a(t_3, \mathbf{r}_3)$ and their Fourier transforms $\bar{V}_a(t_3, \mathbf{q})$ are defined on the interval $t_3 \in [t_0, t_1]$ on the upper or lower Keldysh contour for $a = F$ or B , respectively (i.e. the time argument of V_a is understood to carry an implicit index a). By using Eqs. (B.28a) to rewrite all \hat{U}_{Ia} in Eq. (B.27b) in terms of $\hat{\mathcal{U}}_a$, the reduced density matrix can be expressed as

$$\tilde{\rho}_{11'}(t_1, t_0) = \langle \tilde{\rho}_{11'}(t_1, t_0) \rangle_V, \quad (\text{B.29a})$$

$$\tilde{\rho}_{11'}(t_1, t_0) \equiv \frac{\langle \hat{\mathcal{U}}_B^\dagger(t_1, t_0) \hat{n}_{11'I}(t_1) \hat{\mathcal{U}}_F(t_1, t_0) \rangle_0}{Z(t_1, t_0)}, \quad (\text{B.29b})$$

$$Z(t_1, t_0) \equiv \langle \hat{\mathcal{U}}_B^\dagger(t_1, t_0) \hat{\mathcal{U}}_F(t_1, t_0) \rangle_0, \quad (\text{B.29c})$$

$$\langle \mathcal{F}[V_a] \rangle_V \equiv \frac{\int \mathcal{D}V_F \int \mathcal{D}V_B \mathcal{F}[V_a] e^{iS_V^{\text{tot}}(t_1, t_0)/\hbar}}{\int \mathcal{D}V_F \int \mathcal{D}V_B e^{iS_V^{\text{tot}}(t_1, t_0)/\hbar}}, \quad (\text{B.29d})$$

$$iS_V^{\text{tot}}(t_1, t_0) \equiv i(S_V^{0F} - S_V^{0B}) + \hbar \ln Z. \quad (\text{B.29e})$$

In Eq. (B.29a), the reduced density matrix $\tilde{\rho}_{11'}$ is expressed as a functional average, over all configurations of the fields V_a , of the functional $\tilde{\rho}_{11'}(t_1, t_0)$. The latter, defined in Eq. (B.29b) (and called ρ_V by GZ), is the reduced density matrix corresponding to a particular configuration of the fields V_a . For any such functional $\mathcal{F}[V_a]$, the functional average is defined by the functional integral (B.29d), with an effective action S_V^{tot} given by (B.29e). Note that S_V^{tot} , via its dependence on Z , depends on the source field \tilde{v} .

B.4. Roadmap for GZ's Strategy

If, in Eq. (B.29b) for $\tilde{\rho}_{11'}(t_1, t_0)$, the evolution operators $\hat{\mathcal{U}}_a$ are expanded in powers of the \hat{V}_a 's, the standard Keldysh perturbation expansion for these correlators would result (as recapitulated in App. E). The approach of AAG¹⁷ amounts to doing just such an expansion to order \hat{V}_a^2 . However, such a perturbation expansion has infrared divergencies which are cured only when the leading divergencies are summed to all orders (or by introducing an infrared cut-off by hand, such as an external magnetic field, as done by AAG). At present, no exact way of summing the entire perturbation series is known. Already in 1982, AAK¹⁰ were able to perform a summation of the leading infrared divergencies by treating \hat{V}_a as a classical field; this indeed cured the infrared problems, but neglects the quantum nature of \hat{V}_a , hence corrections to AAK's calculation are to be expected at sufficiently low temperatures.

GZ attempted to proceed both beyond AAK's calculation (by including quantum corrections) and beyond perturbation theory (by summing an infinite subset of the perturbation series). The essence of their idea was to integrate out all electron degrees of freedom but one, the "singled-out electron", thereby deriving an influ-

ence functional describing the effect of the other electrons (an effective dissipative environment) on the diffusive motion of the singled-out electron. To this end, they adopted the following strategy, which we shall repeat below in our own notation:

- (A)** An exact equation of motion is derived for $\tilde{\rho}_{11'}(t, t_0)$ [(GZ-II.24), our (B.33)].
- (B)** From this, another exact equation of motion is derived for the linear response $\delta\tilde{\rho}_{11'}(t_1, t_0)$ to the source field \tilde{v} [(GZ-II.39), our (B.35)], together with the form of the effective Hamiltonian \tilde{H}_{ij}^a [(GZ-II.40), our (B.36)] which governs the dynamics of $\delta\tilde{\rho}_{11'}(t_1, t_0)$.
- (C)** This second equation of motion is integrated exactly [(GZ-II.41), our (B.38)] in terms of effective evolution matrix functions $\tilde{U}_{ij}^a(t, t')$ [(GZ-II.42), our (B.40)].
- (D)** A functional derivative of $\delta\tilde{\rho}_{11'}(t_1, t_0)$ w.r.t. to the source field \tilde{v} is taken to obtain an expression for the conductivity [(GZ-II.49), our (B.53) or (B.55)], which involves a functional average of the form $\langle \tilde{U}^F \tilde{\rho}^0 \tilde{U}^B \rangle_V$ over the fields V_a [Eqs. (B.52)], where $\tilde{\rho}^0 \equiv \tilde{\rho}_{V_a=0}$ is the (initial) density matrix in the absence of interactions. The purpose of the subsequent steps **(E)** to **(G)** is to facilitate the evaluation of this functional average.
- (E)** The evolution functions \tilde{U}_{ij}^a introduced in **(C)** are represented as path integrals over the degrees of freedom of a single electron, whose Hamiltonian depends on the fields V_a . We shall use a coordinate-space-only path integral $\int \tilde{\mathcal{D}}'(\mathbf{R})$ [Eq. (B.56)], thereby deviating somewhat from GZ, who use position-momentum space integrals $\int \mathcal{D}\mathbf{R}^a \mathcal{D}\mathbf{P}^a$ [(GZ-II.44), our Eq. (D.1a)]. The relation between GZ's position-momentum and our coordinates-only path integrals is explained in time-slicing detail in App. D.
- (F)** The action S_V^{tot} (more specifically, the term $\ln Z$) that governs the weights of different configurations of the fields V_a in the functional average $\langle \tilde{U}^F \tilde{\rho}^0 \tilde{U}^B \rangle_V$, is expanded to second order in \hat{V}_a , corresponding to the standard RPA approximation [(GZ-II.30), our Eqs. (B.62) and (B.68)].
- (G)** The density matrix $\tilde{\rho}_{ii'}(t_i, t_0)$, wherever it still occurs, is approximated by its noninteracting ($V_a = 0$) version $\tilde{\rho}_{ii'}^0$. [GZ make this approximation twice: (i) in the propagators \tilde{U}_{ij}^a , to obtain (GZ-II.43), and (ii) in the initial-time thermal averaging, to obtain (GZ-II.49); we use the analogue of (i) [Sec. B.5.7], but do not need (ii).]
- (H)** The functional average $\langle \cdot \rangle_V$, which through the approximations **(F)** and **(G)** has been reduced to a Gaussian functional integral, is performed to yield an effective action $i\tilde{S}_R + \tilde{S}_I$ [(GZ-II.54), (GZ-II.55), our (B.79), (B.83)]. This effective action determines the influence functional of the environment (the other electrons) on the singled-out electron.

In GZ's paper the above steps are presented in a somewhat different order: approximation **(F)** is discussed already after **(B)**, and approximation **(G)** is made directly after **(C)**. We prefer to carry out the steps in the order stipulated above, because this allows us to postpone each approximation to the latest possible stage.

The results derived by the above steps are used in Secs. B.6 and C.3 to make contact with diagrammatic perturbation theory, and in the main text [Sec. 4] to

calculate the decoherence time. For the latter, we continue to follow GZ's approach in spirit, but use a more careful treatment of a certain "Pauli factor"; remarkably, this turns out to lead to AAK's result for τ_φ instead of GZ's. Although the details of this calculation are presented in the main text, we shall now summarize them here, too, in order that the present brief overview of GZ's strategy be complete.

(I) The term $i\tilde{S}_R$ in the effective action turns out to depend on a certain "Pauli factor" ($\tilde{\delta} - 2\tilde{\rho}^0$), which we treat differently from GZ: In their position-momentum path integral it is represented as $[1 - 2n_0(\tilde{h}_0)]$, where $\tilde{h}_0(\mathbf{R}(t), \mathbf{P}(t))$ is the single-particle energy of the singled-out electron, which GZ assume to remain constant during the diffusive motion. In our opinion, this assumption neglects recoil effects associated with electron-electron interactions [see Sec. B.6.2]. Therefore, we instead use a Fourier representation of the effective action, in which the Pauli factor is represented as $[1 - 2n_0(\hbar(\varepsilon - \bar{\omega}))]$ [Eq. (B.91)], where $\hbar\varepsilon$ corresponds to GZ's \tilde{h}_0 , and $\bar{\omega}$ is the frequency transfer upon emission or absorption of a photon.

(J) The path integrals $\int \tilde{\mathcal{D}}\mathbf{R}'$ for the singled-out electron are performed in the saddle point approximation, meaning that only the contributions of pairs of time-reversed diffusive (or "random walk") paths are retained.

(K) The average of the influence functional over all such random walk paths, namely $\langle e^{-(i\tilde{S}_R + \tilde{S}_I)} \rangle_{\text{rw}}$, is approximated by the exponentiating the average of the effective action, $e^{-\langle i\tilde{S}_R + \tilde{S}_I \rangle_{\text{rw}}}$ [(GZ-II.67), our Sec. 4].

(M) The exponent $F(\tau) = \langle i\tilde{S}_R + \tilde{S}_I \rangle_{\text{rw}}$, a growing function of time, is evaluated by Fourier transforming the effective action into the frequency-momentum domain and averaging the Fourier exponents, using $\langle e^{i\tilde{\mathbf{q}} \cdot [\mathbf{R}(t_3) - \mathbf{R}(t_4)]} \rangle_{\text{rw}} \simeq e^{-\tilde{\mathbf{q}}^2 D |t_{34}|}$ [our Eq. (6)].

(L) The resulting function $F(\tau)$ is used to identify the decoherence time as the time for which $F(\tau_\varphi)$ becomes of order unity [(GZ-II.67), (GZ-II.70), or (GZ-III.6) (GZ-III.22), or our Eq. (18)].

B.5. Repeating GZ's Strategy in Detail

The remainder of this appendix is devoted to a detailed discussion of steps **(A)** to **(I)**, using our own notation.

B.5.1. Exact Equation of Motion for $\tilde{\rho}_{i'i''}(t, t_0)$

To derive an exact equation of motion for $\tilde{\rho}_{i'i''}(t, t_0)$, we start from the simple relations

$$i\hbar\partial_t \hat{\psi}_I(t, x) = h_0(x) \hat{\psi}_I(t, x), \quad (\text{B.30a})$$

$$i\hbar\partial_t \hat{\mathcal{U}}_a(t) = [\hat{V}_a(t) + \hat{v}_I(t)] \hat{\mathcal{U}}_a(t). \quad (\text{B.30b})$$

Since all functions in Eqs. (B.30) are evaluated at the same time t , as are all other functions needed below up to Eq. (B.37), we shall suppress the time argument below

38 *Jan von Delft*

and use the shorthand notation

$$\tilde{\rho}_{ii'} = \tilde{\rho}_{ii'}(t, t_0), \quad \hat{\mathcal{U}}_a \equiv \hat{\mathcal{U}}_a(t, t_0), \quad \hat{n}_{ii'} = \hat{n}_{ii'}(t), \quad (\text{B.31a})$$

$$h_{0i} \equiv h_0(x_i), \quad V_{ai} \equiv V_a(t, \mathbf{r}_i), \quad \tilde{\delta}_{ii'} = \delta^{(d)}(\mathbf{r}_i - \mathbf{r}_{i'})\delta_{\sigma_i\sigma_{i'}}. \quad (\text{B.31b})$$

From Eqs. (B.30), we then readily find

$$i\hbar\partial_t\tilde{\rho}_{ii'} = Z^{-1} \left[i\hbar\partial_t \langle \hat{\mathcal{U}}_B^\dagger \hat{n}_{ii'} \hat{\mathcal{U}}_F \rangle_0 - \tilde{\rho}_{ii'} i\partial_t Z \right], \quad (\text{B.32a})$$

$$i\hbar\partial_t Z = \int dx_k (eV_{Fk} - eV_{Bk}) \langle \hat{\mathcal{U}}_B^\dagger : \hat{n}_{kk} : \hat{\mathcal{U}}_F \rangle_0, \quad (\text{B.32b})$$

$$\begin{aligned} i\hbar\partial_t \langle \hat{\mathcal{U}}_B^\dagger \hat{n}_{ii'} \hat{\mathcal{U}}_F \rangle_0 &= (h_{0i} - h_{0i'}) \langle \hat{\mathcal{U}}_B^\dagger \hat{n}_{ii'} \hat{\mathcal{U}}_F \rangle_0 \\ &+ \int dx_k \langle \hat{\mathcal{U}}_B^\dagger \left[\hat{n}_{ii'} (eV_{Fk} : \hat{n}_{kk} :) - (eV_{Bk} : \hat{n}_{kk} :) \hat{n}_{ii'} \right] \hat{\mathcal{U}}_F \rangle_0 \\ &+ \int dx_{k,\bar{k}} v_{\bar{k}k} \langle \hat{\mathcal{U}}_B^\dagger [\hat{n}_{ii'}, \hat{n}_{k\bar{k}}] \hat{\mathcal{U}}_F \rangle_0. \end{aligned} \quad (\text{B.32c})$$

Eq. (B.32a) can be brought into the form

$$\begin{aligned} i\hbar\partial_t\tilde{\rho}_{ii'} &= \left[h_{0i} + eV_{Fi} \right] \tilde{\rho}_{ii'} - \tilde{\rho}_{ii'} \left[h_{0i'} + eV_{B'i'} \right] \\ &- \int dx_k \left[\tilde{\rho}_{ik} (eV_{Fk} - eV_{Bk}) \tilde{\rho}_{ki'} + \tilde{\rho}_{ik} \tilde{v}_{ki'} - \tilde{v}_{ik} \tilde{\rho}_{ki'} \right] \end{aligned} \quad (\text{B.33})$$

by using the identities

$$\begin{aligned} \hat{n}_{ii'} \hat{n}_{k\bar{k}} &= \hat{\psi}_{i'}^\dagger \left[\tilde{\delta}_{i\bar{k}} - \hat{\psi}_{\bar{k}}^\dagger \hat{\psi}_i \right] \hat{\psi}_k = \hat{n}_{ki'} \tilde{\delta}_{i\bar{k}} + \hat{\psi}_{i'}^\dagger \hat{\psi}_{\bar{k}}^\dagger \hat{\psi}_k \hat{\psi}_i \\ \hat{n}_{k\bar{k}} \hat{n}_{ii'} &= \hat{\psi}_{\bar{k}}^\dagger \left[\tilde{\delta}_{ki'} - \hat{\psi}_i^\dagger \hat{\psi}_k \right] \hat{\psi}_i = \hat{n}_{i\bar{k}} \tilde{\delta}_{ki'} + \hat{\psi}_i^\dagger \hat{\psi}_{\bar{k}}^\dagger \hat{\psi}_k \hat{\psi}_i, \\ Z^{-1} \langle \hat{\mathcal{U}}_B^\dagger \hat{\psi}_{i'}^\dagger \hat{\psi}_{\bar{k}}^\dagger \hat{\psi}_k \hat{\psi}_i \hat{\mathcal{U}}_F \rangle_0 &= \tilde{\rho}_{ii'} \tilde{\rho}_{k\bar{k}} - \tilde{\rho}_{i\bar{k}} \tilde{\rho}_{ki'}. \end{aligned} \quad (\text{B.34})$$

The last of these can be checked by expanding both sides in powers of \hat{V}_a , and evaluating each term in the expansion using Wick's theorem. Since \hat{V}_a is quadratic in $\hat{\psi}$'s, one readily finds that the combinatorial factor for each topologically distinct diagram is just equal to 1, and that the left- and right-hand sides of Eq. (B.34) generate precisely the same set of topologically distinct diagrams.

Eq. (B.33) is the desired equation of motion for $\tilde{\rho}_{ii'}$. [It reduces to (GZ-II.24) upon setting the source fields to zero, $\tilde{v} = 0$ and recalling our footnote a.] The term on the right-hand side of Eq. (B.33) that contains a term *quadratic* in $\tilde{\rho}$, coupling to $e(V_F - V_B)$, will be seen below to be responsible for enforcing the Pauli principle. Note that Eq. (B.33) contains *only* *c*-number functions (no hats occur). Hence the order of factors in products does not matter as long as their subscripts are displayed explicitly (the derivatives contained in the functional operator $h_{0i'}$ should be understood to act on index i' of $\tilde{\rho}_{ii'}$ even if we write them in the order $\tilde{\rho}_{ii'}, h_{0i'}$). Nevertheless, the subscripts do imply that the products have the structure of matrix multiplication in coordinate space; we hence chose to write the factors in an order that is suggestive of this matrix multiplication. [This order conforms to

that used by GZ, in whose notation the coordinate indices are not displayed, but are implicit.]

B.5.2. Equation of Motion for $\delta\tilde{\rho}_{i\bar{i}'}(t, t_0)$

Next, we expand the reduced density matrix to linear order in the source field (which is sufficient for a linear response calculation of the conductivity) by writing $\tilde{\rho}_{i\bar{i}'} = \tilde{\rho}_{i\bar{i}'}^{(\text{ns})} + \delta\tilde{\rho}_{i\bar{i}'}$, where the superscript (ns) denotes “no sources” and $\delta\tilde{\rho}_{i\bar{i}'}$ is linear in \tilde{v} . It satisfies the following equation of motion, found by expanding Eq. (B.33),

$$i\hbar\partial_t\delta\tilde{\rho}_{i\bar{i}'} = \tilde{D}_{i\bar{i}'} + \int dx_{\bar{i}} \tilde{H}_{i\bar{i}}^F \delta\tilde{\rho}_{\bar{i}\bar{i}'} - \int dx_{\bar{i}'} \delta\tilde{\rho}_{i\bar{i}'} \tilde{H}_{\bar{i}\bar{i}'}^B, \quad (\text{B.35a})$$

$$\tilde{D}_{i\bar{i}'} \equiv \int dx_{\bar{i}} \tilde{v}_{i\bar{i}} \tilde{\rho}_{\bar{i}\bar{i}'}^{(\text{ns})} - \int dx_{\bar{i}'} \tilde{\rho}_{i\bar{i}'}^{(\text{ns})} \tilde{v}_{\bar{i}'\bar{i}'}, \quad (\text{B.35b})$$

where the effective Hamiltonians \tilde{H}^F and \tilde{H}^B are defined as follows:^c

$$\tilde{H}_{i\bar{i}}^F \equiv h_{0i} \tilde{\delta}_{i\bar{i}} + \tilde{h}_{V_{i\bar{i}}}^F, \quad \tilde{H}_{\bar{i}\bar{i}'}^B \equiv \tilde{\delta}_{\bar{i}\bar{i}'} h_{0i} + \tilde{h}_{V_{\bar{i}\bar{i}'}}^B, \quad (\text{B.36a})$$

$$\tilde{h}_{V_{i\bar{i}}}^F = \tilde{\delta}_{i\bar{i}} eV_{F\bar{i}} - \tilde{\rho}_{i\bar{i}}(eV_{F\bar{i}} - eV_{B\bar{i}}) = \sum_{\alpha=\pm} \tilde{w}_{i\bar{i}}^{F\alpha} V_{\alpha\bar{i}}, \quad (\text{B.36b})$$

$$\tilde{h}_{V_{\bar{i}\bar{i}'}}^B = eV_{B\bar{i}} \tilde{\delta}_{\bar{i}\bar{i}'} + (eV_{F\bar{i}} - eV_{B\bar{i}}) \tilde{\rho}_{\bar{i}\bar{i}'} = \sum_{\alpha=\pm} V_{\alpha\bar{i}} \tilde{w}_{\bar{i}\bar{i}'}^{B\alpha},$$

$$\tilde{w}_{i\bar{i}}^{a+} \equiv e \tilde{\delta}_{i\bar{i}}, \quad \tilde{w}_{i\bar{i}}^{a-} \equiv s_a \frac{1}{2} e (\tilde{\delta}_{i\bar{i}} - 2\tilde{\rho}_{i\bar{i}}^{(\text{ns})}). \quad (\text{B.36c})$$

[Eqs.(B.36) correspond to (GZ-II.39,40); their $-eV_x(\mathbf{r}_i)$ corresponds to our \tilde{v}_{ii} .] In Eqs. (B.35), the combination of indices $i\bar{i}$ or $\bar{i}'\bar{i}'$, one without bar, one with, will always refer to two independent position indices associated with the *same* time (i.e. $t_{\bar{i}} \equiv t_{i'}$). The Hamiltonians \tilde{H}^F and \tilde{H}^B are associated with propagation along the upper and lower Keldysh contours, which is why in Eq. (B.35a) they are contracted from the left or right with the first or second index of $\delta\tilde{\rho}_{i\bar{i}'}$. In Eq. (B.36c) for the vertices $\tilde{w}_{i\bar{i}}^{a\alpha}$ and elsewhere below, the symbol s_a stands for “sign of a ”, with $s_{F/B} = \pm 1$. The fields $V_{\alpha\bar{i}} = V_{\alpha\bar{i}}(t_{\bar{i}}, \mathbf{r}_{\bar{i}})$ (with $\alpha = \pm$) occurring in Eq. (B.36b) are defined as symmetric and antisymmetric linear combinations of the fields $V_{\alpha\bar{i}}$ (i.e. the time and coordinate arguments of $V_{+\bar{i}}$ and $V_{-\bar{i}}$ on the upper and lower Keldysh contours are *both* equal to $(t_{\bar{i}}, \mathbf{r}_{\bar{i}})$):

$$\begin{pmatrix} V_{+\bar{i}} \\ V_{-\bar{i}} \end{pmatrix} \equiv \begin{pmatrix} 1/2 & 1/2 \\ 1 & -1 \end{pmatrix} \begin{pmatrix} V_{F\bar{i}} \\ V_{B\bar{i}} \end{pmatrix}. \quad (\text{B.37})$$

^c Note that $\tilde{H}_{i\bar{i}}^a$, like h_{0i} , is a c -number functional operator – the derivatives contained in $h_{0i}\tilde{\delta}_{i\bar{i}}$ get “transferred” onto the function it multiplies:

$$\int dx_{\bar{i}} (\nabla_{\bar{i}}^2 \tilde{\delta}_{i\bar{i}}) \delta\tilde{\rho}_{\bar{i}k} = \nabla_{\bar{i}}^2 \delta\tilde{\rho}_{i\bar{k}}, \quad \int dx_{\bar{i}} \delta\tilde{\rho}_{i\bar{i}} (\nabla_{\bar{i}}^2 \tilde{\delta}_{i\bar{k}}) = \nabla_{\bar{k}}^2 \delta\tilde{\rho}_{i\bar{k}}.$$

Since both $H_{\bar{i}\bar{i}}^F$ and $H_{\bar{i}\bar{i}}^B$ depend, through $V_{\alpha\bar{i}}$, on both $V_{F\bar{i}}$ and $V_{B\bar{i}}$, crossterms will occur below that link the forward and backward Keldysh contours. Note that the field $V_{\alpha\bar{i}}$, which shall always carry a “barred” index below, is contracted with the second index of $w_{\bar{i}\bar{i}}^{F\alpha}$ in $\tilde{h}_{\bar{i}\bar{i}}^F$ or the first index of $\tilde{w}_{\bar{i}\bar{i}}^{B\alpha}$ in $\tilde{h}_{\bar{i}\bar{i}}^B$, respectively. Thus V_- and \tilde{w}^{a-} “do not commute”, which will be important below. The factor $(\tilde{\delta} - 2\tilde{\rho})$ in \tilde{w}^{a-} will be seen below to account for the Pauli principle.

All functions occurring in Eqs. (B.36) depend on the same time argument t , which we henceforth display explicitly again. It is worth emphasizing that, through their dependence on $\tilde{\rho}_{\bar{i}\bar{i}}^{(\text{ns})}(t, t_0)$, the expressions $\delta\tilde{\rho}_{\bar{i}\bar{i}'}$, $\tilde{D}_{\bar{i}\bar{i}}$, $\tilde{H}_{\bar{i}\bar{i}}^a$ and $\tilde{U}_{\bar{i}\bar{j}}^a$ [defined below in Eqs. (B.40)] all explicitly depend on the initial time t_0 , too, although, for notational brevity, this t_0 -dependence will be displayed below only for $\tilde{\rho}_{\bar{i}\bar{i}}^{(\text{ns})}(t, t_0)$.

B.5.3. Exact Expression for $\delta\tilde{\rho}_{\bar{i}\bar{i}'}(t, t_0)$

The formally exact solution of Eqs. (B.35) can be written in the form

$$\delta\tilde{\rho}_{\bar{i}\bar{i}'}(t) = -i \int_{t'_0}^t dt' \int dx_{k,\bar{k}} \tilde{U}_{\bar{i}k}^F(t, t') \tilde{D}_{k\bar{k}}(t') \tilde{U}_{\bar{k}\bar{i}'}^B(t', t), \quad (\text{B.38})$$

where the functions $\tilde{U}_{\bar{i}\bar{j}}^F(t, t')$ and $\tilde{U}_{\bar{j}\bar{i}}^B(t', t)$ are defined by the requirements that

$$\tilde{U}_{\bar{i}\bar{j}}^F(t, t) = \tilde{U}_{\bar{j}\bar{i}}^B(t, t) = \tilde{\delta}_{\bar{i}\bar{j}}, \quad (\text{B.39a})$$

$$i\hbar\partial_t \tilde{U}_{\bar{i}\bar{j}}^F(t, t') = \int dx_{\bar{i}} \tilde{H}_{\bar{i}\bar{i}}^F(t) \tilde{U}_{\bar{i}\bar{j}}^F(t, t'), \quad (\text{B.39b})$$

$$i\hbar\partial_t \tilde{U}_{\bar{j}\bar{i}}^B(t', t) = - \int dx_{\bar{i}} \tilde{U}_{\bar{j}\bar{i}}^B(t', t) \tilde{H}_{\bar{i}\bar{i}}^B(t). \quad (\text{B.39c})$$

Eqs. (B.39) are fulfilled by time-ordered exponentials

$$\tilde{U}_{\bar{i}\bar{j}}^F(t, t') = \left[\mathcal{T} e^{-\frac{i}{\hbar} \int_{t'}^t dt_3 \tilde{H}^F(t_3)} \right]_{\bar{i}\bar{j}}, \quad (\text{B.40a})$$

$$\equiv \tilde{\delta}_{\bar{i}\bar{j}} - \frac{i}{\hbar} \int_{t'}^t dt_3 \tilde{H}_{\bar{i}\bar{j}}^F(t_3) - \frac{1}{\hbar^2} \int_{t'}^t dt_3 \int_{t'}^{t_3} dt_4 \int dx_k \tilde{H}_{\bar{i}k}^F(t_3) \tilde{H}_{k\bar{j}}^F(t_4) + \dots$$

$$\tilde{U}_{\bar{j}\bar{i}}^B(t', t) = \left[\overline{\mathcal{T}} e^{\frac{i}{\hbar} \int_{t'}^t dt_3 \tilde{H}^B(t_3)} \right]_{\bar{j}\bar{i}}, \quad (\text{B.40b})$$

$$\equiv \tilde{\delta}_{\bar{i}\bar{j}} + \frac{i}{\hbar} \int_{t'}^t dt_3 \tilde{H}_{\bar{j}\bar{i}}^B(t_3) - \frac{1}{\hbar^2} \int_{t'}^t dt_4 \int_{t'}^{t_4} dt_3 \int dx_k \tilde{H}_{\bar{j}k}^B(t_3) \tilde{H}_{k\bar{i}}^B(t_4) + \dots$$

where we always take $t > t'$, and where each “internal” product of two factors $\tilde{H}_{\bar{i}k}^a \tilde{H}_{k\bar{j}}^a$ that arises when expanding the exponential involves a further coordinate integral $\int dx_k$. [Below, we shall often suppress time arguments and use the shorthand $\tilde{U}_{\bar{i}\bar{j}}^a \equiv \tilde{U}_{\bar{i}\bar{j}}^a(t_i, t_j)$ and likewise $\tilde{U}_{\bar{j}\bar{i}}^a \equiv \tilde{U}_{\bar{j}\bar{i}}^a(t_i, t_j)$.] Note that the time-ordered exponentials (B.40a) and (B.40b) for $\tilde{U}_{\bar{i}\bar{j}}^F$ and $\tilde{U}_{\bar{j}\bar{i}}^B$ are *defined* in terms of the power series expansions indicated above; the same is true for all path integral representations of $\tilde{U}_{\bar{i}\bar{j}}^F$ and $\tilde{U}_{\bar{j}\bar{i}}^B$ to be used below. Note also that $\tilde{U}_{\bar{i}\bar{j}}^a$ is spin-diagonal, since this is the case for $\tilde{H}_{\bar{i}\bar{i}}^a(t) = \delta_{\sigma_i\sigma_{\bar{i}}} \tilde{H}^a(t, \mathbf{r}_i, \mathbf{r}_{\bar{i}})$ and $\tilde{\rho}_{\bar{i}\bar{i}}(t, t_0) = \delta_{\sigma_i\sigma_{\bar{i}}} \tilde{\rho}(t, t_0; \mathbf{r}_i, \mathbf{r}_{\bar{i}})$.

Eq. (B.38) corresponds to GZ's exact Eq. (GZ-II.41). Note that the procedure by which it was obtained, namely, first differentiating $\tilde{\rho}$ and then integrating $\delta\tilde{\rho}$ w.r.t. t , has produced a result in which the reduced density matrix $\rho^{(\text{ns})}$ appears in the exponent, via its occurrence in \tilde{H}_{ij}^a and \tilde{U}_{ij}^a . Accordingly, the effective action to be derived below will likewise depend on $\rho^{(\text{ns})}$.

Let us now also derive an equation of motion for the time evolution of the density matrix in the *absence* of source fields, $\tilde{\rho}_{ij'}^{(\text{ns})}$, since we need it in Eq. (B.38), where it enters via the \tilde{D} of Eq. (B.35b). [This point is not discussed by GZ, who simply replace $\tilde{\rho}_{ij'}^{(\text{ns})}$ in Eq. (B.38) by $\tilde{\rho}_{ij'}^0$, as discussed in Section B.5.7.] Evidently, the desired equation of motion for $\tilde{\rho}_{ij'}^{(\text{ns})}$ is the $\tilde{v} = 0$ version of that of $\tilde{\rho}_{ij'}$, namely Eq. (B.33) $_{\tilde{v}=0}$, which can, in analogy to Eq. (B.35a) (without its first term), be rewritten as

$$i\hbar\partial_t\tilde{\rho}_{ij'}^{(\text{ns})} = \int dx_{i'}\tilde{H}_{ii'}^a\tilde{\rho}_{ij'}^{(\text{ns})} - \int dx_{j'}\tilde{\rho}_{ij'}^{(\text{ns})}\tilde{H}_{j'j'}^B. \quad (\text{B.41})$$

Here the primed Hamiltonians $\tilde{H}_{ii'}^a$ are defined by equations identical to Eqs. (B.36) for the unprimed ones, except that the vertices $\tilde{w}_{ii}^{a\alpha}$ of Eq. (B.36c) are replaced by primed vertices $\tilde{w}_{ii}^{\prime a\alpha}$ that are defined as follows:^d

$$\tilde{w}_{ii}^{\prime a+} \equiv e\tilde{\delta}_{ii}, \quad \tilde{w}_{ii}^{\prime a-} \equiv s_a\frac{1}{2}e(\tilde{\delta}_{ii} - y^a 2\tilde{\rho}_{ii}^{(\text{ns})}). \quad (\text{B.42})$$

Here the $y^{F/B} \in [0, 1]$ are (arbitrary) real numbers, with $y^F + y^B \equiv 1$. It will turn out below to be convenient to let the choice of values for $y^{\tilde{a}}$ depend on which contour the current vertex at time $t_{2_{\tilde{a}}}$ is located: if it is on contour F/B , we shall choose $y^{F/B} = 0 = 1 - y^{B/F}$ (compactly: $y^{\tilde{a}} = 0$ for $\hat{j}(t_{2_{\tilde{a}}})$ on contour \tilde{a} ; Fig. B1 below shows an example with $\tilde{a} = F$). The solution of Eq. (B.41) can be expressed as

$$\tilde{\rho}_{ij'}^{(\text{ns})}(t, t_0) = \tilde{U}_{ik}^{\prime F}(t, t_0)\tilde{\rho}_{k\bar{k}}^0\tilde{U}_{k'j'}^{\prime B}(t_0, t), \quad \text{with } y^F + y^B = 1, \quad (\text{B.43a})$$

$$= \begin{cases} \tilde{U}_{ik}^{\prime F}(t, t_0)\Big|_{y^F=0}\tilde{\rho}_{k\bar{k}}^0\tilde{U}_{k'j'}^{\prime B}(t_0, t) & \text{if } y^F = 0, y^B = 1, \\ \tilde{U}_{ik}^{\prime F}(t, t_0)\tilde{\rho}_{k\bar{k}}^0\tilde{U}_{k'j'}^{\prime B}(t_0, t)\Big|_{y^B=0} & \text{if } y^B = 0, y^F = 1, \end{cases} \quad (\text{B.43b})$$

The primed propagators $\tilde{U}_{ij'}^{\prime a}$ are defined analogously to Eqs. (B.40), but with $\tilde{H} \rightarrow \tilde{H}'$ everywhere. In Eqs. (B.43) we have implemented the standard initial condition

^dThe reason for the extra y^a in front of $\tilde{\rho}_{ii}^{(\text{ns})}$ for $\tilde{w}_{ii}^{\prime a-}$, which is the only difference compared to \tilde{w}_{ii}^{a-} of Eq. (B.36c), is as follows: The linear response equation of motion for $\delta\tilde{\rho}_{ii'}$ contains two *different* contributions that are quadratic in $\tilde{\rho}$, namely $\tilde{\rho}_{ik}^{(\text{ns})}eV_{-k}\delta\tilde{\rho}_{ki'}$ and $\delta\tilde{\rho}_{ik}eV_{-k}\tilde{\rho}_{ki'}^{(\text{ns})}$, which in Eq. (B.35a) were grouped with the first and second terms of respectively. In contrast, the equation of motion for $\tilde{\rho}_{ij'}^{(\text{ns})}$ turns out to contain on the right-hand side just one type of term quadratic in $\tilde{\rho}$, namely $\tilde{\rho}_{ik}^{(\text{ns})}eV_{-k}\tilde{\rho}_{ki'}^{(\text{ns})}$, with total weight 1. By using $y^F + y^B = 1$ in Eq. (B.42), we have distributed this term with weights y^F and y^B among the two terms on the right-hand side of Eq. (B.41).

for the Keldysh approach, namely that at time $t = t_0$, the density matrix was free, i.e. $\tilde{\rho}_{ij'}^{(\text{ns})}(t_0, t_0) \equiv \tilde{\rho}_{ij'}^0$. Below [cf. Eq. (B.51b)], we shall insert Eqs. (B.43b), with $t_0 \rightarrow -\infty$, into Eq. (B.38), where it enters via the \tilde{D} of Eq. (B.35b), to ensure that thermal averaging is done in the infinite past. This is an important improvement relative to an approximation used by GZ, who simply replace $\tilde{\rho}_{ij'}^{(\text{ns})}(t, t_0)$ in Eq. (B.38) by $\tilde{\rho}_{ij'}^0$; they thereby effectively perform thermal averaging with a nonequilibrium initial density matrix, as discussed in Section B.5.7.

The way in which \tilde{U}_{ij}^F , \tilde{U}_{ij}^B and $\tilde{\rho}_{ij}^{(\text{ns})}$ differ from their free versions is evidently through their dependence on the fields V_a and the density matrix $\tilde{\rho}_{ij}$ in Eqs. (B.36). Let us now briefly discuss their free versions. First, in the absence of all interactions the expression for the reduced density matrix $\tilde{\rho}_{ij}^{(\text{ns})}$ reduces to the form

$$\tilde{\rho}_{ij}^0 = \sum_{\lambda} \psi_{\lambda}(x_i) \psi_{\lambda}^*(x_j) n_0(\xi_{\lambda}) = (\tilde{\rho}_{ji}^0)^* , \quad (\text{B.44a})$$

where $n_0(\xi_{\lambda}) = [e^{\xi_{\lambda}/T} + 1]^{-1}$ is the Fermi function, and $\psi_{\lambda}(x_i)$ are the exact single-particle eigenfunctions of \tilde{h}_{0i} , with eigenvalues ξ_{λ} [cf. Eq. (B.15)]. Next, let \tilde{U}_{ij}^{0a} denote the propagator to which \tilde{U}_{ij}^a reduces in the absence of interactions, i.e. for $V_{ai} = 0$ in Eqs. (B.36) [so that $\tilde{H}_{ij}^a = h_{0i}\delta_{ij}$]. Its explicit form is easily found by constructing an object satisfying the defining Eqs. (B.39) for $V_{ai} = 0$; the result is independent of whether $a = F$ or B , and given by:

$$\tilde{U}_{ij}^{0a} \equiv \tilde{U}_{ij}^0 = \sum_{\lambda} \psi_{\lambda}(x_i) \psi_{\lambda}^*(x_j) e^{-i\xi_{\lambda} t_{ij}/\hbar} = i\hbar(\tilde{G}_{ij}^R - \tilde{G}_{ij}^A) , \quad (\text{B.45})$$

where $\tilde{G}_{ij}^{R/A} = \pm\theta(\pm t_{ij})(\tilde{G}_{ij}^> - \tilde{G}_{ij}^<)$ are the standard free retarded and advanced electron Green's functions, with

$$\mp i\hbar \tilde{G}_{ij}^{</>} \equiv \left\{ \begin{array}{l} \langle \hat{\psi}_I^{\dagger}(t_j, x_j) \hat{\psi}_I(t_i, x_i) \rangle_0 \\ \langle \hat{\psi}_I(t_i, x_i) \hat{\psi}_I^{\dagger}(t_j, x_j) \rangle_0 \end{array} \right\} = \sum_{\lambda} \psi_{\lambda}(x_i) \psi_{\lambda}^*(x_j) e^{-i\xi_{\lambda} t/\hbar} n_0(\pm\xi_{\lambda}) . \quad (\text{B.46})$$

It follows that for a given time order, as occurs under a time-ordered integral, \tilde{U}_{ij}^{0a} is equal to *either* a retarded *or* an advanced Green's function; e.g., for $t_i > t_j$, we have $\tilde{U}_{ij}^{0F} = i\hbar\tilde{G}_{ij}^R$ and $\tilde{U}_{ji}^{0B} = -i\hbar\tilde{G}_{ji}^A$. Nevertheless, it will be useful to generally retain both terms in Eq. (B.45), because that allows expressions involving the free reduced density matrix to be simplified by Fourier transforming from the time to the frequency domain: for example, denoting the frequency Fourier transform of $\tilde{U}_{ij}^0(t)$ by $\tilde{U}_{ij}^0(\omega)$, we immediately find the exceedingly useful relations:

$$\int dx_{\bar{i}} \tilde{\rho}_{i\bar{i}}^0 \tilde{U}_{ij}^0(\omega) = n_0(\hbar\omega) \tilde{U}_{ij}^0(\omega) = -i\hbar\tilde{G}_{ij}^<(\omega) , \quad (\text{B.47a})$$

$$\int dx_{\bar{i}} [\tilde{\delta} - 2\tilde{\rho}_{i\bar{i}}^0] \tilde{U}_{ij}^0(\omega) = [1 - 2n_0(\hbar\omega/2T)] \tilde{U}_{ij}^0(\omega) = i\hbar\tilde{G}_{ij}^K(\omega) , \quad (\text{B.47b})$$

where $G_{ij}^K = \tilde{G}_{ij}^> + \tilde{G}_{ij}^<$ is the Keldysh function. Note, in particular, that by passing to the frequency representation, the Pauli factor $(\tilde{\delta} - 2\tilde{\rho}^0)$ in Eq. (B.47b) gets mapped

onto $[1 - 2n_0(\hbar\omega/2T)] = \tanh(\hbar\omega/2T)$, a fact that will be very useful in Sec. B.6.2 below.

For future reference, we note that when the matrix propagators \tilde{U}_{ij}^F and \tilde{U}_{ij}^B [with $t > t'$] are expanded in powers of \tilde{h}_V^a [i.e. in powers of the fields V_α , see Eqs. (B.36b)], they take the form of time-ordered or anti-time-ordered power series, respectively:

$$\left. \begin{aligned} \tilde{U}_{ij}^F(t, t') \\ \tilde{U}_{ji}^B(t', t) \end{aligned} \right\} = \sum_{N=0}^{\infty} \frac{1}{\hbar^N} \int_{t_j}^{t_i} dt_1 \int_{t_j}^{t_1} dt_2 \dots \int_{t_j}^{t_{N-1}} dt_N \int dx_{1,\bar{1}} dx_{2,\bar{2}} \dots dx_{N,\bar{N}} \times \begin{cases} (-i)^N \tilde{U}_{i\bar{1}}^{0F} \tilde{h}_{V\bar{1}\bar{1}}^F \tilde{U}_{\bar{1}\bar{2}}^{0F} \dots \tilde{h}_{V\bar{N}\bar{N}}^F \tilde{U}_{\bar{N}j}^{0F} \\ (+i)^N \tilde{U}_{j\bar{N}}^{0B} \tilde{h}_{V\bar{N}\bar{N}}^B \dots \tilde{U}_{\bar{2}\bar{1}}^{0B} \tilde{h}_{V\bar{1}\bar{1}}^B \tilde{U}_{\bar{1}i}^{0B} \end{cases} . \quad (\text{B.48})$$

These expansions [illustrated in App. D by the third row of Fig. D1] are alternative but equivalent to those of Eqs. (B.40), and, just as the latter, can be regarded as formal *definitions* of \tilde{U}_{ij}^a , and of all path-integral representations thereof to be used below. Note that for each occurrence of a “vertex” $\tilde{h}_{V\bar{l}_F\bar{l}_F}^F$ or $\tilde{h}_{V\bar{l}_B\bar{l}_B}^B$, the vertex coordinates x_{l_a} and $x_{\bar{l}_a}$ are both associated with the *same* time t_l , and both are integrated over in $\int dx_{l,\bar{l}}$ [cf. Eq. (B.6)]. This need for a double position integral at each vertex is a direct consequence of the fact that the effective Hamiltonians \tilde{H}_{ij}^a of Eqs. (B.36) are nonlocal in space. Since the integrals in Eq. (B.48) are time-ordered, each \tilde{U}^{0F} occurring in \tilde{U}^F can be replaced by $i\hbar\tilde{G}^R$, and each \tilde{U}^{0B} in \tilde{U}^B by $-i\hbar\tilde{G}^A$ [see Eq. (D.11c)]. Indeed, the latter replacements are, in effect, used in the path integral representation of \tilde{U}^a to be introduced below [Eq. (B.56)]. We have nevertheless chosen to write Eq. (B.48) in terms of \tilde{U}^{0a} functions, as a reminder that the density matrices occurring in the interaction vertices \tilde{h}_V^a can be converted to Fermi functions using Eqs. (B.47).

B.5.4. Exact Expression for Conductivity

The density-density commutator $\tilde{\mathcal{C}}_{[11',22']}$ [Eqs. (B.19), (B.27), (B.29a) and (B.38)] can now be obtained by taking the functional derivative of $\delta\tilde{\rho}_{12}(t)$ with respect to the source field \tilde{v} [occurring in (B.38) via \tilde{D} of (B.35b)]. Henceforth writing $t \equiv t_1$ and $t' \equiv t_2$, the result can be written as

$$\tilde{\mathcal{C}}_{[11',22']}(t_1 - t_2) = \sum_{\tilde{a}=F,B} \tilde{J}_{12',21'}^{(\tilde{a})}(t_1, t_2; t_0) + \tilde{\mathcal{C}}_{[11',22']}^{\text{Hartree}}, \quad (\text{B.49})$$

44 *Jan von Delft*

where $\tilde{\mathcal{C}}_{[11',22']}^{\text{Hartree}}$ is a contribution irrelevant for weak localization, which will be dropped henceforth.^e The $\tilde{J}^{(\tilde{a})}$'s are defined in terms of the correlator

$$\tilde{J}_{12',2\bar{2}',\bar{2}1'}^V(t_1, t_2; t_0) \equiv \frac{1}{\hbar} \tilde{U}_{12'}^F(t_1, t_2) \tilde{\rho}_{2\bar{2}'}^{(\text{ns})}(t_2, t_0) \tilde{U}_{\bar{2}1'}^B(t_2, t_1) \quad (\text{B.51a})$$

$$= \frac{1}{\hbar} \int dx_{0,\bar{0}} \tilde{U}_{12'}^F(t_1, t_2) \tilde{U}'_{20}(t_2, t_0) \tilde{\rho}_{0\bar{0}}^0 \tilde{U}'_{0\bar{2}'}(t_0, t_2) \tilde{U}_{\bar{2}1'}^B(t_2, t_1), \quad (\text{B.51b})$$

[the second line follows via Eq. (B.43a)] by:

$$\begin{aligned} \tilde{J}_{12',21'}^{(F)}(t_1, t_2; t_0) &\equiv \int dx_{\bar{2}} \left\langle \tilde{J}_{12',2\bar{2}',\bar{2}1'}^V(t_1, t_2; t_0) \right\rangle_{V,\text{ns}} \quad (\text{B.52a}) \\ &= \int dx_{0,\bar{0}} \frac{1}{\hbar} \left\langle \tilde{U}_{12'}^F \tilde{U}'_{20} \tilde{\rho}_{0\bar{0}}^0 \tilde{U}_{0\bar{1}'}^B \right\rangle_{V,\text{ns}}^{y^F=0}, \end{aligned}$$

$$\begin{aligned} \tilde{J}_{12',21'}^{(B)}(t_1, t_2; t_0) &\equiv - \int dx_{\bar{2}} \left\langle \tilde{J}_{12',2\bar{2}',21'}^V(t_1, t_2; t_0) \right\rangle_{V,\text{ns}} \quad (\text{B.52b}) \\ &= - \int dx_{0,\bar{0}} \frac{1}{\hbar} \left\langle \tilde{U}_{10}^F \tilde{\rho}_{0\bar{0}}^0 \tilde{U}'_{0\bar{2}'}^B \tilde{U}_{21'}^B \right\rangle_{V,\text{ns}}^{y^B=0}. \end{aligned}$$

$\tilde{J}^{(F)}$ [illustrated in Fig. B1] and $\tilde{J}^{(B)}$ denote correlators that have a current vertex inserted on the forward or backward Keldysh contours, respectively. As a notational reminder, the indices 2, 2', and $\bar{2}$ here all refer to the same time, t_2 in this case, and after performing the derivatives implicit in $\mathbf{j}_{11'}$ and $h_{22'}^{\text{ext}}$, we have to set $2 = 2'$. However, $x_{\bar{2}}$ in Eqs. (B.52) is an independent integration variable. The subscript ns (for “no sources”) in $\langle \rangle_{V,\text{ns}}$ indicates that, following the prescription of Eq. (B.27a), all remaining \tilde{v} -dependencies are to be dropped henceforth by setting $\tilde{v} = 0$. The second lines of Eqs. (B.52a) and (B.52b), in which we set $y^{\tilde{a}} = 0$ for the correlator $\tilde{J}^{(\tilde{a})}$ containing the current vertex on contour \tilde{a} , follow from Eq. (B.51b) for $\tilde{J}_{12',2\bar{2}',\bar{2}1'}^V$ by using the first or second line of Eq. (B.43b) for $\tilde{U}'^F \tilde{\rho}^0 \tilde{U}'^B$, respectively

^e The term $\tilde{\mathcal{C}}_{[11',22']}^{\text{Hartree}}$ in Eq. (B.49) has the form

$$\begin{aligned} \tilde{\mathcal{C}}_{[11',22']}^{\text{Hartree}} &= i \langle \tilde{\rho}_{12}(t_1, t_0) \frac{\delta \ln Z}{\delta \tilde{v}_{2'2}(t_2)} \rangle_{V,\text{ns}} - i \langle \tilde{\rho}_{12}(t_1, t_0) \rangle_{V,\text{ns}} \langle \frac{\delta \ln Z}{\delta \tilde{v}_{2'2}(t_2)} \rangle_{V,\text{ns}}, \\ \frac{\delta \ln Z}{\delta \tilde{v}_{2'2}(t_2)} &= -i \frac{1}{\hbar Z} \left[\langle \hat{U}_B^\dagger(t_1, t_0) \hat{U}_F(t_1, t_2) \hat{n}_{22'I}(t_2) \hat{U}_F(t_2, t_0) \rangle_0 \right. \\ &\quad \left. - \langle \hat{U}_B^\dagger(t_2, t_0) \hat{n}_{22'I}(t_2) \hat{U}_B^\dagger(t_1, t_2) \hat{U}_F(t_2, t_0) \rangle_0 \right], \end{aligned}$$

and arises since the effective action S_V^{tot} of Eq. (B.29e) in the functional average (B.29d) depends, via $\ln Z$, on \tilde{v} too. $\tilde{\mathcal{C}}_{[11',22']}^{\text{Hartree}}$ corresponds to (GZ-II.47) and is neglected by GZ [see the discussion after (GZ-II.47)], because in the absence of interactions, it vanishes entirely, and hence does not contribute to the weak localization correction to the conductivity (in other words, $\tilde{\mathcal{C}}_{[11',22']}^{\text{Hartree}}$ is irrelevant to the question how this correction is affected by interactions). We shall not consider it further either, since in diagrammatic terms it corresponds to Hartree contributions to the electron Green's functions, which merely renormalize the magnitude of the conductivity (and were neglected by AAG¹⁷, too).

[thereby conveniently avoiding primed propagators \tilde{U}' under the $x_{\bar{2}}$ -integrals on the “other” contour $\tilde{a}' \neq \tilde{a}$, which thus have the form $\int dx_{\bar{2}} \tilde{U}'_{i\bar{2}} \tilde{U}_{\bar{2}j} = \tilde{U}'_{ij}$; the latter composition rule follows from Eq. (B.45) and the completeness of the wavefunctions $\psi_{\lambda}(x_i)$ occurring therein.]

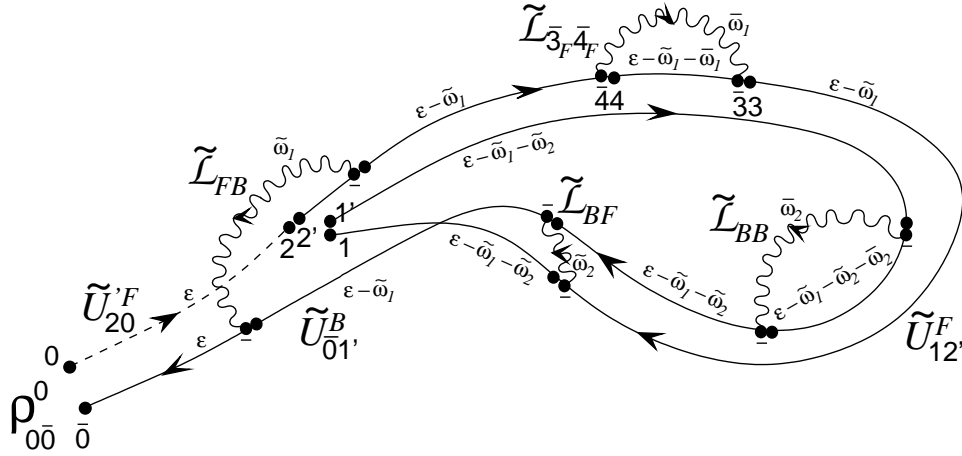


Fig. B1. A pair of backward (B) and forward (F) paths contributing to $\tilde{J}_{12',21'}^{(F)}(t_1, t_2; t_0)$, with $t_1 > t_2 > t_0$. There are two ways to view this figure: (i) Ignore the wavy interaction lines, double dot vertices and frequency assignments; then this figure illustrates the second line of Eq. (B.52a), and the solid or dashed lines represent the full unprimed ($\tilde{U}^{F/B}$) or primed ($\tilde{U}'^{F/B}$) propagators, respectively. (ii) Imagine the propagators $\tilde{U}^{F/B}$ and $\tilde{U}'^{F/B}$ to have been expanded in powers of the interaction [as in Eq. (B.48)]. This generates a forward and backward backbone of free propagators \tilde{U}_{ij}^{0F} or $\tilde{U}_{j\bar{i}}^{0B}$ (represented by either solid or dashed lines, which now have identical meanings), which are respectively decorated by the vertices $\tilde{h}_{V\bar{i}\bar{i}}^F$ and $\tilde{h}_{V\bar{i}\bar{i}}^B$ (represented by a pair of dots; both dots are associated with the same time, but the one drawn on the side of earlier times is distinguished by a bar; the origin of this convention is explained in App. D, Fig. D1). The vertices generate, after averaging over the fields $V_{a\bar{i}}$, the wavy interaction lines $\tilde{L}_{i\bar{a}j\bar{a}'}$, connected to the barred dots. [The interaction lines are labelled according to Eq. (B.84) below: $\tilde{L}_{aa'}$ stands for $\tilde{L}_{i\bar{a}j\bar{a}'}$, $\tilde{L}_{i\bar{a}j\bar{a}'}$ or $\tilde{L}_{j\bar{a}'i\bar{a}}$, if generated by $\langle V_{+\bar{i}a} V_{+\bar{j}a'} \rangle_V$, $\langle V_{+\bar{i}a} V_{-\bar{j}a'} \rangle_V$, or $\langle V_{-\bar{i}a} V_{+\bar{j}a'} \rangle_V$, respectively, cf. Eq. (B.75b).] For both cases (i) and (ii), arrows are drawn to point from the second index to the first index of each of $\tilde{U}_{ij}^{F/B}$, $\tilde{U}_{j\bar{i}}^{B/F}$ and $\tilde{L}_{i\bar{a}j\bar{a}'}$. Thus, they point from later to earlier times along the backward Keldysh contour, and from earlier to later times along the forward Keldysh contour (i.e. they form a continuous loop, starting on the backward contour from t_1 backwards to $t_0 = -\infty$, then continuing on the forward contour from $t_0 = -\infty$ forwards via t_2 to t_1). Finally, the frequencies label the interaction correlators $\tilde{L}_{aa'}(\omega)$ and Green's functions $\tilde{G}^{R/A}(\omega)$ and $\tilde{G}^K(\omega) = \tanh(\hbar\omega/2T)[\tilde{G}^R - \tilde{G}^A](\omega)$ that arise (before disorder averaging) upon Fourier transforming from the time to the frequency domain, as for Eqs. (B.86) or (C.16) below. The effective action defined in Eqs. (2) to (4a) of the main text neglects the frequency transfers ω_i in the arguments of all retarded and advanced electron Green's functions [$\tilde{G}^{R/A}(\epsilon - \omega_i - \dots) \rightarrow \tilde{G}^{R/A}(\epsilon)$], but, for every $\tilde{L}^{R/A}(\omega_i)\tilde{G}^K(\epsilon - \omega_i)$, retains it in the factor $\tanh[\hbar(\epsilon - \omega_i)/\hbar]$ of the accompanying \tilde{G}^K function. [As discussed in Sec. 3 or B.6.2, this is justified by the fact that all integrals over frequency transfer variables are limited by Fermi factors to the range $|\hbar\omega_i| \lesssim T$].

Inserting Eq. (B.49) for $\tilde{C}_{[11',22']}$ into Eq. (B.22a), the expression for σ_{DC} that

46 *Jan von Delft*

results upon representing the applied field in terms of a scalar potential, and then relabelling $x_2 \leftrightarrow x_{\bar{2}}$ in the term containing $\tilde{J}^{(B)}$, we find:

$$\sigma_{\text{DC}} = \frac{e^2}{2m d} \sum_{\sigma_1} \int_{-\infty}^{t_1} dt_2 \int dx_{2,\bar{2}} \quad (\text{B.53})$$

$$[\mathbf{r}_2 - \mathbf{r}_{\bar{2}}] \cdot (\nabla_1 - \nabla_{1'}) \langle \tilde{J}_{12',2\bar{2},\bar{2}1'}^V(t_1, t_2; t_0) \rangle_{V, \text{ns}} .$$

Eq. (B.53) for the DC conductivity is analogous (but, as discussed below, not identical) to (GZ-II.49) [the factor $\tilde{U}_{12'}^F(t_1, t_2) \tilde{U}_{\bar{2}1'}^B(t_2, t_1)$ which occurs in our $J_{12',2\bar{2},\bar{2}1'}(t_1, t_2; t_0)$ is the analogue of the function $J(t_1, t_2; \mathbf{r}_1, \mathbf{r}'_1; \mathbf{r}_2, \mathbf{r}_2)$ occurring in Eqs. (GZ-II.49) and (GZ-II.50)]. In deriving Eq. (B.53), no approximations have been made, apart from not displaying the Hartree terms [cf. footnote e].

Instead of (B.22a) and (B.53), it will be more convenient for our purposes to use Eq. (B.22b) as alternative expression for σ_{DC} , derived by representing the applied external field via a vector potential. The correlator $\tilde{J}_{12',21'}(\omega_0)$ occurring therein can [via Eq. (B.49)] be expressed as:

$$\tilde{J}_{12',21'}(\omega_0) \equiv \int_{-\infty}^{\infty} dt_{12} e^{i\omega_0 t_{12}} \lim_{t_0 \rightarrow -\infty} \sum_{\bar{a}=F,B} \theta_{12} \tilde{J}_{12',21'}^{(\bar{a})}(t_1, t_2; t_0) . \quad (\text{B.54})$$

Since $\tilde{J}_{12',21'}$ stems from the commutator $\tilde{C}_{[11',22']}$ [Eq. (B.19)], whose terms satisfy $\langle \hat{n}_{11'H} \hat{n}_{22'H} \rangle = \langle \hat{n}_{22'H} \hat{n}_{11'H} \rangle^*$, the correlators $\tilde{J}^{(a)}$ satisfy

$$\tilde{J}_{12',21'}^{(B)}(t_1, t_2; t_0) = -\tilde{J}_{1'2,2'1}^{(F)*}(t_1, t_2; t_0) , \quad \tilde{J}_{12',21'}^{(B)}(\omega_0) = -[\tilde{J}_{1'2,2'1}^{(F)}(-\omega_0)]^*$$

The first of these [which implies the second] is manifestly obeyed by Eqs. (B.52). Taylor-expanding Eq. (B.22b) using $\tilde{J}(\omega_0) = \tilde{J}(0) + \omega_0 \tilde{J}'(0) + \dots$, and separating $\sigma_{\text{DC}} = \sigma_{\text{DC,real}} + i\sigma_{\text{DC,imag}}$ into real and imaginary parts, we obtain

$$\sigma_{\text{DC,real}} = \sum_{\sigma_1} \frac{1}{d} \int dx_2 \mathbf{j}_{11'} \cdot \mathbf{j}_{22'} \tilde{J}'_{12',21'}(0) , \quad (\text{B.55a})$$

$$i\sigma_{\text{DC,imag}} = \lim_{\omega_0 \rightarrow 0} \frac{1}{\omega_0} \sum_{\sigma_1} \left[\frac{ie^2 \langle \hat{n}_{11H} \rangle}{m} + \frac{1}{d} \int dx_2 \mathbf{j}_{11'} \cdot \mathbf{j}_{22'} \tilde{J}_{12',21'}(0) \right] . \quad (\text{B.55b})$$

Since we have taken the DC-limit $\omega_0 \rightarrow 0$, the imaginary part $\sigma_{\text{DC,imag}}$ must be strictly equal to 0 (to all orders in the interaction), which is a useful consistency check.

In App. C we show how Eqs. (B.55) can be massaged into more familiar expressions for σ_{DC} , both in the absence and presence of interactions [cf. Eqs. (C.3), (C.8b), (C.28b)].

B.5.5. Coordinate-Space Path-Integral Representation for \tilde{U}_{ij}^a

In this subsection we shall derive path integral expressions for the objects in terms of which the conductivity is expressed in Eq. (B.55a), namely the propagators \tilde{U}_{ij}^a

[Eq. (B.40)] and the interaction-averaged correlators $\langle \tilde{J}^{(\tilde{a})} \rangle_V$ [Eqs. (B.52)]. We deviate from GZ's approach, who used a path integral $\int \mathcal{D}\mathbf{R} \int \mathbf{P}$ over both coordinate and momentum space, in that we shall use coordinate-space-only path integrals $\int \tilde{\mathcal{D}}'(\mathbf{R})$, because that makes possible a more accurate treatment of the crucial nonlocal Pauli factors $(\tilde{\delta} - 2\tilde{\rho})$ in the effective Hamiltonian \tilde{H}^a of Eq. (B.36).

We begin from the power series expansions (B.48) of the evolution matrix functions $\tilde{U}_{ij}^a(t, t')$ of Eqs. (B.40) in powers of \tilde{h}_V^a , and introduce, as a shorthand for these expansions, the following coordinate space path integrals:

$$\left. \begin{aligned} \tilde{U}_{ij}^F(t, t') \\ \tilde{U}_{ji}^B(t', t) \end{aligned} \right\} = \int_{\mathbf{R}^a(t')=\mathbf{r}_j}^{\mathbf{R}^a(t)=\mathbf{r}_i} \tilde{\mathcal{D}}' \mathbf{R}^a e^{i s_a \tilde{S}_0^a(t, t')/\hbar} \exp \left[\frac{-i s_a}{\hbar} \int_{t'}^t dt_3 \left\{ \tilde{h}_{V_{3F\bar{3}F}}^F \right. \right. \\ \left. \left. \tilde{h}_{V_{\bar{3}B3B}}^B \right\} \right]. \quad (\text{B.56})$$

Here s_a stands for $s_{F/B} = \pm$, and the index value $a = F$ or B should be used for the upper or lower term in the curly bracket, respectively. The coordinate-space path integral is over all paths $\mathbf{R}^a(t_3)$ that begin at time t' at point \mathbf{r}_j and end at time t at point \mathbf{r}_i ; the time t_3 that is used to parametrize this path $\mathbf{R}^a(t_3)$ is understood to refer to the upper or lower Keldysh contour for $a = F$ or B , respectively [in this sense, an index a on t_3 is implicit, as in $\mathbf{R}^a(t_{3_a})$]. The objects \tilde{S}_0^a and \tilde{h}_V^a in the exponential factors in Eq. (B.56) are both functionals of the path $\mathbf{R}^a(t_3)$: S_0^a is the standard action for a noninteracting electron in a disorder potential,

$$\tilde{S}_0^a(t, t')[\mathbf{R}^a(t_3)] \equiv \int_{t'}^t dt_3 \left[\frac{1}{2} m \dot{\mathbf{R}}^{a2}(t_3) - V_{\text{imp}}(\mathbf{R}^a(t_3)) \right], \quad (\text{B.57})$$

whereas in the second exponential, we used the following shorthand notation:

$$\tilde{h}_{V_{3F\bar{3}F}}^F = \sum_{\alpha=\pm} \tilde{w}_{3F\bar{3}F}^{F\alpha} V_{\alpha\bar{3}F} = \sum_{\alpha=\pm} \tilde{w}^{F\alpha} [t_3, \mathbf{r}_3^F(t_3), \mathbf{r}_3^F(t_3)] V_{\alpha} [t_3, \mathbf{r}_3^F(t_3)], \quad (\text{B.58a})$$

$$\tilde{h}_{V_{\bar{3}B3B}}^B = \sum_{\alpha=\pm} V_{\alpha\bar{3}B} \tilde{w}_{\bar{3}B3B}^{B\alpha} = \sum_{\alpha=\pm} V_{\alpha} [t_3, \mathbf{r}_3^B(t_3)] \tilde{w}^{B\alpha} [t_3, \mathbf{r}_3^B(t_3), \mathbf{r}_3^B(t_3)]. \quad (\text{B.58b})$$

In App. D we give an explicit definition of the path integral Eq. (B.56) by time-slicing the time interval $[t', t]$ [Sec. D.4], and a detailed demonstration that it satisfies the defining Eqs. (B.39) [Sec. D.2]. The explicit derivation given there shows that, when writing down the path integral (B.56), the following points are to be implicitly understood [see also Fig. D1 of App. D]: (i) The path integral (B.56) is simply a short-hand for the time-ordered power series expansion (B.48), with $(-i/\hbar)\tilde{U}_{iFjF}^{0F}$ replaced by \tilde{G}_{iFjF}^R and $(i/\hbar)\tilde{U}_{jB\bar{i}B}^{0B}$ by $\tilde{G}_{jB\bar{i}B}^A$ [cf. Eq. (D.11c)]. (ii) For each occurrence of a ‘‘vertex’’ $\tilde{h}_{V_{3F\bar{3}F}}^F$ or $\tilde{h}_{V_{\bar{3}B3B}}^B$, the vertex coordinates $\mathbf{r}_3^a(t_3)$ and $\mathbf{r}_3^a(t_3)$ are both associated with the *same* time t_3 , and both are assumed to be integrated over in the path integral [as in Eq. (B.48)], thereby taking into account the nonlocal nature of the Hamiltonians $\tilde{h}_{V_{ij}}^a$. (iii) The associated integrations $\int dx_{3,\bar{3}}$ are understood to be included in the measure $\int \tilde{\mathcal{D}}' \mathbf{R}^a$ (the prime serves as reminder of this fact), in addition to the integrations associated with propagators between vertices. (iv) Vertices are connected by propagators of the form \tilde{G}_{iFjF}^R or $\tilde{G}_{jB\bar{i}B}^A$ on the forward or backward Keldysh contours, respectively. However, since these propagators occur under

time-ordered integrals anyway, they can equally well also be written as $(-i/\hbar)\tilde{U}_{i_F j_F}^{0F}$ or $(i/\hbar)\tilde{U}_{j_B i_B}^{0B}$, as is convenient [in order to exploit Eq. (B.47)] whenever they are contracted with a density matrix $\tilde{\rho}_{i_F i_F}^0$ or $\tilde{\rho}_{i_B i_B}^0$.

Now use the path integral representation (B.56) (twice) in Eq. (B.51b) for $\langle \tilde{J}^V \rangle_{V, \text{ns}}$, and interchange the order of averages, $\langle \int \tilde{\mathcal{D}}'(\mathbf{R}) \dots \rangle_V \rightarrow \int \tilde{\mathcal{D}}'(\mathbf{R}) \langle \dots \rangle_V$. [The latter step could have been postponed until the beginning of Section B.5.8, but is used already here, since it simplifies subsequent expressions. Its use, sooner or later, is a crucial ingredient in GZ's approach. Its far-reaching consequences are discussed in detail in App. A.4.] We obtain

$$\begin{aligned} \langle \tilde{J}_{12', 2\bar{2}', 21'}^V(t_1, t_2; t_0) \rangle_{V, \text{ns}} &= \frac{1}{\hbar} \int dx_{0_F, \bar{0}_B} \tilde{\rho}_{0_F \bar{0}_B} \\ &\times \int_{2'_F}^{1_F} \int_{\bar{2}_B}^{1'_B} \tilde{\mathcal{D}}'(\mathbf{R}) \int_{0_F}^{2_F} \int_{\bar{0}_B}^{2'_B} \tilde{\mathcal{D}}'(\mathbf{R}) \tilde{\mathcal{F}}_{(t_1, t_0)}[\mathbf{R}^a], \end{aligned} \quad (\text{B.59})$$

where $\int_{j_F}^{i_F} \int_{\bar{j}_B}^{\bar{i}_B} \tilde{\mathcal{D}}'(\mathbf{R})$ is used as a shorthand for the following forward and backward path integral between the specified initial and final coordinates and times:

$$\begin{aligned} \int_{j_F}^{i_F} \int_{\bar{j}_B}^{\bar{i}_B} \tilde{\mathcal{D}}'(\mathbf{R}) \dots &\equiv \int_{\mathbf{R}^F(t_j^F)=\mathbf{r}_j^F}^{\mathbf{R}^F(t_i^F)=\mathbf{r}_i^F} \tilde{\mathcal{D}}' \mathbf{R}^F(t_3) e^{i\tilde{S}_0^F(t_i^F, t_j^F)/\hbar} \\ &\times \int_{\mathbf{R}^B(t_j^B)=\mathbf{r}_j^B}^{\mathbf{R}^B(t_i^B)=\mathbf{r}_i^B} \tilde{\mathcal{D}}' \mathbf{R}^B(t_3) e^{-i\tilde{S}_0^B(t_i^B, t_j^B)/\hbar} \dots \end{aligned} \quad (\text{B.60})$$

The influence functional $\tilde{\mathcal{F}}_{(t_1, t_0)}[\mathbf{R}^a]$ in Eq. (B.59) is defined by the following functional integral over all configurations of the fields $V_{\pm 3} = V_{\pm}(t_3, \mathbf{r}_3)$ of Eqs. (B.37), with $t_3 \in [t_0, t_1]$:

$$\tilde{\mathcal{F}}_{(t_1, t_0)}[\mathbf{R}^F(t_3); \mathbf{R}^B(t_3)] \equiv \frac{\int \mathcal{D}V_+ \int \mathcal{D}V_- e^{\frac{i}{\hbar}[S_V^{\text{tot}} - \tilde{\mathcal{B}} \cdot \mathcal{V}](t_1, t_0)}}{\int \mathcal{D}V_+ \int \mathcal{D}V_- e^{\frac{i}{\hbar}S_V^{\text{tot}}(t_1, t_0)}}, \quad (\text{B.61a})$$

$$\tilde{\mathcal{B}} \cdot \mathcal{V}(t_1, t_0) \equiv \int_{t_0}^{t_1} dt_3 \int d\mathbf{r}_3 \sum_{\alpha=\pm} \tilde{\mathcal{B}}_{\alpha}(t_3, \mathbf{r}_3) V_{\alpha}(t_3, \mathbf{r}_3), \quad (\text{B.61b})$$

$$\tilde{\mathcal{B}}_{\alpha}(t_3, \mathbf{r}_3) \equiv s_F \tilde{W}_{3_F 3_F}^{F\alpha} \delta(\mathbf{r}_3 - \mathbf{r}_{3_F}) + s_B \tilde{W}_{3_B 3_B}^{B\alpha} \delta(\mathbf{r}_3 - \mathbf{r}_{3_B}), \quad (\text{B.61c})$$

$$\tilde{W}_{33}^{a\alpha} \equiv \theta_{32} \tilde{w}_{33}^{a\alpha} + \theta_{23} \tilde{w}'_{33}{}^{a\alpha}. \quad (\text{B.61d})$$

Here $S_V^{\text{tot}}(t_1, t_0)$ is given by Eq. (B.29e), and Eq. (B.61c), which defines the field $\tilde{\mathcal{B}}_{\alpha 3} = \mathcal{B}_{\alpha}(t_3, \mathbf{r}_3)$, follows from using Eqs. (B.58) or a primed version thereof, for $t_3 > t_2$ or $t_3 < t_2$, respectively. The distinction between the two time orderings, which is reflected in the definition (B.61d) of the vertices $\tilde{W}_{33}^{a\alpha}$ (and not noted by GZ, since they set $t_0 = t_2$), is necessary, since Eq. (B.51b) correspondingly features unprimed or primed propagators \tilde{U}_{ij}^a or $\tilde{U}'_{ij}{}^a$, respectively, which have different vertices [compare Eqs. (B.36c) and (B.42)]. Note that $\tilde{\mathcal{B}}_{\alpha 3}$ is itself a functional of

both the paths $\mathbf{R}^F(t_3)$ and $\mathbf{R}^B(t_3)$. The influence functional^f $\tilde{\mathcal{F}}_{(t_1, t_0)}[\mathbf{R}^a]$ describes the effect of all other electrons on a pair (forward and backward) of singled-out electron trajectories $\mathbf{R}^F(t_3)$ and $\mathbf{R}^B(t_3)$ between the initial time t_0 and final time t_1 . Importantly, this influence functional incorporates the Pauli principle, via the presence of the Pauli factor $(\tilde{\delta} - 2\tilde{\rho})$ in \tilde{w}^{a-} .

B.5.6. RPA Approximation

To evaluate the influence functional $\tilde{\mathcal{F}}_{(t_1, t_0)}$ explicitly, our next task is to perform the functional integrals $\int \mathcal{D}V_\alpha$ stipulated in Eq. (B.61a). As a first (standard) step toward making these integrals Gaussian, i.e. doable, we apply (following GZ) the RPA approximation: we approximate the effective action S_V^{tot} of Eq. (B.29e) by the part quadratic in the fields V , say

$$iS_V^{(2)}(t_1, t_0) = i(S_V^{0F} - S_V^{0B}) + \hbar Z^{(2)} \equiv -\frac{1}{2} [\mathcal{V} \cdot \tilde{\mathcal{A}} \cdot \mathcal{V}](t_1, t_0) \quad (\text{B.62a})$$

$$= -\frac{1}{2} \int_{t_0}^{t_1} dt_3 \int_{t_0}^{t_1} dt_4 \int d\mathbf{r}_3 d\mathbf{r}_4 \sum_{\alpha\alpha'} V_{\alpha 3} \tilde{\mathcal{A}}_{34}^{\alpha\alpha'} V_{\alpha' 4}, \quad (\text{B.62b})$$

so that Eq. (B.61a) becomes

$$\tilde{\mathcal{F}}_{(t_1, t_0)} \xrightarrow{\text{RPA}} \frac{\int \mathcal{D}V_+ \int \mathcal{D}V_- e^{-\frac{1}{2\hbar} \mathcal{V} \cdot \tilde{\mathcal{A}} \cdot \mathcal{V}} e^{-\frac{i}{\hbar} \tilde{\mathcal{B}} \cdot \mathcal{V}}}{\int \mathcal{D}V_+ \int \mathcal{D}V_- e^{-\frac{1}{2\hbar} \mathcal{V} \cdot \tilde{\mathcal{A}} \cdot \mathcal{V}}}. \quad (\text{B.63})$$

To find $\tilde{\mathcal{A}}$, we have to find an explicit expression for the term $\hbar Z^{(2)}$ in Eq. (B.62a), which arises from expanding the factor $\ln Z = Z^{(2)} + \mathcal{O}(V_a^3)$ to second order in V_a , using

$$Z(t_1, t_0) = 1 + Z^{(1)} + Z^{(2)} + \mathcal{O}(V_a^3), \quad (\text{B.64a})$$

$$Z^{(2)} = -\frac{1}{2\hbar^2} \int_{t_0}^{t_1} dt_3 \int_{t_0}^{t_1} dt_4 \left\{ \langle \mathcal{T} \hat{V}_F(t_3) \hat{V}_F(t_4) \rangle + \langle \bar{\mathcal{T}} \hat{V}_B(t_3) \hat{V}_B(t_4) \rangle - 2 \langle \hat{V}_B(t_3) \hat{V}_F(t_4) \rangle_0 \right\}, \quad (\text{B.64b})$$

and noting that $Z^{(1)}$ vanishes, since \hat{V}_a is normal-ordered [cf. Eq. (B.28d)]. Expressing Eq. (B.64b) through the fields $V_{\alpha i}$ ($\alpha = \pm 1$) of Eq. (B.37), we find

$$\hbar Z^{(2)} = -\int_{t_0}^{t_1} dt_3 \int_{t_0}^{t_1} dt_4 \int d\mathbf{r}_3 d\mathbf{r}_4 \left(iV_{-3} \tilde{\chi}_{34} V_{+4} + V_{-3} \tilde{\eta}_{34} V_{-4} \right), \quad (\text{B.65})$$

where $\tilde{\chi}_{ij}$ (the charge susceptibility) and $\tilde{\eta}_{ij}$ (characterizing charge fluctuations) are defined as

$$\tilde{\chi}_{ij} \equiv -i \frac{2e^2}{\hbar} \theta(t_{ij}) \langle [\hat{n}_{iiI}(t_1), \hat{n}_{jjI}(t_j)] \rangle_0 = 4e^2 \hbar \text{Im} [\tilde{G}_{ij}^R \tilde{G}_{ji}^<], \quad (\text{B.66a})$$

^f The term ‘‘influence functional’’ is used here in precisely the sense in which Feynman used it: Our $\tilde{\mathcal{F}}_{23}[\mathbf{R}^a]$ is analogous to the quantity $F[q(t), q'(t)]$ of Eq. (12-90) of R. P. Feynman and A. R. Hibbs, ‘‘Quantum Mechanics and Path Integrals’’, McGraw-Hill (1965).

50 *Jan von Delft*

$$\tilde{\eta}_{ij} \equiv \frac{e^2}{2\hbar} \langle \{ : \hat{n}_{iiI}(t_i) :, : \hat{n}_{jjI}(t_j) : \} \rangle_0 = -e^2 \hbar \operatorname{Re} [\tilde{G}_{ij}^> \tilde{G}_{ji}^<] , \quad (\text{B.66b})$$

with equal spins, $\sigma_i = \sigma_j$ (for $\sigma_i \neq \sigma_j$, both these quantities vanish). [Eqs. (B.66) correspond to (GZ-II.31) and (GZ-II.32).] The right-most equalities were obtained by using Wick's theorem to rewrite the correlators in terms of the single-particle Green's functions $\tilde{G}^{<,>}$ [Eqs. (B.46)]. The Fourier transforms of $\tilde{\chi}_{ij}$ and $\tilde{\eta}_{ij}$ satisfy $\bar{\chi}_{-\mathbf{k}}^*(-\omega) = \bar{\chi}_{\mathbf{k}}(\omega) = \bar{\chi}_{-\mathbf{k}}(\omega)$ and $\bar{\eta}_{-\mathbf{k}}(-\omega) = \bar{\eta}_{\mathbf{k}}(\omega)$ (thus the latter is real), and are related by the fluctuation dissipation theorem [(GZ-II.33)]:

$$\bar{\eta}_{\mathbf{k}}(\omega) = -\frac{1}{2} \coth(\hbar\omega/2T) \operatorname{Im} \bar{\chi}_{\mathbf{k}}(\omega) . \quad (\text{B.67})$$

Now, if we write the second-order contribution $iS_V^{(2)}(t, t_0)$ in the form of Eq. (B.62b), and Fourier transform,[§] we obtain from Eqs. (B.28b) and (B.65):

$$\mathcal{V} \cdot \bar{\mathcal{A}} \cdot \mathcal{V} = \int \frac{d\mathbf{k} d\omega}{(2\pi)^{d+1}} \sum_{\alpha\alpha'} \bar{V}_{\alpha, -\mathbf{k}}(-\omega) \bar{\mathcal{A}}_{\mathbf{k}}^{\alpha\alpha'}(\omega) \bar{V}_{\alpha', \mathbf{k}}(\omega) , \quad (\text{B.68a})$$

$$\bar{\mathcal{A}}_{\mathbf{k}}^{\alpha\alpha'}(\omega) = -i \begin{pmatrix} 0 & \frac{\bar{\varepsilon}_{-\mathbf{k}}(-\omega)}{\bar{V}^{\text{int}}(\mathbf{k})} \\ \frac{\bar{\varepsilon}_{\mathbf{k}}(\omega)}{\bar{V}^{\text{int}}(\mathbf{k})} & 2i\bar{\eta}_{\mathbf{k}}(\omega) \end{pmatrix}_{\alpha\alpha'} , \quad (\text{B.68b})$$

where $\bar{\varepsilon}_{\mathbf{k}}(\omega) \equiv 1 - \bar{V}^{\text{int}}(\mathbf{k}) \bar{\chi}_{\mathbf{k}}(\omega)$ is the dielectric susceptibility. [The latter relation is a generalized version of (GZ-II.35); in (GZ-II.36), GZ added to $\bar{\varepsilon}_{\mathbf{k}}(\omega)$ an electron-phonon contribution, which is not important for the present discussion and neglected by GZ themselves later on, after (GZ-II.75).]

Having found $\bar{\mathcal{A}}$, let us now also find and discuss some useful properties of its inverse, $\bar{\mathcal{A}}^{-1}$ [it will be needed in the next section after evaluating the functional integral Eq. (B.63)]. Using $\bar{\varepsilon}_{-\mathbf{k}}(-\omega) = \bar{\varepsilon}_{\mathbf{k}}^*(\omega)$, we find

$$(\bar{\mathcal{A}}^{-1})_{\mathbf{k}}^{\alpha\alpha'}(\omega) = \begin{pmatrix} \bar{I}_{\mathbf{k}}(\omega) & i\bar{R}_{\mathbf{k}}(\omega) \\ i\bar{R}_{-\mathbf{k}}(-\omega) & 0 \end{pmatrix} , \quad (\text{B.69})$$

with matrix elements given by

$$\bar{R}_{\mathbf{k}}(\omega) = \frac{\bar{V}^{\text{int}}(\mathbf{k})}{\bar{\varepsilon}_{\mathbf{k}}(\omega)} , \quad (\text{B.70a})$$

$$\bar{I}_{\mathbf{k}}(\omega) = \frac{2\bar{\eta}_{\mathbf{k}}(\omega) |\bar{V}^{\text{int}}(\mathbf{k})|^2}{|\bar{\varepsilon}_{\mathbf{k}}(\omega)|^2} = -\coth(\hbar\omega/2T) \operatorname{Im} \bar{R}_{\mathbf{k}}(\omega) , \quad (\text{B.70b})$$

where the last equality in Eq. (B.70b) follows from Eq. (B.67). Note that the assumptions [stated before Eq. (B.14)] that $\bar{V}^{\text{int}}(\mathbf{k})$ is real and symmetric, imply that

$$\bar{R}_{-\mathbf{k}}^*(-\omega) = \bar{R}_{\mathbf{k}}(\omega) = \bar{R}_{-\mathbf{k}}(\omega) , \quad \bar{I}_{-\mathbf{k}}^*(-\omega) = \bar{I}_{\mathbf{k}}(\omega) = \bar{I}_{-\mathbf{k}}(\omega) = \bar{I}_{\mathbf{k}}(-\omega) , \quad (\text{B.71})$$

[§]Strictly speaking the Fourier transform (B.68a) is an exact representation of $\mathcal{V} \cdot \bar{\mathcal{A}} \cdot \mathcal{V}$ only if the time integrals in Eq. (B.62b) are unbounded, e.g. for $t_0 = -\infty$ and $t_1 = \infty$. In our formalism, this indeed is the case, since we do take the limit $t_0 \rightarrow -\infty$, and may also take $t_1 \rightarrow +\infty$ (because the t_1 -dependence drops out, anyway).

so that the functions \tilde{R}_{ij} and \tilde{I}_{ij} are both purely real: $\tilde{R}_{ij} = \tilde{R}_{ij}^*$ and $\tilde{I}_{ij} = \tilde{I}_{ij}^* = \tilde{I}_{ji}$. For reference purposes, we note also that their frequency Fourier transforms, denoted by $\tilde{R}_{ij}(\omega)$ and $\tilde{I}_{ij}(\omega)$, satisfy the relations $\tilde{R}_{ij}(\omega) = \tilde{R}_{ji}(\omega) = \tilde{R}_{ij}^*(-\omega)$ and

$$\tilde{I}_{ij}(\omega) = \tilde{I}_{ji}(\omega) = \tilde{I}_{ij}^*(-\omega) = \tilde{I}_{ij}(-\omega) = -\coth(\hbar\omega/2T)\text{Im}[\tilde{R}_{ij}(\omega)]. \quad (\text{B.72})$$

Furthermore, $\tilde{R}_{ij}(\omega)$ is analytic in the upper half plane, implying that \tilde{R}_{ij} is proportional to $\theta(t_{ij})$. In contrast, \tilde{I}_{ij} is symmetric in its indices and thus nonzero for both $t_{ij} > 0$ and < 0 .

The components of $\tilde{\mathcal{A}}^{-1}$ are of course related to field correlation functions of the type $\langle V_{\alpha i} V_{\alpha' j} \rangle_{V, \text{ns}}$, as follows from a simple exercise in Gaussian integration: Introducing the generating functional

$$Q[\zeta] \equiv \langle e^{-\frac{i}{\hbar}\zeta \cdot \mathcal{V}} \rangle_{V, \text{ns}}, \quad (\text{B.73a})$$

$$[\zeta \cdot \mathcal{V}](t_1, t_0) \equiv \int_{t_0}^{t_1} dt_3 \int d\mathbf{r}_3 \sum_{\alpha=\pm} \zeta_{\alpha 3} V_{\alpha 3}, \quad (\text{B.73b})$$

where $\zeta_{\alpha i} = \zeta_{\alpha}(t_i, \mathbf{r}_i)$, with $\alpha = \pm 1$, are two real source fields, we find

$$Q[\zeta] \xrightarrow{\text{RPA}} \frac{\int \mathcal{D}V_+ \int \mathcal{D}V_- e^{-\frac{1}{2\hbar}\mathcal{V} \cdot \tilde{\mathcal{A}} \cdot \mathcal{V}} e^{-\frac{i}{\hbar}\zeta \cdot \mathcal{V}}}{\int \mathcal{D}V_+ \int \mathcal{D}V_- e^{-\frac{1}{2\hbar}\mathcal{V} \cdot \tilde{\mathcal{A}} \cdot \mathcal{V}}} = e^{-\frac{1}{2\hbar}\zeta \cdot \tilde{\mathcal{A}}^{-1} \cdot \zeta}. \quad (\text{B.74a})$$

The field correlators are then easily found to have the form

$$\frac{1}{\hbar} \langle V_{\alpha i} V_{\alpha' j} \rangle_{V, \text{ns}} = -\hbar \frac{\delta^2 Q[\zeta]}{\delta \zeta_{\alpha i} \delta \zeta_{\alpha' j}} \Big|_{\zeta=0} = (\tilde{\mathcal{A}}^{-1})_{ij}^{\alpha\alpha'} = \begin{pmatrix} \tilde{I}_{ij} & i\tilde{R}_{ij} \\ i\tilde{R}_{ji} & 0 \end{pmatrix}_{\alpha\alpha'} \quad (\text{B.75a})$$

$$= -\frac{i}{e^2} \begin{pmatrix} \frac{1}{2}\tilde{\mathcal{L}}_{ij}^K & \tilde{\mathcal{L}}_{ij}^R \\ \tilde{\mathcal{L}}_{ij}^A & 0 \end{pmatrix}_{\alpha\alpha'}. \quad (\text{B.75b})$$

where Eq. (B.69) has been used, and the functions [cf. (GZ-II.56) and (GZ-II.57)]

$$(\tilde{R}/\tilde{I})_{ij} = \int (d\mathbf{k})(d\omega) e^{-i\omega(t_i - t_j) + i\mathbf{k} \cdot (\mathbf{r}_i - \mathbf{r}_j)} (\tilde{R}/\tilde{I})_{\mathbf{k}}(\omega) \quad (\text{B.76})$$

are defined via their Fourier transforms, given by Eqs. (B.70a) and (B.70b) above. Eq. (B.75b) expresses the general fact [reviewed in App. E.2] that the field correlators can also be written in terms of the standard retarded, advanced and Keldysh components of the interaction propagator, $\tilde{\mathcal{L}}_{ij}^R$, $\tilde{\mathcal{L}}_{ij}^A$ and $\tilde{\mathcal{L}}_{ij}^K$, implying that these are proportional to \tilde{R}_{ij} , \tilde{R}_{ji} and \tilde{I}_{ij} [cf. (GZ-III.A14)]. This implies that \tilde{R}_{ij} is a retarded propagator and thereby confirms that it is proportional to $\theta(t_{ij})$ [as had already been concluded above from the analytic properties of $\tilde{R}_{ij}(\omega)$].

To obtain explicit expressions for $\tilde{R}_{\mathbf{k}}(\omega)$, one needs $\bar{\varepsilon}_{\mathbf{k}}(\omega)$ and hence $\bar{\chi}_{\mathbf{k}}(\omega)$, for which one has to calculate a polarization bubble [see App. F, Fig. F1(e)]. If $\bar{V}^{\text{int}}(\mathbf{k}) = 4\pi/\mathbf{k}^2$ represents the unscreened Coulomb interaction [Eq. (B.14) with $\lambda_0 = 0$] and, as is usually the case in the presence of disorder, only small frequencies

52 *Jan von Delft*

and wave numbers are of interest, a standard calculation yields [cf. Eq. (F.5e) and (GZ-II.36)]:

$$\bar{\chi}_{\mathbf{k}}(\omega) = -\frac{\mathbf{k}^2 \sigma_{\text{DC}}^{\text{Drude}}}{D\mathbf{k}^2 - i\omega}, \quad \bar{\varepsilon}_{\mathbf{k}}(\omega) = 1 + \frac{4\pi\sigma_{\text{DC}}^{\text{Drude}}}{D\mathbf{k}^2 - i\omega}, \quad \bar{R}_{\mathbf{k}}(\omega) = \frac{D\mathbf{k}^2 - i\omega}{e^2 2\nu D\mathbf{k}^2}. \quad (\text{B.77})$$

B.5.7. Approximating $\tilde{\rho}_{ij}^{(\text{ns})}$ by $\tilde{\rho}_{ij}^0$

Even after having made the RPA approximation, the functional integral in Eq. (B.63) over all field configurations of V_α is not yet Gaussian. The reason is that the term $\mathcal{B}' \cdot \mathcal{V}$ in the exponent depends, via \tilde{w}^{a-} , on the full, interacting density matrix $\tilde{\rho}_{ij}^{(\text{ns})}(t')$, which depends on the fields V_α too, in a highly nontrivial way. To make further progress, we shall ultimately have to neglect the effect of interactions on the single-particle density matrix, by replacing $\tilde{\rho}_{ij}^{(\text{ns})}(t')$ by its noninteracting (and hence time-independent) version $\tilde{\rho}_{ij}^0$:

$$\tilde{\rho}_{ij}^{(\text{ns})}(t') \xrightarrow{\text{approx}} \tilde{\rho}_{ij}^0 \equiv \langle \hat{n}_{ijS} \rangle_0. \quad (\text{B.78})$$

GZ use this approximation at two points in their calculation [see the comment after (GZ-II.43)]: (GZi) to simplify the propagators \tilde{U}_{ij}^a , namely when passing from (GZ-II.40) to (GZ-II.43); and (GZii) to simplify the thermal weighting factor describing the initial distribution of electrons, namely to obtain the explicit factor ρ_0 in (GZ-II.49). In our formalism, (GZii) would correspond to setting $t_0 \rightarrow t_2$, i.e. making the replacement $\tilde{\rho}_{2\bar{2}'}^{(\text{ns})}(t_2, t_0) \rightarrow \rho_{2\bar{2}'}^0$, in Eq. (B.51a) for $\tilde{J}_{12', 2\bar{2}', \bar{2}1'}^V(t_1, t_2; t_0)$ and inserting the result into Eq. (B.53), since this would reproduce (GZ-II.49).

We shall use similar but weaker approximations, and proceed in two separate steps:

(i) We “linearize” the exponential factor $\tilde{\mathcal{B}} \cdot \mathcal{V}$ in Eq. (B.63) by making the replacement $\tilde{\mathcal{B}}[\tilde{\rho}_{ij}^{(\text{ns})}] \rightarrow \tilde{\mathcal{B}}[\tilde{\rho}_{ij}^0]$, so that the functional integral (B.63) becomes truly Gaussian in \mathcal{V} and can readily be performed [see Sec. B.5.8]. We thereby neglect the effect of interactions on all occurrences (via \tilde{w}^{a-} in \tilde{h}_V^a) of $\tilde{\rho}^{(\text{ns})}$ in the propagators \tilde{U}_{ij}^a , the rationale being that in order to calculate the decoherence rate, we are interested in how the interaction affects the time-evolved *propagation* of electrons along time-reversed paths, and not how it modifies equal-time objects like $\tilde{\rho}_{ij}$. Diagrammatically, this corresponds to neglecting diagrams which modify the Keldysh Green’s function without affecting the retarded or advanced ones, i.e. which modify only the tanh factor, but not the propagator \tilde{U}_{ij} in Eq. (B.47b).

(ii) For the propagator $J^{(\tilde{a})}$, which is defined as the sum of all terms for which the current vertex $j_{2\bar{2}'}$ occurs on contour \tilde{a} at time $t_{2\bar{a}}$, we neglect all interaction vertices that occur on the *same* contour \tilde{a} at earlier times $t_{3\bar{a}}$ or $t_{4\bar{a}} \in [t_0, t_{2\bar{a}}]$. Thus, in the second lines of Eqs. (B.52a) and (B.52b), we make the replacements $\tilde{U}_{20}^{F'} \rightarrow \tilde{U}_{20}^0$ and $\tilde{U}_{02'}^{B'} \rightarrow U_{02'}^0$. However, for the opposite contour containing no current vertex, we include interaction vertices for all times $\in [t_0, t_1]$. The rationale for this is that, in diagrammatic language, this approximation retains only those dia-

grams for which *both* current vertices $\hat{j}_{22'}$ and $\hat{j}_{11'}$ are always sandwiched between a \tilde{G}^R - and a \tilde{G}^A -function, i.e. $\tilde{G}^R \hat{j} \tilde{G}^A$. These are the ones relevant for the Cooperon; the contributions thereby neglected correspond to the so-called “interaction corrections”, which feature at least on current vertex sandwiched between two retarded or advanced functions, i.e. $\tilde{G}^R \hat{j} \tilde{G}^R$ or $\tilde{G}^A \hat{j} \tilde{G}^A$.

Note that this approximation (ii) is much weaker than (GZii): we do *not* replace $\tilde{\rho}_{22'}^{(\text{ns})}$ by $\tilde{\rho}_{22'}^0$, in Eq. (B.51a) (i.e. we do not set $t_0 \rightarrow t_2$), but instead use $\tilde{\rho}_{22'}^{(\text{ns})}(t_2, t_0) = \tilde{U}_{20}^F \tilde{\rho}_{00}^0 \tilde{U}_{02'}^B$, [Eq. (B.43a)] and send $t_0 \rightarrow -\infty$. Also, we wish to emphasize that “interaction correction” terms *can* be calculated from our formalism if one so chooses, by avoiding our approximation (ii) altogether and keeping track of all interaction insertions on the entire interval $[t_0, t_1]$ of *both* contours [Eqs. (C.10c) and (C.10d) give examples of such contributions]. For the sake of greater generality, we shall thus for the moment use only approximation (i), and postpone the use of (ii) to Sec. B.6.

B.5.8. Integrating out the Fields V_α to obtain $i\tilde{S}_R + \tilde{S}_I$

The approximations discussed in the previous two subsections render the functional integral (B.63) for $\tilde{\mathcal{F}}_{(t_1, t_0)}[\mathbf{R}^a]$ Gaussian. In fact, Eq. (B.63) is just of the form (B.74a), with $\zeta \cdot \mathcal{V}$ replaced by $\tilde{\mathcal{B}} \cdot \mathcal{V}$ of Eq. (B.61c), so that we get

$$\tilde{\mathcal{F}}_{(t_1, t_0)}[\mathbf{R}^a] = e^{-\frac{1}{2\hbar} \tilde{\mathcal{B}} \cdot \tilde{\mathcal{A}}^{-1} \cdot \tilde{\mathcal{B}}} \equiv e^{-[i\tilde{S}_R + \tilde{S}_I](t_1, t_0)/\hbar}. \quad (\text{B.79})$$

The exponent $(i\tilde{S}_R + \tilde{S}_I)[\mathbf{R}^a] \equiv \frac{1}{2} \tilde{\mathcal{B}} \cdot \tilde{\mathcal{A}}^{-1} \cdot \tilde{\mathcal{B}}$, which is a functional of the paths \mathbf{R}^a , can be regarded as an “effective action” that describes the effect of interactions on the “singled-out” electron traveling along the paths \mathbf{R}^a . The indices R, I are meant to distinguish terms depending on the interaction propagators \tilde{R} and \tilde{I} . Before working out the effective action explicitly form, however, let us first collect results to obtain path integral expressions for the correlators $\tilde{J}_{12', 21'}^{(F/B)}$ of Eqs. (B.52). These contain the correlators $\langle \tilde{J}_{12', 22', 21'}^V \rangle_{V, (\text{ns})}$, for which we use Eq. (B.59), with $\tilde{\mathcal{F}}_{(t_1, t_0)}$ given by Eq. (B.79), and $\int dx_{\tilde{2}}$ integrals, which we perform in the same way as for the second equalities of Eqs. (B.52):

$$\begin{aligned} \tilde{J}_{12', 21'}^{(F/B)}(t_1, t_2; t_0) &= \pm \frac{1}{\hbar} \int dx_{0_F, \bar{0}_B} \tilde{\rho}_{0_F \bar{0}_B}^0 \\ &\times \left\{ \begin{array}{l} \int_{2'_F}^{1_F} \int_{0_F}^{2_F} \int_{\bar{0}_B}^{1'_B} \tilde{\mathcal{D}}'(\mathbf{R}) \\ \int_{0_F}^{1_F} \int_{2_B}^{1'_B} \int_{\bar{0}_B}^{2'_B} \tilde{\mathcal{D}}'(\mathbf{R}) \end{array} \right\} e^{-[i\tilde{S}_R + \tilde{S}_I](t_1, t_0)/\hbar} \Big|_{y^{F/B}=0}. \end{aligned} \quad (\text{B.80})$$

Combined with the current vertex insertions $\int dx_2 \mathbf{j}_{22'} \cdot \mathbf{j}_{11'}$ of Eq. (B.55a), we obtain

$$\int dx_2 \mathbf{j}_{22'} \cdot \mathbf{j}_{11'} \sum_{\bar{a}=F, B} \tilde{J}_{12', 21'}^{(\bar{a})}(t_1, t_2; t_0) = \int dx_{0_F, \bar{0}_B} \tilde{\rho}_{0_F \bar{0}_B}^0 \int_{0_F}^{1_F} \int_{\bar{0}_B}^{1'_B} \tilde{\mathcal{D}}'(\mathbf{R}) \quad (\text{B.81})$$

54 Jan von Delft

$$\times \frac{1}{\hbar} \left\{ \left[\hat{\mathbf{j}}(t_{2F}) \hat{\mathbf{j}}(t_1) e^{-[i\tilde{S}_R + \tilde{S}_I](t_1, t_0)/\hbar} \right]_{y^F=0} - \left[\hat{\mathbf{j}}(t_{2B}) \hat{\mathbf{j}}(t_1) e^{-[i\tilde{S}_R + \tilde{S}_I](t_1, t_0)/\hbar} \right]_{y^B=0} \right\}.$$

This expression, which is the first central result of our formalism, has a simple interpretation: thermal averaging with $\tilde{\rho}_{00}^0$ at time t_0 ($\rightarrow -\infty$) is followed by propagation, in the presence of interactions (described by $e^{-[i\tilde{S}_R + \tilde{S}_I]}$), along all possible paths from time t_0 up to time t_1 , with insertions of current vertices $\hat{\mathbf{j}}(t_{2a})$ at time t_2 on either the upper or lower Keldysh contour, and another current vertex $\hat{\mathbf{j}}(t_1)$ at the final time.

Let us now determine the effective action explicitly, by using Eq. (B.61c) for $\tilde{\mathcal{B}}$ to evaluate $\frac{1}{2} \tilde{\mathcal{B}} \cdot \tilde{\mathcal{A}}^{-1} \cdot \tilde{\mathcal{B}}$:

$$\begin{aligned} [i\tilde{S}_R + \tilde{S}_I](t_1, t_0)[\mathbf{R}^a] &= \frac{1}{2} \sum_{\alpha\alpha'} \int_{t_0}^{t_1} dt_3 \int_{t_0}^{t_1} dt_4 \\ &\times \left[2\theta_{34} s_F \tilde{W}_{3F3F}^{F\alpha} (\tilde{\mathcal{A}}^{-1})_{3F4F}^{\alpha\alpha'} s_F \tilde{W}_{4F4F}^{F\alpha'} + s_B \tilde{W}_{3B3B}^{B\alpha} (\tilde{\mathcal{A}}^{-1})_{3B4F}^{\alpha\alpha'} s_F \tilde{W}_{4F4F}^{F\alpha'} \right. \\ &\left. + s_F \tilde{W}_{3F3F}^{F\alpha} (\tilde{\mathcal{A}}^{-1})_{3F4B}^{\alpha\alpha'} s_B \tilde{W}_{4B4B}^{B\alpha'} + 2\theta_{34} s_B \tilde{W}_{3B3B}^{B\alpha} (\tilde{\mathcal{A}}^{-1})_{3B4B}^{\alpha\alpha'} s_B \tilde{W}_{4B4B}^{B\alpha'} \right]. \end{aligned} \quad (\text{B.82})$$

There are now two somewhat different routes to proceed, which lead to two somewhat different (but equivalent) representations for the effective action. The first, followed in the present section, exploits symmetries under $3 \leftrightarrow 4$ write the effective action in terms of as few terms as possible, leading to expressions [(B.83), (B.84), or (A.7), (A.8)] useful for recovering the Keldysh diagrammatic results for the Cooperon self energy [(B.89) or (A.10)]. The second, summarized in Section B.6.3, does not combine similar-looking terms, and is useful for establishing contact with other, more standard influence-functional approaches.

Let us proceed with the first route. Since $(\tilde{\mathcal{A}}^{-1})_{34}^{\alpha\alpha'} = (\mathcal{A}^{-1})_{43}^{\alpha'\alpha}$, the integrand in Eq. (B.82) for $\tilde{\mathcal{B}} \cdot \tilde{\mathcal{A}}^{-1} \cdot \tilde{\mathcal{B}}$ is symmetric under the exchange of variables $\sum_{\alpha} \int dt_3 d\mathbf{r}_3 \leftrightarrow \sum_{\alpha'} \int dt_4 d\mathbf{r}_4$. We have exploited this fact to insert a factor of $2\theta_{34}$ into the first and last terms of Eq. (B.82), which both *individually* have this symmetry, to obtain time-ordered integrals for these, which has the advantage of reducing the number of terms in subsequent expressions. (We could similarly have inserted $2\theta_{34}$ into the second and third terms of Eq. (B.82), too, but since only their *sum* has the above-mentioned symmetry, this turns out to be inconvenient.)

More explicit expressions for $\tilde{S}_{R/I}$ can be found with the help of Eqs. (B.61d) for $\tilde{W}_{ij}^{a\alpha}$, Eq. (B.75) for $\tilde{\mathcal{A}}^{-1}$ and recalling that $\theta_{34} \tilde{R}_{43} = 0$. Using the shorthand $(i\tilde{R}/\tilde{S}_I)$ to present two similar equations in one line, and writing $(i\tilde{R}/\tilde{I})_{\bar{i}a\bar{j}a'} = (i\tilde{R}/\tilde{I})[t_{ij}, \mathbf{r}_{\bar{i}}^a(t_i) - \mathbf{r}_{\bar{j}}^{a'}(t_j)]$, where $t_{ij} = t_i - t_j$ [and likewise for $\mathcal{L}_{\bar{i}a\bar{j}a'}^{R,A,K}$], we find:

$$[i\tilde{S}_R/\tilde{S}_I](t_1, t_0)[\mathbf{R}^a] \equiv \sum_{\alpha\alpha'} \int_{t_0}^{t_1} dt_{3a} \int_{t_0}^{t_1} dt_{4a'} (i\tilde{L}^R/\tilde{L}^I)_{3a4a'}[\mathbf{R}^a], \quad (\text{B.83})$$

$$\begin{aligned}
 - (i\tilde{L}^R/\tilde{L}^I)_{3_F 4_F} &= -\theta_{34} s_F s_F \widetilde{W}_{3_F \bar{3}_F}^{F+} \widetilde{W}_{4_F \bar{4}_F}^{F\mp} (i\tilde{R}/\tilde{I})_{\bar{3}_F \bar{4}_F} \\
 &= \frac{1}{2} i \tilde{\delta}_{3_F \bar{3}_F} \left\{ \begin{array}{c} [\tilde{\delta} - (\theta_{42} + y^F \theta_{24}) 2\tilde{\rho}^0]_{4_F \bar{4}_F} \\ \theta_{34} \tilde{\delta}_{4_F \bar{4}_F} \end{array} \right\} \tilde{\mathcal{L}}_{\bar{3}_F \bar{4}_F}^{R/K}, \quad (\text{B.84a})
 \end{aligned}$$

$$\begin{aligned}
 - (i\tilde{L}^R/\tilde{L}^I)_{3_B 4_F} &= -\frac{1}{2} s_B s_F \widetilde{W}_{4_F \bar{4}_F}^{F\mp} (2i\tilde{R}/\tilde{I})_{\bar{3}_B \bar{4}_F} \widetilde{W}_{\bar{3}_B 3_B}^{B+} \\
 &= -\frac{1}{2} i \left\{ \begin{array}{c} [\tilde{\delta} - (\theta_{42} + y^F \theta_{24}) 2\tilde{\rho}^0]_{4_F \bar{4}_F} \\ \frac{1}{2} \tilde{\delta}_{4_F \bar{4}_F} \end{array} \right\} \tilde{\mathcal{L}}_{\bar{3}_B \bar{4}_F}^{R/K} \tilde{\delta}_{\bar{3}_B 3_B}, \quad (\text{B.84b})
 \end{aligned}$$

$$\begin{aligned}
 - (i\tilde{L}^R/\tilde{L}^I)_{3_F 4_B} &= -\frac{1}{2} s_F s_B \widetilde{W}_{3_F \bar{3}_F}^{F+} (2i\tilde{R}/\tilde{I})_{\bar{3}_F \bar{4}_B} \widetilde{W}_{\bar{4}_B 4_B}^{B\mp} \\
 &= \pm \frac{1}{2} i \tilde{\delta}_{3_F \bar{3}_F} \tilde{\mathcal{L}}_{\bar{4}_B \bar{3}_F}^{A/K} \left\{ \begin{array}{c} [\tilde{\delta} - (\theta_{42} + y^B \theta_{24}) 2\tilde{\rho}^0]_{\bar{4}_B 4_B} \\ \frac{1}{2} \tilde{\delta}_{\bar{4}_B 4_B} \end{array} \right\}, \quad (\text{B.84c})
 \end{aligned}$$

$$\begin{aligned}
 - (i\tilde{L}^R/\tilde{L}^I)_{3_B 4_B} &= -\theta_{34} s_B s_B (i\tilde{R}/\tilde{I})_{\bar{3}_B \bar{4}_B} \widetilde{W}_{\bar{3}_B 3_B}^{B+} \widetilde{W}_{\bar{4}_B 4_B}^{B\mp} \\
 &= \mp \frac{1}{2} i \tilde{\mathcal{L}}_{\bar{4}_B \bar{3}_B}^{A/K} \tilde{\delta}_{\bar{3}_B 3_B} \left\{ \begin{array}{c} [\tilde{\delta} - (\theta_{42} + y^B \theta_{24}) 2\tilde{\rho}^0]_{\bar{4}_B 4_B} \\ \theta_{34} \tilde{\delta}_{\bar{4}_B 4_B} \end{array} \right\}. \quad (\text{B.84d})
 \end{aligned}$$

The $\tilde{\delta}_{\bar{i}i}$ functions in the second lines of Eq. (B.84) will remove one of the coordinate integrations $\int dx_{\bar{i},i}$ that are contained in the path integral $\int \tilde{\mathcal{D}}(\mathbf{R})$. The second and third terms of Eq. (B.82) are equal, as can be seen by setting $3 \leftrightarrow 4$ and $\alpha \leftrightarrow \alpha'$ in the third and recalling that $(\tilde{\mathcal{A}}^{-1})_{43}^{\alpha'} = (\tilde{\mathcal{A}}^{-1})_{34}^{\alpha}$; we exploited this property above to combine those contributions from these terms that are proportional to $\tilde{R}_{\bar{3}_B \bar{4}_F}$ [or $\tilde{R}_{\bar{3}_F \bar{4}_B}$] together into Eq. (B.84b) [or Eq. (B.84c)], hence the factors of $2\tilde{R}$ in these equations.

Note that if we make approximation (ii) of Sec. B.5.7, a useful simplification occurs [which was exploited in App. A to obtain Eqs. (A.8) from Eqs. (B.84)]: all the factors $(\theta_{4_{a'},2} + y^{a'} \theta_{24_{a'}})$ above then reduce^h to 1, because $y^{a'} \neq 1$ was needed only to deal with interaction vertices occurring at times $t_{4_{a'}}$ earlier than a current vertex on the same contour a' , and these are precisely the ones that are dropped under approximation (ii).

Eqs. (B.84) for the effective action $(i\tilde{S}_I + \tilde{S}_R)$ constitute the second central result of this section. It should be emphasized that in the path integral (B.81), the Pauli

^h To see this explicitly, we argue as follows, discussing in parallel the cases of $\tilde{J}^{(\tilde{a}=F/B)}$, having a current vertex on the upper/lower contour and for which we have decided to use $y^{\tilde{a}=F/B} = 0$: if an interaction vertex lies on the same contour as the current vertex, i.e. for $\tilde{J}^{(\tilde{a}=F/B)}$ on the upper/lower contour at time $t_{4_{F/B}}$ (hence $a' = F/B$), approximation (ii) says that it must lie at greater times than the current vertex, $t_{4_{F/B}} > t_{2_{F/B}}$, implying that $(\theta_{4_{F/B},2} + y^{F/B} \theta_{24_{F/B}}) = 1$. If instead the interaction vertex lies on the opposite contour than the current vertex, i.e. for $\tilde{J}^{(\tilde{a}=F/B)}$ on the lower/upper contour at time $t_{4_{B/F}}$ (hence $a' = B/F$), the fact that $y^F + y^B = 1$ (always) and that we chose $y^{\tilde{a}=F/B} = 0$, implying $y^{B/F} = 1$, also gives $(\theta_{4_{B/F},2} + y^{B/F} \theta_{24_{B/F}}) = 1$, independent of the value of $t_{4_{B/F}}$.

principle is fully accounted for by the Pauli factors $(\tilde{\delta} - 2\tilde{\rho})$ in \tilde{S}^R . The ability to incorporate the Pauli principle into an influence functional for interacting electrons may be regarded as one of the main achievements of the formalism developed so far.

This concludes our rederivation of GZ's influence functional. In the remaining section B.6, where we show how it is related to diagrammatic Keldysh perturbation theory, and in the main text, where we use it to calculate the decoherence rate γ_φ , our analysis differs significantly from GZ's, since we come to different conclusions.

Let us here just mention one such difference: According to the first lines of Eqs. (B.84), $i\tilde{S}_R$ and \tilde{S}_I are, respectively, purely imaginary or purely real functionals of the paths \mathbf{R}^a , since $\tilde{W}^{a\alpha}$, \tilde{R}_{ij} and \tilde{I}_{ij} are all purely real functions. GZ have used this fact to argue that after averaging $e^{-(i\tilde{S}_R + \tilde{S}_I)}$ over all paths [as required by the path integrals in Eq. (B.80)], $e^{-\tilde{S}_I/\hbar}$ will produce an exponentially *decaying* function of time and thereby determine the interaction-induced decoherence rate, whereas $e^{-i\tilde{S}_R}$ will just produce an *oscillating* time dependence, and hence, quite generally, cannot contribute to decoherence; in particular, they argued that “ $i\tilde{S}_R$ can never cancel any contribution from \tilde{S}_I ” [discussion before (GZ-III.22)]. This general argument would work if the measure used in the path integral were real; however, it does not apply to the present case of Eq. (B.80) where the measure $e^{\pm iS_0^{F/B}/\hbar}$ is *complex*, since the average of a purely oscillatory function, using a complex measure, can well contain a decaying component, too. Indeed, it is shown in the main text [end of Sec. 4] that contributions from $i\tilde{S}_R$ and \tilde{S}_I *do* partially cancel each other.

B.6. Influence Functional vs. Keldysh Diagrammatics

To check the general formalism developed above, it is important and instructive to verify that it can reproduce the standard results of diagrammatic Keldysh perturbation theory, *before disorder averaging*. We shall do this by expanding the path integrals (B.80) in powers of the effective action $(i\tilde{S}_R + \tilde{S}_I)$:

$$\begin{aligned} \int_{0_F}^{1_F} \int_{0_B}^{1'_B} \tilde{\mathcal{D}}'(\mathbf{R}) e^{-(i\tilde{S}_R + \tilde{S}_I)/\hbar} &= \sum_{N=0}^{\infty} \frac{1}{N!} \int_{0_F}^{1_F} \int_{0_B}^{1'_B} \tilde{\mathcal{D}}'(\mathbf{R}) \\ &\times \left[\frac{-1}{\hbar} \sum_{a a'} \int_{t_0}^{t_1} dt_{3a} \int_{t_0}^{t_1} dt_{4a'} [i\tilde{L}_{3a4a'}^R + \tilde{L}_{3a4a'}^I] \right]^N. \end{aligned} \quad (\text{B.85})$$

Now and henceforth using approximation (ii) of Sec. B.5.7, we shall use this expansion to reproduce the Keldysh expressions for the conductivity in first order perturbation theory [Eqs. (B.86)], and to obtain general expressions for the first order contributions to the Cooperon before disorder averaging [Eqs. (B.89)], thereby reproducing the familiar Keldysh diagrams for the Cooperon self energy [Fig. A1 of App. A].

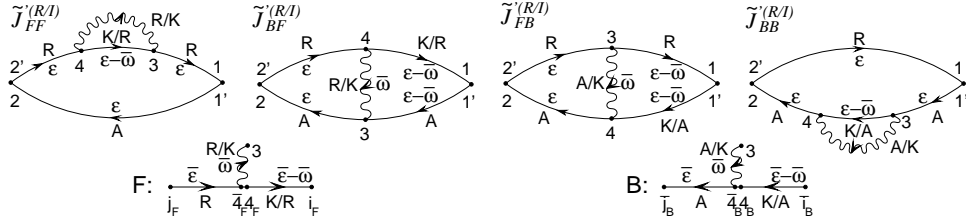


Fig. B2. Feynman diagrams for the first-order correlators $\tilde{J}_{aa'}^{(R/I)}$ of Eq. (B.86), and for the vertices of Eqs. (B.92).

B.6.1. First Order Terms and Cooperon Self Energy $\tilde{\Sigma}^{R/I}$

The $N = 1$ terms of Eq. (B.85) can be used to obtain the first order contributions, $\tilde{J}_{12',21'}^{(1)}$ (0), to the correlators needed for $\sigma_{\text{DC,real}}$ [Eq. (B.55a)]. This straightforward, if tedious, exercise is discussed in App. C.3. The result can be written as $\tilde{J}_{12',21'}^{(1)}(0) = \int (d\varepsilon) \tilde{J}_{12',21'}^{(1)\varepsilon}$, where [see Fig. B2]

$$\tilde{J}_{12',21'}^{(1)\varepsilon} = [-n'_0(\hbar\varepsilon)] \left(-\frac{1}{2}i\hbar^3\right) \int (d\bar{\omega}) \sum_{aa'} \left[\tilde{J}_{aa'}^{(R)} + \tilde{J}_{aa'}^{(I)} \right], \quad (\text{B.86a})$$

$$\tilde{J}_{FF}^{(R/I)} = \tilde{G}_{13}^R(\varepsilon) \tilde{G}_{34}^{K/R}(\varepsilon - \bar{\omega}) \tilde{G}_{42'}^R(\varepsilon) \tilde{G}_{21'}^A(\varepsilon) (\tilde{\mathcal{L}}^R / \tilde{\mathcal{L}}^K)_{34}(\bar{\omega}), \quad (\text{B.86b})$$

$$\tilde{J}_{BF}^{(R/I)} = \tilde{G}_{14}^{K/R}(\varepsilon - \bar{\omega}) \tilde{G}_{42'}^R(\varepsilon) \tilde{G}_{23}^A(\varepsilon) \tilde{G}_{31'}^A(\varepsilon - \bar{\omega}) (\tilde{\mathcal{L}}^R / \frac{1}{2}\tilde{\mathcal{L}}^K)_{34}(\bar{\omega}), \quad (\text{B.86c})$$

$$\tilde{J}_{FB}^{(R/I)} = \tilde{G}_{13}^R(\varepsilon - \bar{\omega}) \tilde{G}_{32'}^R(\varepsilon) \tilde{G}_{24}^A(\varepsilon) \tilde{G}_{41'}^{K/A}(\varepsilon - \bar{\omega}) (\tilde{\mathcal{L}}^A / \frac{1}{2}\tilde{\mathcal{L}}^K)_{43}(\bar{\omega}), \quad (\text{B.86d})$$

$$\tilde{J}_{BB}^{(R/I)} = \tilde{G}_{12'}^R(\varepsilon) \tilde{G}_{24}^A(\varepsilon) \tilde{G}_{43}^{K/A}(\varepsilon - \bar{\omega}) \tilde{G}_{31'}^A(\varepsilon) (\tilde{\mathcal{L}}^A / \tilde{\mathcal{L}}^K)_{43}(\bar{\omega}), \quad (\text{B.86e})$$

where $\tilde{J}_{aa'}^{(R/I)}$ denotes a first-order contribution from $(i\tilde{S}^R/\tilde{S}^I)$, with interaction vertices that lie on contours a and a' . These expressions agree with those of standard diagrammatic Keldysh perturbation theory. Thus, the basic building blocks of the influence functional approach, including its treatment of the Pauli principle, have survived their first test.

Next, we shall derive a general expression for the self energy of the Cooperon propagator. Usually, the Cooperon self energy is defined, after Fourier transforming to momentum space and disorder averaging, by a Dyson equation of the form $\bar{\mathcal{C}}_q = \bar{\mathcal{C}}_q^0 + \bar{\mathcal{C}}_q^0 \bar{\Sigma}_q \bar{\mathcal{C}}_q$, where $\bar{\mathcal{C}}_q^0$, the free Cooperon in the absence of interactions, is the contribution to $\langle \tilde{G}^R \tilde{G}^A \rangle_{\text{dis}}$ of time-reversed paths [cf. Eq. (F.3b)]. To identify a similar structure in position space and before disorder averaging, we need to write the first order ($N = 1$) term of Eq. (B.85) in the form $\tilde{U}_B^F \cdot \tilde{\Sigma} \cdot \tilde{U}_B^F$, i.e. a self-energy insertion sandwiched by two forward-backward propagators ($\tilde{U}_B^F)_{j_B i_B}^{i_F j_F} \equiv \tilde{U}^{0F, \bar{i}_F j_F} \tilde{U}_{j_B i_B}^{0B} = \hbar^2 \tilde{G}^{R, \bar{i}_F j_F} \tilde{G}_{j_B i_B}^A$ (each of which will produce a Cooperon upon disorder averaging):

$$-\frac{1}{\hbar} \rlap{-}\int_{j_F}^{i_F} \rlap{-}\int_{j_B}^{i_B} \tilde{\mathcal{D}}'(\mathbf{R})(i\tilde{\mathcal{L}}^R/\tilde{\mathcal{L}}^I)_{aa'}(t_3, t_4) = (\tilde{U}_B^F \cdot \tilde{\Sigma}_{aa'}^{R/I} \cdot \tilde{U}_B^F)_{j_B i_B}^{i_F j_F} \quad (\text{B.87a})$$

$$= \int dx_{3_F} dx_{\bar{4}_B} \int dx_{\bar{4}_F} dx_{3_B} (\tilde{U}_B^F)_{j_B \bar{4}_B}^{i_F 3_F} \left(\tilde{\Sigma}_{aa'}^{R/I} \right)_{\bar{4}_B 3_B}^{3_F \bar{4}_F} (\tilde{U}_B^F)_{3_B i_B}^{\bar{4}_F j_F}. \quad (\text{B.87b})$$

(For ease of recognition, we here and henceforth in this section write indices associated with the forward (F) or backward (B) paths as superscripts or subscripts, respectively). As made explicit by Eq. (B.87b), the first (or second) dot product on the right-hand side of Eq. (B.87a) indicates integration over the two coordinates associated with the two “outgoing” (or the two “incoming”) vertices at the corners of the self-energy box [see Fig. A1a]. Now, the left-hand side of Eq. (B.87a) contains *two* vertices, associated with the indices of $(i\tilde{L}^R/\tilde{L}^I)_{3_a \bar{4}_{a'}}$ [Eqs. (B.84)], as insertions into a double path integral, and therefore contains *four* Green’s functions \tilde{G} [cf. the rule of thumb (D.10) of App. D.3]; however, for $\tilde{U}_B^F \cdot \tilde{\Sigma} \cdot \tilde{U}_B^F$, we formally need *six* Green’s functions \tilde{G} and *four* vertices, one for each corner of the self-energy box. To achieve this, we proceed as follows: the two corners to which the interaction lines are connected [black dots in Fig. A1] can be naturally labelled by a and a' , which take the values F/B , according to the contour that the corner sits on; let \bar{a} and \bar{a}' similarly label the other two, “free” corners [empty circles in Fig. A1]. For the free corner \bar{a} (and similarly for \bar{a}'), we use the identity (t_k is an arbitrary time between t_i and t_j)

$$\tilde{G}_{i_{\bar{a}} j_{\bar{a}}}^{R/A} = (s_{\bar{a}} i\hbar) \int dx_{k_{\bar{a}}, \bar{k}_{\bar{a}}} \tilde{G}_{i_{\bar{a}} k_{\bar{a}}}^{R/A} \tilde{\delta}_{k_{\bar{a}} \bar{k}_{\bar{a}}} \tilde{G}_{\bar{k}_{\bar{a}} j_{\bar{a}}}^{R/A}, \quad (\text{B.88})$$

taking R/A and $s_{\bar{a}} = \pm 1$ if $\bar{a} = F/B$, to write one Green’s function as the convolution of two, and regard the $\tilde{\delta}_{\bar{a}}$ function as the “vertex” at the corresponding free corner of the self energy box.ⁱ In this way, the self-energy contributions $\tilde{\Sigma}_{aa'}^{R/I}$ are found to be given by the first lines of the following equations (summarized diagrammatically in Fig. A1):

$$\begin{aligned} \left(\tilde{\Sigma}_{FF}^{R/I} \right)_{\bar{4}_B 3_B}^{3_F \bar{4}_F} &= \theta_{34} \left(\widetilde{W}^{F+} \tilde{\delta}_B \cdot \tilde{U}_B^F \cdot \tilde{\delta}_B \widetilde{W}^{F\mp} \right)_{\bar{4}_B 3_B}^{3_F \bar{4}_F} \frac{1}{\hbar} (i\tilde{R}/\tilde{I})_{3_F \bar{4}_F} \\ &= -\frac{i\hbar}{2} (\tilde{G}^{K/R})_{3_F \bar{4}_F} \tilde{G}_{\bar{4}_B 3_B}^A (\tilde{\mathcal{L}}^R/\tilde{\mathcal{L}}^K)_{3_F \bar{4}_F}, \end{aligned} \quad (\text{B.89a})$$

$$\begin{aligned} \left(\tilde{\Sigma}_{BF}^{R/I} \right)_{\bar{4}_B 3_B}^{3_F \bar{4}_F} &= \left(\tilde{\delta}^F \tilde{\delta}_B \cdot \tilde{U}_B^F \cdot \widetilde{W}_{B+} \widetilde{W}^{F\mp} \right)_{\bar{4}_B 3_B}^{3_F \bar{4}_F} \frac{1}{\hbar} (i\tilde{R}/\tilde{I})_{3_B \bar{4}_F} \\ &= -\frac{i\hbar}{2} (\tilde{G}^{K/R})_{3_F \bar{4}_F} \tilde{G}_{\bar{4}_B 3_B}^A (\tilde{\mathcal{L}}^R/\frac{1}{2}\tilde{\mathcal{L}}^K)_{3_B \bar{4}_F}, \end{aligned} \quad (\text{B.89b})$$

$$\left(\tilde{\Sigma}_{FB}^{R/I} \right)_{\bar{4}_B 3_B}^{3_F \bar{4}_F} = \left(\widetilde{W}^{F+} \widetilde{W}_{B\mp} \cdot \tilde{U}_B^F \cdot \tilde{\delta}_B \tilde{\delta}^F \right)_{\bar{4}_B 3_B}^{3_F \bar{4}_F} \frac{1}{\hbar} (i\tilde{R}/\tilde{I})_{3_F \bar{4}_B}$$

ⁱ By using Eq. (B.88) twice at the two free corners, an extra overall phase factor of $(is_{\bar{a}})(is_{\bar{a}'}) = -s_a s_{a'}$ is generated. The latter cancels the overall phase factor $(-s_a s_{a'})$ occurring in the first lines of Eqs. (B.83) for $(i\tilde{L}^R/\tilde{L}^I)$, which is why this factor does not occur in the first lines of Eqs. (B.89).

Influence functional calculation of decoherence in weak localization 59

$$= -\frac{i\hbar}{2} \tilde{G}^{iR,3F\bar{4}F} (\tilde{G}^{K/A})_{\bar{4}B3B} (\tilde{\mathcal{L}}^A / \frac{1}{2} \tilde{\mathcal{L}}^K)_{\bar{4}B}{}^{3F}, \quad (\text{B.89c})$$

$$\begin{aligned} \left(\tilde{\Sigma}_{BB}^{R/I} \right)_{\bar{4}B3B}^{3F\bar{4}F} &= \theta_{34} \left(\tilde{\delta}^F \tilde{W}_{B\mp} \cdot \tilde{U}_B^F \cdot \tilde{W}_{B+} \tilde{\delta}^F \right)_{\bar{4}B3B}^{3F\bar{4}F} \frac{1}{\hbar} (i\tilde{R}/\tilde{I})_{3B\bar{4}F} \\ &= -\frac{i\hbar}{2} \tilde{G}^{iR,3F\bar{4}F} (\tilde{G}^{K/A})_{\bar{4}B3B} (\tilde{\mathcal{L}}^A / \tilde{\mathcal{L}}^K)_{\bar{4}B3B}. \end{aligned} \quad (\text{B.89d})$$

To obtain the second lines of Eqs. (B.89) from the respective first lines, we proceed similarly as for Eqs. (B.84) [but now with $\theta_{42} + y^{a'}\theta_{24} = 1$, since we use approximation (ii), as explained in the paragraph after Eqs. (B.84)]. In particular, we exploit the fact that the time-integrals in a path integral are time-ordered for the upper contour and anti-time-ordered for the lower contour to replace \tilde{U}^{0F} by $i\hbar\tilde{G}^R$ and \tilde{U}^{0B} by $-i\hbar\tilde{G}^A$ [cf. Eq. (B.46)], or, if they are pre- or post-contracted with $(\tilde{\delta} - 2\tilde{\rho}_0)$, by $i\hbar\tilde{G}_K$ [Eqs. (B.47b)]. For example, to obtain Eqs. (B.89a) and (B.89d) for $\tilde{\Sigma}_{FF/BB}^R$, we used:

$$\left(\tilde{W}^{F+} \tilde{\delta}_B \cdot \tilde{U}_B^F \cdot \tilde{\delta}_B \tilde{W}^{F-} \right)_{\bar{4}B3B}^{3F\bar{4}F} \quad (\text{B.90a})$$

$$\begin{aligned} &= \int dx_{\bar{3}F} dx_{4B} \int dx_{4F} dx_{\bar{3}B} \tilde{\delta}^{3F\bar{3}F} \tilde{\delta}_{\bar{4}B4B} \tilde{U}^{0F,3F4F} \tilde{U}_{\bar{4}B3B}^{0B} \tilde{\delta}_{\bar{3}B3B} \frac{1}{2} s_F (1 - 2\tilde{\rho}_0)^{4F\bar{4}F} \\ &= +\frac{1}{2} (i\hbar \tilde{G}^{K,3F\bar{4}F}) (-i\hbar \tilde{G}_{\bar{4}B3B}^A), \end{aligned} \quad (\text{B.90b})$$

$$\left(\tilde{\delta}^F \tilde{W}_{B-} \cdot \tilde{U}_B^F \cdot \tilde{W}_{B+} \tilde{\delta}^F \right)_{\bar{4}B3B}^{3F\bar{4}F} \quad (\text{B.90c})$$

$$\begin{aligned} &= \int dx_{\bar{3}F} dx_{4B} \int dx_{4F} dx_{\bar{3}B} \tilde{\delta}^{3F\bar{3}F} \frac{1}{2} s_B (1 - 2\tilde{\rho}_0)_{\bar{4}B4B} \tilde{U}^{0F,\bar{3}F4F} \tilde{U}_{\bar{4}B3B}^{0B} \tilde{\delta}_{\bar{3}B3B} \tilde{\delta}^{4F\bar{4}F} \\ &= -\frac{1}{2} (i\hbar \tilde{G}^{R,3F\bar{4}F}) (i\hbar \tilde{G}_{\bar{4}B3B}^K). \end{aligned} \quad (\text{B.90d})$$

Satisfactorily, the second lines of Eqs. (B.89), summarized diagrammatically in Fig. A1, are identical to what one obtains from Keldysh perturbation theory, as can easily be verified starting from Eq. (E.24) of App. E.3. Moreover, they are evidently consistent with the first order results listed in Eqs. (B.86) above. (In fact, the latter could have been used to guess Eqs. (B.89); the reason for nevertheless going through the above analysis was to check that the signs can be organized in a manner that allows for a series to be summed up.) In Sec. F.2, we shall calculate the Cooperon self-energy explicitly by starting from Eqs. (B.87b) and (B.89) and performing the disorder averaging diagrammatically.

B.6.2. Fate of the Pauli Factor $(\tilde{\delta} - 2\tilde{\rho}^0)$

One instructive outcome of the analysis of the previous section is that we have learnt quite generally how to deal with the Pauli factors $(\tilde{\delta} - 2\tilde{\rho}^0)$ occurring in \tilde{S}_R : All Keldysh functions in Eqs. (B.86) and (B.89) arose from exploiting the identities

60 *Jan von Delft*

$\tilde{U}_{i\bar{i}}^0(\tilde{\delta} - 2\tilde{\rho}^0)_{i\bar{i}} = (\tilde{\delta} - 2\tilde{\rho}^0)_{i\bar{i}}\tilde{U}_{i\bar{i}}^0 = i\hbar\tilde{G}_{ij}^K$ [Eq. (B.47b)]. Since its frequency Fourier transform obeys [Eq. (B.47b)] $\tilde{G}_{ij}^K(\varepsilon) = [1 - 2n_0(\hbar\varepsilon)][\tilde{G}_{ij}^R - G_{ij}^A](\varepsilon)$, and in Eqs. (B.86) and (B.89) all Keldysh functions come in the combination $\tilde{G}^K(\varepsilon - \bar{\omega})\tilde{\mathcal{L}}^{R/A}(\bar{\omega})$, we can deduce a rule of thumb: by transforming to the coordinate-frequency representation, one generates the replacement

$$(\tilde{\delta} - 2\tilde{\rho}^0)\tilde{\mathcal{L}}^{R/A} \rightarrow \tanh\left[\frac{\hbar(\varepsilon - \bar{\omega})}{2T}\right]\tilde{\mathcal{L}}^{R/A}(\bar{\omega}). \quad (\text{B.91})$$

Actually, in deriving the general structure of the self-energy above [Eq. (B.89)], this replacement has, in effect, already been deduced directly, and to all orders in the interaction, from the general form of $i\tilde{L}_{aa'}^R$, in Eqs. (B.84), by exploiting the fact that in the path integral, each $\tilde{L}_{aa'}^R$ is sandwiched between propagators \tilde{U}^0 . Since this point is so important, let us spell it out once more: depending on whether a vertex at time $t_{4'_a}$ sits on the forward (time-ordered) or backward (anti-time-ordered) contour ($a' = F/B$), the factor $(\tilde{\delta} - 2\tilde{\rho}^0)\tilde{\mathcal{L}}^{R/A}$ occurring in $\tilde{L}_{aa'}^R$ is sandwiched as follows between two $\tilde{G}^R \dots \tilde{G}^R$ or $\tilde{G}^A \dots \tilde{G}^A$ functions [see bottom two diagrams of Fig. B2]:

$$\left[\tilde{G}_{i_F 4_F}^R(\tilde{\delta} - 2\tilde{\rho}^0)_{4_F \bar{4}_F}\right]\tilde{\mathcal{L}}_{3\bar{4}_F}^R\tilde{G}_{\bar{4}_F j_F}^R \rightarrow \tilde{G}_{i_F \bar{4}_F}^K(\bar{\varepsilon} - \bar{\omega})\tilde{\mathcal{L}}_{3\bar{4}_F}^R(\bar{\omega})\tilde{G}_{\bar{4}_F j_F}^R(\bar{\varepsilon}), \quad (\text{B.92a})$$

$$\tilde{G}_{\bar{j}_B \bar{4}_B}^A\tilde{\mathcal{L}}_{\bar{4}_B 3}^A\left[(\tilde{\delta} - 2\tilde{\rho}^0)_{\bar{4}_B 4_B}\tilde{G}_{4_B \bar{i}_B}^A\right] \rightarrow -\tilde{G}_{\bar{j}_B \bar{4}_B}^A(\bar{\varepsilon})\tilde{\mathcal{L}}_{\bar{4}_B 3}^A(\bar{\omega})\tilde{G}_{4_B \bar{i}_B}^K(\bar{\varepsilon} - \bar{\omega}). \quad (\text{B.92b})$$

Here the left- and right-hand sides are written in the time and frequency domains, respectively, and the replacement rule (B.91) follows from Eqs. (B.92) since $\tilde{G}^K(\bar{\varepsilon} - \bar{\omega})$ contains a factor $\tanh[\hbar(\bar{\varepsilon} - \bar{\omega})/2T]$. To be very explicit, the arrows in Eqs. (B.92) are shorthands for the following series of manipulations on the above factors of $\tilde{G}_{i_F 4_F}^R(\tilde{\delta} - 2\tilde{\rho}^0)_{4_F \bar{4}_F}$ or $(\tilde{\delta} - 2\tilde{\rho}^0)_{\bar{4}_B 4_B}\tilde{G}_{4_B \bar{i}_B}^A$ occurring on the forward or backward contours [indices are now dropped, for brevity]:

$$\begin{aligned} \tilde{G}^R(\tilde{\delta} - 2\tilde{\rho}^0) &= [\tilde{G}^R - G^A](\tilde{\delta} - 2\tilde{\rho}^0) = \tilde{G}^K \xrightarrow{(1)} [\tilde{G}^R - \tilde{G}^A] \tanh \xrightarrow{(2)} \tilde{G}^R \tanh, \\ (\tilde{\delta} - 2\tilde{\rho}^0)\tilde{G}^A &= (\tilde{\delta} - 2\tilde{\rho}^0)[\tilde{G}^A - G^R] = -\tilde{G}^K \xrightarrow{(1)} -[\tilde{G}^R - \tilde{G}^A] \tanh \xrightarrow{(2)} \tilde{G}^A \tanh. \end{aligned} \quad (\text{B.93})$$

Beginning in the position-time representation on the left hand side, we exploit the fact that the upper or lower contours are time- or anti-time-ordered to add an extra $-\tilde{G}^{A/R} = 0$ inside the square brackets, thereby obtaining a $\pm\tilde{G}^K$. Step (1) indicates Fourier transforming to the position-frequency domain, in which the tanh factor becomes explicit. (Step (2) will be discussed later below.) The expressions obtained after step (1) are the ones used to produce the right-hand sides of Eqs. (B.92); satisfyingly, the latter are precisely the combinations produced by the Feynman rules of diagrammatic Keldysh perturbation theory, illustrated in Fig. B2. [As Eqs. (B.89) show, the signs work out correctly, too, if the bookkeeping is done sufficiently carefully]. The above argument is indeed completely general, and holds for each vertex

separately (but with different $\hbar\bar{\varepsilon}$'s at each vertex), to all orders in perturbation theory. Thus, we have succeeded in recovering the Feynman rules from the influence functional approach.

In Eqs. (B.91) and (B.92), the variable $\hbar\bar{\varepsilon}$ represents the energy of the electron line on the upper (or lower) Keldysh contour before it enters (or after it leaves) an interaction vertex at which its energy decreases (or increases) by $\hbar\bar{\omega}$ [see lowest two figures in Fig. B2]. The subtraction of $\bar{\omega}$ in the argument of \tanh thus reflects the physics of recoil: emitting or absorbing a photon causes the electron energy to change by $\hbar\bar{\omega}$, and it is this changed energy $\hbar(\bar{\varepsilon} - \bar{\omega})$ that enters the Fermi functions for the accessible final states. (A standard back-of-the-envelope argument for the origin of the Pauli factor, based on the availability of initial and final states, is given in MDSA-I²⁰, Section V.A.) Of course, $\hbar\bar{\varepsilon}$ will have different values from one vertex to the next, reflecting the history of energy changes of an electron line as it proceeds through a Feynman diagram.

The final step (2) in Eqs. (B.93) [not contained in Eq. (B.92)] indicates an approximation that occurs *if* one chooses to evaluate the path integral by including only time-reversed paths [as GZ do, see Sec. 4 of main text]: one thereby drops terms containing interaction vertices at which \tilde{G}^R changes to \tilde{G}^A on the upper contour, or \tilde{G}^A changes to \tilde{G}^R on the lower contour [so-called Hikami box terms], and thus drops $\tilde{G}^{A/R} \tanh$ terms on the upper/lower contour. Of course, this last step (2) is *optional*; the Hikami terms *can* be retained, if one so chooses, and we do so in App. F.2 when diagrammatically deriving a Dyson equation for the Cooperon that includes the Hikami box terms. The result of that analysis is used in the main text [Sec. 5] to calculate the decoherence rate; remarkably and unexpectedly, it turns out that the Hikami-box contribution to the decoherence rate happens to be zero for the special form of the interaction propagator used in the main text, namely the unitary limit of Eq. (4a). This fact implies that, for the specific purpose of deriving the *decoherence rate* (but not necessarily for other, more general quantities) from an influence functional, we *may* indeed adopt step (2) and drop Hikami-box terms. We shall do so henceforth. For the remaining terms, comparison of the very left and right-hand sides of Eqs. (B.93) clearly shows that one really *can* simply replace $(\tilde{\delta} - 2\tilde{\rho}^0)$ by \tanh , without worrying about signs, etc., as specified in Eq. (B.91).

Having adopted step (2) of dropping Hikami-box terms, our rule of thumb replacement (B.91) can quite easily be implemented “to all orders” in the influence functional approach: Fourier-transform the kernels $(\tilde{i}L^R/\tilde{L}^I)_{3a_4a'}$ [Eqs. (B.84)] of the effective action $(i\tilde{S}_R + \tilde{S}_I)$ [Eq. (B.83)], and simply make the replacement (B.91) in the Fourier-transformed version of $i\tilde{L}^R$, now using the *same* energy $\hbar\bar{\varepsilon} \equiv \hbar\varepsilon$ as that which enters the overall weighting factor $[-n'_0(\hbar\varepsilon)]$. The resulting form of the effective action is summarized in Eqs. (2) to (4) of the main text, which serve as the starting point of our calculation of the decoherence rate there.

Diagrammatically speaking, the procedure just proposed amounts to using the *same* ε inside each $\tanh[\hbar(\varepsilon - \bar{\omega})/2T] \tilde{\mathcal{L}}^{R/A}(\bar{\omega})$. *If* one intends to consider *only*

self-energy diagrams and to treat infrared divergent frequency integrals with a self-consistently-determined lower cutoff $1/\tau_\varphi$ (as GZ in fact do themselves in GZ99³, and as discussed in detail in Sec. 4 and 5 of the main text) then this procedure would in fact not introduce any further approximations: the energy entering and leaving each self-energy insertion then is indeed the same for all such insertions, so they all *should* have the same $\tanh[\hbar(\varepsilon - \bar{\omega})/2T] \tilde{\mathcal{L}}^{R/A}(\bar{\omega})$ factors.

Of course, once one includes vertex diagrams too, as needed if one wants to cure infrared problems “properly” (as in GZ99⁴) instead of “by hand” (as in GZ99⁴), then the proposed procedure of using the same ε everywhere amounts to a further approximation, since it neglects the accumulation of energy changes that are generated by vertex terms transferring energy between the forward and backward contours [as illustrated by the frequencies $\tilde{\omega}_1$ and $\tilde{\omega}_2$ in Fig. B1]. Nevertheless, the mistake incurred by this approximation is insignificant, since the vertex terms are not ultraviolet divergent, and the frequency transfers contained therein are limited to the range $\hbar|\bar{\omega}| \ll T$, just as for self-energy terms. In fact, vertex terms become important only in the *infrared* limit where $\bar{\omega} \simeq 1/t$ (as required, of course, to cure infrared problems of the self-energy diagrams), so that we may replace $\bar{\omega}$ by 0 wherever else it occurs in a diagram. More formally, it suffices to treat the $\bar{\omega}$ -dependence explicitly only for that part of a diagram where it occurs as energy transfer, while Taylor-expanding in $\bar{\omega}$ all other factors of the diagram to which this $\bar{\omega}$ -dependence has propagated; only the zeroth-order terms of this Taylor expansion need to be retained, since the others contain higher powers of $\bar{\omega} \sim 1/t$, and hence produce contributions with a subleading time dependence.

Note also that the accumulation of energy transfers manifests itself only in diagrams of second or higher order in the interaction propagator. However, the influence functional approach proposed by GZ and rederived here features an effective action that is linear in the interaction propagator, and hence is equivalent to re-exponentiating the *first* order term in the expansion of the Cooperon in powers of the interaction propagator (as shown explicitly in DMSA-II²⁰). Hence an accurate treatment of effects occurring only in second or higher order is beyond the accuracy of the influence functional approach, in both GZ’s original formulation and the modified version proposed here. The accumulation of energy transfers is such an effect. Fortunately, it only produces corrections that are subleading in time, as argued above.

It is shown in the main text that if the replacement Eq. (B.91) is used in a “nonperturbative calculation” of τ_φ à la GZ, a result consistent with conventional wisdom is obtained. Conversely, the reason why GZ obtained a different result is that they, in effect, omitted the $-\bar{\omega}$ in the tanh-function in Eq. (B.91), and hence lost the physics of recoil, as first suspected by Eriksen and Hedegard¹¹.

B.6.3. Alternative Representation of Effective Action

To facilitate a comparison of the influence functional approach developed in the present review with that of MDSA-I²⁰, it is convenient to rewrite the effective action derived in Section B.5.8 and summarized in Eqs. (A.7), (A.8), in the following form (to be compared to Eqs. (21) of MDSA-I²⁰):

$$[i\tilde{S}_R + \tilde{S}_I](t_1, t_0) = \frac{1}{2} \int_{t_0}^{t_1} dt_3 \int_{t_0}^{t_1} dt_4 \sum_{aa'=F/B} s_a s_{a'} (-\frac{1}{2}i) \tilde{\mathcal{L}}_{3_a 4_{a'}}^{aa'}. \quad (\text{B.94})$$

In particular, the integrands are to contain nonzero contributions not only for $t_{34} > 0$ [as is the case in Eqs. (A.8)] but also for $t_{34} < 0$. To this end, we follow the second of the routes mentioned after Eq. (B.82). We start from the latter, but instead of exploiting any $3 \leftrightarrow 4$ symmetries and inserting any factors of $2\theta_{34}$, as done in Section B.5.8 (“route one”), we now write out all terms explicitly, while still making approximation (ii) of Sec. B.5.7, namely to replace all factors of $(\theta_{4_{a'}2} + y^{a'}\theta_{24_{a'}})$ and $(\theta_{4_{a'}2} + y^{a'}\theta_{24_{a'}})$ by 1. [A perhaps quicker way to obtain the same results is to start directly from Eqs. (B.83), (A.8), but to symmetrize the integrands w.r.t. $3 \leftrightarrow 4$ by replacing $\sum_{aa'} \mathcal{L}_{3_a 4_{a'}}$ by $\sum_{aa'} \frac{1}{2} [\mathcal{L}_{3_a 4_{a'}} + \mathcal{L}_{4_a 3_{a'}}]$.] The result can be written in the form of Eq. (B.94), with $\mathcal{L}_{3_a 4_{a'}}^{aa'}$ being a shorthand for the following expressions:

$$\begin{aligned} \tilde{\mathcal{L}}_{3\bar{3},4\bar{4}}^{FF} &= \tilde{\delta}_{3_F\bar{3}_F} \tilde{\mathcal{L}}_{3_F\bar{4}_F}^K \tilde{\delta}_{4_F\bar{4}_F} + \tilde{\delta}_{3_F\bar{3}_F} \tilde{\mathcal{L}}_{3_F\bar{4}_F}^R [\tilde{\delta} - 2\tilde{\rho}^0]_{4_F\bar{4}_F} + [\tilde{\delta} - 2\tilde{\rho}^0]_{3_F\bar{3}_F} \tilde{\mathcal{L}}_{3_F\bar{4}_F}^A \tilde{\delta}_{4_F\bar{4}_F} \\ \tilde{\mathcal{L}}_{3\bar{3},4\bar{4}}^{BF} &= \tilde{\delta}_{3_B\bar{3}_B} \tilde{\mathcal{L}}_{3_B\bar{4}_F}^K \tilde{\delta}_{4_F\bar{4}_F} + \tilde{\delta}_{3_B\bar{3}_B} \tilde{\mathcal{L}}_{3_B\bar{4}_F}^R [\tilde{\delta} - 2\tilde{\rho}^0]_{4_F\bar{4}_F} - [\tilde{\delta} - 2\tilde{\rho}^0]_{3_B\bar{3}_B} \tilde{\mathcal{L}}_{3_B\bar{4}_F}^A \tilde{\delta}_{4_F\bar{4}_F} \\ \tilde{\mathcal{L}}_{3\bar{3},4\bar{4}}^{FB} &= \tilde{\delta}_{3_F\bar{3}_F} \tilde{\mathcal{L}}_{3_F\bar{4}_B}^K \tilde{\delta}_{4_B\bar{4}_B} - \tilde{\delta}_{3_F\bar{3}_F} \tilde{\mathcal{L}}_{3_F\bar{4}_B}^R [\tilde{\delta} - 2\tilde{\rho}^0]_{4_B\bar{4}_B} + [\tilde{\delta} - 2\tilde{\rho}^0]_{3_F\bar{3}_F} \tilde{\mathcal{L}}_{3_F\bar{4}_B}^A \tilde{\delta}_{4_B\bar{4}_B} \\ \tilde{\mathcal{L}}_{3\bar{3},4\bar{4}}^{BB} &= \tilde{\delta}_{3_B\bar{3}_B} \tilde{\mathcal{L}}_{3_B\bar{4}_B}^K \tilde{\delta}_{4_B\bar{4}_B} - \tilde{\delta}_{3_B\bar{3}_B} \tilde{\mathcal{L}}_{3_B\bar{4}_B}^R [\tilde{\delta} - 2\tilde{\rho}^0]_{4_B\bar{4}_B} - [\tilde{\delta} - 2\tilde{\rho}^0]_{3_B\bar{3}_B} \tilde{\mathcal{L}}_{3_B\bar{4}_B}^A \tilde{\delta}_{4_B\bar{4}_B}. \end{aligned} \quad (\text{B.95})$$

[The double spatial indices, $3\bar{3}$ for the forward and $\bar{3}3$ for the backward contour, are associated with the same time t_3 and are both integrated over in the path integral (similarly for $4\bar{4}, \bar{4}4$ and t_4), see point (iii) after Eq. (B.58)]. As explained in Sec. B.6.2, upon Fourier transforming, the Pauli factors can be converted via Keldysh Green’s functions into tanh functions. However, we now need to use a more general replacement rule (of which the one discussed in Sec. B.6.2 was a special case), involving either of the expressions $\text{th}_\mp \equiv \tanh[\hbar(\varepsilon \mp \bar{\omega})/2T]$. The reason is that we now have to distinguish two types of vertices: For vertices of “type one” [Fig. B3(a)], the arrows of the $\tilde{L}^{R/A}$ and \tilde{G}^K correlators that get generated both point in the *same* direction (i.e. both away from or both towards the same vertex), in which case we get the combination $\tilde{L}^{R/A}(\bar{\omega})\tilde{G}^K(\varepsilon - \bar{\omega})$:

$$\tilde{L}_{3_a\bar{4}_F}^R [\tilde{\delta} - 2\tilde{\rho}^0]_{4_F\bar{4}_F} \rightarrow \text{th}_- \bar{\mathcal{L}}_{\bar{q}}^R(\bar{\omega}), \quad [\tilde{\delta} - 2\tilde{\rho}^0]_{\bar{3}_B\bar{3}_B} \tilde{L}_{\bar{3}_B\bar{4}_{a'}}^A \rightarrow \text{th}_- \bar{\mathcal{L}}_{\bar{q}}^A(\bar{\omega}). \quad (\text{B.96a})$$

For vertices of “type two” (the occurrence of which was studiously avoided in Section B.5.8), the arrows point in *opposite* directions (one toward, the other away from the same vertex), [Fig. B3(b)], which gives the combination $\tilde{L}^{R/A}(\bar{\omega})\tilde{G}^K(\varepsilon + \bar{\omega})$:

$$\tilde{L}_{3_a\bar{4}_B}^R [\tilde{\delta} - 2\tilde{\rho}^0]_{\bar{4}_B\bar{4}_B} \rightarrow \text{th}_+ \bar{\mathcal{L}}_{\bar{q}}^R(\bar{\omega}), \quad [\tilde{\delta} - 2\tilde{\rho}^0]_{3_F\bar{3}_F} \tilde{L}_{3_F\bar{4}_{a'}}^A \rightarrow \text{th}_+ \bar{\mathcal{L}}_{\bar{q}}^A(\bar{\omega}). \quad (\text{B.96b})$$

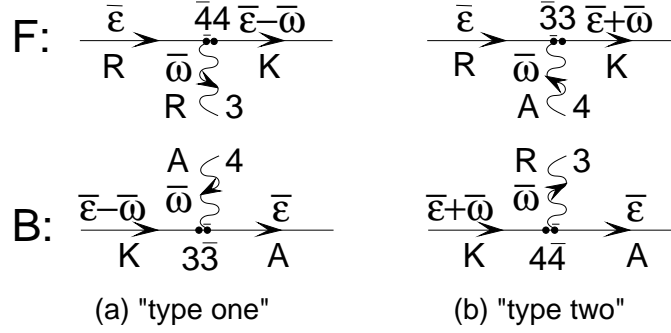


Fig. B.3. (a) Vertices of “type one” and (b) of “type two” arising in Keldysh perturbation theory; the accompanying Keldysh Green’s functions are $\hat{G}^K(\varepsilon \mp \bar{\omega})$, respectively, producing Pauli factors $\tanh[(\varepsilon \mp \bar{\omega})/2T]$ that dress the associated interaction propagators $\bar{\mathcal{L}}_{\bar{q}}^R(\bar{\omega})$ and $\bar{\mathcal{L}}_{\bar{q}}^A(\bar{\omega})$ [Eq. (B.96)].

Using these replacement rules, the effective Fourier representations of Eqs. (B.95) are readily seen to have the following forms:

$$\tilde{\mathcal{L}}_{3_a 4_{a'}} = \int (d\bar{\omega})(d\bar{q}) e^{i\bar{q} \cdot [\mathbf{R}^a(t_{3_a}) - \mathbf{R}^{a'}(t_{4_{a'}})]} e^{-i\bar{\omega}(t_{3_a} - t_{4_{a'}})} \bar{\mathcal{L}}_{\bar{q}}^{aa'}(\bar{\omega}), \quad (\text{B.97a})$$

$$\bar{\mathcal{L}}_{\bar{q}}^{aa'}(\bar{\omega}) = \bar{\mathcal{L}}_{\bar{q}}^K(\bar{\omega}) + s_{a'} \text{th}_{-s_{a'}} \bar{\mathcal{L}}_{\bar{q}}^R(\bar{\omega}) + s_a \text{th}_{+s_a} \bar{\mathcal{L}}_{\bar{q}}^A(\bar{\omega}). \quad (\text{B.97b})$$

Eqs. (B.94) and (B.97) together constitute an alternative and perhaps more compact expression for the effective action of Eqs. (2) to (4).

Appendix C. Relation between Path Integral and Cooperon

In this appendix we show how the general path integral expression derived for the conductivity in the main text in terms of $\tilde{J}_{12',21'}$ [Eqs. (B.55a) and (B.80)], can be rewritten in terms of the Drude conductivity $\sigma_{\text{DC}}^{\text{Drude}}$ and the familiar Cooperon, and thereby clarify how they are related to the standard relations familiar from diagrammatic perturbation theory. We begin [Sec. C.1] by reviewing the noninteracting case before disorder averaging, then [Sec. C.2] recall how disorder averaging produces the standard result for $\sigma_{\text{DC}}^{\text{WL}}$. Next [Sec. C.3] we discuss the first order interaction contribution and subsequently [Sec. C.4] generalize the analysis to include interactions to all orders, before disorder averaging. In particular, we elucidate how the average energy $\hbar\varepsilon$ of the two counterpropagating trajectories is fixed in this formalism. Finally, we perform a disorder average for the general case with interactions [Sec. C.5] to establish a connection to the general Cooperon propagator in the presence of interactions, and [Sec. C.6] review its structure in the coordinate space representation.

C.1. Noninteracting Limit before Disorder Averaging

Let us check that in the noninteracting limit but before disorder averaging, Eqs. (B.55) for σ_{DC} , with $\tilde{J}'(0)$ given by Eqs. (B.54) and (B.52), reproduce familiar expressions for the conductivity $\sigma_{\text{DC}}^{\text{nonint}}$. If interactions are neglected, both \tilde{U}_{ij}^a and $\tilde{U}_{ij}^{t'a}$ in Eq. (B.52) reduce to \tilde{U}_{ij}^0 . Using Eqs. (B.45) and (B.47a) in Eqs. (B.52), one then readily obtains

$$\tilde{J}_{12',21'}^{(0)}(t_1, t_2; t_0) = \sum_{\tilde{a}=F,B} \tilde{J}_{12',21'}^{(0),\tilde{a}}(t_1, t_2; t_0) = \hbar \tilde{G}_{12'}^R \tilde{G}_{21'}^< + \hbar \tilde{G}_{12'}^< \tilde{G}_{21'}^A. \quad (\text{C.1a})$$

Inserting Eq. (C.1a) into Eq. (B.22a), we obtain a standard expression for $\sigma_{\text{DC}}^{\text{nonint}}$, before disorder averaging. To evaluate its real part $\sigma_{\text{DC,real}}^{\text{nonint}}$ [Eq. (B.55a)], we have to Fourier transform \tilde{J} according to Eq. (B.54). Writing the result as $\tilde{J}_{12',21'}^{(0)}(\omega_0) = \int (d\varepsilon) \tilde{J}_{12',21'}^{(0),\varepsilon}(\omega_0)$, we get

$$\tilde{J}_{12',21'}^{(0),\varepsilon}(\omega_0) = \hbar \left[\tilde{G}_{12'}^R(\varepsilon_+) \tilde{G}_{21'}^<(\varepsilon_-) + \tilde{G}_{12'}^<(\varepsilon_+) \tilde{G}_{21'}^A(\varepsilon_-) \right], \quad (\text{C.1b})$$

with $\varepsilon_{\pm} \equiv \varepsilon \pm \frac{1}{2}\omega_0$. Now expand $\tilde{J}^{(0),\varepsilon}(\omega_0) = \tilde{J}^{(0),\varepsilon}(0) + \omega_0 \tilde{J}'^{(0),\varepsilon}(0)$, as needed for Eq. (B.55a). Using $\tilde{G}_{ij}^<(\varepsilon_{\pm}) = -n_0(\hbar\varepsilon_{\pm}) [\tilde{G}_{ij}^R - \tilde{G}_{ij}^A](\varepsilon_{\pm})$, replacing $\tilde{G}^{R/A}(\varepsilon_{\pm})$ by $\tilde{G}^{R/A}(\varepsilon)$, and dropping terms in $\tilde{J}'^{(0),\varepsilon}(0)$ containing $\partial_{\varepsilon} \tilde{G}^{R/A}(\varepsilon)$, since they are smaller than those kept by a factor T/ε_{F} , we obtain

$$\tilde{J}_{12',21'}^{(0),\varepsilon}(0) = -n_0(\hbar\varepsilon) \hbar \left[\tilde{G}_{12'}^R(\varepsilon) \tilde{G}_{21'}^R(\varepsilon) - \tilde{G}_{12'}^A(\varepsilon) \tilde{G}_{21'}^A(\varepsilon) \right], \quad (\text{C.2a})$$

$$\tilde{J}'_{12',21'}^{(0),\varepsilon}(0) = -n'_0(\hbar\varepsilon) \hbar^2 \tilde{G}_{12'}^R(\varepsilon) \tilde{G}_{21'}^A(\varepsilon). \quad (\text{C.2b})$$

Here $n'_0(\xi) \equiv \partial_{\xi} n_0(\xi)$, hence, in the $\tilde{J}'^{(0),\varepsilon}(0)$ correlator of Eq. (C.2b), the energy argument $\hbar\varepsilon$ is constrained to be $\lesssim T$. The desired result for $\sigma_{\text{DC,real}}^{\text{nonint}}$ of Eq. (B.55a) thus is:

$$\sigma_{\text{DC,real}}^{\text{nonint}} = \sum_{\sigma_1} \frac{1}{d} \int (d\varepsilon) \hbar [-n'_0(\hbar\varepsilon)] \int dx_2 \mathbf{j}_{11'} \cdot \mathbf{j}_{22'} \hbar \tilde{G}_{12'}^R(\varepsilon) \tilde{G}_{21'}^A(\varepsilon). \quad (\text{C.3})$$

This is a standard result; it still has to be averaged over disorder, a step that we review in App. C.2.

The $\tilde{J}^{(0),\varepsilon}(0)$ correlator of Eq. (C.2a), in which the energy argument is not constrained, turns out to cancel the (first) diamagnetic term in Eq. (B.55b), implying that $\sigma_{\text{DC,imag}}^{\text{nonint}} = 0$, as expected. This cancellation can be verified, even before disorder averaging, by using an exact identity,

$$\frac{1}{d} \int dx_2 \mathbf{j}_{11'} \cdot [\tilde{G}_{12'}^{R/A}(\varepsilon) \mathbf{j}_{22'} \tilde{G}_{21'}^{R/A}(\varepsilon)] = -\frac{e^2}{m} \tilde{G}_{11}^{R/A}(\varepsilon), \quad (\text{C.4})$$

proven below, to rewrite the contribution from $\tilde{J}^{(0)}(0)$ to Eq. (B.55b) as follows:

$$\begin{aligned} \sum_{\sigma_1} \int dx_2 \mathbf{j}_{11'} \cdot \mathbf{j}_{22'} \frac{\tilde{J}_{12',21'}^{(0)}(0)}{\omega_0 d} &= \frac{\hbar e^2}{\omega_0 m} \sum_{\sigma_1} \int (d\varepsilon) n_0(\hbar\varepsilon) \left[\tilde{G}_{11}^R(\varepsilon) - \tilde{G}_{11}^A(\varepsilon) \right] \\ &= -\frac{\hbar e^2}{\omega_0 m} \sum_{\sigma_1} \int (d\varepsilon) G_{11}^<(\varepsilon) = -\sum_{\sigma_1} \frac{ie^2 \langle \hat{n}_{11H} \rangle}{\omega_0 m}, \end{aligned} \quad (\text{C.5})$$

which indeed cancels the first term of Eq. (B.55b). Since the DC conductivity is a real quantity, the latter cancellation of the two contributions to $\sigma_{\text{imag}}^{\text{DC}}$, namely the diamagnetic term and a term containing an integral $\int d\varepsilon n_0(\hbar\varepsilon)$ over the entire Fermi sea, must hold order for order, to all orders, in perturbation theory in the interaction. Therefore, we shall henceforth not keep track of these terms, and take \tilde{J} to represent only those terms that end up containing a factor $-n'_0(\hbar\varepsilon)$ that restricts ε to the vicinity of the Fermi surface, as in Eq. (C.2b) for $\tilde{J}'^{(0)}$.

It remains to prove Eq. (C.4). It follows directly from another exact identity,

$$\int dx_l \mathbf{j}_{l\nu} [\tilde{G}_{i\nu}^{R/A}(\varepsilon) \tilde{G}_{lj}^{R/A}(\varepsilon)] = -\frac{ie \mathbf{r}_{ij}}{\hbar} \tilde{G}_{ij}^{R/A}(\varepsilon), \quad (\text{C.6})$$

which can be derived¹⁷ before disorder averaging by evoking gauge invariance: let $\psi_\lambda(x_i) = \langle x_i | \lambda \rangle$ and ξ_λ be exact eigenfunctions and eigenvalues of the single-particle Hamiltonian \hat{H}_0 [i.e. $\hat{H}_0 | \lambda \rangle = \xi_\lambda | \lambda \rangle$, cf. Eq. (B.15)], and let \mathbf{A} be a spatially uniform vector potential. Then the gauge-transformed wave-functions $e^{-ie\mathbf{A}\cdot\mathbf{r}_i/\hbar} \psi_\lambda(x_i) \equiv \tilde{\psi}_\lambda(x_i) \equiv \langle x_i | \tilde{\lambda} \rangle$ are eigenfunctions of the gauge-transformed Hamiltonian $\tilde{H}_0 \equiv \hat{H}_0(\hat{\mathbf{P}} + e\mathbf{A}) = \hat{H}_0(\hat{\mathbf{P}}) + \mathbf{A} \cdot \hat{\mathbf{j}} + \frac{e^2 \mathbf{A}^2}{2m}$, again with eigenvalue ξ_λ , i.e. $\tilde{H}_0 | \tilde{\lambda} \rangle = \xi_\lambda | \tilde{\lambda} \rangle$. Consequently, the gauge-transformed version of $\tilde{G}_{ij}^{R/A}(\varepsilon)$ can be written in two equivalent ways, as follows:

$$e^{-ie\mathbf{A}\cdot\mathbf{r}_{ij}/\hbar} \tilde{G}_{ij}^{R/A}(\varepsilon) = \sum_\lambda \langle x_i | \tilde{\lambda} \rangle \frac{1}{\hbar\varepsilon - \xi_\lambda \pm i\alpha} \langle \tilde{\lambda} | x_j \rangle = \langle x_i | \frac{1}{\hbar\varepsilon - \tilde{H}_0 \pm i\alpha} | x_j \rangle.$$

Expanding both the left- and right-hand sides to linear order in \mathbf{A} , and representing the latter in terms of the non-gauge transformed wave functions $\langle x_i | \lambda \rangle = \psi_\lambda(x_i)$, we obtain

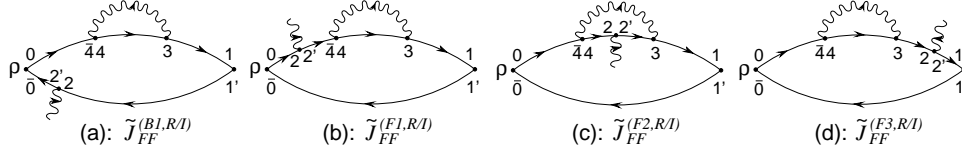
$$-\frac{ie\mathbf{A}\cdot\mathbf{r}_{ij}}{\hbar} \tilde{G}_{ij}^{R/A}(\varepsilon) = \sum_{\lambda'\lambda} \psi_{\lambda'}(x_i) \frac{1}{\hbar\varepsilon - \xi_{\lambda'} \pm i\alpha} \langle \lambda' | \mathbf{A} \cdot \hat{\mathbf{j}} | \lambda \rangle \frac{1}{\hbar\varepsilon - \xi_\lambda \pm i\alpha} \psi_\lambda(x_j).$$

This readily yields Eq. (C.6), since the matrix elements of the current operator are given by $\langle \lambda' | \hat{\mathbf{j}} | \lambda \rangle = \int dx_l \mathbf{j}_{l\nu} [\psi_{\lambda'}^*(x_l) \psi_\lambda(x_l)]$.

C.2. Disorder Average of Noninteracting Case

Evaluating the disorder average $\langle \tilde{G}^R \tilde{G}^A \rangle_{\text{dis}}$ needed in Eq. (C.3) is a textbook exercise: Introducing an extra dummy integration $\text{Vol}^{-1} \int d\mathbf{r}_1$ into Eq. (B.55a), using Eqs. (F.1) and (F.3) from App. F and performing the momentum integrals using Eq. (F.6b), we find:

$$\begin{aligned} \sigma_{\text{DC}}^{\text{nonint}} &= \int (d\varepsilon) [-n'_0(\hbar\varepsilon)] \frac{2e^2 \hbar^4}{dm^2 \text{Vol}} \sum_{\mathbf{p}\mathbf{p}'} \mathbf{p} \cdot \mathbf{p}' \bar{\mathcal{G}}_{\mathbf{p}}^R(\varepsilon) \bar{\mathcal{G}}_{\mathbf{p}'}^A(\varepsilon) \\ &\quad \times \left[\delta_{\mathbf{p},\mathbf{p}'} + \frac{\bar{\mathcal{G}}_{\mathbf{p}'}^R(\varepsilon) \bar{\mathcal{G}}_{\mathbf{p}}^A(\varepsilon) \bar{\mathcal{C}}_{\mathbf{p}+\mathbf{p}'}^0(0)}{\text{Vol} 2\pi\nu\tau_{\text{el}}^2/\hbar} \right] \end{aligned} \quad (\text{C.8a})$$


 Fig. C1. Feynman diagrams for the correlators $\tilde{J}_{aa'}^{(R/I)}$ of Eqs. (C.10).

$$\simeq \sigma_{\text{DC}}^{\text{Drude}} \left[1 - \frac{1}{\pi\nu\hbar} \int d\varepsilon \hbar [-n'_0(\hbar\varepsilon)] \int (d\mathbf{q}) \int_0^\infty d\tau \tilde{C}_{\mathbf{q}}^0(\tau) \right]. \quad (\text{C.8b})$$

Here $\sigma_{\text{DC}}^{\text{Drude}} = 2e^2\nu D$ is the Drude conductivity and $D = v_F^2\tau_{\text{el}}/d$ is the diffusion constant. For the second term of Eq. (C.8b), we introduced the variable $\mathbf{q} = \mathbf{p} + \mathbf{p}'$ and set $\mathbf{q} = 0$ everywhere except in $\tilde{C}_{\mathbf{q}}^0(\omega = 0)$, because the latter's infrared singularity as $\mathbf{q} \rightarrow 0$ dominates the $\int (d\mathbf{q})$ integral. [Since $\overline{D}_{2\mathbf{p}}^0(0)$ from Eq. (F.3b) has no singularities, its contribution to Eq. (C.8b) was dropped.] The $\int d\varepsilon$ integral in Eq. (C.8b), which trivially equals one, is displayed here explicitly only for the sake of comparison with later results.

The fact that the weak localization correction is small compared to the Drude term is often made explicit by expressing the prefactor of the Cooperon term in terms of the dimensionless conductance $g_{\bar{d}}(L)$ [see Eq. (B.9), and the discussion thereafter]: Using $\int (d\mathbf{q}) = a^{\bar{d}-d} \int d^{\bar{d}}q / (2\pi)^{\bar{d}}$ for the momentum integral over the diffusive motion, and introducing, e.g., the dimensionless variables $u \equiv \tau_{12}/\tau_H$ and $z \equiv qL_H$ (with $L_H = \sqrt{D\tau_H}$) [if more convenient, e.g. in the absence of a magnetic field, one could replace τ_H by τ_φ here) we obtain from Eq. (C.8b) (times $a^{d-\bar{d}}$):

$$\sigma_{\bar{d},\text{DC}}^{\text{nonint}} = \sigma_{\bar{d}} \left[1 - \frac{1}{g_{\bar{d}}(L_H)} \frac{2}{\pi} \int \frac{d^{\bar{d}}z}{(2\pi)^{\bar{d}}} \int_{\tau_{\text{el}}/\tau_H}^\infty du \tilde{C}_{z/L_H}^0(u\tau_H) \right], \quad (\text{C.9})$$

where we inserted an ultraviolet cutoff at small times, needed for $\bar{d} = 2, 3$. Appealingly, the prefactor of the Cooperon term manifestly displays the smallness of $\sigma_{\bar{d}}^{\text{WL}}$, via the largeness of $g_{\bar{d}}$.

C.3. First order Calculation of \tilde{J}'

In this section, we illustrate the structure of the perturbation expansion generated when the influence functional is expanded in powers of the effective action ($i\tilde{S}_R + \tilde{S}_I$), as in Eq. (B.85): using approximation (ii) of Sec. B.5.7, we explicitly calculate the first order contribution $\tilde{J}_{12',21'}^{(1)}(0)$ to the correlator of Eq. (B.55a), i.e. the $\omega_0 = 0$ value of first derivative ∂_{ω_0} of the ω_0 -Fourier transform of $\theta_{12} \tilde{J}_{12',21'}^{(1)}(t_1, t_2; t_0) \equiv \sum_{aa'} [\tilde{J}_{aa'}^{(R)} + \tilde{J}_{aa'}^{(I)}]$. Here $\tilde{J}_{aa'}^{(R/I)} = \sum_{\tilde{a}} \tilde{J}_{aa'}^{(\tilde{a}, R/I)}$ denotes the first-order contribution to $\tilde{J}^{(1)}$ that arises from ($i\tilde{S}^R/\tilde{S}^I$) and has interaction vertices lying on contours a and a' , while the index \tilde{a} in $\tilde{J}_{aa'}^{(\tilde{a}, R/I)}$ indicates which contour the current vertex is located on.

Our starting point is Eq. (B.80), expanded to first order in $-(i\tilde{S}_R/\tilde{S}_I)/\hbar$, using Eq. (B.83):

$$\begin{aligned}\tilde{J}_{aa'}^{(F,R/I)} &\equiv -\frac{\theta_{12}}{\hbar^2} \int dx_{0_F, \bar{0}_B} \tilde{\rho}_{0_F \bar{0}_B}^0 \rlap{-}\int_{2'_F}^{1_F} \rlap{-}\int_{0_F}^{2_F} \rlap{-}\int_{\bar{0}_B}^{1'_B} \tilde{\mathcal{D}}'(\mathbf{R}) \int_{t_0}^{t_1} dt_{3_a} dt_{4_{a'}} \left\{ \begin{array}{l} i\tilde{L}^R \\ \tilde{L}^I \end{array} \right\}_{3_a 4_{a'}}^{y_F=0} \\ \tilde{J}_{aa'}^{(B,R/I)} &\equiv \frac{\theta_{12}}{\hbar^2} \int dx_{0_F, \bar{0}_B} \tilde{\rho}_{0_F \bar{0}_B}^0 \rlap{-}\int_{0_F}^{1_F} \rlap{-}\int_{2_B}^{1'_B} \rlap{-}\int_{\bar{0}_B}^{2'_B} \tilde{\mathcal{D}}'(\mathbf{R}) \int_{t_0}^{t_1} dt_{3_a} dt_{4_{a'}} \left\{ \begin{array}{l} i\tilde{L}^R \\ \tilde{L}^I \end{array} \right\}_{3_a 4_{a'}}^{y_B=0}\end{aligned}$$

If interaction and current vertices occur on the same part (forward or backward) of the Keldysh contour, then, depending on the relative time orderings of the vertices, there can be more than one contribution to each of these quantities, which we shall denote by $\tilde{J}_{aa'}^{(\bar{i},R/I)}$, with $i = 1, 2, 3$, etc.

Consider $\tilde{J}_{FF}^{(B1,R/I)}$ [see Fig. C1(a)], which has two interaction vertices on the forward contour at times t_3 and t_4 satisfying $t_0 < t_4 < t_3 < t_1$, and a current vertex on the backward contour at time t_2 satisfying $t_0 < t_2 < t_1$ [in GZ's approach, who take $t_0 = t_2$, cf. Section B.5.7, these two sets of inequalities are replaced by a single one instead, namely $t_2 < t_4 < t_3 < t_1$]. Inserting Eq. (B.84a) for $(i\tilde{L}^R/\tilde{L}^I)_{3_F 4_F}$ into the first of the above equations, we obtain:

$$\begin{aligned}\tilde{J}_{FF}^{(B1,R/I)} &= \frac{i\theta_{12}}{2\hbar^2} \int_{t_0}^{t_1} dt_{3_F} \int_{t_0}^{t_{3_F}} dt_{4_F} \int dx_{0_F, \bar{0}_B} \tilde{U}_{1_F 3_F}^0 \delta_{3_F \bar{3}_F} \tilde{U}_{3_F 4_F}^0 \left\{ \begin{array}{l} (\tilde{\delta} - 2\tilde{\rho}^0)_{4_F \bar{4}_F} \\ \theta_{34} \tilde{\delta}_{4_F \bar{4}_F} \end{array} \right\} \tilde{\mathcal{L}}_{3_F \bar{4}_F}^{R/K} \\ &\quad \times \tilde{U}_{4_F 0_F}^0 \tilde{\rho}_{0_F \bar{0}_B}^0 \tilde{U}_{\bar{0}_B 2'_B}^0 \tilde{U}_{2_B 1'_B}^0 \\ &= \frac{1}{2} i \hbar^2 \int_{-\infty}^{\infty} dt_3 \int_{-\infty}^{\infty} dt_4 \tilde{G}_{13}^R \tilde{G}_{34}^{K/R} \tilde{G}_{42'}^< \tilde{G}_{21'}^A \tilde{\mathcal{L}}_{34}^{R/K}.\end{aligned}\quad (\text{C.10a})$$

Here integration over repeated spatial indices such as 0_F or $\bar{0}_B$ or 3_F is implied; those over time are displayed explicitly, to keep track of the integration boundaries.] Eq. (C.10a) [whose index contractions are illustrated in Fig. B2(a)] follows from the first line by relations such as Eqs. (B.45) and (B.47) (and dropping the subscripts F, B on indices). Moreover, taking the limit $t_0 \rightarrow -\infty$ [but keeping t_1 fixed], the time integrals were extended to range over $[-\infty, \infty]$. This is possible, since \tilde{G}_{ij}^R contains a factor θ_{ij} , \tilde{G}_{ij}^A a θ_{ji} , and $\tilde{\mathcal{L}}_{34}^R$ a θ_{34} , so that the product of Green's functions under the time integrals automatically vanishes for time arguments lying outside the integration ranges stipulated by the integration boundaries and θ -functions occurring in the first line. [However, if t_0 had erroneously been replaced by t_2 in the first line above, as GZ do, the second line would have integration limits $\int_{t_2}^{\infty} dt_{4_F} \int_{t_4}^{\infty} dt_{3_F}$, since $G_{42'}^<$ contains no θ_{42} .]

The case of $\tilde{J}_{FF}^{(Fi,R/I)}$ is similar, but since both the interaction vertices at times t_3 , t_4 and the current vertex at time t_2 all reside on the forward contour, three separate cases have to be considered [see Fig. C1(b) to (d)], corresponding to the three possible time orderings, namely (1): $t_0 < t_2 < t_4 < t_3 < t_1$, or (2): $t_0 < t_4 < t_2 < t_3 < t_1$, or (iii): $t_0 < t_4 < t_3 < t_2 < t_1$ [since GZ implicitly take $t_0 = t_2$, the latter two cases

do not occur in their approach]:

$$\begin{aligned}
 \tilde{J}_{FF}^{(F1,R/I)} &= \frac{i\theta_{12}}{2\hbar^2} \int_{t_2}^{t_1} dt_{3F} \int_{t_2}^{t_{3F}} dt_{4F} \int dx_{0F, \bar{0}B} \tilde{U}_{1F3F}^0 \delta_{3F\bar{3}F} \tilde{U}_{3F4F}^0 \left\{ \begin{array}{l} (\tilde{\delta} - 2\tilde{\rho}^0)_{4F\bar{4}F} \\ \theta_{34} \tilde{\delta}_{4F\bar{4}F} \end{array} \right\} \tilde{\mathcal{L}}_{3F4F}^{R/K} \\
 &\quad \times \tilde{U}_{4F2F}^0 \tilde{U}_{2F0F}^0 \tilde{\rho}_{0F\bar{0}B}^0 \tilde{U}_{0B1B}^0 \\
 &= -\frac{1}{2} i\hbar^2 \int_{-\infty}^{\infty} dt_3 \int_{-\infty}^{\infty} dt_4 \tilde{G}_{13}^R \tilde{G}_{34}^{K/R} \tilde{G}_{42'}^R \tilde{G}_{21'}^< \tilde{\mathcal{L}}_{34}^{R/K} . \quad (C.10b)
 \end{aligned}$$

$$\begin{aligned}
 \tilde{J}_{FF}^{(F2,R/I)} &= \frac{i\theta_{12}}{2\hbar^2} \int_{t_2}^{t_1} dt_{3F} \int_{t_0}^{t_2} dt_{4F} \int dx_{0F, \bar{0}B} \tilde{U}_{1F3F}^0 \delta_{3F\bar{3}F} \tilde{U}_{3F2F}^0 \tilde{U}_{2F4F}^0 \left\{ \begin{array}{l} \tilde{\delta}_{4F\bar{4}F} \\ \theta_{34} \tilde{\delta}_{4F\bar{4}F} \end{array} \right\} \tilde{\mathcal{L}}_{3F4F}^{R/K} \\
 &\quad \times \tilde{U}_{4F0F}^0 \tilde{\rho}_{0F\bar{0}B}^0 \tilde{U}_{0B1B}^0 \\
 &= -\frac{1}{2} i\hbar^2 \int_{-\infty}^{\infty} dt_3 \int_{-\infty}^{\infty} dt_4 \tilde{G}_{13}^R \tilde{G}_{32'}^R \tilde{G}_{24}^R \tilde{G}_{41'}^< \tilde{\mathcal{L}}_{34}^{R/K} , \quad (C.10c)
 \end{aligned}$$

$$\begin{aligned}
 \tilde{J}_{FF}^{(F3,R/I)} &= \frac{i\theta_{12}}{2\hbar^2} \int_{t_0}^{t_2} dt_{3F} \int_{t_0}^{t_2} dt_{4F} \int dx_{0F, \bar{0}B} \tilde{U}_{1F2F}^0 \tilde{U}_{2F3F}^0 \delta_{3F\bar{3}F} \tilde{U}_{3F4F}^0 \left\{ \begin{array}{l} \tilde{\delta}_{4F\bar{4}F} \\ \theta_{34} \tilde{\delta}_{4F\bar{4}F} \end{array} \right\} \tilde{\mathcal{L}}_{3F4F}^{R/K} \\
 &\quad \times \tilde{U}_{4F0F}^0 \tilde{\rho}_{0F\bar{0}B}^0 \tilde{U}_{0B1B}^0 \\
 &= -\frac{1}{2} i\hbar^2 \int_{-\infty}^{\infty} dt_3 \int_{-\infty}^{\infty} dt_4 \tilde{G}_{12'}^R \tilde{G}_{23}^R \tilde{G}_{34}^R \tilde{G}_{41'}^< \tilde{\mathcal{L}}_{34}^{R/K} . \quad (C.10d)
 \end{aligned}$$

Eqs. (C.10b) corresponds to Figs. B2(b). The absence of a factor $(\tilde{\delta} - 2\tilde{\rho}^0)$ in the first lines of Eqs. (C.10c) and (C.10d), and the corresponding absence of a \tilde{G}^K -function in the respective second lines, reflects the fact that we took $y^F = 0$ and that $t_4 < t_2$ in these integrals, so that the factor $(\theta_{42} + y_F \theta_{24}) 2\tilde{\rho}^0$ in Eq. (B.84a) for $(i\tilde{L}^R/\tilde{L}^I)_{3F4F}$ vanishes. Eqs. (C.10c) and (C.10d) are examples of contributions for which one or more interaction vertices occur on the same contour as the current vertex, but at *earlier* times. As discussed in approximation (ii) of Sec. B.5.7, such terms contribute to “interaction corrections” but not to decoherence, and thus will henceforth be excluded from our considerations.

Adding the two terms [(C.10a), (C.10b)] that survive under the said approximation (ii), we obtain $\tilde{J}_{FF}^{(R/I)} = \sum_{\bar{a}} \tilde{J}_{FF}^{(\bar{a}1,R/I)}$. The other three correlators, $\tilde{J}_{BF}^{(R/I)}$, $\tilde{J}_{FB}^{(R/I)}$ and $\tilde{J}_{BB}^{(R/I)}$, can be calculated in an entirely analogous manner. The results are:

$$\tilde{J}_{FF}^{(R/I)} = -\frac{1}{2} i\hbar^2 \int_{-\infty}^{\infty} dt_3 dt_4 \tilde{G}_{13}^R \tilde{G}_{34}^{K/R} \left[\tilde{G}_{42'}^R \tilde{G}_{21'}^< + \tilde{G}_{42'}^< \tilde{G}_{21'}^A \right] (\tilde{\mathcal{L}}^R/\tilde{\mathcal{L}}^K)_{34} , \quad (C.11a)$$

$$\tilde{J}_{BF}^{(R/I)} = -\frac{1}{2} i\hbar^2 \int_{-\infty}^{\infty} dt_3 dt_4 \tilde{G}_{14}^{K/R} \left[\tilde{G}_{42'}^R \tilde{G}_{23}^< + \tilde{G}_{42'}^< \tilde{G}_{23}^A \right] \tilde{G}_{31}^A (\tilde{\mathcal{L}}^R/\frac{1}{2}\tilde{\mathcal{L}}^K)_{34} , \quad (C.11b)$$

$$\tilde{J}_{FB}^{(R/I)} = -\frac{1}{2} i\hbar^2 \int_{-\infty}^{\infty} dt_3 dt_4 \tilde{G}_{13}^R \left[\tilde{G}_{32'}^R \tilde{G}_{24}^< + \tilde{G}_{32'}^< \tilde{G}_{24}^A \right] \tilde{G}_{41'}^{K/A} (\tilde{\mathcal{L}}^A/\frac{1}{2}\tilde{\mathcal{L}}^K)_{43} , \quad (C.11c)$$

$$\tilde{J}_{BB}^{(R/I)} = -\frac{1}{2} i\hbar^2 \int_{-\infty}^{\infty} dt_3 dt_4 \left[\tilde{G}_{12'}^R \tilde{G}_{24}^< + \tilde{G}_{12'}^< \tilde{G}_{24}^A \right] \tilde{G}_{43}^{K/A} \tilde{G}_{31'}^A (\tilde{\mathcal{L}}^A/\tilde{\mathcal{L}}^K)_{43} . \quad (C.11d)$$

Satisfactorily, these expressions agree completely with those [Eqs. (E.31)] obtained in App. E.4] using diagrammatic Keldysh perturbation theory.

To obtain $\tilde{J}'(0)$, we have to Fourier transform these equations w.r.t. t_{12} , and then calculate $J_{aa'}^{(R/I)}(0) = [\partial_{\omega_0} J_{aa'}^{(R/I)}(\omega_0)]_{\omega_0=0}$. For example, $\tilde{J}_{FF}^{(R/I)}(\omega_0)$ is given by

$$\begin{aligned} \tilde{J}_{FF}^{(R/I)}(\omega_0) = & -\frac{1}{2}i\hbar \int (d\varepsilon)(d\bar{\omega}) \tilde{G}_{13}^R(\varepsilon_+) \tilde{G}_{34}^{K/R}(\varepsilon_+ - \bar{\omega}) \tilde{\mathcal{L}}_{34}^{R/K}(\bar{\omega}) \\ & \times \hbar \left[\tilde{G}_{42'}^R(\varepsilon_+) \tilde{G}_{21'}^<(\varepsilon_-) + \tilde{G}_{42'}^<(\varepsilon_+) \tilde{G}_{21'}^A(\varepsilon_-) \right], \end{aligned} \quad (\text{C.12})$$

and $\tilde{J}_{FF}^{(R/I)}(0)$ is easily calculated by noting that the factor in the second line of Eq. (C.12) equals $\tilde{J}_{42',21'}^{(0)}(\omega_0)$ [cf. Eq. (C.1b)], whose first derivative is given by Eq. (C.2b), namely $\tilde{J}_{42',21'}^{(0),\varepsilon}(0) = -n'_0(\hbar\varepsilon) \hbar^2 \tilde{G}_{42'}^R(\varepsilon) \tilde{G}_{21'}^A(\varepsilon)$. Thus, the final result for $\tilde{J}_{FF}^{(R/I)}(0)$ is

$$\tilde{J}_{FF}^{(R/I)}(0) = -\frac{1}{2}i\hbar^3 \int (d\varepsilon)(d\bar{\omega}) [-n'_0(\hbar\varepsilon)] \tilde{G}_{13}^R(\varepsilon) \tilde{G}_{34}^{K/R}(\varepsilon - \bar{\omega}) \tilde{G}_{42'}^R(\varepsilon) \tilde{G}_{21'}^A(\varepsilon) \tilde{\mathcal{L}}_{34}^{R/K}(\bar{\omega}).$$

Similar expressions for the other contributions $\tilde{J}_{aa'}^{(R/I)}(0)$ can be derived from Eqs. (C.11) in an entirely analogous manner, and are given in Eq. (B.86) of App. B.6.2. In each case the combination $\hbar[\tilde{G}_{i2'}^R, \tilde{G}_{2j}^< + \tilde{G}_{i2'}^<, \tilde{G}_{2j}^A]$ produces a factor $\hbar^2[-n'_0(\hbar\varepsilon)]\tilde{G}_{i2'}^R(\varepsilon)\tilde{G}_{2j}^A(\varepsilon)$.

Actually, it is clear from the above derivation that in *every* order of perturbation theory in the interaction, such a factor will be produced for *all* terms that survive the abovementioned approximation (ii): in analogy to Eqs. (C.10a) and (C.10b), it will arise from a factor

$$-\frac{1}{\hbar} \int dx_{0F, \bar{0}B} \left[\tilde{U}_{iF0F}^0 \tilde{\rho}_{0F\bar{0}B}^0 \tilde{U}_{0B2'B}^0 \tilde{U}_{2BjB}^0 - \tilde{U}_{iF2'F}^0 \tilde{U}_{2F0F}^0 \tilde{\rho}_{0F\bar{0}B}^0 \tilde{U}_{0BjB}^0 \right], \quad (\text{C.13})$$

where t_{iF} and t_{jB} are the times of the *earliest* interaction vertex on the upper or lower Keldysh contour, respectively.

To conclude this section, we wish to emphasize once more the significance of the fact, illustrated by Eqs. (C.11) but valid for all contributions to $\tilde{J}^{(1)}$ (including the “interaction corrections”), that all time integrals occurring in Keldysh perturbation theory can be extended to range over the *entire* real axis. Importantly, this implies that the Fourier transforms that are needed to obtain $\tilde{J}^{(1)}(\omega_0)$ (and from there the conductivity) are *always* given by simple convolution integrals, such as Eq. (C.12). In contrast, in GZ’s calculations all time integrals $\int dt_3 dt_4$ have t_2 as lower limit, see e.g. (GZ-III.A20) and (GZ-III.A23) in GZ00⁴, whose t' corresponds to our t_2 . This means that instead of obtaining simple convolution integrals, they erroneously end up with sin and cos functions, see (GZ-III.58) and (GZ-III.61). This leads to numerous incorrect complications and conclusions, such as the claimed existence of an “oscillating cos-term” in (GZ-III.70). Thus, GZ’s perturbative analysis in Sec. IV of GZ00⁴, in particular their discussion of the “breakdown of the Fermi golden rule approximation” in Sec. IV.B, is invalid, since its starting point is based on the

replacement $t_0 \rightarrow t_2$, which is incorrect (and unnecessary, since the correct limit $t_0 \rightarrow -\infty$ can be incorporated into GZ's approach, as emphasized in Sec. B.5.7 and illustrated explicitly above).

C.4. Thermal Weighting and Path Integral, before Disorder Averaging

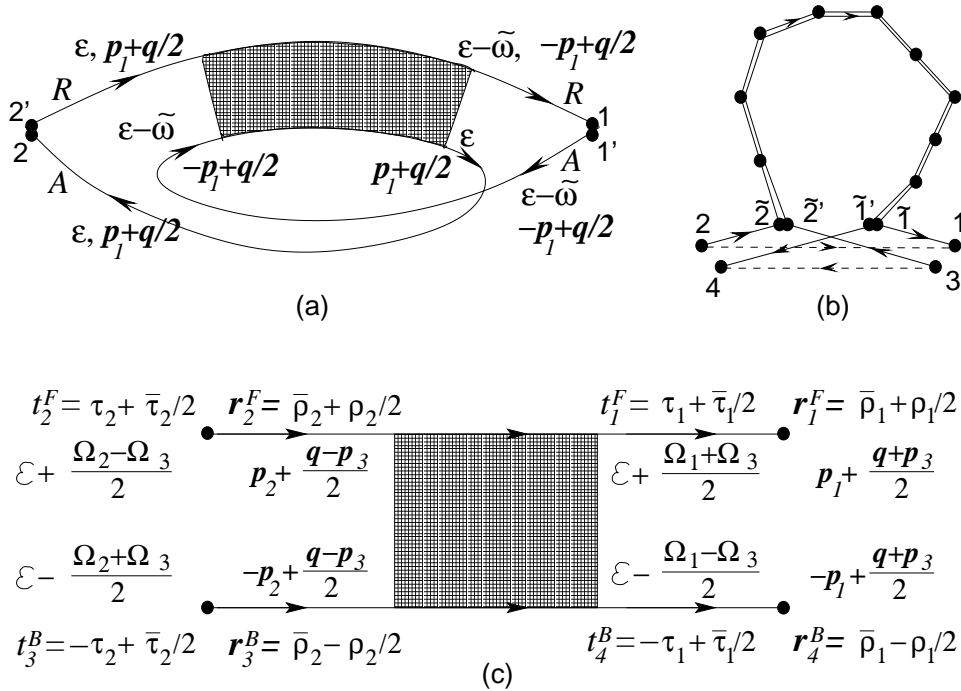


Fig. C2. (a) Diagrammatic depiction of Eqs. (C.18) for $\tilde{J}'_{12',21'}$ or Eq. (C.29) for $\sigma_{\text{DC}}^{\text{WL}}$. Before disorder averaging the black box represents $\tilde{\mathcal{P}}_{21'}^{12'}(\varepsilon - \frac{1}{2}\tilde{\omega}; -\tilde{\omega}, \tilde{\omega})$, thereafter it represents $\tilde{\mathcal{C}}_q^{\varepsilon - \frac{1}{2}\tilde{\omega}}(-\tilde{\omega}, \tilde{\omega})/(2\pi\nu\tau_{\text{el}}^2/\hbar)$. (b) Real-space depiction of a typical pair of Drude (dashed) and time-reversed (solid) trajectories contributing to $\tilde{P}_{43}^{12, \text{Drude}}$ and $\tilde{P}_{43}^{12, \text{WL}}$, corresponding to Eqs. (C.31a) and (C.31b), respectively. (c) Definition of variables used for Fourier-transforming the double path integral $\tilde{P}_{43}^{12}(\mathcal{E}, \Omega_1, \Omega_2)$ of Eq. (C.16). In (c), frequency and momentum variables are chosen such that Ω_1 and Ω_2 are, respectively, the outgoing and incoming ‘‘Cooperon frequencies’’ (i.e. frequency differences between upper and lower lines); $q \pm p_3$ are the outgoing and incoming ‘‘Cooperon momenta’’ (i.e. sum of momenta of upper and lower lines); $\mathcal{E} \pm \Omega_3/2$ are the average (between upper and lower) frequencies flowing out of our into the Cooperon, respectively. The time variables $\tau_{1,2}$ and $\bar{\tau}_{1,2}$ and coordinate variables $\rho_{1,2}$ and $\bar{\rho}_{1,2}$ are purposefully defined in such a way [Eqs. (C.17a), (C.32)] that the Fourier exponents in Eqs. (C.16b), (C.16c) and (C.35) are free of factors of 2. (Our labelling convention differs from that of AAK¹⁰, which has typos involving factors of 2.)

The presence of interactions will, in general, modify the result (C.8b) for $\sigma_{\text{DC}}^{\text{nonint}}$

in two ways: firstly, it can renormalize the value of $\sigma_{\text{DC}}^{\text{Drude}}$, but this effect is not interesting for present purposes and will be ignored here. Secondly, it can reduce the life-time of the Cooperon propagator, thereby contributing to decoherence, which is the effect we are interested in. Our goal in this section is to express the conductivity of Eq. (B.55a) in terms of double path integral expressions for $\tilde{J}'_{12',21'}(0)$, obtained from Eq. (B.80), in a way that is generally valid in the presence of interactions, *before* disorder averaging, and properly accounts for thermal weighting via a factor $[-n'_0(\hbar\varepsilon)]$, as in Eq. (C.8b). Hence, we will have to find appropriate Fourier transforms of our path integral expressions that relate them to the energy $\hbar\varepsilon$.

An important first clue comes from the first order relations (B.86) for $\tilde{J}'_{12',21'}(0)$: each term contains a factor $\int(d\varepsilon)\hbar^2[-n'_0(\hbar\varepsilon)]\tilde{G}_{i2'}^R(\varepsilon)\tilde{G}_{2j}^A(\varepsilon)$, thus the current vertex $\mathbf{j}_{22'}$ is always sandwiched between a retarded and advanced function with energy ε , $\tilde{G}_{i2'}^R(\varepsilon)\mathbf{j}_{22'}\tilde{G}_{2j}^A$, and thermal weighting is always governed by a factor $[-n'_0(\hbar\varepsilon)]$. As explained after in App. C.3 [just before Eq. (C.13)] these properties actually hold in *every* order of perturbation theory in the interaction, for *all* terms that survive approximation (ii). Of course, the other current vertex $\mathbf{j}_{11'}$ is similarly sandwiched, too, but in general with a different energy argument, $\tilde{G}_{j1'}^A(\varepsilon - \tilde{\omega})\mathbf{j}_{11'}\tilde{G}_{1i}^R(\varepsilon - \tilde{\omega})$. The general expression for that part of the conductivity containing the Cooperon propagator, relevant for weak localization, is by definition the sum to all orders of all such terms containing $[-n'_0]\tilde{G}_{i2'}^R\mathbf{j}_{22'}\tilde{G}_{2j}^A \dots \tilde{G}_{j1'}^R\mathbf{j}_{11'}\tilde{G}_{1i}^A$. In path integral language, it will thus have the following form,

$$\sigma_{\text{DC}} = \sum_{\sigma_1} \frac{1}{d} \int dx_2 \mathbf{j}_{11'} \cdot \mathbf{j}_{22'} \int (d\varepsilon) \tilde{J}'_{12',21'}^\varepsilon, \quad (\text{C.14})$$

written in analogy to Eq. (B.55a) for $\sigma_{\text{DC,real}}$, where the integral equals $\tilde{J}'_{12',21'}(0)$, and $\tilde{J}'_{12',21'}^\varepsilon$ equals $[-n'_0(\hbar\varepsilon)]$ times some suitable frequency Fourier transform (needed to set the energy to ε) of a double path integral whose forward path connects the points $\mathbf{r}_{2'}$ and \mathbf{r}_1 , while the backward path connects \mathbf{r}_2 and $\mathbf{r}_{1'}$. To find the appropriate expression, we begin by considering the general double path integral

$$\tilde{P}_{43}^{12} \equiv \theta_{12} \theta_{34} \rlap{-}\int_{\mathbf{R}^F(t_2^F)=\mathbf{r}_2^F}^{\mathbf{R}^F(t_1^F)=\mathbf{r}_1^F} \rlap{-}\int_{\mathbf{R}^B(t_4^B)=\mathbf{r}_4^B}^{\mathbf{R}^B(t_3^B)=\mathbf{r}_3^B} \tilde{\mathcal{D}}'(\mathbf{R}) e^{-[i\tilde{S}_R + \tilde{S}_I]/\hbar}, \quad (\text{C.15})$$

depicted schematically in Figs. C2(b) and C2(c). It ranges from \mathbf{r}_2^F at time t_2^F to \mathbf{r}_1^F at time t_1^F ($> t_2^F$) on the forward contour and from \mathbf{r}_4^B at time t_4^B to \mathbf{r}_3^B at time t_3^B ($> t_4^B$) on the backward contour. These times are understood to be the limits of the $\int dt_a$ time integrals in \tilde{S}_0^a and $(i\tilde{S}_R + \tilde{S}_I)$, and t_4^B, t_3^B are in general not equal to t_2^F, t_1^F , since they will have to be Fourier transformed independently [as required, e.g., to properly define the variable ε in Eq. (C.14)]. For general time arguments, we adopt the following conventions, depicted in Fig. C2(c), for Fourier transforming from the time to frequency domain and back:

$$\tilde{P}_{43}^{12} \equiv \int (d\mathcal{E})(d\Omega_1)(d\Omega_2)(d\Omega_3) 2\pi\delta(\Omega_3) \tilde{\mathcal{P}}_{43}^{12}(\mathcal{E}; \Omega_1, \Omega_2) \exp i \left\{ -t_1^F \left[\mathcal{E} + \frac{\Omega_1 + \Omega_3}{2} \right] \right\}$$

$$+ t_2^F \left[\mathcal{E} + \frac{\Omega_2 - \Omega_3}{2} \right] - t_4^B \left[\mathcal{E} - \frac{\Omega_1 - \Omega_3}{2} \right] + t_3^B \left[\mathcal{E} - \frac{\Omega_2 + \Omega_3}{2} \right] \Big\}, \quad (\text{C.16a})$$

$$= \int (d\mathcal{E}) (d\omega) (d\omega') \tilde{\mathcal{P}}_{43}^{12}(\mathcal{E}; \omega + \frac{1}{2}\omega', \omega - \frac{1}{2}\omega') e^{-i[\tilde{\tau}_{12}\mathcal{E} + \tilde{\tau}_{12}\omega' + \tau_{12}\omega]}, \quad (\text{C.16b})$$

$$\tilde{\mathcal{P}}_{43}^{12}(\mathcal{E}; \Omega_1, \Omega_2) = \int d\tau_1 d\tau_2 d\tilde{\tau}_{12} e^{i[\tau_1\Omega_1 - \tau_2\Omega_2 + \tilde{\tau}_{12}\mathcal{E}]} \tilde{P}_{43}^{12}(\tau_{12}, \tilde{\tau}_{12}, \bar{\tau}_{12}). \quad (\text{C.16c})$$

(For \tilde{P} , the indices $_{43}^{12}$ stand for both coordinate and time variables, for its frequency Fourier transform $\tilde{\mathcal{P}}$, distinguished from the former by using calligraphic script, they stand for coordinate variables only; we use a similar convention for the Cooperon, \tilde{C} or $\tilde{\mathcal{C}}$, defined below.) For Eq. (C.16b) we changed frequency variables to $\omega = \frac{1}{2}(\Omega_1 + \Omega_2)$ and $\omega' = \Omega_1 - \Omega_2$, and introduced various sum and difference times [see Fig. C2(c)]:

$$\bar{\tau}_1 \equiv t_1^F + t_4^B, \quad \tau_1 \equiv \frac{t_1^F - t_4^B}{2}, \quad \bar{\tau}_2 \equiv t_2^F + t_3^B, \quad \tau_2 \equiv \frac{t_2^F - t_3^B}{2}, \quad (\text{C.17a})$$

$$\tau_{12} = \tau_1 - \tau_2, \quad \bar{\tau}_{12} = \bar{\tau}_1 - \bar{\tau}_2, \quad \tilde{\tau}_{12} = \frac{\tau_1 + \tau_2}{2}. \quad (\text{C.17b})$$

On the right-hand side of the back transformation (C.16c), $\tilde{P}_{43}^{12}(\tau_{12}, \tilde{\tau}_{12}, \bar{\tau}_{12})$ by definition is given by \tilde{P}_{43}^{12} of Eq. (C.15), with the understanding that the indices 12, 43 now only specify the path end points $\mathbf{r}_1^F, \mathbf{r}_2^F, \mathbf{r}_4^B, \mathbf{r}_3^B$, but that the time arguments $t_1^F, t_2^F, t_3^B, t_4^B$ in Eq. (C.15) are chosen such that Eqs. (C.17) hold.

The frequencies introduced in Eq. (C.16) have evident physical interpretations [see Fig. C2(c)]. The ‘‘Cooperon frequencies’’ Ω_1 and Ω_2 are the outgoing and incoming frequency differences between upper and lower lines, respectively, while $\mathcal{E} \pm \frac{1}{2}\Omega_3$ are the average (between upper and lower) frequencies flowing out of or into the Cooperon. In general, the presence of external time-dependent fields would require Ω_3 , the total frequency difference between outgoing and incoming lines, to be nonzero. However, for the present purpose of calculating the conductivity in linear response, such external fields can be set to zero; hence in Eq. (C.16a) we use a delta-function to set Ω_3 equal to zero, thus recovering translational invariance in time for \tilde{P}_{43}^{12} .

Having identified the meaning of the frequency arguments \mathcal{E} , Ω_1 and Ω_2 [Fig. C2(c)], and inspecting the frequency labels of the standard diagrammatic depiction [Fig. C2(a), where an integral over the ‘‘internal’’ frequency $\tilde{\omega}$ is implied] of the current-current correlator needed for the conductivity, it becomes evident that the average frequency is $\mathcal{E} = \varepsilon - \frac{1}{2}\tilde{\omega}$, while the outgoing and incoming Cooperon frequencies are $\Omega_1 = -\tilde{\omega}$ and $\Omega_2 = \tilde{\omega}$, respectively (i.e. $\omega = 0$ and $\omega' = -2\tilde{\omega}$). Moreover, the upper line runs from $\mathbf{r}_{2'}$ to \mathbf{r}_1 , while the lower line runs backwards in time from $\mathbf{r}_{1'}$ to \mathbf{r}_2 . Thus, the particular Fourier transformed version of \tilde{P} needed for $\tilde{J}_{12', 21'}^\varepsilon$ in Eq. (C.14) is

$$\tilde{J}_{12', 21'}^\varepsilon = [-n'(\hbar\varepsilon)] \int (d2\tilde{\omega}) \tilde{P}_{21'}^{12'}(\varepsilon - \frac{1}{2}\tilde{\omega}; -\tilde{\omega}, \tilde{\omega}). \quad (\text{C.18})$$

To check that the normalization factors and frequency assignments are correct, let us expand $\tilde{P}_{21'}^{12'}$ in Eq. (C.18) to zeroth and first order in the interaction in order to calculate $\tilde{J}_{12',21'}^\varepsilon = [\tilde{J}'^{(0),\varepsilon} + \tilde{J}'^{(1),\varepsilon}]_{12',21'}$, and compare the results to our previously-obtained expressions for these [Eqs. (C.2b) and (B.86)]. To this end, we begin with \tilde{P}_{65}^{12} , as given in Eq. (C.15) and with general indices, expand it to first order in $-[i\tilde{S}_R + \tilde{S}_I]/\hbar$, and express the resulting terms in terms of $\tilde{G}_{ij}^{K/R/A}$ functions. The details are analogous to those presented in Sections C.1 and C.3 to derive $\tilde{J}_{12',21'}^{(0)}$ and $\tilde{J}_{12',21'}^{(1)}$ from $\tilde{J}_{12',21'}^{F/B}$ of Eq. (B.80) (except that the latter's first line is not needed for \tilde{P}_{65}^{12} , and the limits of the path integrals are different). The result can be written as $\tilde{P}_{65}^{12} = \tilde{P}_{12,65}^{(0)} + \sum_{aa'} [\tilde{P}_{aa'}^{(R)} + \tilde{P}_{aa'}^{(I)}]_{12,65}$, where $\tilde{P}_{12,65}^{(0)}$ and $\tilde{P}_{aa'}^{(R/I)}$ are given by Eqs. (C.1a) and (C.11), respectively [with $(12', 21') \rightarrow (12, 65)$], except that all occurrences of the combination $\hbar[\tilde{G}_{i2}^R, \tilde{G}_{2j}^< + \tilde{G}_{i2}^<, \tilde{G}_{2j}^A]$ have to be replaced by $\hbar^2 \tilde{G}_{i2}^R \tilde{G}_{6j}^A$. Fourier transforming the result for \tilde{P}_{65}^{12} [via Eq. (C.16c)] to obtain $\tilde{\mathcal{P}}_{65}^{12}(\mathcal{E}; \Omega_1, \Omega_2)$, specifying the spatial indices as $(12, 65) \rightarrow (12', 21')$ and then integrating as stipulated in Eq. (C.18), one recovers $\tilde{J}_{12',21'}^\varepsilon = [\tilde{J}'^{(0),\varepsilon} + \tilde{J}'^{(1),\varepsilon}]_{12',21'}$, with the first and second terms given by Eqs. (C.2b) and (B.86), respectively, as expected. Thus, our check worked. [Also, the reason for the 2 in $\int(d2\tilde{\omega})$ in Eq. (C.18) becomes clear: $\tilde{\mathcal{P}}_{65}^{12}(\mathcal{E}; \Omega_1, \Omega_2)$ turns out to contain factors of $2\pi\delta(\Omega_1 - \Omega_2)$ or $2\pi\delta(\Omega_1 - \Omega_2 + \dots)$ for self-energy and vertex terms, respectively, which under the integral $\int(d2\tilde{\omega})\tilde{\mathcal{P}}_{21'}^{12'}(\varepsilon - \frac{1}{2}\tilde{\omega}; -\tilde{\omega}, \tilde{\omega})$ of Eq. (C.18) have to collapse to unity, $\int(d2\tilde{\omega})2\pi\delta(\dots - 2\tilde{\omega}) = 1$.]

Finally, let us rewrite Eq. (C.18) in a more suggestive form. Transforming back to the time domain using Eq. (C.16c) and writing the result in terms of the time variables of Eq. (C.17b), we find

$$\tilde{J}_{12',21'}^\varepsilon = [-n'(\hbar\varepsilon)] \int_0^\infty d\tau_{12} \tilde{P}_{21'}^{12',\varepsilon}(\tau_{12}), \quad (\text{C.19a})$$

$$\tilde{P}_{21'}^{12',\varepsilon}(\tau_{12}) = \int_{-\infty}^\infty d\tilde{\tau}_{12} \int(d2\tilde{\omega}) e^{-i2\tilde{\omega}\tilde{\tau}_{12}} \int_{-\infty}^\infty d\bar{\tau}_{12} e^{i\bar{\tau}_{12}(\varepsilon - \frac{1}{2}\tilde{\omega})} \times \tilde{P}_{21'}^{12'}(\tau_{12}, \tilde{\tau}_{12}, \bar{\tau}_{12}), \quad (\text{C.19b})$$

$$= \int_{-\infty}^\infty d\bar{\tau}_{12} e^{i\bar{\tau}_{12}\varepsilon} \tilde{P}_{21'}^{12'}(\tau_{12}, -\frac{1}{4}\bar{\tau}_{12}, \bar{\tau}_{12}). \quad (\text{C.19c})$$

We need to consider $\tilde{P}_{21'}^{12'}$ only in the limit $\mathbf{r}_2 \rightarrow \mathbf{r}_1$, since the Cooperon contribution to it is negligible for $|\mathbf{r}_1 - \mathbf{r}_2| \gtrsim \lambda_F$, where λ_F is the Fermi wavevector (assumed to be much smaller than the mean free path, $\lambda_F \ll l_{\text{el}}$). The purpose of the time integrals in Eq. (C.19b) is to project out from the general path integral $\tilde{P}_{21'}^{12'}$ of Eq. (C.15), defined in the position-time domain, an object depending in an appropriate way on both the average propagation time τ_{12} of the forward and backward paths and the energy ε occurring in the thermal weighting factor. (The simultaneous specification of both a time and an energy does not violate the time-energy uncertainty relation, as incorrectly argued by GZ²⁴, because $\tilde{P}_{21'}^{12',\varepsilon}(\tau_{12})$ is constructed from *two* electron propagators, not one). To see how this projection

works in detail, we use Eqs. (C.17b) to write the time differences τ_{12} , $\tilde{\tau}_{12}$ and $\bar{\tau}_{12}$ as follows:

$$\begin{aligned}\tau_{12} &= \frac{1}{2}[(t_1^F - t_2^F) + (t_3^B - t_4^B)], & \tilde{\tau}_{12} &= \frac{1}{4}[(t_1^F + t_2^F) - (t_3^B + t_4^B)], \\ \bar{\tau}_{12} &= (t_1^F - t_2^F) - (t_3^B - t_4^B).\end{aligned}\quad (\text{C.20})$$

The $\int d\bar{\tau}_{12}$ integral in Eq. (C.19b) fixes the average energy of the upper and lower electron lines (in diagrammatic language) to be $\varepsilon - \tilde{\omega}/2$ [where $\bar{\tau}_{12}$ is the length difference between the forward and backward pieces of the contour]. The $\int(d\tilde{\omega})$ integral averages over all possible frequency differences $\tilde{\omega}$ between the upper and lower electron lines, as is necessary when vertex terms are present that transfer energy between them. And finally, the $\int d\tau_{12}$ integral projects out the $\tilde{\tau}_{12}$ -dependence of $P_{21'}^{12'}$ [where $\tilde{\tau}_{12}$ is half the difference between the midpoints of the forward and backward pieces of the contour]. The only remaining time variable, τ_{12} , is the average of the lengths of the forward and backward pieces, and can be viewed as the ‘‘observation time’’ as a function of which $\tilde{P}_{21'}^{12',\varepsilon}(\tau_{12})$ will decay. $\tilde{P}_{21'}^{12',\varepsilon}(\tau_{12})$ will contain a contribution resulting from time-reversed paths that corresponds to the full Cooperon in the position-time representation, $\tilde{C}_{\rho=0}(\tau_{12})$. The time scale on which it decays is the desired decoherence time τ_φ .

Now, the $\int(d\tilde{\omega})$ integral in Eq. (C.19b) yields $\delta(\tilde{\tau} + \frac{1}{4}\bar{\tau})$ [here and henceforth we drop the subscripts on τ , $\bar{\tau}$ and $\tilde{\tau}$], leaving us to consider a path integral with time arguments $\tilde{P}_{21'}^{12'}(\tau, -\frac{1}{4}\bar{\tau}, \bar{\tau})$, as indicated in Eq. (C.19c). These time arguments can be obtained by choosing, e.g., $t_1 = t_3 = \frac{1}{2}\tau$ and $t_{2,4} = -\frac{1}{2}(\tau \pm \bar{\tau})$, resulting in:

$$\tilde{P}_{21'}^{12',\varepsilon}(\tau) = \int_{-\infty}^{\infty} d\bar{\tau} e^{i\bar{\tau}\varepsilon} \int_{\mathbf{R}^F(-\frac{\tau}{2}-\frac{\bar{\tau}}{2})=\mathbf{r}_{2'}}^{\mathbf{R}^F(\frac{\tau}{2})=\mathbf{r}_1} \int_{\mathbf{R}^B(-\frac{\tau}{2}+\frac{\bar{\tau}}{2})=\mathbf{r}_2}^{\mathbf{R}^B(\frac{\tau}{2})=\mathbf{r}_{1'}} \tilde{D}'(\mathbf{R}) e^{-[i\tilde{S}_R + \tilde{S}_I]/\hbar}. \quad (\text{C.21})$$

Eq. (C.14), together with (C.19a) and (C.21), are the central results of this section, because they express the conductivity in terms of a general path integral influence functional, with thermal weighting taken properly into account. The main difference to the path integral (1b) used in the main text (and by GZ) is that in Eq. (C.21) the duration of the forward and backward paths differs by a time $\bar{\tau}$ that is being integrated over in $\int d\bar{\tau} e^{i\bar{\tau}\varepsilon}$. The remainder of this section is devoted to justifying the replacement of Eq. (C.21) by the simpler Eq. (1b).

The combination $\int d\varepsilon \int d\bar{\tau}$ of integrals from Eqs. (C.14) and (C.21) have the effect of fixing the average energy of the forward and backward trajectories to be close to the Fermi energy, with energy spread of roughly $\pm T$ (in a way reminiscent of App. B of the review²¹ by Chakravarty and Schmid). To see this, consider first the noninteracting limit (i.e. ignore $i\tilde{S}_R + \tilde{S}_I$) in the semiclassical approximation, where the path integrals in Eq. (C.21) are restricted to all possible classical forward and backward paths $\mathbf{r}_{\text{cl}}^{F/B}(t_3)$ having the specified boundary conditions, with corresponding classical actions $S_{0,\text{cl}}^{F/B}(\frac{\tau}{2}, -\frac{\tau}{2} \mp \frac{\bar{\tau}}{2})$. Since these paths follow diffusive trajectories through a disordered potential landscape, for any given τ and $\bar{\tau}$ the path integral still includes many such classical paths, with a range of different classical energies (and correspondingly different diffusion constants). Now, the energy

integral in Eq. (1a) restricts the $\int d\bar{\tau}$ integral in Eq. (C.21) to the range $|\bar{\tau}| \lesssim \hbar/T$, since

$$\int d\varepsilon [-n'(\hbar\varepsilon)] e^{i\varepsilon\bar{\tau}} = \frac{\pi\hbar\bar{\tau}T}{\sinh(\pi\hbar\bar{\tau}T)}. \quad (\text{C.22})$$

The relevant values of $\bar{\tau}$ are thus much smaller than the typical propagation times τ relevant for determining the decoherence time [$\tau \simeq \tau_\varphi \sim \hbar g(L_\varphi)/T \gg \hbar/T$, see Eq. (19)], so that the classical actions can be expanded²¹ to first order in $\bar{\tau}$,

$$S_{0,\text{cl}}^{F/B}(\frac{\tau}{2}, -\frac{\tau}{2} \mp \frac{\bar{\tau}}{2}) \simeq S_{0,\text{cl}}^{F/B}(\frac{\tau}{2}, -\frac{\tau}{2}) \mp \frac{1}{2}\bar{\tau}\mathcal{E}_{\text{cl}}^{F/B}, \quad (\text{C.23})$$

where $\mathcal{E}_{\text{cl}}^{F/B}$ is the classical energy at the endpoint of the corresponding classical path $\mathbf{r}_{\text{cl}}^{F/B}(t_3)$. Using this in Eq. (C.21), the $\int d\bar{\tau}$ integral is seen to fix the average classical energy of the forward and backward classical paths to be close to the Fermi energy $\varepsilon_F = 0$, with an energy spread of order T :

$$\int_{-\infty}^{\infty} d\bar{\tau} \frac{\pi\hbar\bar{\tau}T}{\sinh(\pi\hbar\bar{\tau}T)} e^{i\bar{\tau}\frac{1}{2}(\mathcal{E}_{\text{cl}}^F + \mathcal{E}_{\text{cl}}^B)} = \int d\varepsilon [-n'(\hbar\varepsilon)] \delta\left(\varepsilon - \frac{1}{2}(\mathcal{E}_{\text{cl}}^F + \mathcal{E}_{\text{cl}}^B)\right). \quad (\text{C.24})$$

(The right-hand side follows from using the integral representation (C.22) for the sinh-function.) Note that the energy spread is consistent with the time-energy uncertainty relation in the limit of present interest, $\tau T \gg \hbar$.

Now, in the absence of interactions, the only effect of fixing this average energy ε to be roughly ε_F is that the velocity appearing in the diffusion constant is the Fermi velocity, $D = v_F^2\tau_{\text{el}}/d$. However, in the presence of interactions, the energy ε also plays a role in determining the phase space available for electrons to get scattered upon absorbing or emitting a noise quantum. In particular, in perturbative calculations it shows up in the $\tanh[\hbar(\varepsilon \mp \bar{\omega})/2T]$ -factors of the Keldysh electron Green's functions $\tilde{G}^K(\varepsilon \mp \bar{\omega})$. In our influence functional approach this can be kept track of by replacing Eq. (C.21) by Eq. (1b), which mimicks the effect of the former's integral $\int d\bar{\tau} e^{i\varepsilon\bar{\tau}}$ by using (i) forward and backward paths of equal duration τ and (ii) an effective action whose time integration boundaries are fixed at $\pm\tau/2$, but which *depends explicitly on the average propagation energy* ε . Note that GZ's approach in effect employs the same simplification, since they likewise have no $\int d\bar{\tau} e^{i\varepsilon\bar{\tau}}$ integral and use forward and backward paths of equal duration τ .

The ε -dependence of the effective action enters through the Pauli factor $(\tilde{\delta} - 2\bar{\rho})$ occurring in \tilde{S}_R [Eqs. (A.8) or (B.95)], which we treat differently from GZ. In our approach, it produces factors of $\tanh[\hbar(\varepsilon \mp \bar{\omega})/2T]$ in the frequency representation of \tilde{S}_R [cf. Eqs. (4e) or (B.97)], chosen in such a way as to be consistent with Keldysh perturbation theory, as discussed in Sec 3 and (more extensively) B.6.2, B.6.3. In GZ's approach, the tanh-arguments contain ε instead of $\varepsilon \mp \bar{\omega}$ (i.e. their effective action depends on the average energy too). However, lacking the $\mp\bar{\omega}$ recoil shifts, the tanh-terms turn out to yield zero after averaging over random walks, so that $\langle i\tilde{S}_R^{\text{GZ}} \rangle_{\text{rw}} \simeq 0$.

The strategy just described for arriving at forward and backward paths of equal duration is of course not exact; but it is sufficiently accurate for our purposes: the

errors incurred by it are of order $\hbar/(T\tau)$ ($\ll 1$ for $\tau \sim \tau_\varphi$), as can be shown by a detailed comparison with Keldysh diagrammatic perturbation theory (App. B.6.2 of this review, and App. A.3 of DMSA-II²⁰).

C.5. General Cooperon, after Disorder Averaging

Let us now disorder average Eqs. (C.18), in order to arrive at an expression for $\sigma_{\text{DC}}^{\text{WL}}$ in terms of a general Cooperon propagator, in the presence of interactions. To this end, we have to Fourier transform from position to wave-number variables,

$$\begin{aligned} \tilde{\mathcal{P}}_{43}^{12}(\mathcal{E}; \Omega_1, \Omega_2) = & \frac{1}{\text{Vol}^2} \sum_{\mathbf{p}_1, \mathbf{p}_2, \mathbf{p}_3, \mathbf{q}} \delta_{\mathbf{p}_3, 0} \overline{\mathcal{P}}_{\mathbf{q}, \mathbf{p}_1, \mathbf{p}_2}^{\mathcal{E}, \Omega_1, \Omega_2} \exp i \left\{ \mathbf{r}_1^F \cdot \left[\mathbf{p}_1 + \frac{\mathbf{q} + \mathbf{p}_3}{2} \right] \right. \\ & \left. - \mathbf{r}_2^F \cdot \left[\mathbf{p}_2 + \frac{\mathbf{q} - \mathbf{p}_3}{2} \right] + \mathbf{r}_4^B \cdot \left[-\mathbf{p}_1 + \frac{\mathbf{q} + \mathbf{p}_3}{2} \right] - \mathbf{r}_3^B \cdot \left[-\mathbf{p}_2 + \frac{\mathbf{q} - \mathbf{p}_3}{2} \right] \right\}. \end{aligned} \quad (\text{C.25})$$

as depicted in Fig. C2(c). (Again, the $\delta_{\mathbf{p}_3, 0}$ guarantees translational invariance.) According to the standard diagrammatic approach for disorder averaging [cf. Fig. F1 in App. F], the disorder average of $\overline{\mathcal{P}}_{\mathbf{q}, \mathbf{p}_1, \mathbf{p}_2}^{\mathcal{E}, \Omega_1, \Omega_2}$ can be separated into a ‘‘Drude’’ and a ‘‘weak-localization’’ contribution,

$$\begin{aligned} \langle \overline{\mathcal{P}}_{\mathbf{q}, \mathbf{p}_1, \mathbf{p}_2}^{\mathcal{E}, \Omega_1, \Omega_2} \rangle_{\text{dis}} = & \hbar^2 \overline{\mathcal{G}}_{\frac{1}{2}\mathbf{q} + \mathbf{p}_1}^R(\mathcal{E} + \frac{1}{2}\Omega_1) \overline{\mathcal{G}}_{\frac{1}{2}\mathbf{q} - \mathbf{p}_1}^A(\mathcal{E} - \frac{1}{2}\Omega_1) \left\{ 2\pi(\Omega_1 - \Omega_2) \delta_{\mathbf{p}_1, \mathbf{p}_2} \right. \\ & \left. + \overline{\mathcal{G}}_{\frac{1}{2}\mathbf{q} + \mathbf{p}_2}^R(\mathcal{E} + \frac{1}{2}\Omega_2) \overline{\mathcal{G}}_{\frac{1}{2}\mathbf{q} - \mathbf{p}_2}^A(\mathcal{E} - \frac{1}{2}\Omega_2) \frac{\overline{\mathcal{C}}_{\mathbf{q}}^{\mathcal{E}}(\Omega_1, \Omega_2)}{\text{Vol} 2\pi\nu\tau_{\text{el}}^2/\hbar} \right\}, \end{aligned} \quad (\text{C.26})$$

where in the second term the contributions from the four external electron lines were separated and a conventional prefactor $(2\pi\nu\tau_{\text{el}}^2/\hbar)^{-1}$ was split off. The normalization of the general Cooperon in the presence of interactions, $\overline{\mathcal{C}}_{\mathbf{q}}^{\mathcal{E}}(\Omega_1, \Omega_2)$, is fixed by requiring that when interactions are switched off, it reduces to its free version, $\overline{\mathcal{C}}_{\mathbf{q}}^0(\Omega_1)$, according to

$$\overline{\mathcal{C}}_{\mathbf{q}}^{\mathcal{E}}(\Omega_1, \Omega_2) \xrightarrow{\text{no int}} 2\pi \delta(\Omega_1 - \Omega_2) \overline{\mathcal{C}}_{\mathbf{q}}^0(\Omega_1), \quad \overline{\mathcal{C}}_{\mathbf{q}}^0(\Omega_1) = \frac{1}{D\mathbf{q}^2 - i\Omega_1 + \gamma_H}. \quad (\text{C.27})$$

Just as $\overline{\mathcal{C}}_{\mathbf{q}}^0(\Omega_1)$, the full Cooperon $\overline{\mathcal{C}}_{\mathbf{q}}^{\mathcal{E}}(\Omega_1, \Omega_2)$ does not depend on the external momenta $\mathbf{p}_{1,2}$, because, in diagrammatic terms, it is separated from external lines by impurity lines.

In a purely diagrammatic approach, where one typically works exclusively in the wavenumber-frequency domain, Eq. (C.26) would be the standard starting point for further calculations. Since the dominant contribution to $\overline{\mathcal{C}}_{\mathbf{q}}^{\mathcal{E}}(\Omega_1, \Omega_2)$ typically comes from small \mathbf{q} (with $q l_{\text{el}} \ll 1$) and small $\Omega_{1,2}$ (with $\Omega_{1,2} \tau_{\text{el}} \ll 1$), while \mathcal{E} is likewise small ($\lesssim T$), it is customary to neglect the terms $\pm \frac{1}{2}\mathbf{q}$ and $\mathcal{E} \pm \frac{1}{2}\Omega_{1,2}$ in the arguments of the external $\overline{\mathcal{G}}^{R/A}$ functions, which simplifies the $\int d\mathbf{p}_{1,2}$ integrals. To explore the effects of interactions, one would proceed to expand $\overline{\mathcal{C}}_{\mathbf{q}}^{\mathcal{E}}(\Omega_1, \Omega_2)$ in powers of the interaction propagator, etc.

Instead, here we shall use the general Eqs. (C.25) and (C.26) for $\tilde{\mathcal{P}}_{43}^{12}(\mathcal{E}; \Omega_1, \Omega_2)$ to analyse the general structure of the disorder-averaged version of Eq. (C.14), as needed for $\langle \sigma_{\text{DC}} \rangle_{\text{dis}}$. As intermediate result, we obtain

$$\int dx_2 \mathbf{j}_{11'} \cdot \mathbf{j}_{22'} \langle \tilde{\mathcal{P}}_{21'}^{12'}(\mathcal{E}; \Omega_1, \Omega_2) \rangle_{\text{dis}} \quad (\text{C.28a})$$

$$\begin{aligned} &= \frac{e^2 \hbar^4}{4m^2 \text{Vol}^2} \sum_{\mathbf{p}_1 \mathbf{p}_2 \mathbf{q}} (\mathbf{q} + \mathbf{p}_1 - \mathbf{p}_2) \cdot (\mathbf{q} - \mathbf{p}_1 + \mathbf{p}_2) \langle \overline{\mathcal{P}}_{\mathbf{q}, \mathbf{p}_1, \mathbf{p}_2}^{\mathcal{E}, \Omega_1, \Omega_2} \rangle_{\text{dis}} \int d\mathbf{r}_2 e^{i(\mathbf{r}_1 - \mathbf{r}_2) \cdot (\mathbf{p}_1 - \mathbf{p}_2)} \\ &= \sigma_{\text{DC}}^{\text{Drude}} 2\pi\hbar \left[2\pi(\Omega_1 - \Omega_2) - \frac{1}{\pi\nu\hbar} \int (d\mathbf{q}) \overline{\mathcal{C}}_{\mathbf{q}}^{\mathcal{E}}(\Omega_1, \Omega_2) \right], \end{aligned} \quad (\text{C.28b})$$

where Eq. (F.6b) was used (under neglect of $\mathcal{E} \pm \frac{1}{2}\Omega_{1/2}$ in the frequency arguments of all electron Green's functions) to perform the momentum integrals, i.e. the $\int (d\mathbf{q})$ integral for the Drude contribution to $\overline{\mathcal{P}}_{\mathbf{q}, \mathbf{p}_1, \mathbf{p}_2}^{\mathcal{E}, \Omega_1, \Omega_2}$, and the $\int (d\mathbf{p}_1)$ integral for the Cooperon contribution (for the latter, the $\frac{1}{2}\mathbf{q}$ arguments in the external electron leg Green's functions were neglected). Inserting Eqs. (C.18) and (C.28b) into Eq. (C.14), we readily find:

$$\sigma_{\text{DC}} = \sigma_{\text{DC}}^{\text{Drude}} \left[1 - \frac{1}{\pi\nu\hbar} \int d\varepsilon \hbar [-n'_0(\hbar\varepsilon)] \int (d\mathbf{q}) \int (d2\tilde{\omega}) \overline{\mathcal{C}}_{\mathbf{q}}^{\varepsilon - \frac{1}{2}\tilde{\omega}}(-\tilde{\omega}, \tilde{\omega}) \right]. \quad (\text{C.29})$$

Eq. (C.29) is the desired generalization of Eq. (C.8b) [and in the absence of interactions, duly reduces to the latter, via Eq. (C.27)].

C.6. Cooperon in Position-Time Domain

For our present purpose of relating the diagrammatic and path integral approaches to each other, it is instructive to understand the consequences of Eq. (C.26) also in path integral language. To this end, let us transcribe Eq. (C.26) back into the position-time domain, in which the Cooperon is defined as:

$$\tilde{\mathcal{C}}_{\rho}^{\mathcal{E}}(\tau_1, \tau_2) \equiv \int (d\mathbf{q})(d\Omega_1)(d\Omega_2) e^{i(\rho \cdot \mathbf{q} - \Omega_1 \tau_1 + \Omega_2 \tau_2)} \overline{\mathcal{C}}_{\mathbf{q}}^{\mathcal{E}}(\Omega_1, \Omega_2). \quad (\text{C.30})$$

Inserting Eqs. (C.25) and (C.26) into Eq. (C.16a) yields $\langle \tilde{P} \rangle_{\text{dis}} = \tilde{P}^{\text{Drude}} + \tilde{P}^{\text{WL}}$, with

$$\tilde{P}_{43}^{12, \text{Drude}} = \hbar^2 \tilde{\mathcal{G}}_{\mathbf{r}_{12}}^R(t_{12}) \tilde{\mathcal{G}}_{\mathbf{r}_{43}}^A(t_{43}), \quad (\text{C.31a})$$

$$\begin{aligned} \tilde{P}_{43}^{12, \text{WL}} &= \int \frac{d\tilde{\mathbf{r}}_1 d\tilde{\mathbf{r}}_2 d\tilde{t}_1 d\tilde{t}'_1 d\tilde{t}_2 d\tilde{t}'_2 (d\mathcal{E})}{2\pi\nu\tau_{\text{el}}^2/\hbar} e^{-i\mathcal{E}(\tilde{t}_1 + \tilde{t}'_1 - \tilde{t}_2 - \tilde{t}'_2)} \tilde{\mathcal{C}}_{\tilde{\mathbf{r}}_1 - \tilde{\mathbf{r}}_2}^{\mathcal{E}}\left(\frac{1}{2}(\tilde{t}_1 - \tilde{t}'_1), \frac{1}{2}(\tilde{t}_2 - \tilde{t}'_2)\right) \\ &\quad \times \hbar^2 \tilde{\mathcal{G}}_{\mathbf{r}_1 - \tilde{\mathbf{r}}_1}^R(t_1 - \tilde{t}_1) \tilde{\mathcal{G}}_{\mathbf{r}_4 - \tilde{\mathbf{r}}_1}^A(t_4 - \tilde{t}'_1) \tilde{\mathcal{G}}_{\tilde{\mathbf{r}}_2 - \mathbf{r}_2}^R(\tilde{t}_2 - t_2) \tilde{\mathcal{G}}_{\tilde{\mathbf{r}}_2 - \mathbf{r}_3}^A(\tilde{t}'_2 - t_3). \end{aligned} \quad (\text{C.31b})$$

Fig. C2(b) offers an intuitive interpretation of these expressions: $\tilde{P}_{43}^{12, \text{Drude}}$ gives the amplitude for propagation from $(\mathbf{r}_2, t_2) \rightarrow (\mathbf{r}_1, t_1)$ (forward in time) times that for $(\mathbf{r}_3, t_3) \rightarrow (\mathbf{r}_4, t_4)$ (backward in time). And $\tilde{P}_{43}^{12, \text{WL}}$ gives the amplitude for forward propagation from $(\mathbf{r}_2, t_2) \rightarrow (\tilde{\mathbf{r}}_2, \tilde{t}_2) \rightarrow (\tilde{\mathbf{r}}_1, \tilde{t}'_1) \rightarrow (\mathbf{r}_1, t_1)$, times that for backward propagation from $(\mathbf{r}_3, t_3) \rightarrow (\tilde{\mathbf{r}}_2, \tilde{t}'_2) \rightarrow (\tilde{\mathbf{r}}_1, \tilde{t}'_1) \rightarrow (\mathbf{r}_4, t_4)$. The middle part of the

forward and backward paths have the same beginning and end points in space, albeit not in time, and hence can interfere constructively if the paths connecting them are time-reversed partners.

The approximation mentioned above of neglecting $\pm \frac{1}{2}\mathbf{q}$ and $\mathcal{E} \pm \frac{1}{2}\Omega_{1,2}$ in the arguments of external $\bar{\mathcal{G}}^{R/A}$ functions has a counterpart in the position-time domain: when performing the integrals in Eq. (C.31b), it corresponds to exploiting the fact that $\tilde{\mathcal{G}}_{\mathbf{r}}(\tilde{t})$ has a short range in space ($|\mathbf{r}| \lesssim \tau_{\text{el}}$) and time ($|\tilde{t}| \lesssim l_{\text{el}}$) [cf. Eq. (F.2d)]. To be explicit, the latter fact means that the disordered Green's functions occurring in the second line of Eq. (C.31b) act effectively as delta-functions in time as far as the factor $e^{-i\mathcal{E}(\cdot)}\tilde{C}_{\tilde{\mathbf{r}}_1-\tilde{\mathbf{r}}_2}^{\mathcal{E}}(\cdot)$ is concerned. Thus, in the latter we may make the replacements $\tilde{t}_1 \rightarrow t_1$, $\tilde{t}'_1 \rightarrow t_4$, $\tilde{t}_2 \rightarrow t_2$, $\tilde{t}'_2 \rightarrow t_3$, after which the four time-integrals each yield a zero-frequency Green's function, $\int d\tilde{t} \tilde{\mathcal{G}}_{\mathbf{r}}(\tilde{t}) = \tilde{\mathcal{G}}_{\mathbf{r}}(\mathcal{E} = 0)$. Introducing the sum and difference coordinates

$$\bar{\boldsymbol{\rho}}_1 \equiv \frac{\mathbf{r}_1^F + \mathbf{r}_4^B}{2}, \quad \boldsymbol{\rho}_1 \equiv \mathbf{r}_1^F - \mathbf{r}_4^B, \quad \bar{\boldsymbol{\rho}}_2 \equiv \frac{\mathbf{r}_2^F + \mathbf{r}_3^B}{2}, \quad \boldsymbol{\rho}_2 \equiv \mathbf{r}_2^F - \mathbf{r}_3^B, \quad (\text{C.32})$$

recalling similar definitions (C.17) for the time variables, and shifting the space integrations according to $\tilde{\mathbf{r}}_i \rightarrow \tilde{\mathbf{r}}_i + \bar{\boldsymbol{\rho}}_i$ for $i = 1, 2$, Eq. (C.31b) gives:

$$\begin{aligned} \tilde{P}_{43}^{12,\text{WL}} &= \int d\tilde{\mathbf{r}}_1 d\tilde{\mathbf{r}}_2 \int (d\mathcal{E}) e^{-i\mathcal{E}\bar{\tau}_{12}} \frac{\tilde{C}_{\bar{\boldsymbol{\rho}}_1-\bar{\boldsymbol{\rho}}_2+\tilde{\mathbf{r}}_1-\tilde{\mathbf{r}}_2}^{\mathcal{E}}(\tau_1, \tau_2)}{2\pi\nu\tau_{\text{el}}^2/\hbar} \\ &\quad \times \hbar^2 \tilde{\mathcal{G}}_{\frac{1}{2}\boldsymbol{\rho}_1-\tilde{\mathbf{r}}_1}^R(0) \tilde{\mathcal{G}}_{-\frac{1}{2}\boldsymbol{\rho}_1-\tilde{\mathbf{r}}_1}^A(0) \tilde{\mathcal{G}}_{\tilde{\mathbf{r}}_2-\frac{1}{2}\boldsymbol{\rho}_2}^R(0) \tilde{\mathcal{G}}_{\tilde{\mathbf{r}}_2+\frac{1}{2}\boldsymbol{\rho}_2}^A(0). \end{aligned} \quad (\text{C.33})$$

Since the zero-frequency Green's functions $\tilde{\mathcal{G}}_{\mathbf{r}}^R(0)$ decay with distance as $e^{-|\mathbf{r}|/2l_{\text{el}}}$, we note that $\tilde{\mathbf{r}}_i \simeq \frac{1}{2}\boldsymbol{\rho}_i \simeq -\tilde{\mathbf{r}}_i$, which implies that $|\tilde{\mathbf{r}}_i| \lesssim l_{\text{el}}$ and $|\boldsymbol{\rho}_i| \lesssim l_{\text{el}}$. Thus, we may drop the terms $\tilde{\mathbf{r}}_1 - \tilde{\mathbf{r}}_2$ from the argument of $\tilde{C}^{\mathcal{E}}$ in Eq. (C.33), whereupon the spatial integrations can be performed explicitly, using

$$\int_{-\infty}^{\infty} d\tilde{t}_i \int_{-\infty}^{\infty} d\tilde{t}_j \int d\tilde{\mathbf{r}}_l \tilde{\mathcal{G}}_{il}^{R/A}(\tilde{t}_i) \tilde{\mathcal{G}}_{lj}^{A/R}(\tilde{t}_j) = \frac{\delta_{l_{\text{el}}}(r_{ij})}{\varepsilon_{\text{F}}^2}, \quad (\text{C.34a})$$

$$\tilde{\delta}_{l_{\text{el}}}(r_{ij}) \equiv \left(\frac{l_{\text{el}} k_{\text{F}}^3}{4\pi} \right) e^{-r_{ij}/2l_{\text{el}}} \frac{\sin(k_{\text{F}} r_{ij})}{r_{ij}}, \quad (\text{C.34b})$$

where $\tilde{\delta}_{l_{\text{el}}}(r_{ij})$ is a ‘‘smeared-out delta function’’ of normalization $\int d\mathbf{r}_{ij} \tilde{\delta}_{l_{\text{el}}}(r_{ij}) = 1$ and width $\simeq 1/k_{\text{F}}$, the Fermi wavelength (since $1/k_{\text{F}} \ll l_{\text{el}}$, the width is set by the oscillating factor $\sin(k_{\text{F}} r)/r$, not by the exponential $e^{-r/2l_{\text{el}}}$). Thus, Eq. (C.33) becomes:

$$\tilde{P}_{43}^{12,\text{WL}} = \frac{\hbar^2}{\varepsilon_{\text{F}}^4} \tilde{\delta}_{l_{\text{el}}}(\boldsymbol{\rho}_1) \tilde{\delta}_{l_{\text{el}}}(\boldsymbol{\rho}_2) \int (d\mathcal{E}) e^{-i\mathcal{E}(\bar{\tau}_1-\bar{\tau}_2)} \frac{\tilde{C}_{\bar{\boldsymbol{\rho}}_1-\bar{\boldsymbol{\rho}}_2}^{\mathcal{E}}(\tau_1, \tau_2)}{2\pi\nu\tau_{\text{el}}^2/\hbar}. \quad (\text{C.35})$$

This useful result clarifies the relation between the coordinates 1,2,3,4 of $\tilde{P}_{43}^{12,\text{WL}}$, and the times and spatial coordinates relevant for the Cooperon. In particular, we see that $\tilde{P}_{43}^{12,\text{WL}}$ is nonzero only for $|\boldsymbol{\rho}_1| = |\mathbf{r}_1 - \mathbf{r}_4| \lesssim 1/k_{\text{F}}$ and $|\boldsymbol{\rho}_2| = |\mathbf{r}_2 - \mathbf{r}_3| \lesssim 1/k_{\text{F}}$. Moreover, if we want to describe a Cooperon with a specified average energy \mathcal{E} , we need to Fourier-transform $\tilde{P}_{43}^{12,\text{WL}}$ with $\int d\bar{\tau}_{12} e^{i\mathcal{E}\bar{\tau}_{12}}$. Note that for

$\tilde{P}_{21'}^{12',\text{WL}}$, as needed in Eqs. (C.19), the Cooperon position argument is identically zero, $\bar{\rho}_1 - \bar{\rho}_2 = 0$, while $|\rho_1| = |\mathbf{r}_1 - \mathbf{r}_2|$ ensures that \mathbf{r}_1 and \mathbf{r}_2 lie close together.

Appendix D. Time-Slicing of Path Integral for \tilde{U}_{ij}^a

In this appendix, we give an explicit time-slicing definition for the path integral representation (B.56) of the propagators \tilde{U}_{ij}^a used in the main text, and derive various properties thereof. Our discussion is very (perhaps overly) detailed, since the object of interest is somewhat unconventional, namely a path integral for a non-local hamiltonian. We begin [Secs. D.1 to D.3] by defining it in terms of a path integral $\int \mathcal{D}\mathbf{R} \int \mathcal{D}\mathbf{P}$ over paths in both coordinate and momentum space, which is the form used by GZ; then [Sec. D.4] we explicitly perform the $\int \mathcal{D}\mathbf{P}$ integral to arrive at a “coordinate-space-only” path integral $\int \tilde{\mathcal{D}}\mathbf{R}$, which is the form used in App. B.5 to B.8. Finally [Sec. D.5] we present explicit expressions for the effective Hamiltonian \tilde{H}_n^a in the position-momentum representation used by GZ, and [Sec. D.6] recover from this GZ’s expressions for the effective action $(i\tilde{S}_R + \tilde{S}_I)[\mathbf{R}^a, \mathbf{P}^a]$.

D.1. Time-Slicing Definition

The propagators \tilde{U}_{ij}^a are defined by the requirement that they have to satisfy both the conditions Eqs. (B.39). This fact can be used to give meaning to the formal path integral of Eq. (B.56), by using the standard time-slicing procedure to construct an object that satisfies this requirement. To this end, we divide the interval $[t', t]$ into $M = (t - t')/\epsilon$ time intervals, with $t_n = t' + n\epsilon$ for $n = 0, \dots, M$, and write $\mathbf{r}_n^a = \mathbf{r}^a(t_n)$ [$\mathbf{r}_0^a = \mathbf{r}_j$, $\mathbf{r}_M^a = \mathbf{r}_i$] and $\mathbf{p}_n^a = \mathbf{p}^a(t_n)$. Then the following construction, illustrated in the first row of Fig. D1, has the desired properties:

$$\left. \begin{aligned} \tilde{U}_{ij}^F(t, t') \\ \tilde{U}_{ji}^B(t', t) \end{aligned} \right\} \equiv \delta_{\sigma_i, \sigma_j} \lim_{M \rightarrow \infty} \prod_{n=1}^{M-1} \left(\int d\mathbf{r}_n^a \right) \prod_{n=1}^M \left(\int \frac{d\mathbf{p}_n^a}{(2\pi)^d} \right) e^{(is_a\epsilon/\hbar) \sum_{n=1}^M \bar{L}_n^a} \quad (\text{D.1a})$$

$$\equiv \int \mathcal{D}\mathbf{R} \int \mathcal{D}\mathbf{P} e^{(is_a/\hbar) \bar{S}^a[\mathbf{R}^a, \mathbf{P}^a]}. \quad (\text{D.1b})$$

The second line, with action $\bar{S}^a = \epsilon \sum_n \bar{L}_n^a$, is a formal shorthand for the detailed time-slicing construction of the first line. Here and below, $t > t'$, the index value $a = F$ or B should be used for the upper or lower term in the curly bracket, and s_a stands for $s_{F/B} = \pm$. The multiple products in Eq. (D.1a) contain one momentum integral (M in total) for each interval, and one position integral ($M - 1$ in total) for each boundary between intervals (see Fig. D1). The Lagrangian \bar{L}_n^a and Hamiltonian $\tilde{H}_n^a \equiv \tilde{H}^a(t_n, \mathbf{R}_n^a, \mathbf{P}_n^a)$ associated with the n -th interval are given by (here $\mathbf{P}_n^a \equiv \hbar \mathbf{p}_n^a$):

$$\bar{L}_n^a \equiv \mathbf{P}_n^a \cdot \frac{\delta \mathbf{r}_n^a}{\epsilon} - \tilde{H}_n^a, \quad (\text{D.2a})$$

$$\tilde{H}_n^a \equiv \int d(\delta \mathbf{r}_n^a) e^{-is_a \mathbf{p}_n^a \cdot \delta \mathbf{r}_n^a} \tilde{H}^a(t_n, \mathbf{R}_n^a + s_a(1 - b_a) \delta \mathbf{r}_n^a, \mathbf{R}_n^a - s_a b_a \delta \mathbf{r}_n^a). \quad (\text{D.2b})$$

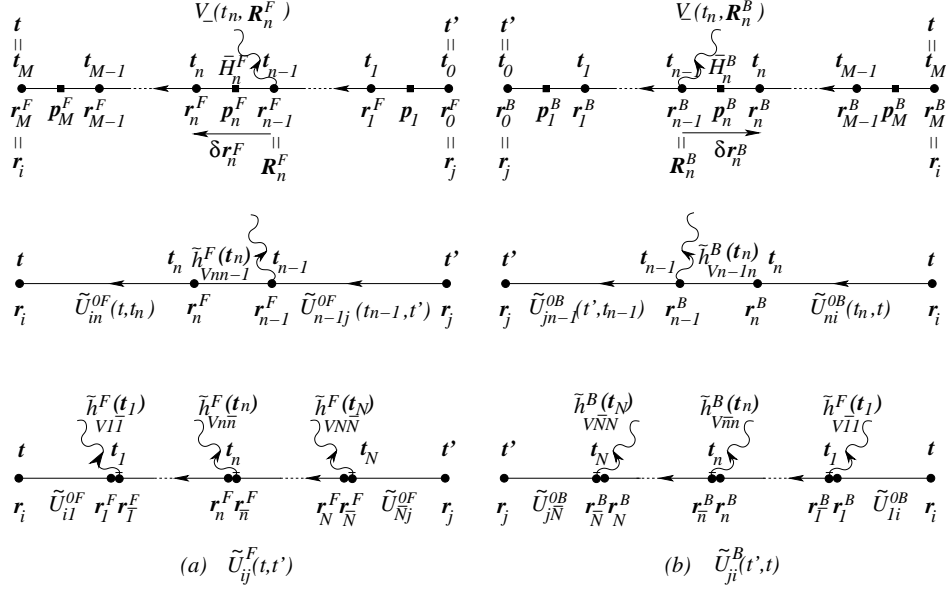


Fig. D1. Three representations of the propagators (a) $\tilde{U}_{ij}^F(t, t')$ and (b) $\tilde{U}_{ji}^B(t', t)$, with $t > t'$. Arrow point from the second to the first index of propagators. The first row illustrates the position-momentum (dots-squares) time-sliced path integral representation of Eq. (D.1a) (with the choice $b_a = \delta_{aB}$ in cf. Eq. (D.3), so that $\mathbf{R}_n^a = \mathbf{r}_{n-1}^a$); the wavy line indicates which end of the n -th time slice the interaction field $V_-(t_n, \mathbf{r}_{n-1}^a)$ is attached to. The second row depicts the first order perturbation expansion of Eq. (D.8b), obtained after performing the momentum path integral, using Eq. (D.9) to convert \tilde{h}_V^a to \tilde{h}_V^a . The third row shows the N -th order perturbation term of Eq. (D.11b). The double dots remind us that the vertices $\tilde{h}_{V_{n\bar{n}}}^F$ and $\tilde{h}_{V_{n\bar{n}}}^B$ are nonlocal (since they contain factors of $\tilde{\rho}_{n\bar{n}}$ or $\tilde{\rho}_{\bar{n}n}$): they arise from “pulling together” the two local vertices at times t_n and t_{n-1} of the second row of this figure into a single nonlocal vertex at time t_n , with which we hence associate a double integration $\int dx_{n\bar{n}}^F$ or $\int dx_{n\bar{n}}^B$. The dot carrying a bar indicates which of these two integration variables occurs in the argument of $V_-(\mathbf{r}_{\bar{n}})$, namely the one drawn on the side of earlier times.

Here we introduced relative and “asymmetric center-of-mass” coordinates for the n -th interval,

$$\delta \mathbf{r}_n^a = \mathbf{r}_n^a - \mathbf{r}_{n-1}^a, \quad \mathbf{R}_n^a = \left\{ \begin{array}{l} \mathbf{r}_{n-1}^F \\ \mathbf{r}_n^B \end{array} \right\} + s_a b_a \delta \mathbf{r}_n^a = \left\{ \begin{array}{l} \mathbf{r}_n^F \\ \mathbf{r}_{n-1}^B \end{array} \right\} - s_a (1 - b_a) \delta \mathbf{r}_n^a, \quad (\text{D.3})$$

where the “asymmetry parameter” b_a is a real number with $0 \leq b_a \leq 1$, which in general can be different for $a = F$ or B . The actual values chosen for b_a do not affect any of the final results, hence they can be chosen according to taste or convenience, or left unspecified, as we shall do for now. It is to be understood that under the path integral, the notation $\mathbf{R}^a(t_n)$ and $\mathbf{P}^a(t_n)$ [e.g. as arguments of the fields $V_{\pm}(t_n, \mathbf{R}^a(t_n))$], should be interpreted as \mathbf{R}_n^a and \mathbf{P}_n^a , respectively.

The arguments of \tilde{H}^a in Eq. (D.2b) were purposefully constructed such that the

inverse Fourier transform of Eq. (D.2b) yields

$$\int \frac{d\mathbf{p}_n^a}{(2\pi)^d} e^{is_a \mathbf{p}_n^a \cdot \delta \mathbf{r}_n^a} \bar{H}^a(t_n, \mathbf{R}_n^a, \mathbf{P}_n^a) = \begin{cases} \tilde{H}^F(t_n, \mathbf{r}_n^F, \mathbf{r}_{n-1}^F), \\ \tilde{H}^B(t_n, \mathbf{r}_{n-1}^B, \mathbf{r}_n^B). \end{cases} \quad (\text{D.4})$$

This equation can be regarded as the defining relation for \bar{H}_n^a (and Eq. (D.2b) as its consequence): \bar{H}_n^a is the (generally asymmetric) Fourier transform, with respect to the relative coordinate $\delta \mathbf{r}_n^a$, of $\tilde{H}^a(t_n)$, in which the position arguments \mathbf{r}_n^a and \mathbf{r}_{n-1}^a occur in a time-ordered or anti-time-ordered fashion for $a = F$ or B , respectively (i.e. the coordinate associated with the later time, t_n , appears to the left or right of the earlier time, t_{n-1} , respectively). This, of course, is required to ensure that the path integral representation for $\tilde{U}_{ij}^F(t, t')$ and $\tilde{U}_{ji}^B(t', t)$ produces time-ordered and anti-time-ordered expressions, respectively, as illustrated in Fig. D1. The reason for using a factor s_a in the Fourier transform exponentials $e^{-is_a \mathbf{r}^a \cdot \mathbf{p}^a}$ in the definition (D.2b) of \bar{H}_n^a and its inverse, Eq. (D.4), is simply that the factor $e^{is_a \mathbf{r}^a \cdot \mathbf{p}^a}$ occurring in the latter is generated by the combination $is_a \bar{L}_n^a$ in the action of Eq. (D.1a). Finally, note also that $\bar{H}^a(\mathbf{R}^a, \mathbf{P}^a)$ is independent of \mathbf{P}^a if and only if $\tilde{H}^a(\mathbf{r}_i^a, \mathbf{r}_i^a)$ is proportional to $\tilde{\delta}(\mathbf{r}_i^a - \mathbf{r}_i^a)$.

D.2. Verifying the Defining Equations and Composition Rule

It is straightforward to verify that Eq. (D.1a) satisfies all the requirements expected of a propagator. We shall now first show that it fulfills the defining conditions for \tilde{U}_{ij}^a , namely Eqs. (B.39), and then check that it satisfies the usual composition rule. Since the manipulations for $a = F$ and $a = B$ are very similar, but differ in numerous minor details, we shall mostly consider the former case only. Hence, a will be understood to stand for F below, except when explicitly noted otherwise.

Normalization: To recover the normalization condition Eq. (B.39a), take the limit $t \rightarrow t'$ by taking $M = 1$ and $\epsilon \rightarrow 0$. Then the entire path integral reduces simply to

$$\lim_{t \rightarrow t'} \tilde{U}_{ij}^a(t, t') = \delta_{\sigma_i, \sigma_j} \int \frac{d\mathbf{p}_1^a}{(2\pi)^d} e^{i\mathbf{p}_1^a \cdot (\mathbf{r}_i^a - \mathbf{r}_j^a)} = \tilde{\delta}_{ij}. \quad (\text{D.5})$$

Equation of motion: To recover the equation of motions for \tilde{U}_{ij}^F and \tilde{U}_{ji}^B , namely Eqs. (B.39b) and (B.39c), add one time slice in Eq. (D.1a) ($M \rightarrow M + 1$, so that now $\mathbf{r}_i^a = \mathbf{r}_{M+1}^a$), and expand the corresponding exponential $e^{(is_a \epsilon / \hbar) L_{M+1}^a}$ to first order in ϵ :

$$\begin{aligned} \tilde{U}_{ij}^F(t + \epsilon, t') &= \sum_{\sigma_M} \delta_{\sigma_i, \sigma_M} \int d\mathbf{r}_M^F \int \frac{d\mathbf{p}_{M+1}^F}{(2\pi)^d} e^{i\mathbf{p}_{M+1}^F \cdot \delta \mathbf{r}_{M+1}^F} \left[1 - \frac{i\epsilon}{\hbar} \bar{H}_{M+1}^F \right] U_{Mj}^F(t, t') \\ &= U_{ij}^F(t, t') - \frac{i\epsilon}{\hbar} \int d\mathbf{x}_M^F \tilde{H}_{iM}^F(t) \tilde{U}_{Mj}^F(t, t'), \end{aligned} \quad (\text{D.6a})$$

$$\tilde{U}_{ji}^B(t', t + \epsilon) = \sum_{\sigma_M} \delta_{\sigma_i, \sigma_M} \int d\mathbf{r}_M^B \int \frac{d\mathbf{p}_{M+1}^B}{(2\pi)^d} U_{jM}^B(t', t) e^{-i\mathbf{p}_{M+1}^B \cdot \delta \mathbf{r}_{M+1}^B} \left[1 + \frac{i\epsilon}{\hbar} \bar{H}_{M+1}^B \right]$$

$$= U_{ji}^B(t', t) + \frac{i\epsilon}{\hbar} \int dx_M^B \tilde{U}_{jM}^B(t', t) \tilde{H}_{Mi}^B(t). \quad (\text{D.6b})$$

Here Eqs. (D.4) and $\mathbf{r}_{M+1}^a = \mathbf{r}_i^a$ were used to obtain Eqs. (D.6a) and (D.6b), which, in the limit $\epsilon \rightarrow 0$, reproduce Eqs. (B.39b) and (B.39c).

Composition rule: Next we check that Eq. (D.1a) also satisfies the usual composition rules for propagators, namely

$$\int dx_1 U_{i1}^F(t, t_1) U_{1j}^F(t_1, t') = U_{ij}^F(t, t'), \quad \int dx_1 U_{j1}^B(t', t_1) U_{1i}^B(t_1, t) = U_{ji}^B(t', t).$$

To this end, let M_1 be the number of intervals between t_1 and t' , i.e. write $t_1 = t' + \epsilon M_1$ and $\mathbf{r}_1 = \mathbf{r}_{M_1}$. Then, by concatenating two expressions of the form Eq. (D.1a) for U_{i1}^F and U_{1j}^F , we find that the left-hand side of the above equation can be written, up to a factor $\delta_{\sigma_i \sigma_1} \delta_{\sigma_1 \sigma_j}$, as

$$\begin{aligned} & \int d\mathbf{r}_1^F \lim_{M \rightarrow \infty} \prod_{n=M_1+1}^{M-1} \left(\int d\mathbf{r}_n^F \right) \prod_{n=M_1+1}^M \left(\int \frac{d\mathbf{p}_n^F}{(2\pi)^d} \right) e^{(i\epsilon/\hbar) \sum_{n=M_1+1}^M \bar{L}_n^F} \\ & \times \prod_{n=1}^{M_1-1} \left(\int d\mathbf{r}_n^F \right) \prod_{n=1}^{M_1} \left(\int \frac{d\mathbf{p}_n^F}{(2\pi)^d} \right) e^{(i\epsilon/\hbar) \sum_{n=1}^{M_1} \bar{L}_n^F}. \end{aligned} \quad (\text{D.7})$$

This is equal to $\tilde{U}_{ij}^F(t, t')$ as given by Eq. (D.1a), since $\int d\mathbf{r}_1^F = \int d\mathbf{r}_{M_1}^F$. The derivation for \tilde{U}_{ji}^B is entirely analogous.

D.3. Power Series Expansion in \hbar^a :

The power series expansions of $\tilde{U}_{ij}^F(t, t')$ and $\tilde{U}_{ji}^B(t', t)$ in powers of $\tilde{\hbar}_V^F$ and $\tilde{\hbar}_V^B$ are given by Eq. (B.48). To illustrate how they come about from the time-slicing definition (D.1a) of the path integral, we begin by considering only the first order terms (the higher order terms will be discussed subsequently). To this end, we expand each factor $e^{(is_a\epsilon/\hbar)\bar{L}_{n_1}^a}$ in Eq. (D.1a) to linear order in $\bar{\hbar}_{Vn_1}^a$, to obtain $e^{(is_a\epsilon/\hbar)\bar{L}_{n_1}^{0a}} + e^{is_a\mathbf{p}_{n_1}^a \cdot \delta\mathbf{r}_{n_1}^a} (-s_a i\epsilon/\hbar) \bar{\hbar}_{Vn_1}^a$. Here $\bar{L}_{n_1}^{0a}$ is the V -independent part of $\bar{L}_{n_1}^a$, and for the second term, all contributions of order ϵ^2 or higher were dropped (in particular, we replaced $e^{-(is_a\epsilon/\hbar)\bar{\hbar}_{0n_1}^a}$ by 1). Then, to leading order in ϵ , Eq. (D.1a) readily yields the following expression:

$$\begin{aligned} & \left. \begin{aligned} & \tilde{U}_{ij}^F(t, t') - \tilde{U}_{ij}^0(t, t') \\ & \tilde{U}_{ji}^B(t', t) - \tilde{U}_{ji}^0(t', t) \end{aligned} \right\} = \delta_{\sigma_i \sigma_j} \lim_{M \rightarrow \infty} \frac{(-s_a i\epsilon)}{\hbar} \quad (\text{D.8a}) \\ & \times \sum_{n_1=1}^M \left\{ \left[\prod_{n=n_1+1}^{M-1} \left(\int d\mathbf{r}_n^a \right) \prod_{n=n_1+1}^M \left(\int \frac{d\mathbf{p}_n^a}{(2\pi)^d} \right) e^{(is_a\epsilon/\hbar) \sum_{n=n_1+1}^M \bar{L}_n^{0a}} \right] \right. \\ & \times \left[\int d\mathbf{r}_{n_1}^a \int d\mathbf{r}_{n_1-1}^a \int \frac{d\mathbf{p}_{n_1}^a}{(2\pi)^d} e^{is_a\mathbf{p}_{n_1}^a \cdot \delta\mathbf{r}_{n_1}^a} \bar{\hbar}_{Vn_1}^a \right] \\ & \left. \times \left[\prod_{n=1}^{n_1-2} \left(\int d\mathbf{r}_n^a \right) \prod_{n=1}^{n_1-1} \left(\int \frac{d\mathbf{p}_n^a}{(2\pi)^d} \right) e^{(is_a\epsilon/\hbar) \sum_{n=1}^{n_1-1} \bar{L}_n^{0a}} \right] \right\} + \dots \end{aligned}$$

84 Jan von Delft

$$\begin{aligned}
 &= \delta_{\sigma_i \sigma_j} \lim_{\epsilon \rightarrow 0} \frac{(-s_a i \epsilon)}{\hbar} \sum_{n_1=1}^M \int d\mathbf{r}_{n_1}^a \int d\mathbf{r}_{n_1-1}^a \\
 &\quad \times \left\{ \tilde{U}_{in_1}^{0F}(t, t_{n_1}) \tilde{h}_{Vn_1 n_1-1}^F(t_{n_1}) \tilde{U}_{n_1-1j}^{0F}(t_{n_1-1}, t') \right. \\
 &\quad \left. + \tilde{U}_{jn_1-1j}^{0B}(t', t_{n_1-1}) \tilde{h}_{Vn_1-1 n_1}^B(t_{n_1}) \tilde{U}_{n_1 i}^{0B}(t_{n_1}, t) \right\} + \dots \quad (\text{D.8b})
 \end{aligned}$$

$$\begin{aligned}
 &= -\frac{is_a}{\hbar} \int_{t'}^t dt_1 \int dx_{1,\bar{1}} \left\{ \tilde{U}_{i\bar{1}}^{0F} \tilde{h}_{V\bar{1}\bar{1}}^F \tilde{U}_{\bar{1}j}^{0F} \right. \\
 &\quad \left. + \tilde{U}_{j\bar{1}}^{0B} \tilde{h}_{V\bar{1}\bar{1}}^B \tilde{U}_{\bar{1}i}^{0B} \right\} + \dots, \quad (\text{D.8c})
 \end{aligned}$$

in agreement with the $N = 1$ terms of Eq. (B.48). For Eq. (D.8b), which is illustrated in the second row of Fig. D1, we have evoked Eq. (D.4) to make the identification

$$\int \frac{d\mathbf{p}_{n_1}^a}{(2\pi)^d} e^{is_a \mathbf{p}_{n_1}^a \cdot \delta \mathbf{r}_{n_1}^a} \bar{h}_{Vn_1}^a = \begin{cases} \tilde{h}_{Vn_1 n_1-1}^F(t_{n_1}) \\ \tilde{h}_{Vn_1-1 n_1}^B(t_{n_1}) \end{cases}. \quad (\text{D.9})$$

From the above exercise, we extract the following rule of thumb: when a function $\bar{f}^a(t_1) \equiv \bar{f}^a(t_1, \mathbf{R}^a(t_1), \mathbf{P}^a(t_1))$ [e.g. \bar{h}_V^a above] occurs at time t_1 along the forward or backward parts of the Keldysh path integral $\int \mathcal{D}\mathbf{R}^F \mathcal{D}\mathbf{R}^B$, the $\int d\mathbf{p}_{n_1}^a e^{is_a \mathbf{p}_{n_1}^a \cdot \delta \mathbf{r}_{n_1}^a}$ momentum integral at that the corresponding time slice $t_{n_1} = t_1$ converts it into $\tilde{f}_{n_1 n_1-1}^F(t_{n_1})$ or $\tilde{f}_{n_1-1 n_1}^B(t_{n_1})$. Combining this with the propagators implicit in $e^{is_a \bar{S}_0^a}$, generates terms of the form $\tilde{U}_{i\bar{1}}^{0F} \tilde{f}_{\bar{1}\bar{1}}^F \tilde{U}_{\bar{1}j}^{0F}$ or $\tilde{U}_{j\bar{1}}^{0B} \tilde{f}_{\bar{1}\bar{1}}^B \tilde{U}_{\bar{1}i}^{0B}$, respectively [where \bar{f}^a and \tilde{f}^a are Fourier transform pairs, in analogy to \bar{H}^a and \tilde{H}^a of Eqs. (D.2b) and (D.4)]. To be explicit, we have

$$\delta_{\sigma_i \sigma_j} \int_{\mathbf{R}^a(t_j)=\mathbf{r}_j}^{\mathbf{R}^a(t_i)=\mathbf{r}_i} \mathcal{D}\mathbf{R}^a \int \mathcal{D}\mathbf{P}^a e^{is_a \bar{S}_0^a(t, t')} \bar{f}^a(t_1) = \int dx_{1,\bar{1}} \begin{cases} \tilde{U}_{i\bar{1}}^0 \tilde{f}_{\bar{1}\bar{1}}^F \tilde{U}_{\bar{1}j}^0 \\ \tilde{U}_{j\bar{1}}^0 \tilde{f}_{\bar{1}\bar{1}}^B \tilde{U}_{\bar{1}i}^0 \end{cases}. \quad (\text{D.10})$$

Having found the rule (D.10), it is straightforward to go beyond the first order and to recover the full perturbation expansion from the path integral:

$$\left. \begin{aligned} &\tilde{U}_{ij}^F(t_i, t_j) \\ &\tilde{U}_{ji}^B(t_j, t_i) \end{aligned} \right\} = \delta_{\sigma_i \sigma_j} \int_{\mathbf{r}_j}^{\mathbf{r}_i} \mathcal{D}\mathbf{R}^a(t_1) \int \mathcal{D}\mathbf{P}^a(t_1) e^{\pm[i\bar{S}_0^a(t, t') - \int_{t'}^t dt_1 \bar{h}_V^a(t_1)]} \quad (\text{D.11a})$$

$$\begin{aligned}
 &= \delta_{\sigma_i \sigma_j} \int_{\mathbf{r}_j}^{\mathbf{r}_i} \mathcal{D}\mathbf{R}^a(t_1) \int \mathcal{D}\mathbf{P}^a(t_1) e^{\pm i \bar{S}_0^a(t, t')} \\
 &\quad \times \sum_{N=0}^{\infty} \frac{(\mp i)^N}{\hbar^N} \int_{t_j}^{t_i} dt_1 \int_{t_j}^{t_1} dt_2 \dots \int_{t_j}^{t_{N-1}} dt_N \bar{h}_V^a(t_1) \bar{h}_V^a(t_2) \dots \bar{h}_V^a(t_N) \\
 &= \sum_{N=0}^{\infty} \int_{t_j}^{t_i} dt_1 \int_{t_j}^{t_1} dt_2 \dots \int_{t_j}^{t_{N-1}} dt_N \int dx_{1,\bar{1}} dx_{2,\bar{2}} \dots dx_{N,\bar{N}} \\
 &\quad \times \begin{cases} (-i/\hbar)^N \tilde{U}_{i\bar{1}}^{0F} \tilde{h}_{V\bar{1}\bar{1}}^F \tilde{U}_{\bar{1}\bar{2}}^{0F} \dots \tilde{h}_{V\bar{N}\bar{N}}^F \tilde{U}_{\bar{N}j}^{0F} \\ (+i/\hbar)^N \tilde{U}_{j\bar{N}}^{0B} \tilde{h}_{V\bar{N}\bar{N}}^B \dots \tilde{U}_{\bar{2}\bar{1}}^{0B} \tilde{h}_{V\bar{1}\bar{1}}^B \tilde{U}_{\bar{1}i}^{0B} \end{cases}. \quad (\text{D.11b})
 \end{aligned}$$

$$= \sum_{N=0}^{\infty} \int_{t_j}^{t_i} dt_1 \dots dt_N \int dx_{1,\bar{1}} \dots dx_{N,\bar{N}} \left\{ \begin{array}{l} \tilde{G}_{i\bar{1}}^R \tilde{h}_{V\bar{1}\bar{1}}^F \tilde{G}_{\bar{1}\bar{2}}^R \dots \tilde{h}_{V\bar{N}\bar{N}}^F \tilde{G}_{\bar{N}\bar{j}}^R \\ \tilde{G}_{j\bar{N}}^A \tilde{h}_{V\bar{N}\bar{N}}^B \dots \tilde{G}_{\bar{2}\bar{1}}^A \tilde{h}_{V\bar{1}\bar{1}}^B \tilde{G}_{\bar{1}\bar{i}}^A \end{array} \right. . \quad (\text{D.11c})$$

Eq. (D.11b), which is illustrated in the third row of Fig.D1, was obtained from the line preceding it by multiple applications of the rule of thumb (D.10), and reproduces the expansions of Eqs. (B.48). For Eq. (D.11c) we recalled Eq. (B.45) to set $\tilde{U}^{0F/B} = \pm i \hbar \tilde{G}^{R/A}$ along the forward or backward contours, respectively.

D.4. Coordinate-Space-Only Path Integral

Since the power series expansions (D.11b) for \tilde{U}_{ij}^a do not contain any explicit momentum integrals, they may be used as starting points for deriving coordinates-only path integral expressions containing no $\int \mathcal{D}\mathbf{P}^a$ integrations at all, so that only the coordinate integrations $\int \mathcal{D}\mathbf{R}^a$ remain. To this end, we simply perform the $\int \mathcal{D}\mathbf{P}^a$ integrals in the definition of the free propagators \tilde{U}_{ij}^{0a} explicitly, with the well-known result:

$$\left. \begin{array}{l} \tilde{U}_{ij}^{0F}(t, t') \\ \tilde{U}_{ji}^{0B}(t', t) \end{array} \right\} \equiv \delta_{\sigma_i \sigma_j} \lim_{M \rightarrow \infty} \prod_{n=1}^{M-1} \left(\int d\mathbf{r}_n^a \right) \prod_{n=1}^M \left(\int \frac{d\mathbf{p}_n^a}{(2\pi)^d} \right) \\ \times \exp \left[\frac{is_a \epsilon}{\hbar} \sum_{n=1}^M \left(\hbar \mathbf{p}_n^a \cdot \frac{\delta \mathbf{r}_n^a}{\epsilon} - \frac{\hbar^2 \mathbf{p}_n^{a2}}{2m} - V_{\text{imp}}(\mathbf{R}_n^a) \right) \right] \quad (\text{D.12a})$$

$$= \delta_{\sigma_i \sigma_j} \left[\frac{m}{2\pi is_a \epsilon \hbar} \right]^{Md/2} \prod_{n=1}^{M-1} \int d\mathbf{r}_n^a \exp \left[\frac{is_a \epsilon}{\hbar} \sum_{n=1}^M \left(\frac{m}{2} \left[\frac{\delta \mathbf{r}_n^a}{\epsilon} \right]^2 - V_{\text{imp}}(\mathbf{R}_n^a) \right) \right] \\ \equiv \int_{\mathbf{R}^a(t')=\mathbf{r}_j}^{\mathbf{R}^a(t)=\mathbf{r}_i} \tilde{\mathcal{D}}\mathbf{R}^a e^{(is_a/\hbar) \tilde{S}_0^a(t, t')}, \quad (\text{D.12b})$$

$$\tilde{S}_0^a(t, t')[\mathbf{R}^a(t_3)] \equiv \int_{t'}^t dt_3 \left[\frac{1}{2} m \dot{\mathbf{R}}^{a2}(t_3) - V_{\text{imp}}(\mathbf{R}^a(t_3)) \right]. \quad (\text{D.12c})$$

Here \tilde{S}_0^a is the standard action for a noninteracting electron in a disorder potential, and the tilde indicates that [in contrast to \bar{H}^a of Eq. (D.2b)] it is a functional of $\mathbf{R}^a(t_3)$ only, not of $\mathbf{P}^a(t_3)$ too. The tilde on $\int \tilde{\mathcal{D}}\mathbf{R}$ in Eq. (D.12b) indicates that the measure includes the prefactor in the line above it. Now, if we take the power series expansion (D.11b) for \tilde{U}_{ij}^a and insert Eq. (D.12b) for each occurrence of \tilde{U}_{ij}^{0a} , we obtain for \tilde{U}_{ij}^a a coordinate-only path integral expression with a precise (though cumbersome) time-slicing definition. In the main text, we have used for the path integral so obtained the formal path integral notation (B.56), with actions defined by Eqs. (B.57) and (B.58), and measure $\int \tilde{\mathcal{D}}'\mathbf{R}$, where the prime reminds us of the double position integrals $\int dx_{i,\bar{i}}$ occurring in Eq. (D.11b). The points discussed after Eq. (B.58) in the main text all follow directly from the explicit construction given above.

D.5. Explicit Expressions for \bar{H}_n^a

The material presented up to now in this appendix was general, applicable to *any* nonlocal Hamiltonian of the form $\tilde{H}_j^a = \tilde{\delta}_{ij} h_{0j} + \tilde{h}_{V_{ij}}^a$. Let us now be more concrete and specialize to the Hamiltonian defined by Eqs. (B.36), in order to verify GZ's expression for the effective action derived for their $\int \mathcal{D}\mathbf{R} \int \mathcal{D}\mathbf{P}$ path integral.

Inserting Eqs. (B.36) into Eq. (D.2), we readily find that

$$\bar{H}_n^a = \bar{h}_0(\mathbf{R}_n^a, \mathbf{P}_n^a) + \bar{h}_V^a(t_n, t_0; \mathbf{R}_n^a, \mathbf{P}_n^a) = \bar{h}_{0n} + \bar{h}_{V_n}^a, \quad (\text{D.13a})$$

$$\bar{h}_{V_n}^a = \sum_{\alpha=\pm} \bar{w}^{\alpha\alpha}(t_n, t_0; \mathbf{R}_n^a, \mathbf{P}_n^a) V_\alpha(t_n, \mathbf{R}_n^a), \quad (\text{D.13b})$$

$$\bar{h}_0(\mathbf{R}^a, \mathbf{P}^a) \equiv \frac{\mathbf{P}^{a2}}{2m} + V_{\text{imp}}(\mathbf{R}^a) - \mu, \quad (\text{D.13c})$$

$$\bar{w}^{a\pm}(t, t_0; \mathbf{R}^a, \mathbf{P}^a) \equiv \begin{cases} e \\ e s_a \frac{1}{2} e^{-i(b_a - \delta_{aB}) \nabla_{\mathbf{P}^a} \cdot \nabla_{\mathbf{R}^a}} [1 - 2\bar{\rho}^a(t, t_0; \mathbf{R}'^a, \mathbf{P}^a)] \end{cases}, \quad (\text{D.13d})$$

$$\bar{\rho}^a(t, t_0; \mathbf{R}^a, \mathbf{P}^a) = \int d\mathbf{r}^a e^{-i s_a \mathbf{P}^a \cdot \mathbf{r}^a} \tilde{\rho}^{(\text{ns})}(\mathbf{R}^a + s_a(1 - b_a)\mathbf{r}^a, \mathbf{R}^a - s_a b_a \mathbf{r}^a). \quad (\text{D.13e})$$

Here $\bar{h}_0(\mathbf{R}^a, \mathbf{P}^a)$ and $\bar{\rho}^a(t, t_0; \mathbf{R}^a, \mathbf{P}^a)$ are, respectively, the free Hamiltonian and the single-particle density matrix (in the presence of interactions but without source terms) in the mixed representation. In the definition (D.13d) of \bar{w}^{a-} , it is to be understood that \mathbf{R}'^a should be equated to \mathbf{R}^a after evaluating the action of the exponential differential operator on the function $V_-(t_n, \mathbf{R}_n^a)$ to the right of $\bar{w}^{a-}(t, t_0; \mathbf{R}^a, \mathbf{P}^a)$ in Eq. (D.13b), and all equations derived therefrom.

For general choices of b_a , the shift operator $e^{-i(b_a - \delta_{aB}) \nabla_{\mathbf{P}_n^a} \cdot \nabla_{\mathbf{R}_n^a}}$ in Eq. (D.13d) is needed for the following reason: In the defining Eqs. (B.36a) for $\tilde{H}_{i\bar{i}}^F$ and $\tilde{H}_{i\bar{i}}^B$, the arguments of the field $V_{-\bar{i}}$ are evaluated at $\mathbf{r}_{\bar{i}}^F$ and $\mathbf{r}_{\bar{i}}^B$, respectively. When considering the n -th interval (for which $\mathbf{r}_i^a = \mathbf{r}_n^a$, $\mathbf{r}_i^a = \mathbf{r}_{n-1}^a$), these arguments of $V_{-\bar{i}}$ become $\mathbf{r}_{\bar{i}}^F = \mathbf{r}_{n-1}^F = \mathbf{R}_n^F - b_F \delta \mathbf{r}_n^F$ and $\mathbf{r}_{\bar{i}}^B = \mathbf{r}_{n-1}^B = \mathbf{R}_n^B - (1 - b_B) \delta \mathbf{r}_n^B$ [cf. Eq. (D.3)], which are evidently shifted relative to the argument at which the field $V_-(t_n, \mathbf{R}_n^a)$ is evaluated in Eq. (D.13b), namely \mathbf{R}_n^a , by an amount $-s_a(b_a - \delta_{aB}) \delta \mathbf{r}_n^a$. The exponential shift operator implements this shift [as can be verified by inserting Eqs. (D.13) into Eq. (D.4) to recover $H_{i\bar{i}}^F$ and $H_{i\bar{i}}^B$]. Evidently, though, one *can* achieve $\mathbf{R}_n^F = \mathbf{r}_{n-1}^F (= \mathbf{r}_j^F)$ and $\mathbf{R}_n^B = \mathbf{r}_n^B (= \mathbf{r}_i^B)$ and hence avoid the need for shifts, by making the special, “maximally asymmetric” choice $b_a = \delta_{aB}$. Indeed, for this choice, which we shall adopt henceforth, the exponential shift operators $e^{-i(b_a - \delta_{aB}) \nabla_{\mathbf{P}^a} \cdot \nabla_{\mathbf{R}^a}}$ reduce to unity. Moreover, since \mathbf{R}_n^a then depends on only one of the position coordinates \mathbf{r}_n^a and \mathbf{r}_{n-1}^a associated with the n -th time interval, namely the second, so does $\bar{H}_n^a = \bar{H}^a(t_n, \mathbf{r}_{n-1}^a, \mathbf{P}_n^a)$, which greatly simplifies subsequent manipulations. The “price” to be paid for this simplification is not high – one merely has to remember that the definitions (D.2b) of \bar{H}_n^a in terms of the Fourier transforms of \tilde{H}^a and $\tilde{\rho}^a$ with respect to the relative coordinate become fully asymmetric:

$$\bar{H}_n^F \equiv \int d(\delta \mathbf{r}_n^F) e^{-i \mathbf{p}_n^F \cdot \delta \mathbf{r}_n^F} \tilde{H}^F(t_n, \mathbf{r}_{n-1}^F + \delta \mathbf{r}_n^F, \mathbf{r}_{n-1}^F) = \bar{h}_0(\mathbf{r}_{n-1}^F, \mathbf{p}_n^F) + \bar{h}_{V_n}^F, \quad (\text{D.14a})$$

$$\bar{H}_n^B \equiv \int d(\delta \mathbf{r}_n^B) e^{i \mathbf{p}_n^B \cdot \delta \mathbf{r}_n^B} \tilde{H}^B(t_n, \mathbf{r}_{n-1}^B, \mathbf{r}_{n-1}^B - \delta \mathbf{r}_n^B) = \bar{h}_0(\mathbf{r}_{n-1}^B, \mathbf{p}_n^B) + \bar{h}_{V_n}^B, \quad (\text{D.14b})$$

where $\bar{h}_{V_n}^a = \sum_{\alpha=\pm} \bar{w}_n^{a\alpha} V_\alpha(t_n, \mathbf{r}_{n-1}^a)$, with $\bar{w}_n^{a+} = e$ and $\bar{w}_n^{a-} = e \frac{1}{2} s_a [1 - 2\bar{\rho}_n^a]$, and $\bar{\rho}_n^a$ is defined in terms of $\bar{\rho}_{ij}^{(\text{ns})}(t_n, t_0)$ by Fourier transform relations [Eq. (D.13e)] that are analogous to those [Eqs. (D.14)] for \bar{H}_n^a in terms of $\tilde{H}_{ij}^a(t_n)$.

D.6. GZ's Effective Action in Position-Momentum Representation

Having specified the time-sliced versions of \bar{H}^a in the position-momentum representation, it is straightforward to also derive the effective action $(i\bar{S}_R + \bar{S}_I)[\mathbf{R}^a, \mathbf{P}^a]$ for this representation: simply repeat the strategy followed in App. B.5.5 to 5.8, but use the position-momentum representation (denoted by bars instead of tildes) throughout. Since the details are very analogous, we shall be very brief, and indicate only the main differences.

The starting point is again Eq. (B.59) for $\langle J_{12', 2\bar{2}', 21'}^V(t_1, t_2; t_0) \rangle_{V, \text{ns}}$, but with the coordinates-only path integral measure $\int \tilde{\mathcal{D}}(\mathbf{R})$ replaced by a position-momentum path integral measure, $\int \mathcal{D}(\mathbf{R}\mathbf{P})$, which is a shorthand for

$$\int_{j_F}^{i_F} \int_{\bar{j}_B}^{\bar{i}_B} \mathcal{D}(\mathbf{R}\mathbf{P}) \dots \equiv \int_{\mathbf{R}^F(t_j)=\mathbf{r}_j}^{\mathbf{R}^F(t_i)=\mathbf{r}_i} \mathcal{D}\mathbf{R}^F(t_3) \int \mathcal{D}\mathbf{P}^F(t_3) e^{i\bar{S}_0^F(t_i, t_j)/\hbar} \quad (\text{D.15})$$

$$\times \int_{\mathbf{R}^B(t_j)=\mathbf{r}_j}^{\mathbf{R}^B(t_i)=\mathbf{r}_i} \mathcal{D}\mathbf{R}^B(t_3) \int \mathcal{D}\mathbf{P}^B(t_3) e^{-i\bar{S}_0^B(t_i, t_j)/\hbar} \dots \quad (\text{D.16})$$

$\bar{S}_0^a[\mathbf{R}^a(t_3), \mathbf{P}^a(t_3)]$ in the weighting factor is the action for a single, free electron,

$$\bar{S}_0^a(t_i, t_j) = \int_{t_j}^{t_i} dt_3 [\mathbf{P}^a(t_3) \cdot \partial_{t_3} \mathbf{R}^a(t_3) - \bar{h}_0(\mathbf{R}^a(t_3), \mathbf{P}^a(t_3))] , \quad (\text{D.17})$$

and the bar on \bar{S}_0 (and $\bar{\mathcal{B}}$, $\bar{S}_{R/I}$ below) indicates that [in contrast to \tilde{S}_0^a , $\tilde{\mathcal{B}}$, $\tilde{S}_{R/I}$ of App. B] they are functionals of $\mathbf{R}^a(t_3)$ and $\mathbf{P}^a(t_3)$, not of $\tilde{\mathbf{R}}^a(t_3)$ only. In Eqs. (B.61), $\tilde{\mathcal{B}}_{\alpha 3}$ is replaced by

$$\bar{\mathcal{B}}_\alpha(t_3, \mathbf{r}_3) \equiv \sum_a s_a \bar{W}_{3_a}^{a\alpha} \delta(\mathbf{r}_3 - \mathbf{R}^a(t_3)) , \quad \bar{W}_{3_a}^{a+} = e , \quad (\text{D.18a})$$

$$\bar{W}_{3_a}^{a-} = e \frac{1}{2} s_a [1 - (\theta_{32} + y^a \theta_{23}) \bar{\rho}^a(t_3, t_0; \mathbf{R}^a(t_3), \mathbf{P}^a(t_3))] . \quad (\text{D.18b})$$

Now use precisely the same set of approximations and arguments as in App. B.5.6 to B.5.8 to derive the effective action $i\bar{S}_R + \bar{S}_I$. One readily arrives at an equation just like (B.83), but with $(i\tilde{L}^R/\tilde{L}^I)$ of Eqs. (B.84) replaced by^j

$$(i\bar{L}^R/\bar{L}^I)_{3_a 4_{a'}} = \frac{1}{2} s_a s_{a'} \bar{W}_{3_a}^{a+} \bar{W}_{4_{a'}}^{a'+} (2\tilde{R}/\tilde{I})_{3_a 4_{a'}} , \quad (\text{D.19})$$

^jThe $\theta_{34}(i\tilde{R}/\tilde{I})_{34}$ occurring in Eqs. (B.84) was written as $\frac{1}{2}(2i\tilde{R}/\tilde{I})_{34}$ here, exploiting the symmetry $\tilde{I}_{34} = \tilde{I}_{43}$.

where the density matrix occurring in \overline{W}^{a-} now is the free one, $\bar{\rho}_0^a$. Multiplying out the terms in Eq. (D.19) explicitly (and setting $(\theta_{4_{a'},2} + y^{a'}\theta_{24_{a'}}) = 1$ for reasons explained in footnote h on page 55), we find

$$\begin{aligned} \bar{S}_R(t_1, t_0) = & \frac{e^2}{2} \int_{t_0}^{t_1} dt_3 \int_{t_0}^{t_1} dt_4 \left\{ \right. & (D.20a) \\ & \left. \left[1 - 2\bar{\rho}_0^F(\mathbf{R}^F(t_4), \mathbf{P}^F(t_4)) \right] \left(\tilde{R}[t_{34}, \mathbf{R}^F(t_3) - \mathbf{R}^F(t_4)] - \tilde{R}[t_{34}, \mathbf{R}^B(t_3) - \mathbf{R}^F(t_4)] \right) + \right. \\ & \left. \left[1 - 2\bar{\rho}_0^B(\mathbf{R}^B(t_4), \mathbf{P}^B(t_4)) \right] \left(\tilde{R}[t_{34}, \mathbf{R}^F(t_3) - \mathbf{R}^B(t_4)] - \tilde{R}[t_{34}, \mathbf{R}^B(t_3) - \mathbf{R}^B(t_4)] \right) \right\}, \end{aligned}$$

$$\begin{aligned} \bar{S}_I(t_1, t_0) = & \frac{e^2}{2} \int_{t_0}^{t_1} dt_3 \int_{t_0}^{t_1} dt_4 \left\{ \tilde{I}[t_{34}, \mathbf{R}^F(t_3) - \mathbf{R}^F(t_4)] - \tilde{I}[t_{34}, \mathbf{R}^B(t_3) - \mathbf{R}^F(t_4)] \right. \\ & \left. - \tilde{I}[t_{34}, \mathbf{R}^F(t_3) - \mathbf{R}^B(t_4)] + \tilde{I}[t_{34}, \mathbf{R}^B(t_3) - \mathbf{R}^B(t_4)] \right\}. \quad (D.20b) \end{aligned}$$

This reproduces GZ's expressions for the effective action, since Eqs. (D.20) are the analogues of (GZ-II.54) and (GZ-II.55) [our 1st, 2nd, 3rd and 4th terms, having $aa' = FF, BF, FB, BB$, correspond to GZ's 1st, 4th, 3rd and 2nd terms, respectively]. The only difference is that in their Pauli factor, GZ have evidently replaced our $\bar{\rho}_0^a(\mathbf{R}^a(t), \mathbf{P}^a(t))$ by $n(\mathbf{R}^a(t), \mathbf{P}^a(t))$, which they define as the Fermi function $n(\hbar_0)$, evaluated at energy $\hbar_0(\mathbf{R}^a(t), \mathbf{P}^a(t))$.

GZ offered no justification for the latter replacement in GZ99³, but have defended it in subsequent papers⁵ by arguing that it amounts to a quasiclassical approximation that neglects terms of order \hbar . We have argued in a previous publication¹⁵ that the ‘‘small parameter’’ that would protect this approximation is actually $\tau_{el}\hbar/T$, which evidently is *not* small in the $T \rightarrow 0$ limit of present interest. Much more alarming, though, is that when averaging over all self-returning random walk paths, GZ proceed to make the assumption that ‘‘ n_0 depends only on the energy *and not on time* (our emphasis), because the energy is conserved along the classical path’’ [see discussion after Eq. (GZ-II.68)]. As argued in Sec. 4 of the main text, however, this neglects recoil, and produces incorrect results. A more accurate way of treating the Pauli factor, that properly includes recoil, is discussed in Sec. 3 of the main text.

Appendix E. Diagrammatic Keldysh Approach

In order to facilitate comparison between GZ's notation and our's, this appendix collects some standard definitions (following Rammer and Smith^k) and results for electron and field correlators used in the Keldysh approach. [Where relevant, GZ's notation is given in brackets.] Below, subscripts i are abbreviations for (t_i, x_i) when used for fermion fields or for (t_i, \mathbf{r}_i) when used for interaction fields. \tilde{G}_{ij} is a short-

^k J. Rammer and H. Smith, Rev. Mod. Phys. **58**, 323 (1986).

hand for $\tilde{G}_{ij}(t_{ij}) \equiv G(t_{ij}; x_i, x_j)$ [and similarly for $\tilde{\mathcal{L}}_{ij}$], i.e. the time-argument, when not displayed explicitly, will be understood to be $t_{ij} = t_i - t_j$. As elsewhere, the tilde signifies the matrix structure in coordinate space, while bold symbols are used for matrices in Keldysh space, e.g. $\tilde{\mathbf{G}}_{ij}$.

E.1. Electron Correlators

We begin with the electronic Green's functions \tilde{G}_{ij} , and consider for the moment only those for free, noninteracting electrons (i.e. evaluated for $V_a = 0$): the basic correlators

$$\tilde{G}_{ij}^< \equiv \frac{i}{\hbar} \langle \hat{\psi}_I^\dagger(t_j, x_j) \hat{\psi}_I(t_i, x_i) \rangle_0 \quad [= G_{12}^{\text{GZ}}(ij)], \quad (\text{E.1a})$$

$$\tilde{G}_{ij}^> \equiv -\frac{i}{\hbar} \langle \hat{\psi}_I(t_i, x_i) \hat{\psi}_I^\dagger(t_j, x_j) \rangle_0 \quad [= G_{21}^{\text{GZ}}(ij)], \quad (\text{E.1b})$$

are used as follows to construct the time-ordered, anti-time-ordered, retarded, advanced, Keldysh and contour-ordered Green's functions, respectively:

$$\tilde{G}_{ij}^T \equiv \theta(t_{ij}) \tilde{G}_{ij}^> + \theta(t_{ji}) \tilde{G}_{ij}^< \quad [= G_{11}^{\text{GZ}}(ij)], \quad (\text{E.2a})$$

$$\tilde{G}_{ij}^{\bar{T}} \equiv \theta(t_{ji}) \tilde{G}_{ij}^> + \theta(t_{ij}) \tilde{G}_{ij}^< \quad [= G_{22}^{\text{GZ}}(ij)], \quad (\text{E.2b})$$

$$\tilde{G}_{ij}^R \equiv \theta(t_{ij}) (\tilde{G}_{ij}^> - \tilde{G}_{ij}^<) \quad [= \tilde{G}^{R,\text{GZ}}(ij)], \quad (\text{E.2c})$$

$$\tilde{G}_{ij}^A \equiv -\theta(t_{ji}) (\tilde{G}_{ij}^> - \tilde{G}_{ij}^<) \quad [= G^{A,\text{GZ}}(ij)], \quad (\text{E.2d})$$

$$\tilde{G}_{ij}^T = \tilde{G}_{ij}^< + \tilde{G}_{ij}^R = \tilde{G}_{ij}^> + \tilde{G}_{ij}^A, \quad (\text{E.2e})$$

$$\tilde{G}_{ij}^{\bar{T}} = \tilde{G}_{ij}^< - \tilde{G}_{ij}^A = \tilde{G}_{ij}^> - \tilde{G}_{ij}^R, \quad (\text{E.2f})$$

$$\tilde{G}_{ij}^K \equiv \tilde{G}_{ij}^> + \tilde{G}_{ij}^< = \tilde{G}_{ij}^R - \tilde{G}_{ij}^A + 2\tilde{G}_{ij}^<, \quad (\text{E.2g})$$

$$\tilde{U}_{ij}^0 \equiv i(\tilde{G}_{ij}^R - \tilde{G}_{ij}^A) = i(\tilde{G}_{ij}^> - \tilde{G}_{ij}^<), \quad (\text{E.2h})$$

$$\tilde{G}_{ij}^c \equiv \begin{cases} \tilde{G}_{ij}^> & \text{for } t_i >_c t_j, \\ \tilde{G}_{ij}^< & \text{for } t_i <_c t_j, \end{cases} \quad (\text{E.2i})$$

where $t_i >_c t_j$ means that t_i is further along the Keldysh contour than t_j , and \mathcal{T}_c denotes contour-ordering along this contour. (The Keldysh contour runs from the initial time t_0 to $+\infty$ and back.) Under complex conjugation, the following relations hold:

$$(\tilde{G}_{ij}^{R/A})^* = \tilde{G}_{ji}^{A/R}, \quad (\tilde{G}_{ij}^K)^* = -\tilde{G}_{ji}^K, \quad (\tilde{G}_{ij}^{</>})^* = -\tilde{G}_{ji}^{</>}. \quad (\text{E.3})$$

It is customary to represent the contour-ordered Green's function \tilde{G}_{ij}^c by a 2×2 matrix $\tilde{\mathbf{G}}_{ij}^0$ in Keldysh space, whose components are the quantum-statistical averages of contour-ordered operator products,

$$(\tilde{\mathbf{G}}_{ij}^0)^{aa'} \equiv \langle \hat{\mathbf{G}}_{ij}^{aa'} \rangle_0, \quad \hat{\mathbf{G}}_{ij}^{aa'} \equiv -\frac{i}{\hbar} \mathcal{T}_c \left[\hat{\psi}_I^a(t_i, x_i) \hat{\psi}_I^{a'\dagger}(t_j, x_j) \right], \quad (\text{E.4})$$

and are labeled by indices a, a' that take the values F and B , with the convention that if $a = F$ (or B), then t_i resides on the forward (or backward) part of the

Keldysh contour, and similarly for a' and t_j . In matrix notation, we have

$$\tilde{\mathbf{G}}_{ij}^0 = \langle \hat{\mathbf{G}}_{ij} \rangle_0 = -\frac{i}{\hbar} \langle \mathcal{T}_c \hat{\psi}_i \hat{\psi}_j^\dagger \rangle_0 = \begin{pmatrix} \tilde{G}_{ij}^T & \tilde{G}_{ij}^< \\ \tilde{G}_{ij}^> & \tilde{G}_{ij}^T \end{pmatrix}, \quad (\text{E.5})$$

where we used a boldface notation for the fermion fields to indicate that it has two components in Keldysh space, $\hat{\psi}_i \equiv \begin{pmatrix} \hat{\psi}_i^F(t_i, x_i) \\ \hat{\psi}_i^B(t_i, x_i) \end{pmatrix}$. [Note that $(\tilde{\mathbf{G}}_{ij}^0)^{aa'}$ corresponds to GZ's $G_{aa'}^{GZ}(ij)$, with $F \rightarrow 1$ and $B \rightarrow 2$]. A more convenient, since tridiagonal, form is obtained using the representation¹

$$\underline{\hat{\psi}}_i \equiv \mathbf{L} \tau^3 \hat{\psi}_i, \quad \underline{\hat{\psi}}_i^\dagger \equiv \hat{\psi}_i^\dagger \mathbf{L}^\dagger, \quad \tilde{\mathbf{G}}_{ij} \equiv -\frac{i}{\hbar} \left[\mathcal{T}_c \underline{\hat{\psi}}_i \underline{\hat{\psi}}_j^\dagger \right], \quad (\text{E.6a})$$

$$\tilde{\mathbf{G}}_{ij}^0 \equiv \langle \tilde{\mathbf{G}}_{ij} \rangle_0 = \mathbf{L} \tau^3 \tilde{\mathbf{G}}_{ij}^0 \mathbf{L}^\dagger = \begin{pmatrix} \tilde{G}_{ij}^R & \tilde{G}_{ij}^K \\ 0 & \tilde{G}_{ij}^A \end{pmatrix}, \quad (\text{E.6b})$$

where $\tau^{1,2,3}$ denote the Pauli matrices acting in Keldysh space, $\mathbf{L} = \frac{1}{\sqrt{2}} \begin{pmatrix} 1 & -1 \\ 1 & 1 \end{pmatrix}$, and Eq. (E.6b) follows from the definitions (E.2).

For future reference, note also that density operators $\hat{n}_{ijI}^a(t_1)$ located on the forward or backward branches of the Keldysh contour have the following representations (suppressing the time argument), for $a = F, B$:

$$\hat{n}_{ijI}^a = \psi_j^{a\dagger} \psi_i^a = \underline{\hat{\psi}}_j^\dagger \mathbf{P}_a \underline{\hat{\psi}}_i = \underline{\hat{\psi}}_{jI}^\dagger \mathbf{P}_a \underline{\hat{\psi}}_{iI}, \quad (\text{E.7a})$$

$$\mathbf{P}_{F/B} = \frac{1}{2}(\mathbf{1} \pm \tau^3), \quad \underline{\mathbf{P}}_{F/B} = \mathbf{L} \tau^3 \mathbf{P}_{F/B} \mathbf{L}^\dagger = \frac{1}{2}(\tau_1 \pm \mathbf{1}). \quad (\text{E.7b})$$

E.2. Field Correlators

Next we consider the ‘‘interaction propagators’’ $\tilde{\mathcal{L}}_{ij}$, i.e. correlators involving the real, bosonic fields V_i that were introduced via the Hubbard-Stratonovich transformation (B.28a). Below we shall use V_i as a shorthand for $V_a(t_i, \mathbf{r}_i)$, taking it to be understood that if $a = F$ (or B), then t_i resides on the forward (or backward) parts of the Keldysh contour. The basic correlators

$$\tilde{\mathcal{L}}_{ij}^< \equiv \frac{ie^2}{\hbar} \langle V_j V_i \rangle_V \equiv \tilde{\mathcal{L}}_{ji}^>, \quad (\text{E.8})$$

are averaged over all field configurations according to Eq. (B.29d). The definitions of the correlators $\tilde{\mathcal{L}}_{ij}^T, \tilde{\mathcal{L}}_{ij}^{\bar{T}}, \tilde{\mathcal{L}}_{ij}^R, \tilde{\mathcal{L}}_{ij}^A, \tilde{\mathcal{L}}_{ij}^K$ and $\tilde{\mathcal{L}}_{ij}^c$ in terms of $\tilde{\mathcal{L}}_{ij}^<$ and $\tilde{\mathcal{L}}_{ij}^>$ are identical to those of the corresponding electronic \tilde{G}_{ij} 's in terms of $\tilde{G}_{ij}^<$ and $\tilde{G}_{ij}^>$ in Eqs. (E.2). The matrix representation $\tilde{\mathcal{L}}_{ij}$ of the contour-ordered interaction propagator $\tilde{\mathcal{L}}_{ij}^c$, with matrix elements

$$\tilde{\mathcal{L}}_{ij}^{aa'} \equiv \frac{ie^2}{\hbar} \langle \mathcal{T}_c V_{ai} V_{a'j} \rangle_V = \tilde{\mathcal{L}}_{ji}^{a'a}, \quad (\text{E.9a})$$

¹ A. I. Larkin and Yu. N. Ovchinnikov, Zh. Eksp. Theor. Fiz. **68**, 1915 (1975) [Sov. Phys. – JETP **41**, 960 (1975)]. This is also the form used by Rammer and Smith (see footnote k).

takes a form analogous to Eq. (E.5), namely:

$$\tilde{\mathcal{L}}_{ij} \equiv \frac{ie^2}{\hbar} \begin{pmatrix} \langle V_{Fi} V_{Fj} \rangle_V & \langle V_{Fi} V_{Bj} \rangle_V \\ \langle V_{Bi} V_{Fj} \rangle_V & \langle V_{Bi} V_{Bj} \rangle_V \end{pmatrix} = \begin{pmatrix} \tilde{\mathcal{L}}_{ij}^T & \tilde{\mathcal{L}}_{ij}^< \\ \tilde{\mathcal{L}}_{ij}^> & \tilde{\mathcal{L}}_{ij}^T \end{pmatrix}. \quad (\text{E.9b})$$

Following AAG¹⁷, we shall use the transformation $\tilde{\mathbf{L}} = \frac{1}{\sqrt{2}} \begin{pmatrix} 1 & 1 \\ 1 & -1 \end{pmatrix}$ to obtain a tridiagonal representation, reminiscent of Eq. (E.6b),

$$\tilde{\mathcal{L}}_{ij} \equiv \tilde{\mathbf{L}} \tilde{\mathcal{L}}_{ij} \tilde{\mathbf{L}}^\dagger = \begin{pmatrix} \tilde{\mathcal{L}}_{ij}^K & \tilde{\mathcal{L}}_{ij}^R \\ \tilde{\mathcal{L}}_{ij}^A & 0 \end{pmatrix} = \frac{ie^2}{\hbar} \begin{pmatrix} 2\langle V_{+i} V_{+j} \rangle_V & \langle V_{+i} V_{-j} \rangle_V \\ \langle V_{-i} V_{+j} \rangle_V & \frac{1}{2} \langle V_{-i} V_{-j} \rangle_V \end{pmatrix} \quad (\text{E.10a})$$

$$= e^2 \begin{pmatrix} 2i \tilde{I}_{ij} & -\tilde{R}_{ij} \\ -\tilde{R}_{ji} & 0 \end{pmatrix}, \quad (\text{E.10b})$$

with matrix elements to be denoted by $\tilde{\mathcal{L}}_{ij}^{\alpha\alpha'}$, where α, α' take the values \pm . The last equality of Eq. (E.10a) was obtained by using

$$\begin{pmatrix} \sqrt{2} & 0 \\ 0 & \frac{1}{\sqrt{2}} \end{pmatrix} \begin{pmatrix} V_{+i} \\ V_{-i} \end{pmatrix} = \tilde{\mathbf{L}} \begin{pmatrix} V_{Fi} \\ V_{Bi} \end{pmatrix}, \quad (\text{E.11})$$

[cf. Eq. (B.37)] to rewrite $\tilde{\mathbf{L}} \tilde{\mathcal{L}}_{ij} \tilde{\mathbf{L}}^\dagger$ in terms of the correlators $e^2 \langle V_{\alpha i} V_{\alpha' j} \rangle_V$. The relations (E.10a) are general. The explicit expressions for these correlators given by Eq. (E.10b), which are specific for the present model, follow from Eq. (B.75a). [Incidentally, comparing Eqs. (E.10a) and (E.10b) proves Eq. (B.75b)]. Using the explicit forms for \tilde{R}_{ij} and \tilde{I}_{ij} of Eqs. (B.76), it can easily be checked that

$$(\tilde{\mathcal{L}}_{ij}^{R/A})^* = \tilde{\mathcal{L}}_{ij}^{R/A} = \tilde{\mathcal{L}}_{ji}^{A/R}, \quad (\tilde{\mathcal{L}}_{ij}^K)^* = -\tilde{\mathcal{L}}_{ij}^K = -\tilde{\mathcal{L}}_{ji}^K, \quad (\text{E.12})$$

and that their Fourier transforms w.r.t. t_{ij} satisfy the relations

$$\tilde{\mathcal{L}}_{ij}^R(\omega) = \tilde{\mathcal{L}}_{ji}^R(\omega) = \tilde{\mathcal{L}}_{ij}^{R*}(-\omega) = \tilde{\mathcal{L}}_{ij}^{A*}(\omega), \quad \tilde{\mathcal{L}}_{ij}^K(\omega) = \tilde{\mathcal{L}}_{ji}^K(\omega) = -\tilde{\mathcal{L}}_{ij}^{K*}(\omega), \quad (\text{E.13})$$

$$\tilde{\mathcal{L}}_{ij}^K(\omega) = \coth(\hbar\omega/2T) [\tilde{\mathcal{L}}_{ij}^R(\omega) - \tilde{\mathcal{L}}_{ij}^A(\omega)]. \quad (\text{E.14})$$

Eq. (E.14) [cf. Eq. (B.72)] has the form required by the fluctuation-dissipation theorem.

Explicit expressions for the interaction propagators are most readily written down in the Fourier representation. For disordered metals, where small frequencies and wave numbers dominate, we obtain from $\tilde{\mathcal{L}}^R = -e^2 \tilde{R}$ and (B.77) the following relations (in agreement with Eq. (5.8) of AAG¹⁷):

$$\tilde{\mathcal{L}}_q^R(\omega) \simeq -\frac{Dq^2 - i\omega}{2\nu D q^2}, \quad \tilde{\mathcal{L}}_q^K(\omega) = 2i \coth(\hbar\omega/2T) \text{Im} \tilde{\mathcal{L}}_q^R(\omega). \quad (\text{E.15})$$

E.3. Keldysh Perturbation Theory

In this section, we recall how the Feynman rules for Keldysh perturbation theory are derived, and use them to obtain an expression for the self energy $\underline{\Sigma}$ of the Keldysh electron Green's function [Eq. (E.24)].

In the Keldysh approach, expectation values of the form occurring in Eq. (B.27b) are written as follows (following Rammer and Smith, see footnote k):

$$\langle \hat{O}(t) \rangle_K \equiv \frac{\langle \hat{U}_{IB}(t, t_0) \hat{O}_I(t) \hat{U}_{IF}(t, t_0) \rangle_0}{\langle \hat{U}_{IB}(t, t_0) \hat{U}_{IF}(t, t_0) \rangle_0} = \frac{\langle \mathcal{T}_c \hat{S}_{ci} \hat{S}_{c\bar{v}} \hat{O}_I(t) \rangle_0}{\langle \mathcal{T}_c \hat{S}_{ci} \hat{S}_{c\bar{v}} \rangle_0}, \quad (\text{E.16a})$$

$$\hat{S}_{ci} \equiv \mathcal{T}_c e^{-\frac{i}{\hbar} \int_c dt_3 \hat{H}_{iI}(t_3)}, \quad \hat{S}_{c\bar{v}} \equiv \mathcal{T}_c e^{-\frac{i}{\hbar} \int_c dt_3 \hat{v}_I(t_3)}, \quad (\text{E.16b})$$

where $\int_c dt_1$ and \mathcal{T}_c indicate integration and time ordering along the familiar Keldysh contour [\hat{H}_{iI} and \hat{v} are defined in Eqs. (B.11) and (B.27d)]. In Eq. (E.16a), the operator $\hat{O}_I(t)$ can be written as either $\hat{O}_I^F(t)$ or $\hat{O}_I^B(t)$, where the superscripts indicate that the operator resides on the upper or lower branch of the Keldysh contour, since the contribution from the portion of the Keldysh contour from t to ∞ cancels that from ∞ back to t . Consequently, we can also represent $\hat{O}_I(t)$ as $\frac{1}{2}[\hat{O}_I^F + \hat{O}_I^B](t)$, which turns out to be most convenient and will be used henceforth. For examples, the reduced single-particle matrix $\tilde{\rho}_{11'}(t, t_0)$ of Eq. (B.27b) can be written as^m

$$\tilde{\rho}_{11'}(t_1, t_0) = \frac{1}{2} \langle \hat{n}_{11'I}^F + \hat{n}_{11'I}^B \rangle_K = \langle \hat{\psi}_{1'}^\dagger, \frac{1}{2} \boldsymbol{\tau}^1 \hat{\psi}_{1'} \rangle_K = -i\hbar \text{Tr}_K \left[\frac{1}{2} \boldsymbol{\tau}^1 \tilde{\mathbf{G}}_{11'}^{\text{full}} \right], \quad (\text{E.17})$$

Here Tr_K denotes a trace over Keldysh indices, $\tilde{\mathbf{G}}_{11'}^{\text{full}} = \langle \hat{\mathbf{G}}_{ij} \rangle_K$ (and likewise $\tilde{\mathbf{G}}_{11'}^{\text{ns}} = \langle \hat{\mathbf{G}}_{11'} \rangle_{K, \text{ns}}$, which will occur below, too), $\hat{\mathbf{G}}_{ij}$ has the same matrix structure as in Eq. (E.6a), and the superscript “full” (or “ns”) indicates that the average is to be evaluated in the presence of the full interaction and including (or excluding) all external perturbations, i.e. with $\langle \rangle_K$ (or $\langle \rangle_{K, \text{ns}}$) instead of $\langle \rangle_0$. As a check, we note that in the absence of interactions, Eq. (E.17) reduces to $-i\hbar \frac{1}{2} \tilde{\mathbf{G}}_{11'}^K = \frac{1}{2} \langle \psi_{1'}^\dagger, \psi_{1'} - \psi_{1'} \psi_{1'}^\dagger \rangle_0$, which is equal to the desired result of $\langle \psi_{1'}^\dagger, \psi_{1'} \rangle_0$ (recall that $\psi_{1'}^\dagger$ and $\psi_{1'}$ anticommute, since $x_{1'}$ is equated to x_1 only at the very end of the calculation).

By writing $\int_c dt_3 \hat{v}_I(t_3) = \int_{t_0}^\infty dt_3 [\hat{v}_{3I}^F - \hat{v}_{3I}^B]$, and switching to the Keldysh representation of Eq. (E.6a), $S_{c\bar{v}}$ takes the form

$$\hat{S}_{c\bar{v}} = \mathcal{T}_c e^{-\frac{i}{\hbar} \int_{t_0}^\infty dt_3 \int dx_{3,3} \hat{\mathbf{v}}_{33}(t_3)} \quad (\text{E.18a})$$

$$\hat{\mathbf{v}}_{33}(t_3) \equiv \tilde{v}_{33}(t_3) [\hat{n}_{33I}^F - \hat{n}_{33I}^B] = \tilde{v}_{33}(t_3) \hat{\psi}_{\bar{3}}^\dagger \mathbf{1} \hat{\psi}_{\bar{3}}. \quad (\text{E.18b})$$

As a special case of Eq. (E.18b), we note that the external perturbation, \hat{H}_{ext} of Eq. (B.17), generates vertices of the form

$$(-i/\hbar) \hat{h}_{22'}^{\text{ext}} = (-i/\hbar) h_{22'}^{\text{ext}} \hat{\psi}_{\bar{2}'}^\dagger \mathbf{1} \hat{\psi}_{\bar{2}}. \quad (\text{E.19})$$

^mAn alternative but equivalent form to Eq. (E.17) is often used (e.g. by AAG¹⁷, Eq. (5.1), where the factor 2 in front of $\hat{\tau}_1$ is a typo), namely $\tilde{\rho}_{11'} = \langle \hat{\psi}_{1'}^\dagger, \frac{1}{2} (\boldsymbol{\tau}^1 - \mathbf{1}) \hat{\psi}_{1'} \rangle_K = -i\hbar \frac{1}{2} (\boldsymbol{\tau}^1 - \mathbf{1}) \tilde{\mathbf{G}}_{11'}^{\text{full}}$, where it is to be understood that $t_{1'} = t_1 + 0^+$.

To linear order in \hat{h}^{ext} , where each fermion line is simply decorated by the insertion of a single external vertex, we thus have the Feynman rule that each full $\tilde{\mathbf{G}}_{ij}^{\text{full}}$ is to be replaced by

$$h_{22'}^{\text{ext}} \langle \tilde{\mathbf{G}}_{i2'} \mathbf{1} \tilde{\mathbf{G}}_{2j} \rangle_{K,\text{ns}} \rightarrow \frac{i\mathbf{E}(\omega_0) \cdot \mathbf{J}_{22'}}{\omega_0} \langle \tilde{\mathbf{G}}_{i2'} \mathbf{1} \tilde{\mathbf{G}}_{2j} \rangle_{K,\text{ns}}, \quad (\text{E.20})$$

where the subscript “ns” denotes “no (external) sources”, and the term in brackets indicates the form which $h_{22'}^{\text{ext}}$ assumes under Fourier transformation, if we use the gauge of Eq. (B.21b).

For any expectation value of the form $\langle \hat{O}(t) \rangle_K$, the interaction term \hat{H}_{iI} in \hat{S}_{ci} can be decoupled using the Hubbard-Stratonovitch transformation of Eqs. (B.28), just as in Sec. B.3, using the fields V_F and V_B for the forward and backward branches of the Keldysh contour, respectively. One then readily finds that $\langle \hat{O}(t) \rangle_K$ can be expressed as follows as a functional average over all fields $V_{F/B}$:

$$\langle \hat{O}_I(t) \rangle_K = \langle O^V(t, t_0) \rangle_V \quad (\text{E.21a})$$

$$O^V(t, t_0) \equiv \frac{\langle \mathcal{T}_c \hat{S}_{cV} \hat{S}_{c\bar{v}} \hat{O}_I(t) \rangle_0}{Z(t, t_0)}, \quad (\text{E.21b})$$

$$Z(t, t_0) \equiv \langle \mathcal{T}_c \hat{S}_{cV} \hat{S}_{c\bar{v}} \rangle_0, \quad (\text{E.21c})$$

$$\hat{S}_{cV} = \mathcal{T}_c e^{-\frac{i}{\hbar} \int_{t_0}^{\infty} dt_3 \int dx_3 \hat{\mathbf{V}}_3}, \quad (\text{E.21d})$$

$$\hat{\mathbf{V}}_3 \equiv e[\hat{n}_{33'}^F V_F(\mathbf{r}_3) - \hat{n}_{33'}^B V_B(\mathbf{r}_3)] = e[\hat{\psi}_3^\dagger (\mathbf{1} V_{+3} + \frac{1}{2} \boldsymbol{\tau}^1 V_{-3}) \hat{\psi}_3]. \quad (\text{E.21e})$$

Here the functional average $\langle \rangle_V$ over all field configurations is defined, as before, by Eqs. (B.29d), where the functional Z occurring in Eq. (B.29e) is now given by Eq. (E.21c).

To obtain an perturbation expansion within the Keldysh approach, one expands \hat{S}_{cV} in powers of $(-i/\hbar)\hat{\mathbf{V}}_3$, which thus serves as basic interaction vertex, and then applies Wick’s theorem to the fermion fields. In the n -th order term, there are $n!$ equivalent ways to connect the n vertices with n fermion lines of the type $\langle \hat{\psi}_i \hat{\psi}_j^\dagger \rangle_0 = i\hbar \tilde{\mathbf{G}}_{ij}^0$, yielding a combinatorial factor of $(i\hbar)^n n!$ which cancels the $(-i/\hbar)^n / (n!)$ from the expansion of the exponent of \hat{S}_{cV} . Next, the average $\langle \rangle_V$ over all field configurations is to be performed, which yields contractions between the interaction fields pairs of vertices. These contractions have the form

$$\langle \hat{\mathbf{V}}_i \hat{\mathbf{V}}_j \rangle_V = -\frac{1}{2} i\hbar \sum_{\alpha\alpha'} \hat{\psi}_{i'}^\dagger \gamma^\alpha \hat{\psi}_i \tilde{\mathcal{L}}_{ij}^{\alpha\alpha'} \hat{\psi}_{j'}^\dagger \gamma^{\alpha'} \hat{\psi}_j, \quad (\text{E.22})$$

where we introduced the “vertex matrices” $\gamma^+ = \mathbf{1}$ and $\gamma^- = \boldsymbol{\tau}^1$, the field propagator in the Keldysh representation $\tilde{\mathcal{L}}_{ij}^{\alpha\alpha'}$ is given by Eqs. (E.10), and the Feynman diagram corresponding to Eq. (E.22) is the leftmost graph in Fig. E1. Eq. (E.22) implies the following Dyson equation (cf. Eq. (5.6) of AAG¹⁷),

$$\tilde{\mathbf{G}}_{ij}^{\text{full}} = \tilde{\mathbf{G}}_{ij}^0 + \int_{t_0}^{\infty} dt_3 dt_4 \int dx_3 dx_4 \tilde{\mathbf{G}}_{i3}^0 \tilde{\Sigma}_{34} \tilde{\mathbf{G}}_{4j}^{\text{full}}, \quad (\text{E.23})$$

94 Jan von Delft

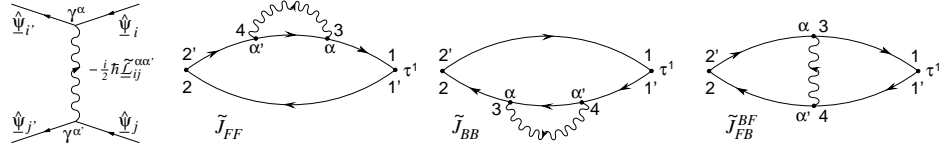


Fig. E1. Feynman diagrams for the interaction propagator [Eq. (E.22)] and the correlators \tilde{J}_{FF} , \tilde{J}_{BB} and \tilde{J}_{FB+BF} [Eqs. (E.28)] that give the leading correction to the conductivity due to electron-electron interaction. Solid lines denote matrix Green's functions $\tilde{\mathbf{G}}_{ij}^0$, wavy lines interaction propagators $\tilde{\mathcal{L}}_{ij}^{\alpha\alpha'}$, and the symbols α and α' the vertices γ^α and $\gamma^{\alpha'}$. Arrows point from the second to the first index of propagators.

where, to lowest order in the interaction, the self-energy is given by

$$\tilde{\Sigma}_{34} = -\frac{1}{2}i\hbar\gamma^\alpha\tilde{\mathbf{G}}_{34}^0\gamma^{\alpha'}\tilde{\mathcal{L}}_{34}^{\alpha\alpha'}. \quad (\text{E.24})$$

E.4. Conductivity

In this section we derive a general expression for conductivity σ_{DC} in the Keldysh approach and expand it to leading order in the interaction propagator. This will allow us to check the perturbative expansion (C.11) of our influence functional $\tilde{J}_{12',21'}$ of Sec. C.3.

We start by using Eq. (E.17) to express the quantum-statistical average of the current density operator $\tilde{\mathcal{J}}_H(t_1, \mathbf{r}_1)$ of Eq. (B.16) as follows,

$$\langle \tilde{\mathcal{J}}_H(t_1, \mathbf{r}_1) \rangle_K = \sum_{\sigma_1} \left[j_{11'} - \frac{e^2}{m} \mathbf{A}(t_1, \mathbf{r}_1) \right] (-i\hbar) \text{Tr}_K \left[\frac{1}{2} \tau^1 \tilde{\mathbf{G}}_{11'}^{\text{full}} \right]. \quad (\text{E.25})$$

Next we expand Eq. (E.25) to first order in \hat{h}_{ext} [using Eq. (E.20)], and then use Eq. (B.20) to calculate σ_{DC} ; the result has the form of Eq. (B.22b), where $\tilde{J}_{12',21'}(\omega_0)$ therein is given by the Fourier transform w.r.t. t_{12} of the following expression:

$$\tilde{J}_{12',21'}^{\text{Keldysh}} = \hbar \text{Tr}_K \left[\frac{1}{2} \tau^1 \langle \tilde{\mathbf{G}}_{12'} \tilde{\mathbf{G}}_{21'} \rangle_{K,\text{ns}} \right]. \quad (\text{E.26})$$

In the absence of electron-electron interactions, this readily reduces to

$$\tilde{J}_{12',21'}^{(0),\text{Keldysh}} = \frac{1}{2}\hbar \left(\tilde{G}_{12'}^R \tilde{G}_{21'}^K + \tilde{G}_{12'}^K \tilde{G}_{21'}^A \right) = \hbar \left(\tilde{G}_{12'}^R \tilde{G}_{21'}^< + \tilde{G}_{12'}^< \tilde{G}_{21'}^A \right). \quad (\text{E.27})$$

The second equality follows from Eq. (E.2g) (with $\tilde{G}_{ij}^{R/A} \tilde{G}_{ji}^{A/R} = 0$) and confirms Eq. (C.1a).

Let us now obtain the leading correction to σ_{DC} due to the electron-electron interaction. To this end, we have to expand Eq. (E.26) for $\tilde{J}_{12',21'}^{\text{Keldysh}}$ to second order in $\hat{\mathbf{V}}_3$. One readily arrives at the following result [which can also be obtained by starting directly from Eq. (E.25), expanding $\tilde{\mathbf{G}}_{11'}^{\text{full}}$ therein to first order in $\tilde{\Sigma}_{34}$ using

Eq. (E.23), and then expanding each $\tilde{\mathbf{G}}_{ij}^0$ in the latter equation to first order in \hat{h}_{ext} using Eq. (E.20)]:

$$\tilde{J}_{12',21'}^{(2),\text{Keldysh}} = -\frac{1}{2}i\hbar^2 \int_{t_0}^{\infty} dt_3 dt_4 \int dx_3 dx_4 \left(\tilde{J}_{FF} + \tilde{J}_{BB} + \tilde{J}_{FB}^{BF} \right),$$

$$\tilde{J}_{FF} = \sum_{\alpha\alpha'} \text{Tr}_K \left[\frac{1}{2} \boldsymbol{\tau}^1 \tilde{\mathbf{G}}_{13}^0 \gamma^\alpha \tilde{\mathbf{G}}_{34}^0 \gamma^{\alpha'} \tilde{\mathbf{G}}_{42'}^0 \tilde{\mathbf{G}}_{21'}^0 \tilde{\mathbf{L}}_{34}^{\alpha\alpha'} \right], \quad (\text{E.28a})$$

$$\tilde{J}_{BB} = \sum_{\alpha\alpha'} \text{Tr}_K \left[\frac{1}{2} \boldsymbol{\tau}^1 \tilde{\mathbf{G}}_{12'}^0 \tilde{\mathbf{G}}_{23}^0 \gamma^\alpha \tilde{\mathbf{G}}_{34}^0 \gamma^{\alpha'} \tilde{\mathbf{G}}_{41'}^0 \tilde{\mathbf{L}}_{34}^{\alpha\alpha'} \right], \quad (\text{E.28b})$$

$$\tilde{J}_{FB}^{BF} = \sum_{\alpha\alpha'} \text{Tr}_K \left[\frac{1}{2} \boldsymbol{\tau}^1 \tilde{\mathbf{G}}_{13}^0 \gamma^\alpha \tilde{\mathbf{G}}_{32'}^0 \tilde{\mathbf{G}}_{24}^0 \gamma^{\alpha'} \tilde{\mathbf{G}}_{41'}^0 \tilde{\mathbf{L}}_{34}^{\alpha\alpha'} \right]. \quad (\text{E.28c})$$

The correlators \tilde{J}_{FF} , \tilde{J}_{BB} and \tilde{J}_{FB}^{BF} are illustrated in Fig. E1, and correspond to self-energy insertions in the upper and lower Keldysh contours, and a vertex correction, respectively. Multiplying out the Keldysh matrices explicitly, taking the trace and omitting all terms involving the combinations $\tilde{G}_{34}^R \tilde{\mathcal{L}}_{34}^A$ or $\tilde{G}_{34}^A \tilde{\mathcal{L}}_{34}^R$, which vanish (since $\theta_{34}\theta_{43} = 0$), we obtain:

$$\begin{aligned} \tilde{J}_{FF} = & \frac{1}{2} \tilde{G}_{13}^R [\tilde{G}_{34}^R \tilde{\mathcal{L}}_{34}^K + \tilde{G}_{34}^K \tilde{\mathcal{L}}_{34}^R] (\tilde{G}_{42'}^R \tilde{G}_{21'}^K + \tilde{G}_{42'}^K \tilde{G}_{21'}^R) \quad (\text{E.29a}) \\ & + \frac{1}{2} [\tilde{G}_{13}^R (\tilde{G}_{34}^K \tilde{\mathcal{L}}_{34}^K + \tilde{G}_{34}^R \tilde{\mathcal{L}}_{34}^R + \tilde{G}_{34}^A \tilde{\mathcal{L}}_{34}^A) + \tilde{G}_{13}^K (\tilde{G}_{34}^A \tilde{\mathcal{L}}_{34}^K + \tilde{G}_{34}^K \tilde{\mathcal{L}}_{34}^A)] \tilde{G}_{42'}^A \tilde{G}_{21'}^A, \end{aligned}$$

$$\begin{aligned} \tilde{J}_{BB} = & \frac{1}{2} (\tilde{G}_{12'}^R \tilde{G}_{23}^K + \tilde{G}_{12'}^K \tilde{G}_{23}^R) [\tilde{G}_{34}^A \tilde{\mathcal{L}}_{34}^K + \tilde{G}_{34}^K \tilde{\mathcal{L}}_{34}^A] \tilde{G}_{41'}^A, \quad (\text{E.29b}) \\ & + \frac{1}{2} \tilde{G}_{12'}^R \tilde{G}_{23}^R [(\tilde{G}_{34}^R \tilde{\mathcal{L}}_{34}^K + \tilde{G}_{34}^K \tilde{\mathcal{L}}_{34}^R) \tilde{G}_{41'}^K + (\tilde{G}_{34}^K \tilde{\mathcal{L}}_{34}^K + \tilde{G}_{34}^R \tilde{\mathcal{L}}_{34}^R + \tilde{G}_{34}^A \tilde{\mathcal{L}}_{34}^A) \tilde{G}_{41'}^A], \end{aligned}$$

$$\begin{aligned} \tilde{J}_{FB}^{BF} = & \frac{1}{2} (\tilde{G}_{32'}^R \tilde{G}_{24}^K + \tilde{G}_{32'}^K \tilde{G}_{24}^R) [\tilde{G}_{41'}^A \tilde{G}_{13}^R \tilde{\mathcal{L}}_{34}^K + \tilde{G}_{41'}^K \tilde{G}_{13}^R \tilde{\mathcal{L}}_{34}^R + \tilde{G}_{41'}^A \tilde{G}_{13}^K \tilde{\mathcal{L}}_{34}^A] \quad (\text{E.29c}) \\ & + \frac{1}{2} \tilde{G}_{32'}^R \tilde{G}_{24}^R [\tilde{G}_{41'}^K \tilde{G}_{13}^R \tilde{\mathcal{L}}_{34}^K + \tilde{G}_{41'}^R \tilde{G}_{13}^R \tilde{\mathcal{L}}_{34}^R + (\tilde{G}_{41'}^K \tilde{G}_{13}^K + \tilde{G}_{41'}^R \tilde{G}_{13}^R) \tilde{\mathcal{L}}_{34}^A] \\ & + \frac{1}{2} \tilde{G}_{32'}^A \tilde{G}_{24}^A [\tilde{G}_{41'}^A \tilde{G}_{13}^K \tilde{\mathcal{L}}_{34}^K + \tilde{G}_{41'}^R \tilde{G}_{13}^R \tilde{\mathcal{L}}_{34}^R + (\tilde{G}_{41'}^K \tilde{G}_{13}^K + \tilde{G}_{41'}^R \tilde{G}_{13}^R) \tilde{\mathcal{L}}_{34}^A]. \end{aligned}$$

Now, terms that involve the combination $\tilde{G}_{i2'}^R \tilde{G}_{2j}^R$ or $\tilde{G}_{i2'}^A \tilde{G}_{2j}^A$ contribute to the so-called interaction corrections, and do not contribute to “decoherence”. Hence, we retain only the first lines of Eqs. (E.29) henceforth. For these, we use the identity [cf. (E.2g)]

$$\frac{1}{2} (\tilde{G}^R \tilde{G}^K + \tilde{G}^K \tilde{G}^A) = \tilde{G}^R \tilde{G}^< + \tilde{G}^< \tilde{G}^A + \frac{1}{2} (\tilde{G}^R \tilde{G}^R - \tilde{G}^A \tilde{G}^A) \quad (\text{E.30})$$

and drop the last term, for the same reason. The remaining terms then take the following form:

$$\tilde{J}_{FF} = \tilde{G}_{13}^R [\tilde{G}_{34}^R \tilde{\mathcal{L}}_{34}^K + \tilde{G}_{34}^K \tilde{\mathcal{L}}_{34}^R] (\tilde{G}_{42'}^R \tilde{G}_{21'}^< + \tilde{G}_{42'}^< \tilde{G}_{21'}^A) \quad (\text{E.31a})$$

$$\tilde{J}_{BB} = (\tilde{G}_{12'}^R \tilde{G}_{23}^< + \tilde{G}_{12'}^< \tilde{G}_{23}^A) [\tilde{G}_{34}^A \tilde{\mathcal{L}}_{34}^K + \tilde{G}_{34}^K \tilde{\mathcal{L}}_{34}^A] \tilde{G}_{41'}^A, \quad (\text{E.31b})$$

$$\tilde{J}_{FB}^{BF} = (\tilde{G}_{32'}^R \tilde{G}_{24}^< + \tilde{G}_{32'}^< \tilde{G}_{24}^A) [\tilde{G}_{41'}^A \tilde{G}_{13}^R \tilde{\mathcal{L}}_{34}^K + \tilde{G}_{41'}^K \tilde{G}_{13}^R \tilde{\mathcal{L}}_{34}^R + \tilde{G}_{41'}^A \tilde{G}_{13}^K \tilde{\mathcal{L}}_{34}^A]. \quad (\text{E.31c})$$

These expressions agree with the expansion (C.11) we obtained from the influence functional approach, as can be seen by relabelling $3 \leftrightarrow 4$ in some terms. [\tilde{J}_{FB}^{BF} here accounts for both \tilde{J}_{BF} and \tilde{J}_{FB} there.]

Appendix F. Diagrammatic Disorder Averaging

In this appendix we summarize, for reference purposes, some standard and well-known conventions and results used for diagrammatically performing disorder averages, using notations summarized at the beginning of App. B.

F.1. Definitions, Standard Results and Useful Tricks

To perform the disorder averages, we take the impurity potential to be short-ranged, $V_{\text{imp}}(\mathbf{r}) = v_{\text{imp}} \sum_i \delta(\mathbf{r} - \mathbf{R}_i)$, (v_{imp} has units of energy times volume), represent the fermion fields as $\psi_\sigma(t, \mathbf{r}) = \text{Vol}^{-1/2} \sum_{\mathbf{p}} e^{i\mathbf{p}\cdot\mathbf{r}} c_{\mathbf{p}}(t)$, and Fourier transform as follows:

$$\tilde{G}_{ij}^{R/A} = \tilde{G}^{R/A}(t_{ij}, x_i, x_j) \equiv \delta_{\sigma_i \sigma_j} \int \frac{d\varepsilon}{2\pi} e^{-i\varepsilon t_{ij}} \frac{1}{\text{Vol}} \sum_{\mathbf{p}; \mathbf{p}_j} e^{i(\mathbf{p}_i \cdot \mathbf{r}_i - \mathbf{p}_j \cdot \mathbf{r}_j)} \bar{G}_{\mathbf{p}; \mathbf{p}_j}^{R/A}(\varepsilon). \quad (\text{F.1})$$

Using standard diagrammatic techniques, the disorder-averaged single-particle propagator is found to have the form [Fig. F1(a)]:

$$\langle \bar{G}_{\mathbf{p}'\mathbf{p}}^{R/A}(\varepsilon) \rangle_{\text{dis}} = \delta_{\mathbf{p}'\mathbf{p}} \bar{\mathcal{G}}_{\mathbf{p}}^{R/A}(\varepsilon), \quad (\text{F.2a})$$

$$\bar{\mathcal{G}}_{\mathbf{p}}^{R/A}(\varepsilon) = \int dt_{ij} \int d\mathbf{r}_{ij} e^{-i\varepsilon t_{ij}} e^{i\mathbf{p}\cdot\mathbf{r}_{ij}} \langle \tilde{G}_{ij}^{R/A} \rangle_{\text{dis}} = \frac{1}{\hbar\varepsilon - \xi_{\mathbf{p}} \pm i\hbar/2\tau_{\text{el}}}. \quad (\text{F.2b})$$

Here $\tau_{\text{el}} = \hbar/(2\pi\nu c_{\text{imp}} v_{\text{imp}}^2)$ is the elastic scattering time, c_{imp} the impurity concentration, $\xi_{\mathbf{p}} = \mathbf{p}^2 \hbar^2 / 2m - \varepsilon_{\text{F}}$, and calligraphic symbols will be used throughout for disorder-averaged quantities. The corresponding position-time expression, found by inverse Fourier transforming, is:

$$\tilde{G}_{ij}^{R/A}(t) = \int (d\mathbf{p}) e^{i\mathbf{p}\cdot\mathbf{r}_{ij}} \int (d\varepsilon) e^{-i\varepsilon t} \bar{\mathcal{G}}_{\mathbf{p}}^{R/A}(\varepsilon), \quad (\text{F.2c})$$

$$= \mp \frac{i}{\hbar} \theta(\pm t) \left(\frac{m}{i2\pi\hbar t} \right)^{d/2} \exp \left[\frac{im\mathbf{r}_{ij}^2}{2\hbar t} \right] e^{i\varepsilon_{\text{F}} t / \hbar} e^{-|t|/2\tau_{\text{el}}}. \quad (\text{F.2d})$$

The disorder-averaged products $\langle \tilde{G}^R \tilde{G}^A \rangle_{\text{dis}}$ have the form [Fig. F1(b)],

$$\langle \bar{G}_{\mathbf{p}'\mathbf{p}}^{R/A}(\varepsilon) \bar{G}_{\bar{\mathbf{p}}'\bar{\mathbf{p}}}^{R/A}(\bar{\varepsilon}) \rangle_{\text{dis}} = \delta_{\mathbf{p}'\mathbf{p}} \delta_{\bar{\mathbf{p}}'\bar{\mathbf{p}}} \bar{\mathcal{G}}_{\mathbf{p}}^{R/A}(\varepsilon) \bar{\mathcal{G}}_{\bar{\mathbf{p}}}^{R/A}(\bar{\varepsilon}), \quad (\text{F.3a})$$

$$\begin{aligned} \langle \bar{G}_{\mathbf{p}'\mathbf{p}}^R(\varepsilon) \bar{G}_{\bar{\mathbf{p}}'\bar{\mathbf{p}}}^A(\bar{\varepsilon}) \rangle_{\text{dis}} &= \delta_{\mathbf{p}'\mathbf{p}} \delta_{\bar{\mathbf{p}}'\bar{\mathbf{p}}} \bar{\mathcal{G}}_{\mathbf{p}}^R(\varepsilon) \bar{\mathcal{G}}_{\bar{\mathbf{p}}}^A(\bar{\varepsilon}) \\ &+ \delta_{\mathbf{p}' + \bar{\mathbf{p}}', \mathbf{p} + \bar{\mathbf{p}}} \bar{\mathcal{G}}_{\mathbf{p}}^R(\varepsilon) \bar{\mathcal{G}}_{\bar{\mathbf{p}}}^R(\varepsilon) \bar{\mathcal{G}}_{\bar{\mathbf{p}}}^A(\bar{\varepsilon}) \bar{\mathcal{G}}_{\mathbf{p}}^A(\bar{\varepsilon}) \frac{\bar{\mathcal{D}}_{\mathbf{p}+\bar{\mathbf{p}}}'^0(\varepsilon - \bar{\varepsilon}) + \bar{\mathcal{C}}_{\mathbf{p}+\bar{\mathbf{p}}}^0(\varepsilon - \bar{\varepsilon})}{\text{Vol} 2\pi\nu\tau_{\text{el}}^2/\hbar}, \end{aligned} \quad (\text{F.3b})$$

$\bar{\mathcal{C}}_{\mathbf{q}}^0(\omega)$ and $\bar{\mathcal{D}}_{\mathbf{q}}^0(\omega)$ being the bare (i.e. without interactions) Cooperon and diffuson, respectively. Fig. F1 summarizes the standard calculations of $\bar{\mathcal{C}}_{\mathbf{q}}^0(\omega)$ and $\bar{\mathcal{D}}_{\mathbf{q}}^0(\omega)$, and of the diffuson-dressed interaction vertex $\bar{\Gamma}_{\mathbf{q}}(\omega)$ and polarization bubble $\bar{\chi}_{\mathbf{q}}(\omega)$, which is defined as the Fourier transform of Eq. (B.66a):

$$\langle \bar{\chi}_{\mathbf{q}}(\omega) \rangle_{\text{dis}} = -i2e^2\hbar \int (d\varepsilon)(d\mathbf{p}) \langle \bar{\mathcal{G}}_{\mathbf{p}+\mathbf{q}}^R(\varepsilon + \omega) \bar{\mathcal{G}}_{\mathbf{p}}^<(\varepsilon) + \bar{\mathcal{G}}_{\mathbf{p}+\mathbf{q}}^<(\varepsilon + \omega) \bar{\mathcal{G}}_{\mathbf{p}}^A(\varepsilon) \rangle_{\text{dis}} \quad (\text{F.4a})$$

(a)
$$j \xrightarrow{R/A} i = \tilde{G}_{ij}^{R/A} \quad \frac{-ie^2(-R_{ij}/2iI_{ij})}{i \text{ wavy line}} = \frac{-ie^2 \mathcal{L}^{R/K}}{2} \Rightarrow \text{wavy line} = \frac{-ie^2 \mathcal{L}^{R/K}}{2}(\omega)$$

(a)
$$\xrightarrow{R/A, \varepsilon, p} = \frac{1}{\hbar \varepsilon - \xi(\mathbf{p}) \pm \hbar i/2\tau_{\text{el}}} \quad \frac{-ie^2(-R_{ji}/2iI_{ji})}{j \text{ wavy line}} = \frac{-ie^2 \mathcal{L}^{A/K}}{2} \Rightarrow \text{wavy line} = \frac{-ie^2 \mathcal{L}^{A/K}}{2}(\omega)$$

(b)
$$\begin{array}{c} \uparrow k \\ \vdots \\ \vdots \\ \vdots \end{array} = \frac{1}{2\pi\nu\tau_{\text{el}}/\hbar} \quad \int (dk) \left(\frac{R, \varepsilon + \omega, k}{A, \varepsilon, q - k} \right) = \bar{\Pi}_q(\omega)$$

(b)
$$\left\langle \begin{array}{c} \mathbf{p} \xrightarrow{R, \varepsilon} \mathbf{p}' \\ \bar{\mathbf{p}} \xrightarrow{A, \bar{\varepsilon}} \bar{\mathbf{p}} \end{array} \right\rangle_{\text{dis}} = \delta_{\mathbf{p}'\mathbf{p}} \delta_{\bar{\mathbf{p}}\bar{\mathbf{p}}} \left(\frac{R, \varepsilon, \mathbf{p}}{A, \bar{\varepsilon}, \bar{\mathbf{p}}} \right) + \frac{\delta_{\mathbf{p}'+\bar{\mathbf{p}}, \mathbf{p}+\bar{\mathbf{p}}}}{\text{Vol}} \left[\begin{array}{c} \frac{R, \varepsilon, \mathbf{p}}{A, \bar{\varepsilon}, \bar{\mathbf{p}}'} \xrightarrow{\varepsilon - \bar{\varepsilon}, \mathbf{p} + \bar{\mathbf{p}}} \frac{R, \varepsilon, \mathbf{p}'}{A, \bar{\varepsilon}, \bar{\mathbf{p}}} \\ + \\ \frac{R, \varepsilon, \mathbf{p}}{A, \bar{\varepsilon}, \bar{\mathbf{p}}} \xrightarrow{\varepsilon - \bar{\varepsilon}, \mathbf{p} + \bar{\mathbf{p}}} \frac{R, \varepsilon, \mathbf{p}'}{A, \bar{\varepsilon}, \bar{\mathbf{p}}'} \end{array} \right]$$

(c)
$$\frac{\bar{C}_q^0(\omega)}{2\pi\nu\tau_{\text{el}}^2/\hbar} = \frac{\varepsilon + \omega, \mathbf{p}}{\varepsilon, \mathbf{q} - \mathbf{p}} \xrightarrow{\omega, \mathbf{q}} \frac{\varepsilon + \omega, \mathbf{p}'}{\varepsilon, \mathbf{q} - \mathbf{p}'} = \frac{\varepsilon + \omega, \mathbf{p}}{\varepsilon, \mathbf{q} - \mathbf{p}} \left[\begin{array}{c} \uparrow \mathbf{p}' - \mathbf{p} \\ \vdots \\ \vdots \\ \vdots \end{array} \right] \xrightarrow{R, \varepsilon + \omega, k} \frac{\varepsilon + \omega, \mathbf{p}'}{\varepsilon, \mathbf{q} - \mathbf{p}'} \left[\begin{array}{c} \leftarrow k - \mathbf{p} \\ \vdots \\ \vdots \\ \vdots \end{array} \right] \xrightarrow{\omega, \mathbf{q}} \frac{\varepsilon + \omega, \mathbf{p}'}{\varepsilon, \mathbf{q} - \mathbf{p}'}$$

(c)
$$= \frac{1}{2\pi\nu\tau_{\text{el}}/\hbar} \left[1 + \bar{\Pi}_q(\omega) \frac{\bar{C}_q^0(\omega)}{2\pi\nu\tau_{\text{el}}^2/\hbar} \right]$$

(c)
$$\frac{\bar{D}_q^0(\omega)}{2\pi\nu\tau_{\text{el}}^2/\hbar} = \frac{\varepsilon + \omega, \mathbf{p}}{\varepsilon, \mathbf{p} - \mathbf{q}} \xrightarrow{\omega, \mathbf{q}} \frac{\varepsilon + \omega, \mathbf{p}'}{\varepsilon, \mathbf{p}' - \mathbf{q}} = \frac{\varepsilon + \omega, \mathbf{p}}{\varepsilon, \mathbf{p} - \mathbf{q}} \left[\begin{array}{c} \uparrow \mathbf{p}' - \mathbf{p} \\ \vdots \\ \vdots \\ \vdots \end{array} \right] \xrightarrow{R, \varepsilon + \omega, k} \frac{\varepsilon + \omega, \mathbf{p}'}{\varepsilon, \mathbf{p}' - \mathbf{q}} \left[\begin{array}{c} \leftarrow k - \mathbf{p} \\ \vdots \\ \vdots \\ \vdots \end{array} \right] \xrightarrow{\omega, \mathbf{q}} \frac{\varepsilon + \omega, \mathbf{p}'}{\varepsilon, \mathbf{p}' - \mathbf{q}}$$

(d)
$$\bar{\Gamma}_q(\omega) = \begin{array}{c} \omega, \mathbf{q} \\ \text{wavy line} \end{array} \begin{array}{c} \nearrow \\ \text{wavy line} \end{array} \begin{array}{c} R, \varepsilon + \omega \mathbf{p} \\ \text{wavy line} \end{array} \begin{array}{c} \searrow \\ \text{wavy line} \end{array} \begin{array}{c} A, \varepsilon, \mathbf{p} - \mathbf{q} \end{array} = \begin{array}{c} \omega, \mathbf{q} \\ \text{wavy line} \end{array} \begin{array}{c} \nearrow \\ \text{wavy line} \end{array} \begin{array}{c} R, \varepsilon + \omega \mathbf{p} \\ \text{wavy line} \end{array} \begin{array}{c} \searrow \\ \text{wavy line} \end{array} \begin{array}{c} A, \varepsilon, \mathbf{p} - \mathbf{q} \end{array}$$

(d)
$$= \begin{array}{c} \omega, \mathbf{q} \\ \text{wavy line} \end{array} \begin{array}{c} \nearrow \\ \text{wavy line} \end{array} \begin{array}{c} R, \varepsilon + \omega \mathbf{p} \\ \text{wavy line} \end{array} \begin{array}{c} \searrow \\ \text{wavy line} \end{array} \begin{array}{c} A, \varepsilon, \mathbf{p} - \mathbf{q} \end{array} + \begin{array}{c} \omega, \mathbf{q} \\ \text{wavy line} \end{array} \begin{array}{c} \nearrow \\ \text{wavy line} \end{array} \begin{array}{c} R, \varepsilon + \omega \mathbf{k} \\ \text{wavy line} \end{array} \begin{array}{c} \searrow \\ \text{wavy line} \end{array} \begin{array}{c} A, \varepsilon, \mathbf{k} - \mathbf{q} \end{array} \begin{array}{c} \nearrow \\ \text{wavy line} \end{array} \begin{array}{c} \varepsilon + \omega \mathbf{p} \\ \text{wavy line} \end{array} \begin{array}{c} \searrow \\ \text{wavy line} \end{array} \begin{array}{c} \varepsilon, \mathbf{p} - \mathbf{q} \end{array} = 1 + \frac{\bar{\Pi}_q(\omega) \bar{D}_q^0(\omega)}{2\pi\nu\tau_{\text{el}}^2/\hbar}$$

(e)
$$\bar{\chi}_q(\omega) = \begin{array}{c} \omega, \mathbf{q} \\ \text{wavy line} \end{array} \begin{array}{c} \nearrow \\ \text{wavy line} \end{array} \begin{array}{c} \varepsilon + \omega, \mathbf{p} + \mathbf{q} \\ \text{wavy line} \end{array} \begin{array}{c} \searrow \\ \text{wavy line} \end{array} \begin{array}{c} \omega, \mathbf{q} \\ \text{wavy line} \end{array} \begin{array}{c} \nearrow \\ \text{wavy line} \end{array} \begin{array}{c} R \\ \text{wavy line} \end{array} \begin{array}{c} \searrow \\ \text{wavy line} \end{array} \begin{array}{c} A \\ \text{wavy line} \end{array} \begin{array}{c} \nearrow \\ \text{wavy line} \end{array} \begin{array}{c} \varepsilon, \mathbf{p} \end{array} + \begin{array}{c} \omega, \mathbf{q} \\ \text{wavy line} \end{array} \begin{array}{c} \nearrow \\ \text{wavy line} \end{array} \begin{array}{c} \varepsilon + \omega, \mathbf{p} + \mathbf{q} \\ \text{wavy line} \end{array} \begin{array}{c} \searrow \\ \text{wavy line} \end{array} \begin{array}{c} \omega, \mathbf{q} \\ \text{wavy line} \end{array} \begin{array}{c} \nearrow \\ \text{wavy line} \end{array} \begin{array}{c} R \\ \text{wavy line} \end{array} \begin{array}{c} \searrow \\ \text{wavy line} \end{array} \begin{array}{c} R \\ \text{wavy line} \end{array} \begin{array}{c} \nearrow \\ \text{wavy line} \end{array} \begin{array}{c} \varepsilon, \mathbf{p} \end{array} + \begin{array}{c} \omega, \mathbf{q} \\ \text{wavy line} \end{array} \begin{array}{c} \nearrow \\ \text{wavy line} \end{array} \begin{array}{c} \varepsilon + \omega, \mathbf{p} + \mathbf{q} \\ \text{wavy line} \end{array} \begin{array}{c} \searrow \\ \text{wavy line} \end{array} \begin{array}{c} \omega, \mathbf{q} \\ \text{wavy line} \end{array} \begin{array}{c} \nearrow \\ \text{wavy line} \end{array} \begin{array}{c} A \\ \text{wavy line} \end{array} \begin{array}{c} \searrow \\ \text{wavy line} \end{array} \begin{array}{c} A \\ \text{wavy line} \end{array} \begin{array}{c} \nearrow \\ \text{wavy line} \end{array} \begin{array}{c} \varepsilon, \mathbf{p} \end{array}$$

Fig. F1. The building blocks of diagrammatic perturbation theory: (a) Basic definitions for the electron lines $\tilde{G}_{ij}^{R/A}$ and $\tilde{G}_p^{R/A}(\varepsilon)$, impurity lines, the function $\bar{\Pi}_q(\omega)$ of Eq. (F.5a), and the interaction lines $\tilde{\mathcal{L}}_{ij}$ or $\bar{\mathcal{L}}_q(\omega)$ of Eq. (B.75b). For all correlators, arrows point from the second to the first index. [creation to annihilation operators] Internal impurity momenta are to be integrated over with $\int (dk)$, as in $\bar{\Pi}_q(\omega)$. (b) Eq. (F.3b). (c) The bare Cooperon $\bar{C}_q^0(\omega)$ [Eq. (F.5b)] and bare diffuson $\bar{D}_q^0(\omega)$ [Eq. (F.5c)]; (d) the diffuson-dressed vertex $\bar{\Gamma}_q(\omega)$ [Eq. (F.5d)] and (e) polarization bubble $\bar{\chi}_q(\omega)$ [Eq. (F.5e)]. For each of $\bar{\Pi}_q(\omega)$, $\bar{C}_q^0(\omega)$ and $\bar{\Gamma}_q(\omega)$, the frequency argument ω is defined as the frequency of the corresponding retarded Green's function minus that of the advanced one.

98 *Jan von Delft*

$$\begin{aligned} &\simeq -i 2e^2 \hbar \int (d\varepsilon)(d\mathbf{p}) \left\langle [-\omega n'_0(\varepsilon)] \bar{\mathcal{G}}_{\mathbf{p}+\mathbf{q}}^R(\varepsilon + \omega) \bar{\mathcal{G}}_{\mathbf{p}}^A(\varepsilon) \right. \\ &\quad \left. - n_0(\varepsilon) \left[\bar{\mathcal{G}}_{\mathbf{p}+\mathbf{q}}^R(\varepsilon + \omega) \bar{\mathcal{G}}_{\mathbf{p}}^R(\varepsilon) - \bar{\mathcal{G}}_{\mathbf{p}+\mathbf{q}}^A(\varepsilon + \omega) \bar{\mathcal{G}}_{\mathbf{p}}^A(\varepsilon) \right] \right\rangle_{\text{dis}}. \end{aligned} \quad (\text{F.4b})$$

The results are:

$$\bar{\Pi}_{\mathbf{q}}(\omega) = \int (d\mathbf{k}) \bar{\mathcal{G}}_{\mathbf{k}}^R(\varepsilon + \omega) \bar{\mathcal{G}}_{\mathbf{q}-\mathbf{k}}^A(\varepsilon) = \frac{2\pi\nu\tau_{\text{el}}}{\hbar} [1 - \tau_{\text{el}}(D\mathbf{q}^2 - i\omega) + \dots], \quad (\text{F.5a})$$

$$\bar{\mathcal{C}}_{\mathbf{q}}^0(\omega) = \frac{\tau_{\text{el}}}{1 - \bar{\Pi}_{\mathbf{q}}(\omega)/(2\pi\nu\tau_{\text{el}}/\hbar)} = \frac{1}{D\mathbf{q}^2 - i\omega + \gamma_H} + \dots, \quad (\text{F.5b})$$

$$\bar{\mathcal{D}}_{\mathbf{q}}^0(\omega) = \frac{\tau_{\text{el}}}{1 - \bar{\Pi}_{\mathbf{q}}(\omega)/(2\pi\nu\tau_{\text{el}}/\hbar)} = \frac{1}{D\mathbf{q}^2 - i\omega} + \dots, \quad (\text{F.5c})$$

$$\bar{\Gamma}_{\mathbf{q}}(\omega) = 1 + \frac{\bar{\Pi}_{\mathbf{q}}(\omega)\bar{\mathcal{D}}_{\mathbf{q}}^0(\omega)}{2\pi\nu\tau_{\text{el}}^2/\hbar} = \frac{1}{\tau_{\text{el}}(D\mathbf{q}^2 - i\omega)} + \dots, \quad (\text{F.5d})$$

$$\bar{\chi}_{\mathbf{q}}(\omega) = -i 2e^2 \left[\frac{\omega\nu}{D\mathbf{q}^2 - i\omega} - i\nu \right] = -\frac{\mathbf{q}^2 \sigma_{\text{DC}}^{\text{Drude}}}{D\mathbf{q}^2 - i\omega} + \dots. \quad (\text{F.5e})$$

Here $D = v_F^2 \tau_{\text{el}}/d$ is the diffusion constant in $d = 3$ or 2 dimensions, γ_H is a magnetic-field cutoff and the dots indicate subleading terms that are small in $\omega\tau_{\text{el}} \ll 1$ and $q\ell_{\text{el}} \ll 1$.

For convenience, we also summarize here some results that are useful for evaluating momentum integrals that arise in diagrammatic perturbation theory. Usually, the energy parameter $\hbar\varepsilon$ of the disorder-averaged Greens' functions $\bar{\mathcal{G}}_{\mathbf{p}}^{R/A}(\varepsilon)$ is confined to the vicinity of ε_F , typically by the presence of a factor $-\partial_\varepsilon n_0(\hbar\varepsilon)$ in an $\int d\varepsilon$ integration, so that terms of order $\hbar\varepsilon/\varepsilon_F$ can be neglected. [The second term of Eq. (F.4b) does not contain a factor $-\partial_\varepsilon n_0$, but one can be generated by integrating by parts.] The explicit form (F.2) for $\bar{\mathcal{G}}_{\mathbf{p}}^{R/A}(\varepsilon)$ then implies the following ‘‘identities’’:

$$\int \frac{(d\mathbf{p})}{2\pi\nu\tau_{\text{el}}/\hbar} \bar{\mathcal{G}}_{\mathbf{p}}^R(\varepsilon) \bar{\mathcal{G}}_{\mathbf{p}}^A(\varepsilon) = 1, \quad \int \frac{(d\mathbf{p})}{2\pi\nu\tau_{\text{el}}/\hbar} \bar{\mathcal{G}}_{\mathbf{p}}^{R/A}(\varepsilon) \bar{\mathcal{G}}_{\mathbf{p}}^{R/A}(\varepsilon) = 0, \quad (\text{F.6a})$$

$$\int \frac{(d\mathbf{p})}{2\pi\nu\tau_{\text{el}}/\hbar} \left[\bar{\mathcal{G}}_{\mathbf{p}}^{R/A}(\varepsilon) \right]^m \left[\bar{\mathcal{G}}_{\mathbf{p}}^{A/R}(\varepsilon) \right]^n = \left(\frac{-i\tau}{\hbar} \right)^{m-1} \left(\frac{i\tau}{\hbar} \right)^{n-1} \binom{m+n-2}{m-1}. \quad (\text{F.6b})$$

Furthermore, in the limit of small frequencies ($\omega, \bar{\omega} \ll 1/\tau_{\text{el}}$) and wavenumbers ($\mathbf{q}^2, \bar{\mathbf{q}}^2 \ll 1/D\tau_{\text{el}}$), integrals of the following kind can be evaluated by a systematic expansion in the small parameters, combined with repeated use of Eqs. (F.6):

$$\int \frac{(d\mathbf{p})}{2\pi\nu\tau_{\text{el}}/\hbar} \bar{\mathcal{G}}_{\mathbf{p}}^{R/A}(\varepsilon) \bar{\mathcal{G}}_{\mathbf{p}+\mathbf{q}}^{A/R}(\varepsilon + \omega) = 1 - \tau_{\text{el}}[D\mathbf{q}^2 \pm i\omega] + \dots, \quad (\text{F.7a})$$

$$\begin{aligned} &\frac{\hbar}{\tau_{\text{el}}} \int \frac{(d\mathbf{p})}{2\pi\nu\tau_{\text{el}}/\hbar} \bar{\mathcal{G}}_{\mathbf{p}}^{R/A}(\varepsilon) \bar{\mathcal{G}}_{\mathbf{p}+\mathbf{q}}^{A/R}(\varepsilon + \omega) \bar{\mathcal{G}}_{\mathbf{p}+\mathbf{q}}^{A/R}(\varepsilon + \bar{\omega}) \\ &\quad = \pm i \left\{ 1 - \tau_{\text{el}}[D(\mathbf{q} + \bar{\mathbf{q}})^2 \pm i(\omega + \bar{\omega})] \right\} + \dots, \end{aligned} \quad (\text{F.7b})$$

$$\begin{aligned} \frac{\hbar^2}{\tau_{\text{el}}^2} \int \frac{(d\mathbf{p})}{2\pi\nu\tau_{\text{el}}/\hbar} \left[\bar{\mathcal{G}}_{\mathbf{p}}^{R/A}(\varepsilon) \right]^2 \bar{\mathcal{G}}_{\mathbf{p}+\mathbf{q}}^{A/R}(\varepsilon + \omega) \bar{\mathcal{G}}_{\mathbf{p}+\bar{\mathbf{q}}}^{A/R}(\varepsilon + \bar{\omega}) \\ = 2 - \tau_{\text{el}} \left[4D(\mathbf{q} + \bar{\mathbf{q}})^2 \pm 3i(\omega + \bar{\omega}) \right] + \dots, \end{aligned} \quad (\text{F.7c})$$

$$\begin{aligned} \frac{\hbar^2}{\tau_{\text{el}}^2} \int \frac{(d\mathbf{p})}{2\pi\nu\tau_{\text{el}}/\hbar} \bar{\mathcal{G}}_{\mathbf{p}}^{R/A}(\varepsilon) \bar{\mathcal{G}}_{\mathbf{p}+\mathbf{q}'}^{R/A}(\varepsilon + \omega') \bar{\mathcal{G}}_{\mathbf{p}+\mathbf{q}}^{A/R}(\varepsilon + \omega) \bar{\mathcal{G}}_{\mathbf{p}+\bar{\mathbf{q}}}^{A/R}(\varepsilon + \bar{\omega}) \\ = 2 - \tau_{\text{el}} \left[D[4(\mathbf{q} + \bar{\mathbf{q}})^2 + 4(\mathbf{q}')^2 - 6\mathbf{q}' \cdot (\mathbf{q} + \bar{\mathbf{q}})] \pm 3i(\omega + \bar{\omega} - \omega') \right] + \dots. \end{aligned} \quad (\text{F.7d})$$

F.2. Cooperon Self Energy

In this section, we provide some details for how the Cooperon self energy can be calculated by performing the disorder average diagrammatically. As starting point we use Eqs. (B.89), which we derived in Sec. B.6.1 from the influence functional approach, but which are equivalent to the standard Keldysh expressions following from Eq. (E.24). According to Eqs. (B.89), there are four self-energy contributions to the Cooperon self energy, which we write as:

$$\bar{\Sigma}_{\mathbf{q}}^{\text{self}}(\omega) \equiv \frac{1}{\hbar} \int \frac{d\bar{\omega}}{2\pi} \int (d\bar{\mathbf{q}}) \left[\bar{\Sigma}_{FF}^I + \bar{\Sigma}_{BB}^I + \bar{\Sigma}_{FF}^R + \bar{\Sigma}_{BB}^R \right]. \quad (\text{F.8})$$

The diagrams for $\bar{\Sigma}_{aa}^I$ are depicted in Fig. F2(b), those for $\bar{\Sigma}_{aa}^R$ in Fig. F2(c) to F2(f) (which correspond one-to-one to Fig. 2(b) to 2(f) of AAV¹⁸). Starting from Eq. (B.89), the corresponding algebraic expressions can be written as:

$$\bar{\Sigma}_{FF}^I = -\frac{1}{2} i \bar{\mathcal{L}}_{\bar{\mathbf{q}}}^K(\bar{\omega}) \bar{\mathcal{C}}_{\mathbf{q}-\bar{\mathbf{q}}}^0(\omega - \bar{\omega}) Y_F^{(1)} \quad (\text{F.9})$$

$$\bar{\Sigma}_{BB}^I = -\frac{1}{2} i \bar{\mathcal{L}}_{\bar{\mathbf{q}}}^K(\bar{\omega}) \bar{\mathcal{C}}_{\mathbf{q}-\bar{\mathbf{q}}}^0(\omega + \bar{\omega}) Y_B^{(1)},$$

$$\bar{\Sigma}_{FF}^R = -\frac{1}{2} i \bar{\mathcal{L}}_{\bar{\mathbf{q}}}^R(\bar{\omega}) \tanh[\hbar(\varepsilon + \omega - \bar{\omega})/2T] \left\{ \bar{\mathcal{C}}_{\mathbf{q}-\bar{\mathbf{q}}}^0(\omega - \bar{\omega}) Y_F^{(1)} - \tau_{\text{el}} \bar{\Gamma}_{\bar{\mathbf{q}}}^2(\bar{\omega}) \sum_{n=2}^4 Y_F^{(n)} \right\},$$

$$\bar{\Sigma}_{BB}^R = -\frac{1}{2} i \bar{\mathcal{L}}_{\bar{\mathbf{q}}}^A(\bar{\omega}) \tanh[\hbar(\varepsilon - \bar{\omega})/2T] \left\{ -\bar{\mathcal{C}}_{\mathbf{q}-\bar{\mathbf{q}}}^0(\omega + \bar{\omega}) Y_B^{(1)} + \tau_{\text{el}} \bar{\Gamma}_{-\bar{\mathbf{q}}}^2(-\bar{\omega}) \sum_{n=2}^4 Y_B^{(n)} \right\}.$$

In the expressions for $\bar{\Sigma}_{aa}^R$, the minus signs before $Y_F^{(2)}$, $Y_F^{(3)}$, $Y_F^{(4)}$ and $Y_B^{(1)}$ arise from the minus sign in $\bar{\mathcal{G}}^K = \tanh(\cdot) [\bar{\mathcal{G}}^R - \bar{\mathcal{G}}^A]$, and the Y 's represent integrals over internal momenta, that can be performed using variations of Eqs. (F.7):

$$\begin{aligned} Y_F^{(1)} &= \frac{\hbar}{\tau_{\text{el}}} \int \frac{(d\mathbf{p})}{2\pi\nu\tau_{\text{el}}/\hbar} \bar{\mathcal{G}}_{\mathbf{q}-\mathbf{p}}^A(\varepsilon) \bar{\mathcal{G}}_{\mathbf{p}}^R(\varepsilon + \omega) \bar{\mathcal{G}}_{\mathbf{p}-\bar{\mathbf{q}}}^R(\varepsilon + \omega - \bar{\omega}) \\ &\quad \times \frac{\hbar}{\tau_{\text{el}}} \int \frac{(d\mathbf{p}')}{2\pi\nu\tau_{\text{el}}/\hbar} \bar{\mathcal{G}}_{\mathbf{q}-\mathbf{p}'}^A(\varepsilon) \bar{\mathcal{G}}_{\mathbf{p}'-\bar{\mathbf{q}}}^R(\varepsilon + \omega - \bar{\omega}) \bar{\mathcal{G}}_{\mathbf{p}'}^R(\varepsilon + \omega) \\ &= (-i)^2 \left\{ 1 - \tau_{\text{el}} \left[D(2\mathbf{q} - \bar{\mathbf{q}})^2 - i(2\omega - \bar{\omega}) \right] + \dots \right\}^2, \end{aligned} \quad (\text{F.10})$$

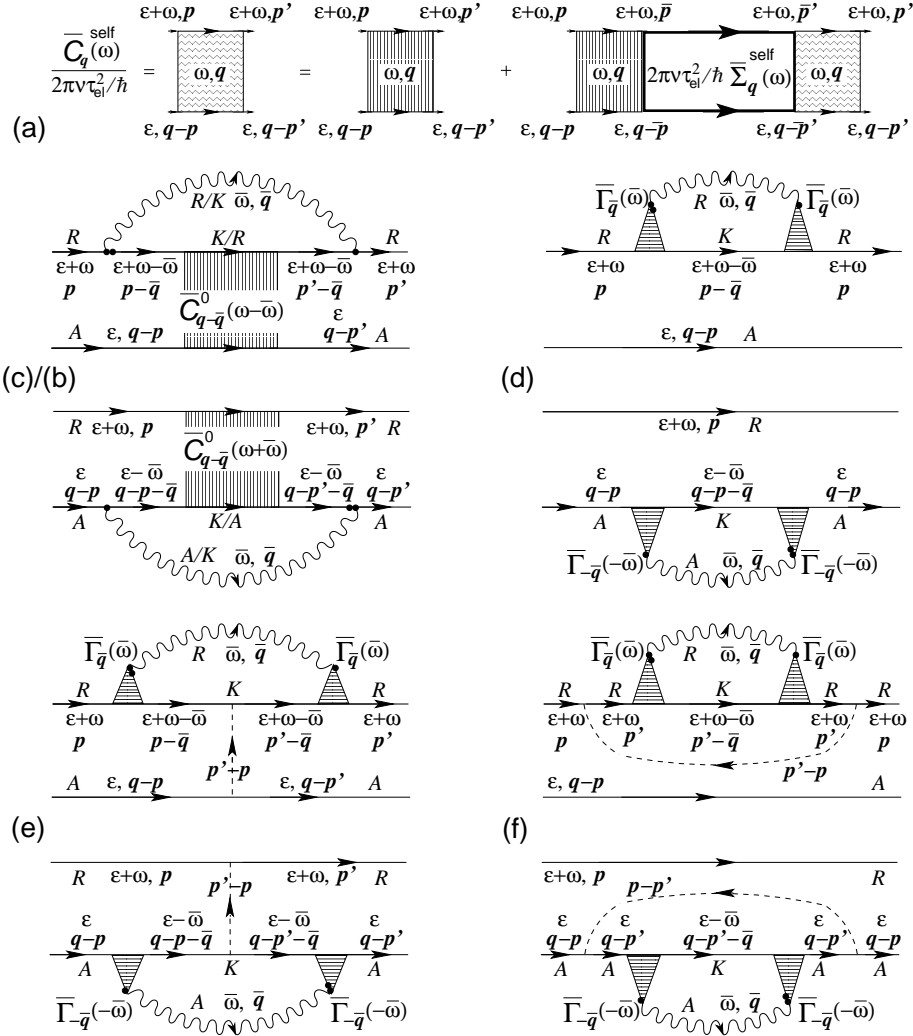


Fig. F2. (a) Dyson equation [Eq. (12)] for the Cooperon, for the case that the Cooperon self energy contains only self-energy contributions. The latter are shown in diagrams (b) to (f), which depict how to perform the disorder average of the various contributions $\bar{\Sigma}_{aa'}^{I/R}$ to the Cooperon self energy, leading to Eqs. (F.9) and (F.10). Diagrams (b) depict $\bar{\Sigma}_{FF/BB}^I$; the diagrams (c) + (d) + (e) + (f) depict $\bar{\Sigma}_{FF/BB}^R$, the four contributions corresponding to the terms in Eqs. (F.10) that contain $Y_a^{(1)}$, $Y_a^{(2)}$, $Y_a^{(3)}$ and $Y_a^{(4)}$, respectively. [To avoid cluttering the figure with factors of $\frac{1}{2}$, the energy and momentum labels ε , ω and \mathbf{q} used here were assigned in a less symmetrical way between upper and lower lines than in Fig. C2(c); to transcribe the expressions used in this section into the notation used there, make the replacements $(\varepsilon + \omega)_{\text{here}} \rightarrow (\varepsilon + \frac{1}{2}\omega)$, $\mathbf{p}'_{\text{here}} \rightarrow (\mathbf{p}_1 + \frac{1}{2}\mathbf{q})$, $\mathbf{p}_{\text{here}} \rightarrow (\mathbf{p}_2 + \frac{1}{2}\mathbf{q})$, and identify $(\mathcal{E} + \frac{1}{2}\Omega_1)_{\text{there}} = (\mathcal{E} + \frac{1}{2}\Omega_2)_{\text{there}} = \varepsilon + \frac{1}{2}\omega$.]

$$Y_F^{(2)} = \frac{\hbar^2}{\tau_{\text{el}}^2} \int \frac{(d\mathbf{p})}{2\pi\nu\tau_{\text{el}}/\hbar} [\bar{\mathcal{G}}_p^R(\varepsilon + \omega)]^2 \bar{\mathcal{G}}_{p-\bar{q}}^A(\varepsilon + \omega - \bar{\omega}) \bar{\mathcal{G}}_{q-p}^A(\varepsilon)$$

$$\begin{aligned}
 &= 2 - \tau_{\text{el}} \left[4D(\mathbf{q} + \bar{\mathbf{q}})^2 - 3i(\omega + \bar{\omega}) \right], \\
 Y_F^{(3)} &= \frac{\hbar}{\tau_{\text{el}}} \int \frac{(d\mathbf{p})}{2\pi\nu\tau_{\text{el}}/\hbar} \bar{\mathcal{G}}_{\mathbf{p}}^R(\varepsilon + \omega) \bar{\mathcal{G}}_{\mathbf{p}-\bar{\mathbf{q}}}^A(\varepsilon + \omega - \bar{\omega}) \bar{\mathcal{G}}_{\mathbf{q}-\mathbf{p}}^A(\varepsilon) \\
 &\quad \frac{\hbar}{\tau_{\text{el}}} \int \frac{(d\mathbf{p}')}{2\pi\nu\tau_{\text{el}}/\hbar} \bar{\mathcal{G}}_{\mathbf{p}'}^R(\varepsilon + \omega) \bar{\mathcal{G}}_{\mathbf{p}'-\bar{\mathbf{q}}}^A(\varepsilon + \omega - \bar{\omega}) \bar{\mathcal{G}}_{\mathbf{q}-\mathbf{p}'}^A(\varepsilon) \\
 &= (i)^2 \left\{ 1 - \tau_{\text{el}} \left[D(\mathbf{q} + \bar{\mathbf{q}})^2 - i(\omega + \bar{\omega}) \right] + \dots \right\}^2 \\
 Y_F^{(4)} &= \frac{\hbar^2}{\tau_{\text{el}}^2} \int \frac{(d\mathbf{p})(d\mathbf{p}')}{(2\pi\nu\tau_{\text{el}}/\hbar)^2} \bar{\mathcal{G}}_{\mathbf{q}-\mathbf{p}}^A(\varepsilon) [\bar{\mathcal{G}}_{\mathbf{p}}^R(\varepsilon + \omega)]^2 \bar{\mathcal{G}}_{\mathbf{p}'-\bar{\mathbf{q}}}^A(\varepsilon + \omega - \bar{\omega}) [\bar{\mathcal{G}}_{\mathbf{p}'}^R(\varepsilon + \omega)]^2 \\
 &= (-i)^2 \left\{ 1 - \tau_{\text{el}} \left[D(2\mathbf{q})^2 - i2\omega \right] + \dots \right\}^2 \left\{ 1 - \tau_{\text{el}} \left[D(2\bar{\mathbf{q}})^2 - i2\bar{\omega} \right] + \dots \right\}^2
 \end{aligned}$$

Performing a similar set of integrals for the $Y_B^{(n)}$'s, we readily find that $Y_B^{(n)}(\bar{\omega}) = Y_F^{(n)}(-\bar{\omega})$. Note that the sums $\sum_{n=2}^4 Y_{F/B}^{(n)}$, which are associated with the so-called ‘‘Hikami-box’’ diagrams of Fig. F2(d) to F2(f), add up to zero in leading order, which is why the next order had to be included. Finally, the results for $\bar{\Sigma}^{I,\text{self}}$ and $\bar{\Sigma}^{R,\text{self}}$, given by Eqs. (13b) in the main text, are obtained by inserting Eqs. (F.10) into Eqs. (F.9) and (F.8), and making the replacement $\varepsilon_{\text{here}} \rightarrow \varepsilon - \frac{1}{2}\omega$ (cf. caption of Fig.F2).

References

1. Jan von Delft, ‘‘Influence functional for Decoherence of Interacting Electrons in Disordered Conductors’’, in *Fundamental Problems of Mesoscopic Physics*, ed. I. V. Lerner, B.L. Altshuler, and Y. Gefen (eds.), Kluwer, London (2004), pp. 115-138. This publication contains, modulo minor revisions, the main text and appendices A.1 to A.3 of the present review.
2. D. S. Golubev and A. D. Zaikin, *Phys. Rev. Lett.* **81**, 1074, (1998).
3. D. S. Golubev and A. D. Zaikin, *Phys. Rev.* **B59**, 9195, (1999).
4. D. S. Golubev and A. D. Zaikin, *Phys. Rev.* **B62**, 14061 (2000).
5. D. S. Golubev, A. D. Zaikin, and G. Schön, *J. Low Temp. Phys.* **126**, 1355 (2002) [cond-mat/0110495].
6. D. S. Golubev and A. D. Zaikin, *J. Low Temp. Phys.* **132**, 11 (2003) [cond-mat/0208140].
7. D. S. Golubev, C. P. Herrero, Andrei D. Zaikin, *Europhys. Lett.* **63**, 426 (2003) [cond-mat/0205549].
8. P. Mohanty, E. M. Q. Jariwala, and R. A. Webb, *Phys. Rev. Lett.* **78**, 3366 (1997); *Fortschr. Phys.* **46**, 779 (1998).
9. Most relevant references can be found in the review⁵ by Golubev, Zaikin and Schön, which gives a useful overview of the controversy from GZ’s point of view.
10. B. L. Altshuler, A. G. Aronov, and D. E. Khmel’nitskii, *J. Phys.* **C15**, 7367 (1982).
11. K. A. Eriksen and P. Hedegard, cond-mat/9810297; GZ replied in cond-mat/9810368.
12. M. Vavilov and V. Ambegaokar, cond-mat/9902127.
13. T.R. Kirkpatrick, D. Belitz, cond-mat/0112063, cond-mat/0111398.
14. Y. Imry, cond-mat/0202044.

102 *Jan von Delft*

15. J. von Delft, *J. Phys. Soc. Jpn.* **72** (2003), Suppl. A pp. 24-29 [cond-mat/0210644].
16. F. Marquardt, cond-mat/0207692.
17. I. Aleiner, B. L. Altshuler, and M. E. Gershenson, *Waves and Random Media* **9**, 201 (1999) [cond-mat/9808053]; *Phys. Rev. Lett.* **82**, 3190 (1999).
18. I. L. Aleiner, B. L. Altshuler, M. G. Vavilov, *J. Low Temp. Phys.* **126**, 1377 (2002) [cond-mat/0110545].
19. I. L. Aleiner, B. L. Altshuler, M. G. Vavilov, cond-mat/0208264.
20. (MDSA-I) F. Marquardt, J. von Delft, R. Smith and V. Ambegaokar, *Phys. Rev.* **B76**, 195331 (2007) [cond-mat/0510556], and (DMSA-II) J. von Delft, F. Marquardt, R. Smith and V. Ambegaokar, *Phys. Rev.* **B76**, 195332 (2007) [cond-mat/0510557].
21. S. Chakravarty and A. Schmid, *Phys. Rep.* **140**, 193 (1983).
22. H. Fukuyama and E. Abrahams, *Phys. Rev.* **B27**, 5976 (1983).
23. The expressions for $\tilde{\Sigma}$ that we published in ¹⁵, Eqs. (A.16), contain incorrect signs and missing factors of $\frac{1}{2}$, and should be replaced by Eqs. (A.10) of this review.
24. D. S. Golubev and A. D. Zaikin, cond-mat/0512411.